

**Czech Technical University in Prague**  
Faculty of Civil Engineering  
Department of Concrete and Masonry Structures



**Analysis of Concrete Structures after Fire**

*Analýza betonových konstrukcí po požáru*

**DOCTORAL THESIS**

Author:	Ing. Petr Müller
Doctoral Degree Programme:	Civil Engineering
Branch of Study:	Building and Structural Engineering
Supervisor:	prof. Ing. Jaroslav Procházka, CSc.
Co-supervisor:	Ing. Radek Štefan, Ph.D.

Prague 2022



# Declaration

Author: Petr Müller

Thesis: Analysis of Concrete Structures after Fire

I hereby affirm that this doctoral thesis has been written by myself, under the supervision of prof. Jaroslav Procházka and Dr. Radek Štefan.

Some parts of this thesis have already been published in scientific papers co-authored by myself. All sources of information that have been used in the dissertation are acknowledged in the text and listed in the Bibliography, in accordance with the requirements given by the CTU Guideline<sup>1</sup>.

.....

Petr Müller

In Prague, 21 August 2022

---

<sup>1</sup> See Metodický pokyn č. 1/2009 O dodržování etických principů při přípravě vysokoškolských závěrečných prací (in Czech).





## Abstract

The Doctoral Thesis is focused on analysis of concrete structures after fire. The topic of structural post-fire assessment is still very actual and situations when such assessment is the only way how to make informed decision about fire-damaged building occur. The Thesis brings both theoretical and practical findings to the investigation process after the end of fire and describes the approach step-by-step. At the same time, the Thesis deals only with reinforced concrete structures made of normal strengths concrete used in building constructions.

At the beginning material properties of concrete and reinforcement steel at high temperatures and after cooling down are described in the state-of-art form. Then the investigation process is discussed in detail: preliminary and detail inspection of the subjected building with estimation of damage extent and severity, conducting on-site material tests, extracting samples for laboratory tests. One chapter is dedicated to the structural diagnosis with special attention to the nature of damage caused by fire. Another chapter deals with global action of fire and temperature-induced forces with respect to both directly and indirectly affected parts and mutual interaction. Chapter dedicated to estimation of residual load-bearing capacity ends the main part of the Thesis. Several worked examples of whole post-fire assessment are given in the annex.

Special attention was dedicated to make the investigation and its conclusions organised, clear and easy-to-read.

## Key words

Concrete; Reinforcement; Fire event; Damage; Fire Scenario Approximation; Structural Diagnosis; Global Analysis; Residual Load-bearing Capacity; Post-fire Structural Assessment

<https://doi.org/10.14311/dis.fsv.2022.011>

## Abstrakt

Disertační práce je zaměřena na analýzu betonových konstrukcí po požáru. Téma statického posuzování po požáru je stále velmi aktuální a dochází k situacím, kdy je takovýto posudek jediným způsobem, jak učinit informované rozhodnutí o budově poškozené požárem. Práce přináší teoretické i praktické poznatky k procesu vyšetřování po skončení požáru a popisuje tento postup krok za krokem. Zároveň se práce zabývá pouze železobetonovými konstrukcemi z betonu normálních pevností v pozemních stavbách.

V úvodu jsou popsány materiálové vlastnosti betonu a betonářské výztuže při vysokých teplotách a po ochlazení ve *state-of-art* podobě. Poté je podrobně rozebrán postup vyšetřování: předběžná a detailní prohlídka zasaženého objektu s odhadem rozsahu a závažnosti poškození, provádění materiálových zkoušek na místě, odběr vzorků pro laboratorní zkoušky. Jedna kapitola je věnována diagnostice konstrukcí se zvláštním zřetelem na charakter poškození požárem. Další kapitola se zabývá globální analýzou konstrukce s ohledem na účinky požáru, především potom přídavné vnitřní síly od teploty a dále interakci mezi přímo a nepřímo zasaženými částmi konstrukce. Hlavní část práce uzavírá kapitola věnovaná výpočtu zbytkové únosnosti. V příloze práce je vypracováno několik vzorových příkladů kompletního posouzení po požáru.

Zvláštní pozornost byla věnována organizaci a přehlednosti procesu posouzení po požáru a souvisejících závěrů.

## Klíčová slova

Beton; výztuž; požární událost; poškození; rekonstrukce požární události; diagnostika konstrukce; globální analýza; zbytková únosnost; statické posouzení po požáru

## Acknowledgements

Sincerely I would like to thank my supervisor, prof. Jaroslav Procházka for his both theoretical and practical advices, for leading me and sharing his enormous knowledge and experience, and being kind and positive all the time.

At the same time, I would like to thank my supervisor-specialist, Dr. Radek Štefan for guiding me as well, reviewing my articles, providing me theoretical and mathematical insight to the problems and discussing various topics in detail.

I also thank to my colleagues Ph.D. students Martin Benýšek and Jakub Holan for collaboration and many enriching discussions.

My gratitude also goes to prof. Antonio Marí from Universitat Politecnica de Catalunya, who supervised my work during short study stay in Barcelona, which was ended early due to beginning of COVID-19 pandemic situation.

I am grateful for financial support provided by following organisations:

- Grant Agency of the Czech Technical University in Prague
  - Grant No. SGS21/040/OHK1/1T/11 (research team member),
  - Grant No. SGS20/041/OHK1/1T/11 (research team member),
  - Grant No. SGS19/034/OHK1/1T/11 (research team member),
  - Grant No. SGS18/038/OHK1/1T/11 (research team member),
  - Grant No. SGS17/044/OHK1/1T/11 (research team member),
- Czech Science Foundation
  - GAČR 17-23067S (research team member).

I am also grateful to Petr Žalský and Tomáš Křivka, my colleagues and directors of structural office STATIKON Solutions s.r.o. for their patience, support and understanding.

Last but not least, I thank to my family and girlfriend Stanislava for their never-ending patience, support and love.

Thank you all.



# Contents

<b>DECLARATION</b> .....	<b>III</b>
<b>ABSTRACT</b> .....	<b>V</b>
<b>ABSTRAKT</b> .....	<b>VI</b>
<b>ACKNOWLEDGEMENTS</b> .....	<b>VII</b>
<b>1 INTRODUCTION</b> .....	<b>10</b>
1.1 Fire Safety & Structural Engineering .....	10
1.2 Motivation and Outline of the Thesis .....	18
<b>2 PROPERTIES OF CONCRETE AND REINFORCEMENT SUBJECTED TO FIRE (STATE-OF-ART)</b> .....	<b>19</b>
2.1 Mechanical and Thermal Properties of Concrete at Elevated Temperatures .....	20
2.1.1 <i>Mechanical Properties</i> .....	20
2.1.2 <i>Thermal Properties</i> .....	26
2.1.3 <i>Effect of Aggregate Content</i> .....	29
2.1.4 <i>Effect of Moisture Content &amp; Explosive Spalling</i> .....	31
2.2 Mechanical and Thermal Properties of Reinforcing Steel at Elevated Temperatures .....	32
2.3 Determination of Concrete Mechanical Properties at Elevated Temperatures by Laboratory Tests ....	35
2.4 Residual Properties of Concrete and Reinforcing Steel after Exposure to Elevated Temperatures .....	37
2.4.1 <i>Residual Properties of Concrete</i> .....	37
2.4.2 <i>Residual Properties of Reinforcing Steel</i> .....	39
2.5 Stress-Strain Diagrams & Thermal Strains.....	41
2.5.1 <i>Stress-Strain Diagram of Concrete</i> .....	41
2.5.2 <i>Stress-Strain Diagram of Reinforcing Steel</i> .....	46
2.6 Approaches to Estimate Fire Resistance.....	48
<b>3 POST-FIRE PROCEDURE</b> .....	<b>51</b>
3.1 General Aspects of Post-Fire Procedure .....	51
3.2 Approach to Post-Fire Structural Assessment .....	54
<b>4 PRELIMINARY INSPECTION OF DAMAGED BUILDING</b> .....	<b>61</b>
4.1 General Aspects of Preliminary Inspection .....	61
4.2 Classification to Damage Classes .....	62
4.3 Output of Preliminary Inspection .....	64
<b>5 DETAILED INSPECTION OF DAMAGED BUILDING</b> .....	<b>66</b>
5.1 Amending Information from Detailed Post-Fire Inspection .....	66
5.2 Fire Scenario Approximation .....	68
5.3 Approach to Damaged Structural Elements.....	78



<b>6</b>	<b>POST-FIRE STRUCTURAL DIAGNOSIS.....</b>	<b>79</b>
6.1	General Aspects of Post-Fire Structural Diagnosis .....	79
6.2	Overview of Post-Fire Diagnosis Methods.....	81
6.2.1	<i>Non-Destructive Diagnosis Methods</i> .....	83
6.2.2	<i>Destructive Diagnosis Methods</i> .....	97
6.3	Evaluation of Results.....	102
<b>7</b>	<b>GLOBAL STRUCTURAL ANALYSIS.....</b>	<b>108</b>
7.1	Importance of Conducting Global Analysis .....	108
7.2	Estimating Fire Resistance with Respect to Global Analysis .....	113
7.3	Incorporation of Thermal Loading into the Assessment.....	114
<b>8</b>	<b>ESTIMATION OF RESIDUAL LOAD-BEARING CAPACITY.....</b>	<b>129</b>
8.1	Aspects to Be Taken into Account Prior to Post-Fire Assessment .....	129
8.2	Methods of Residual Load-Bearing Capacity Estimation.....	132
8.3	Quick Estimations of Load-Bearing Capacity Decay .....	142
8.4	Brief Commentary to Strengthening Design and Final Refurbishment .....	143
<b>9</b>	<b>DISCUSSION .....</b>	<b>145</b>
9.1	General Conclusions.....	145
9.2	Recommendation for Further Research .....	145
	<b>AUTHOR'S PUBLICATIONS.....</b>	<b>146</b>
	<b>REFERENCES .....</b>	<b>147</b>
	<b>LIST OF FIGURES .....</b>	<b>153</b>
	<b>LIST OF TABLES.....</b>	<b>157</b>
	<b>ANNEX – WORKED EXAMPLES OF COMPLETE FIRE AND POST-FIRE RESISTANCE ASSESSMENT .....</b>	<b>158</b>
	Case no. 1 – Assessment of RC Column and Lintels after Fire .....	158
	Case no. 2 – Assessment of RC Floor Slabs and Walls in Global Fire Action .....	168



# 1 Introduction

## 1.1 Fire Safety & Structural Engineering

### Fire Safety Measures, Statistics

The attention dedicated to fire safety in buildings was firstly paid in case of timber structures due to their combustible nature and often cases of their fires. In case of houses with masonry walls and timber-beam floors the first fire engineering solution was usage of protective soffits. Structures made of steel and concrete were not in the scope of fire engineering for a long time due to their incombustible nature, although this fact does not provide any particular fire resistance. More attention to this topic has been paid by civil engineers and local authorities from approximately 1950s. From that time on, various regulations have been implemented in national building codes. Nature of the fire protection can be either preventive (ensuring fire not to start or to reduce its spread and severity) or suppressive (ensuring effective and successful fire extinguishing). The fire safety measures are understood to be a part of fire prevention and can be then divided into:

- *Active measures* – preventing fire from reaching the moment of *flashover* (when all combustible items in the room catch on fire due to high temperatures), such as the intervention of fire brigade, presence of fire extinguishers in the building, fire alarm electronic system, smoke and heat ventilation system, etc.
- *Passive measures* – preventing fire from spreading to another rooms and floors or at least slowing the process down after the flashover effect happened, such as dividing the internal space into fire compartments, using non-combustible materials on compartment boundary structures, sufficient fire resistance of load- and nonload-bearing structures, etc.

The development of fire safety measures still continues and stricter ones are gradually being accepted. It has always been a strong impulse to rise the pace of introducing new stricter regulations after situations when severe fire of big extent with human life losses happened, see e.g. [1, 2, 3, 4]. The intention of fire safety measures and regulations together is to:

- Limit the probability of fire start and if happens so, to limit the spread of fire and smoke to another fire compartments and floors.
- Avoid spreading fire to adjacent buildings.
- Ensure fire resistance of structures for sufficiently long time (either load- and nonload-bearing structures serving as compartment enclosure).
- Ensure safe and effective evacuation of habitants.
- Ensure safe and effective intervention and extinguishing of fire brigade.

From the list of aspects which fire safety measures should ensure or contribute to, one aspect has to be highlighted – ensuring safe evacuation of people out of the burning building is generally considered to be the absolute priority and main objective, because the cost of human life is priceless and incomparable to the losses of possession. In Fig. 1-1 a long-term statistics of human life losses attributed to fire accidents from different world regions can be seen. From the overall trend it can be stated the numbers of human victims are still decreasing which is positive of course and from majority it is result of fire safety regulations which have been implemented over the years. Interesting fact is that the statistics of victims in North America and Eastern Europe are quite similar, whereas situation in Western Europe have been significantly better in the studied time period. In recent years, number of victims in Eastern Europe and North America are finally getting close to those in Western Europe.

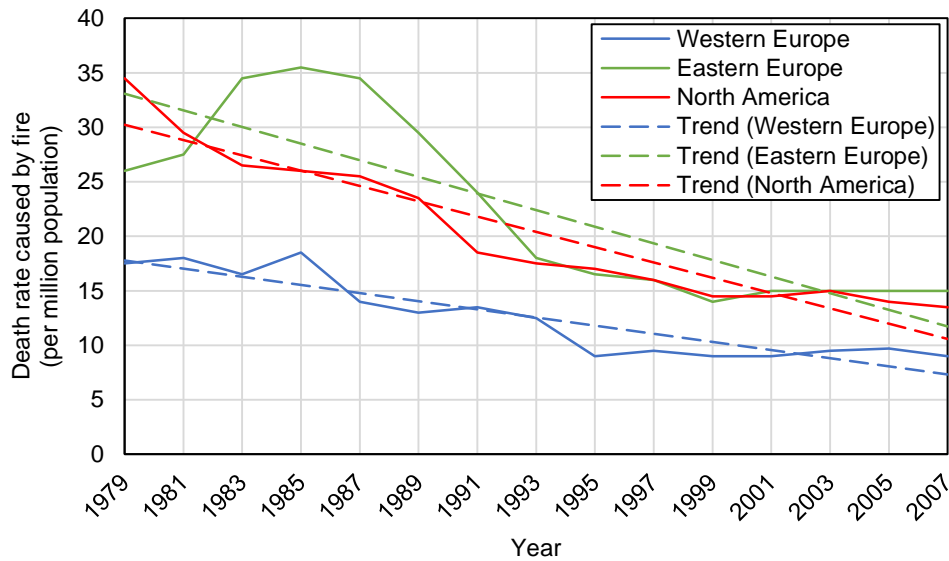


Fig. 1-1. Evolution of human life losses caused by fire, taken over [5].

Another interesting data can be seen in Fig. 1-2 which refers to the official statistics of Czech fire brigade [6] over last years and shows average data per one month. It can be stated that every month there were nearly 30 serious fire accidents<sup>2</sup> with financial harm over 1 million Kč<sup>3</sup> and even 5-10 human life losses attributed to the fire, which are numbers that one would probably not expect in these days. In Fig. 1-3 fire statistics over year 2019 from the same source is shown. Similar trend of data can be observed herein. The worst month of 2019 from this point of view seems to be April when 44 serious fires and even 13 deaths were registered.

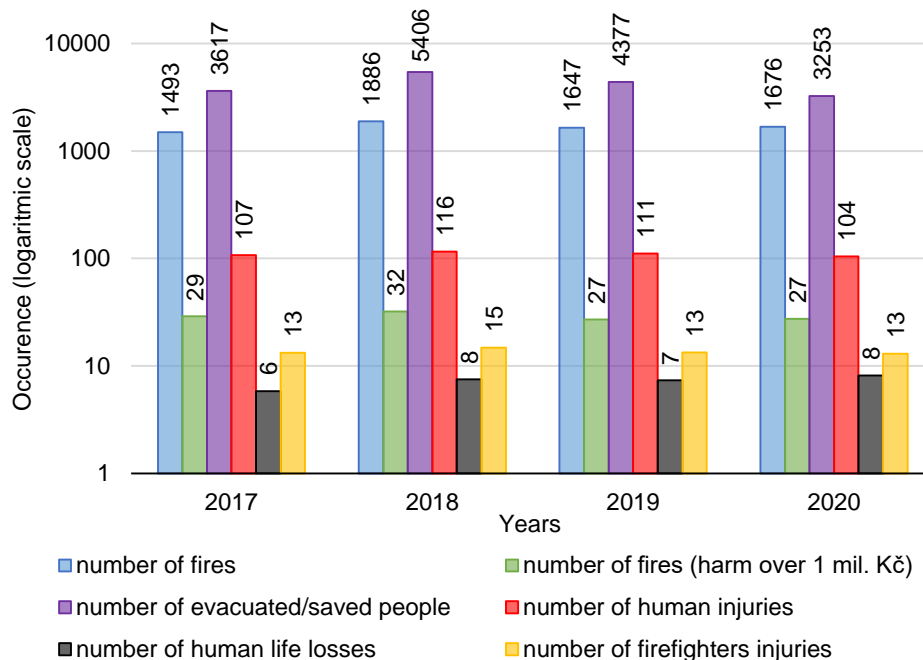
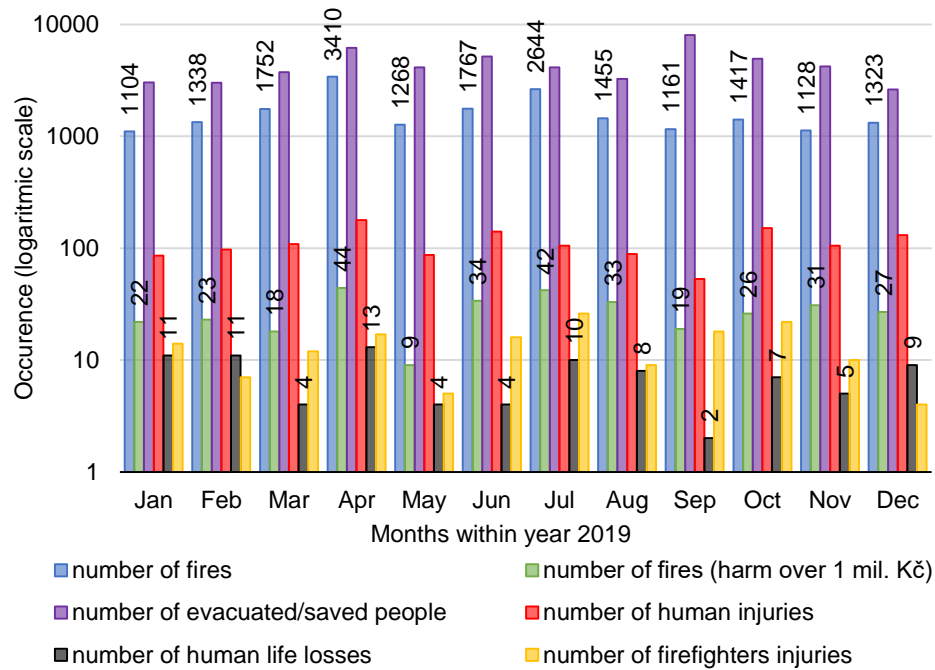


Fig. 1-2. Official Czech fire brigade statistics per one month (average) over last 4 years [6].

<sup>2</sup> All fire accidents are counted together (in buildings, car accidents, agricultural on fields, in forests, etc.), however it can be assumed fires in buildings represent the majority.

<sup>3</sup> According to the long-term exchange rate 1 million Czech crowns (Kč) is approximately equal to €40 000.



*Fig. 1-3. Official Czech fire brigade statistics during year 2019 [6].*

It is interesting to mention that in Czech Republic not reporting fire to fire brigade by a witness is considered to be a civil offense and can be punished by high fines. When speaking about most usual causes of fire start (only fires in buildings are considered), from the fire brigade statistics it seems reasons in the following list are mentioned most often:

- Technical malfunctions of machines and electrical devices, especially electrical wiring.
- Human inattention and carelessness including smoking.
- Manipulation with fire and hot ash.
- Gross errors in building construction – typically timber elements too close or even inside chimneys.
- Intended set of fire.

### Fire Events & Structures

From the structural point of view fires in buildings always represented big threat. In times when the most popular building material was timber and the structures were primarily made of it, it was quite often the buildings and even all villages or towns burned out completely (e.g. Great Fire of London [7]). It was either due to combustible nature of wood (structure itself is fuel to burn) and also due to completely missing fire safety regulations. The situation got partially better when structures started to be made of masonry which is generally incombustible material (stone or ceramic bricks), however timber elements were still commonly used, mainly in ceilings and roofs. In modern age the most popular structural material became steel and concrete – both of mentioned materials are incombustible as well. Fire resistance of concrete structures often showed to be sufficient with no additional care, however steel structures exhibit poor fire resistance from the beginning of material's use and therefore have to be enhanced somehow. Using timber is still typical for certain types of structures (roofs) and in Czech Republic structures completely made of timber are getting popular again in last decades, whereas e.g. in North America they never lost their popularity. However, use of timber in bigger and higher structures is limited according to fire regulations nowadays. For example, in Czech Republic a building with timber load-bearing structure can be maximally 12 m high [8]. Fire resistance of timber structures is usually not bad, but due to the combustible nature it is limited and thus has to be every time carefully verified.





Fire resistance of structures made of all mentioned materials has been intensively studied during (mainly) second half of 20<sup>th</sup> century and in that time comprehensive database of both structural and material behaviour have been created in means of observing real fires, conducting fire experiments and analytical and later also numerical calculations. Thanks to it, firstly empirical and later on also performance-based methods of fire resistance assessment have been developed for different kinds of materials and structural elements. More complicated issues are being intensively studied thanks to broad possibilities of numerical modelling and computer-aided designs. Using this knowledge, the structures can and should be designed appropriately in order to ensure sufficient fire resistance.

It can be stated that in case of “traditional” and ordinary structures, the general processes causing structural performance to decrease are revealed and described relatively well, and therefore the level of structural safety will probably be high enough. However, at the very same time it must be said there are some situations when extra attention has to be paid. During last decades civil and structural engineering have gone through enormous development. New materials were introduced and the old ones have been enhanced as much as possible. During the process of structural design, it is absolutely common structural engineers use computation and design software and also advanced drawing and modelling software. As a result of this all the materials are now stronger, but more brittle and thus the structures are less ductile. The cross-sections are smaller with higher ratio of acting load-to-bearing capacity. The elements are slenderer and thus more prone to excessive deflections and second-order forces. Structural systems are less regular with longer spans. In the calculations the positive spatial effect is often included directly. Thanks to development of construction processes the structures have irregular skew and variable shapes. Many of mentioned aspects make estimating fire resistance more challenging.

Generally, when structures are exposed to the effect of fire and consequent high temperatures, they suffer and their structural performance decrease, either gradually or rapidly after partial or overall collapses. The risk of structural collapse induced by fire is valid for all kinds of structures, including concrete, steel, timber and masonry ones, as well as family and apartment houses, office and public buildings. Even more pronounced risk is connected to industrial halls (due to nature of their use) and high-rise buildings and especially skyscrapers (due to more complicated and loaded structural systems and limited options of fire brigade intervention).

Overview of buildings from all over the world which went through fire situation with short description can be seen e.g. in [9]. Several cases from the list were chosen to be mentioned separately:

- Fire of *Windsor Tower*, Madrid is shown in Fig. 1-4. The skyscraper caught on fire in 2005 during general refurbishment and burned out completely. Structure suffered partial progressive collapse when not yet fire-protected steel façade columns buckled and lost their bearing capacity (ensuring their fire protection was one of the refurbishment goals). The progressive collapse was stopped by very rigid transition floor (thick concrete slabs supported by deep beams). After detailed assessment local authorities decided the structure to be demolished. More about the post-fire inspection can be found in [10].
- Fire of *Grenfell Tower*, London is shown in Fig. 1-5. The high-rise apartment building caught on fire in 2017 and burned for nearly 60 hours. The concrete structural system consisting of precast floor and wall panels did not collapse even after the extreme fire duration thanks to its rigidity. Unfortunately, many habitants died inside the house mainly due to poor fire safety regulations and very limited possibilities of escape and fire brigade intervention. Several years after the incident the building is still out of use completely and very probably will be pulled down. More about the fire situation can be found e.g. in [3].



- Partially collapsed *Hengzhou building*, Hengyang China is shown in Fig. 1-6. The apartment building caught on fire in 2003 and lasted for about 3 hours. According to the post-fire inspection nearly half of structural elements in ground floor were exposed to temperatures above 800 °C and several elements even to 1300 °C. According to the findings and numerical simulation the progressive collapse was triggered by collapse of two interior columns. As a result, adjacent girders were overloaded and collapsed as well inducing collapse of precast floor panels. During the fire brigade intervention number of firefighters died inside the house. The post-fire process is described in detail in [11].
- Collapsed *Plasco building*, Tehran Iran is shown in Fig. 1-7. The former tallest building in Iran caught on fire in 2017. During firefighting whole north outer wall lost stability and collapsed, inducing collapse of the rest of the building. More about the case can be found in [12].
- Burning *Torch skyscraper*, Dubai is shown in Fig. 1-8. Former tallest apartment building in the world caught on fire even twice, in 2015 and 2017. In both cases firefighters managed to get the fire under control and thus the structure was damaged only marginally. After minor repairs the building is in use again.



*Fig. 1-4. Windsor Tower fire, Madrid 2005 [10].*





*Fig. 1-5. Grenfell Tower fire, London 2017 [3].*



*Fig. 1-6. Partial fire-induced collapse of Hengzhou building, China 2003 [13].*





*Fig. 1-7. Fire-induced collapse of Plasco building, Tehran 2017 [12].*



*Fig. 1-8. Fire of Torch skyscraper, Dubai 2015[14].*



Graphical overview of typical fire event process can be seen in Fig. 1-9. If the load-bearing capacity of structure subjected to fire is high enough, its structural system is robust and/or the structural elements are fire-protected, the structure withstands the event – which is a start of the post-fire assessment.

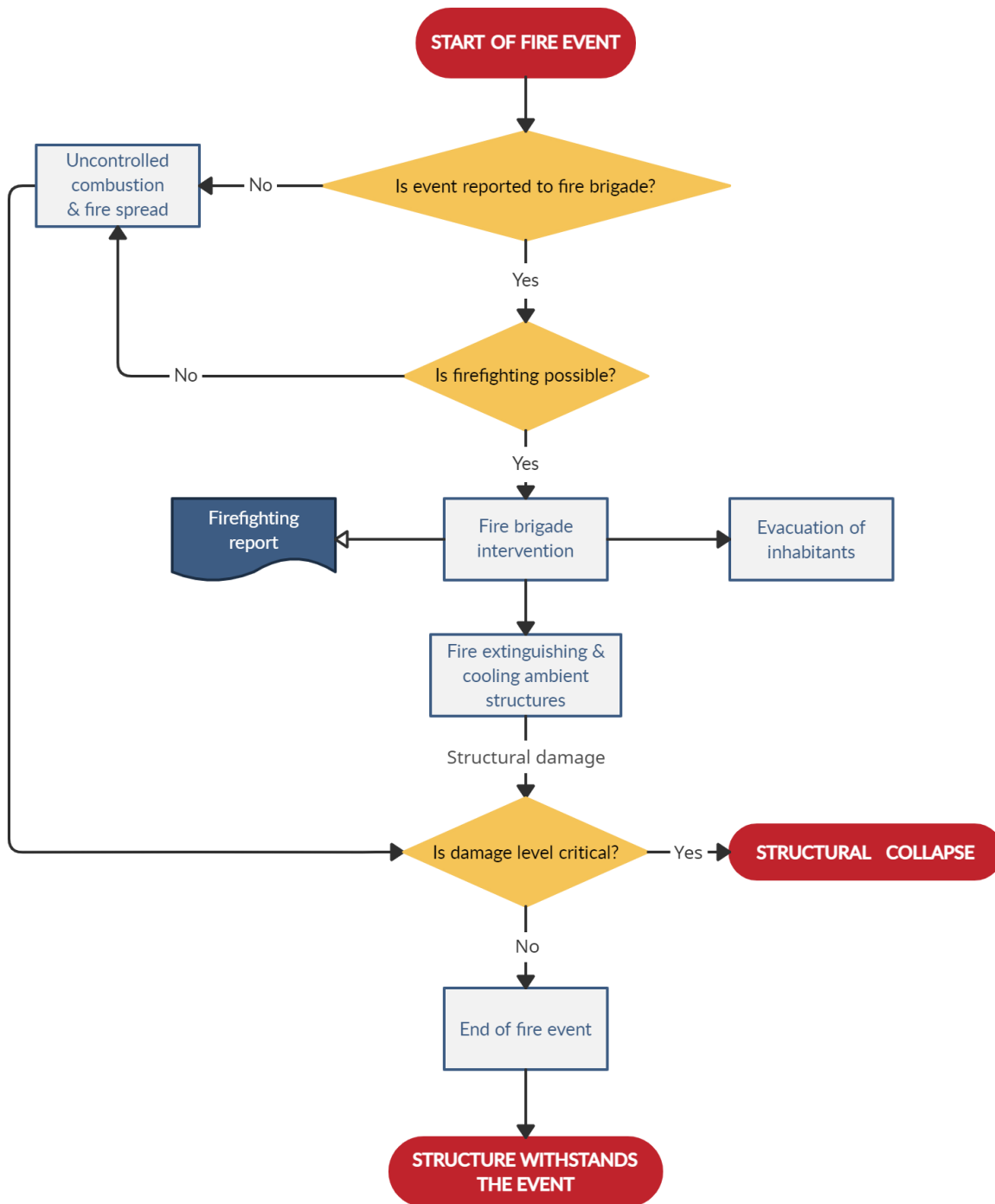


Fig. 1-9. Flowchart of typical fire event.



## 1.2 Motivation and Outline of the Thesis

During second half of 20<sup>th</sup> century civil and structural engineering have gone through enormous development making erecting remarkable buildings possible often moving the limit line of possibilities further. Fire safety engineering have made huge leap as well, especially during last decades in the means of active and passive measures. However, despite the risk of fire start is minimalised thanks to the fire safety engineering measures, it is not completely mitigated – and it seems it is even not possible. Due to it fire situations will happen inevitably in the future, as it is demonstrated by the examples above from recent past. And in every single case the post-fire assessment had to be done in order to set the future of burned-out building and ensure public safety.

The topic of post-fire investigation and assessment is very complex and gets even more challenging in case of modern complicated structural systems and usage of brand-new high-strength or composite materials. The empirical experience from the past tend not to be relevant enough in case of modern and progressive buildings. It is then fair to say the mentioned changes in civil, structural and material engineering are happening so fast that the development of fire safety assessments is often one step behind.

With respect to the difficulties mentioned above on one hand and occurrence of real situations when findings of post-fire structural assessment are the only way to make a decision about future of burned-out building, and also the fact concrete is the most popular building material of last decades, the analysis of concrete structures after fire is considered to be very actual topic according to author's opinion that is worth to study in detail and which has big potential of contribution to engineering practise. General goal of the Thesis is to provide complex methodology of whole process of post-fire structural assessment and making it organised, clear and easy-to-read, since there has been lack of such document in national and even European codes of practise. Attention is dedicated to both theoretical and practical findings. It is also important to mention the Thesis is focused on most common reinforced concrete structures (not pre-stressed) made of normal-strength concrete ( $f_{ck} \leq 50 \text{ MPa}$ ) of building construction (not bridges and other engineering construction).

In the forthcoming chapters following topics are discussed:

- In [Chapter 2](#) theoretical overview of material properties of both concrete and reinforcement steel is given with respect to the state during fire and after its end.
- In [Chapters 3-5](#) the initial steps of post-fire investigation together with recommended approach of preliminary and detailed inspections are given.
- [Chapter 6](#) is dedicated to post-fire structural diagnosis discussing most suitable testing methods for concrete structures with special attention to specific damage caused by fire.
- [Chapter 7](#) deals with global structural effects of fire and possible irreversible changes in structural scheme.
- In [Chapter 8](#) methods of structural assessment of residual load-bearing capacity are discussed.
- Final discussion with recommendations for future work are given in [Chapter 9](#).
- In [Annex 1](#) several examples of complete post-fire assessment are worked out.

[Chapter 2](#) consists of comprehensive state-of-art of published codes, bulletins and scientific papers. In other chapters all information, findings and figures or diagrams taken over from literature are properly cited. Statements, findings, figures or diagrams which are not cited are either commonly known and accepted or they are made on author's own.





## 2 Properties of Concrete and Reinforcement Subjected to Fire (state-of-art)

Earlier it was described that concrete structures have been very popular for almost 100 years already and concrete can be found in nearly every building. Due to such wide use an attention to all design aspects has to be paid very carefully. When speaking about fire situations in concrete buildings, fire resistance of such structures is relatively good with no special treatment or protection, especially when compared to other structural materials. The reason for such performance lies in the nature of concrete structures. Concrete is incombustible material, common concrete elements are rather massive and the thermal properties of concrete are beneficial. Moreover, the thermal conductivity is relatively low and specific heat capacity high (see [Tab. 2-2](#) in [Chapter 2.1](#)). Thus it takes some time before the cross-section is significantly heated and the mechanical parameters deteriorate. Thanks to these features the fire resistance of 60 minutes can be usually achieved without any special treatment or fire protection, assuming the concrete members are correctly designed at ambient temperature and have common load-bearing capacity reserve.

When speaking about steel structures their performance at fire conditions are contrary to concrete structures. Steel is incombustible material as well, but steel structures are light and slender, thermal conductivity of steel is very high and specific heat capacity low (see [Tab. 2-2](#) in [Chapter 2.1](#)). Due to these properties steel members without any protection are heated very quickly which cause rapid deterioration of mechanical properties from certain temperatures, thus reduction of load-bearing capacity and many times even structural collapse. Steel structures without fire protection can usually withstand fire duration up to 15 minutes, but for longer fire durations the fire protection is necessary. Nowadays these types of fire protection are used:

- intumescent coating,
- protective injection,
- protective cladding made of thermal insulation or plasterboards,
- casting in concrete or mortar,
- etc.

When speaking about timber structures, their main disadvantage is that wood is a combustible material. Thus during fire, the cross-sections are getting smaller which leads to reduction of load-bearing capacity and structural collapse in some cases. However, the wood in core of timber elements remains almost undamaged and therefore capable of carrying loads. Modern timber structures often use wood-steel joints which represent problem during fire. Steel bolts, plates and screws are then the weak part which reduces the fire resistance of whole structure. Timber structures can usually withstand fire up to 15-30 minutes with no additional fire protection.

Masonry structures usually do not have a problem with fire resistance, which is mainly a result of their production process. Bricks made of ceramics, aerated concrete or combination of sand and lime are produced at high temperatures, so they are very thermal stable; concrete bricks have the same properties as described above.

Although structures made of concrete exhibit good fire resistance in general, when exposed to fire and high temperatures for longer time the material and whole structure suffer from deterioration of mechanical properties, explosive spalling and decay of load-bearing capacity. The severest fires can end with structural collapse as well. High temperatures affect also the serviceability of the structure – typically growth of deflections and curvature can be seen. Also thermal strains induced by elevated temperatures can affect the behaviour of structure, as members tend to elongate and curve due to thermal expansion.



In the following chapters the effects of elevated temperatures on concrete and reinforcement steel will be described in detail. An attention will be paid on mechanical and thermal properties of both materials at hot state during fire and residual properties after fire, phenomena of explosive spalling, thermal strains, stress-strain diagrams and finally the difficulties of testing of concrete samples subjected to elevated temperatures. An overview of main influences and changes in concrete caused by fire can be seen in Fig. 2-1. Whereas all mentioned influences take place during every fire situation and are caused directly by high temperatures, chemical corrosion is not caused directly by high temperatures, but it is dependent on the nature of things which are on fire. Aggressive and poisonous substances might be released from burning plastics, petrol, oil, etc. Such substances can essentially damage concrete matrix, its constituents or simply accelerate the degradation process. An example of such substances are chlorides.

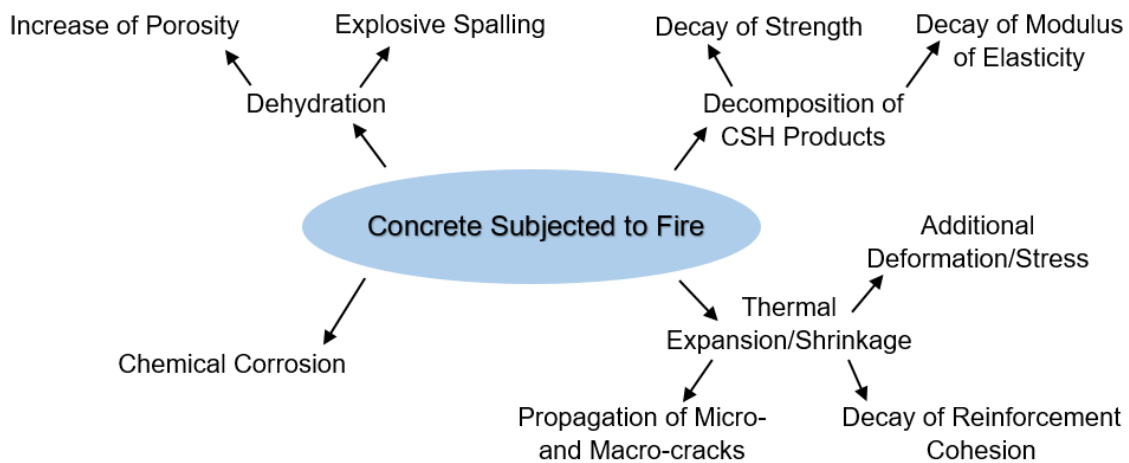


Fig. 2-1. Overview of changes in concrete exposed to fire.

## 2.1 Mechanical and Thermal Properties of Concrete at Elevated Temperatures

### 2.1.1 Mechanical Properties

When concrete is exposed to high temperatures during fire situation many physical and chemical processes take place in the concrete matrix. Most of the changes are irreversible and they are influenced by moisture content of the matrix, thermal properties of used aggregate, heating rate and stress state of given structural member. High temperatures gradually induce dehydration of the matrix, volumetric changes of individual constituents and decomposition of the hydration products. Overview of the main changes can be seen in Tab. 2-1.

Tab. 2-1. Overview of physical and chemical changes in concrete at increasing temperatures [15].

Temperature [°C]	Description of changes
20-200	Secondary hydration of not so far hydrated cement grains takes place. Slight increase of compressive strength might be observed (as pore pressure rise, the process is similar to autoclaving).
100+	Evaporation of free water accelerates.
80-850	Gradual loss of chemically bound water. Decomposition of compounds containing water.
150	First stage of decomposition of calcium silicate hydrate (CSH) culminates.
300+	Disintegration of CSH and $\text{Ca}(\text{OH})_2$ continues. Aggregate starts to be damaged. Incompatibility of volumetric changes between aggregate and cement paste causes creation and propagation of micro-cracks in concrete matrix. <b>First significant decay of compressive strength (~15 %).</b>





374	Critical point of water. Above this temperature water cannot exist in liquid state no matter of its pressure and volume. All free water is evaporated from the matrix.
400-600	Ca(OH) <sub>2</sub> dissociates into CaO and H <sub>2</sub> O. Thermal incompatibility of aggregate and cement paste is significant, so is matrix porosity. <b>All together cause major decay of compressive strength (~40 %). Concrete heated up to 600 °C and more is considered not to contribute to load-bearing capacity.</b>
573	Crystalline grid of quartz (which is a part of sand or siliceous aggregate) changes from α-phase to β-phase. This is connected to another volumetric expansion. Compactness of the matrix is thus more damaged.
700+	Decomposition of Ca(CO) <sub>3</sub> in cement paste and carbonate aggregate into CaO and CO <sub>2</sub> . Second stage of CSH decomposition culminates.
800	Hydraulic bindings created during initial hydration are being replaced by ceramic bindings.
1000+	Individual components of the concrete matrix start to melt.

From the table mentioned above it is clear that when concrete is heated up to 200 °C its strength does not suffer. No or very limited damage happens in the matrix due to the aggregate. With temperature arising, there are two important temperature ranges which are worth to point out. The first is a temperature around 300 °C where first notable compressive strength decay can be observed and which is equal approximately to 15 %. The second range lies in between 500-600 °C and the compressive strength decay is expected to be about 40 %. Concrete heated over 600 °C is then assumed to be damaged to the extent its load-bearing contribution is minimal and thus neglected.

Based on the amount of test results from scientists all over the world a unified approach how to express the strength decay was implemented into the Eurocode 2. Simple equations were introduced (Eq. (2-1, 2-2)), where reduction coefficient  $k_c(\theta)$  and  $k_{c,t}(\theta)$  describes the strength decay which is related right to the hot state of concrete. The coefficients dependent on temperature are plotted in Figs. 2-2 and Fig. 2-3.

- equation for compressive strength decay  $f_{ck}(\theta) = k_c(\theta) * f_{ck,20}$  (2-1)

- equation for tensile strength decay  $f_{ct,t}(\theta) = k_{ct}(\theta) * f_{ctk,20}$  (2-2)

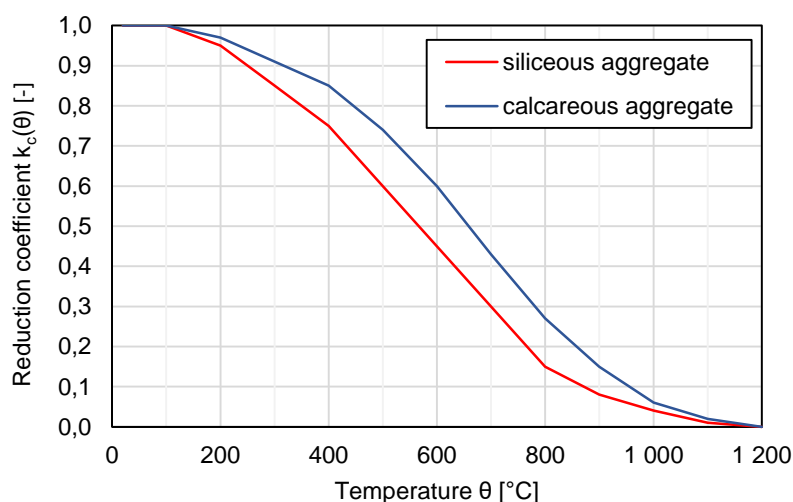


Fig. 2-2. Reduction coefficient of compressive strength according to EC2 [16].



It is known that tensile strength of concrete is very sensitive to high temperatures and decreases rapidly from relatively low temperatures. EC2 suggests linear reduction of tensile strength from 100 °C to 600 °C where tensile strength is expected to be equal to zero. As a result, bending stiffness decreases, flexural cracks create at lower loading and propagate more. Deflections of flexural members increases. Also anchorage of tensile reinforcement suffers and the bond strength decreases as the cohesive forces between steel rods and concrete are dependent on tensile strength of concrete.

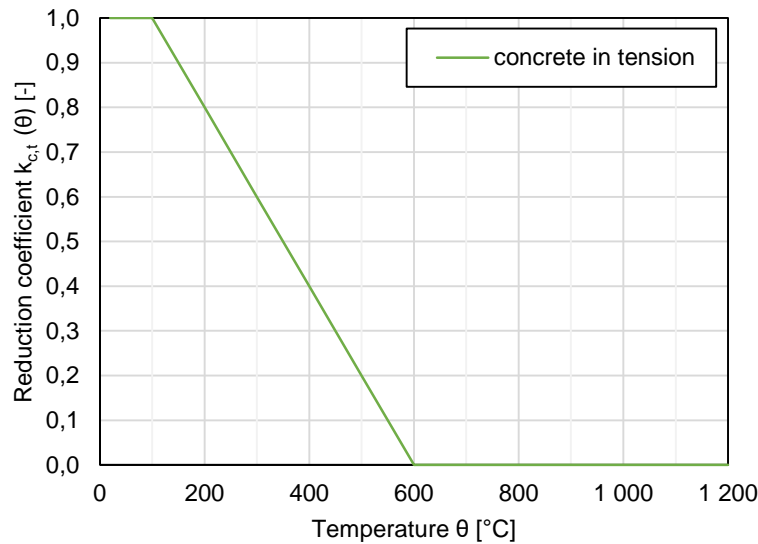


Fig. 2-3. Reduction coefficient of tensile strength according to EC2 [16].

It is worth to mention that EC2 distinguishes the reduction of compressive strength according to aggregate used in the mixture. The idea is based on different thermal stability of siliceous and calcareous aggregate which influence the strength decay. This will be discussed in detail later on in this chapter.

Another interesting thing is that American design code ACI 216.1 [17] also provides diagrams of compressive strength deterioration, but unlike EC2 it distinguishes not only the type of used aggregate, but also whether the concrete is right at hot state or whether it is residual strength. Moreover, there are two curves representing concrete with no compressive stress applied and concrete under compression at a certain level with respect to ultimate strength. This idea is based on the thermal strains mechanism, respectively the difference between free thermal strains and transient thermal strains of a member under compression. This topic will be described in detail in Chapter 2.5. Mentioned diagrams can be seen in Fig. 2-4.

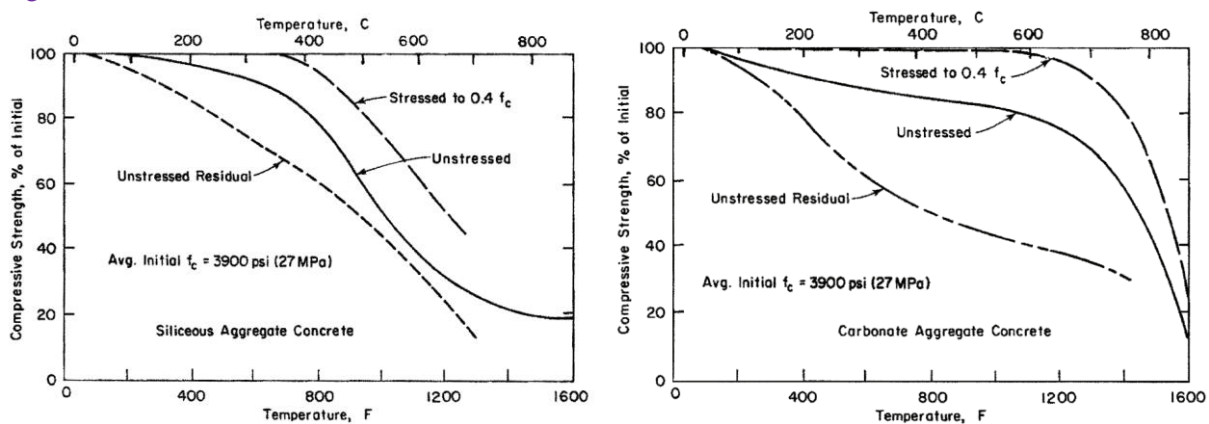


Fig. 2-4. Diagrams of compressive strength reduction according to ACI 216.1 (left: siliceous aggregate concrete, right: calcareous aggregate concrete), taken over [17].



Sensitivity of bond strength between reinforcement and concrete to high temperatures is in aim of growing scientific interest recent years. Many experimental studies have been conducted to prove the material deterioration influences not only the compressive and tensile strength and Young's modulus of concrete, but also the bond strength. The decay seems to be reasonable and not surprising conclusion as the bond strength depends on compressive and tensile strength of concrete directly. However, actual design codes (EC2 [16] and ACI [17]) do not provide any information nor recommendation about the appropriate reduction. Fib Model Code 2010 [18] suggests the reduction should follow the reduction trend of tensile strength at elevated temperature, which means reduction of 50 % when temperature is equal to 300 °C and even 90 % when temperature is equal to 500 °C. However, the reality might be a little bit more favourable. According to test results and test arrangement it seems the bond strength decay lies somewhere between reduction curves of compressive and tensile strength [19, 20]. The reduction diagram gained from series of test results can be seen in Fig. 2-5.

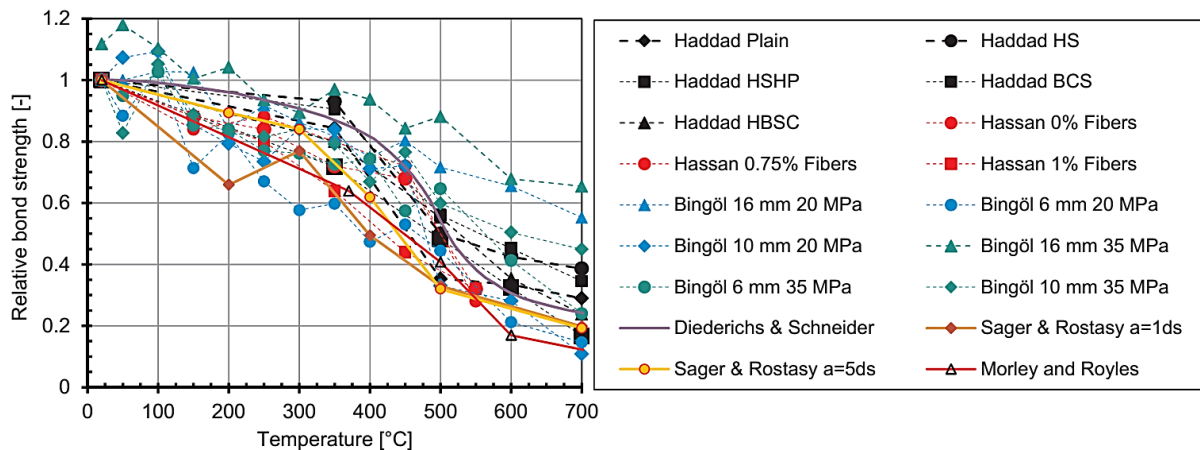
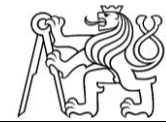


Fig. 2-5. Diagram of bond strength reduction according to experimental results, taken over from [19].

The last mechanical property to mention is the concrete's Young's modulus of elasticity. Its decay is induced by the very same reasons as why compressive and tensile strength decreases – it lies in the damaged microstructure and gradual decomposition of hydration products. When mechanical properties of concrete are compared, with increasing temperatures the fastest decay exhibits modulus of elasticity, then the tensile strength and the slowest decay exhibits compressive strength.

Experimental results, which have been published in literature and which focus on effect of high temperatures on Young's modulus, exhibit relatively large scatter. Test results are influenced by many boundary conditions, most of them are mentioned in Chapter 2.3. Main conditions influencing testing modulus of elasticity are:

- which type of modulus of elasticity is investigated (either initial tangent or secant),
  - if secant modulus of elasticity – which stress level is considered to cross the stress-strain curve;
- whether the test investigates *hot* or *residual* property;
- are specimens during heating subjected to compressive stress, if so to what extent;
- is the mechanical property investigated by ordinary static destructive test or non-destructively using ultrasonic pulse velocity test;
- what type of aggregate is used in the concrete mixture,
  - generally siliceous or calcareous,
  - what modulus of elasticity exhibit the aggregate – can vary greatly (from 10 GPa for sandstone up to 90 GPa for basalt [21]);
- what kind of heat treatment of specimens is proceeded.



According to the comprehensive state-of-art review in [22] the test results scatter can be graphically interpreted as can be seen in Fig. 2-6.

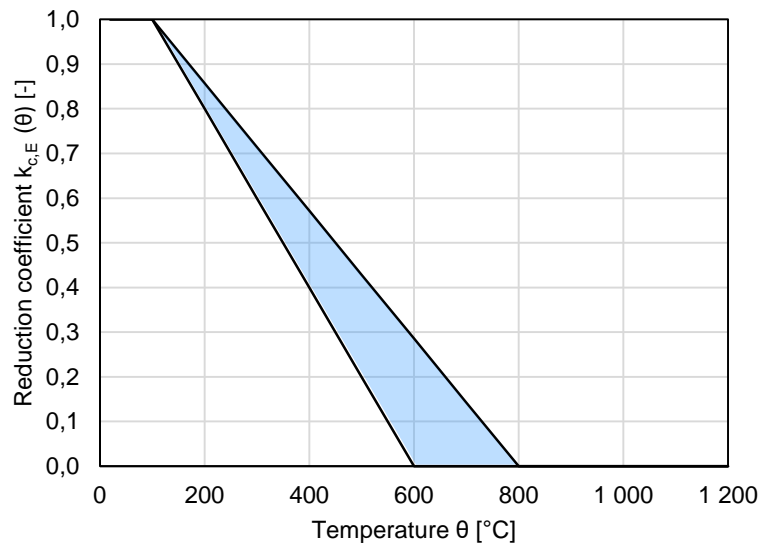


Fig. 2-6. Scatter of Young's modulus decay based on test results according to [22].

Based on the number of test result some authors carried out regression analysis and proposed analytical equations of Young's modulus' dependency on elevated temperatures. Visual interpretation of the equations can be seen in Fig. 2-7. Similar trend can be found among curves, however one has to keep in mind the results are rather informative and approximate than generically usable for design purposes.

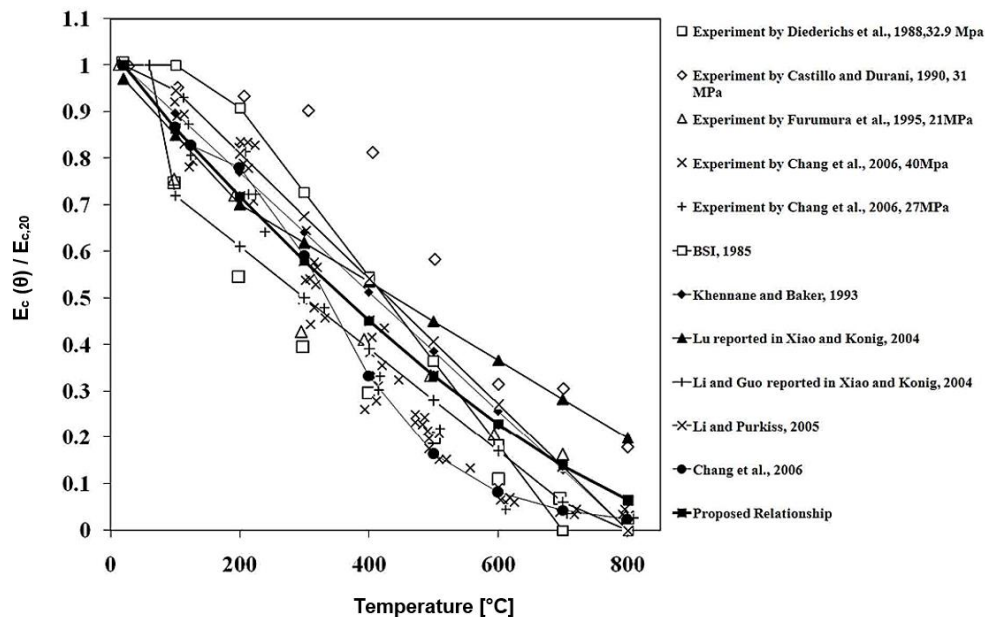
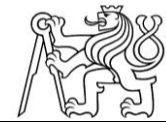


Fig. 2-7. Experimental results of Young's modulus decay at high temperatures, taken over from [23].

At ambient temperatures modulus of elasticity and its decay does not have direct impact on load-bearing capacity of flexural structural members, but it does influence their serviceability. In case of concrete typical example is the creep mechanism. Due to it deflections and curvatures of structural members grow with time. It is also together with crack propagation responsible for internal forces redistribution which indirectly influences also structural load-bearing performance. For slender walls and especially columns the decay of stiffness can highlight second order effect and buckling failure can



occur. When concrete structure is exposed to high temperatures due to material deterioration Young's modulus decreases. The higher the temperatures the more modulus of elasticity decreases. As a result, significant decay of stiffness takes places. Moreover, deflections and curvatures of elements grow considerably and flexural cracks propagate earlier and in larger extent. Redistribution of internal forces is strongly influenced by stiffness evolution along members and also values of additional temperature-induced inner forces are directly dependent on mutual stiffness's ratios, as will be discussed in detail in [Chapter 7](#). Therefore, correct estimation of Young's modulus decay seems to be crucial for calculating fire resistance and residual load-bearing capacity as well.



### 2.1.2 Thermal Properties

Thermal properties of concrete, which describes material response to elevated temperatures and enables conducting thermal analysis, are specific heat capacity and thermal conductivity. The properties are functions of temperature in general and their change is connected to loss of moisture from the matrix. Their definition is provided by EC2.

Specific heat capacity  $c_p$  describes how much energy is needed to warm one kilogram of material by one Kelvin. The diagram can be found in Fig. 2-8. It can be seen each curve is connected to certain moisture content of concrete. If the moisture content is not equal to zero, the peak lies in the range of 100-115 °C and is caused by change of free water state from liquid to gas. From 400 °C on it is assumed there is no free water left in the matrix and therefore the specific heat capacity is constant.

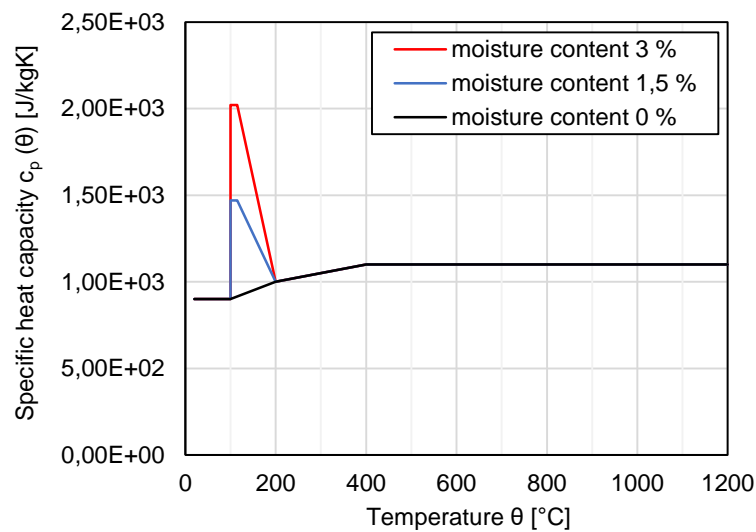


Fig. 2-8. Specific heat capacity of concrete according to EC2 [16].

Bulk density of concrete  $\rho_c$  is also dependent on moisture content of concrete matrix. As water from concrete evaporates (at first free water, later on chemically bounded water from decomposed compounds), the matrix becomes lighter. Increasing porosity is a result of evaporating moisture and propagating micro-cracks and it makes bulk density smaller as well. The decay of relative bulk density according to EC2 can be found in Fig. 2-9.

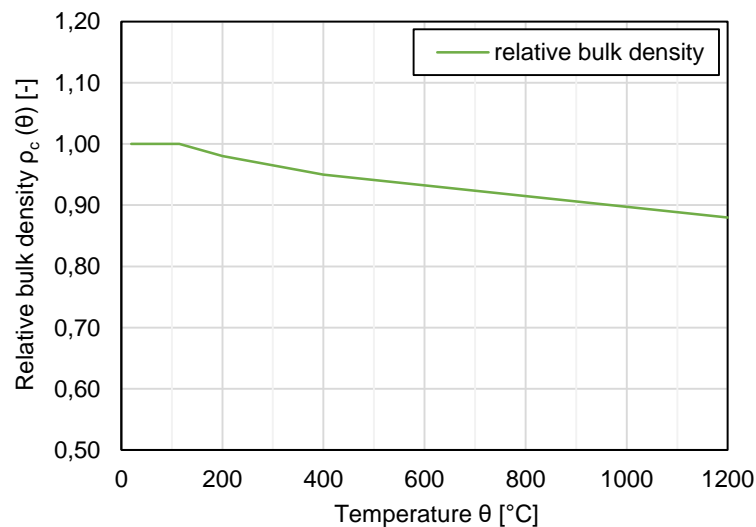
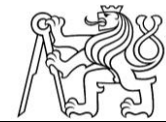


Fig. 2-9. Bulk density of concrete according to EC2 [16].



The second important thermal property of concrete is thermal conductivity  $\lambda_c$ . It describes how fast is heat from one part of material with higher temperature conducted to another part with lower temperature. The heat conduction runs naturally in direction of heat gradient as the system tends to balance itself. The definition of thermal conductivity says how much heat power is needed to rise temperature of material with dimensions of 1 m<sup>2</sup> in area and 1 m in thickness by one Kelvin. As moisture evaporates from concrete with rising temperatures air replaces free space in the matrix. Because air is better thermal insulator than water is, the thermal conductivity decreases with rising temperatures. EC2 suggests curves representing upper and lower limits. According to its instructions the upper limit was derived primarily for composite steel and concrete structures and so lower limit is suggested to be used for reinforced concrete structures. The diagram is shown in Fig. 2-10.

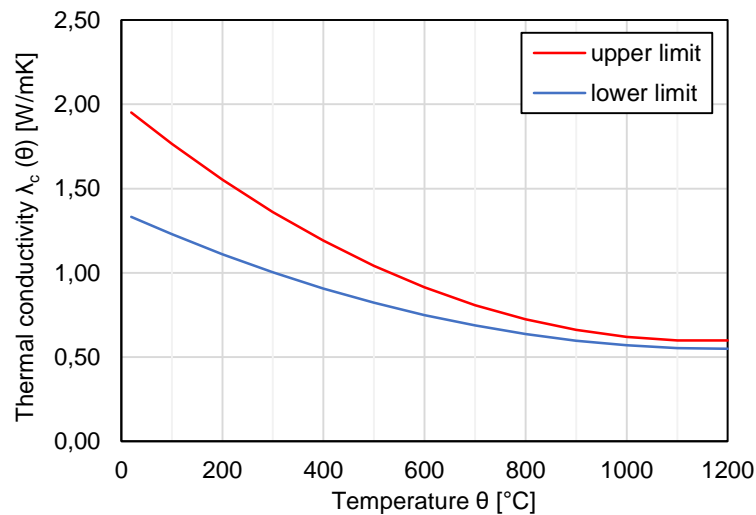


Fig. 2-10. Thermal conductivity of concrete according to EC2 [16].

EC2 also provides equations and chart to estimate thermal strains induced by high temperatures. Again it is distinguished whether siliceous or calcareous aggregate is used in concrete mixture. But it is necessary to mention that the suggested thermal strains are free strains which can be found on test specimens or parts of structure with no compressive stresses [24]. More about thermal strains can be found in Chapter 2.5.

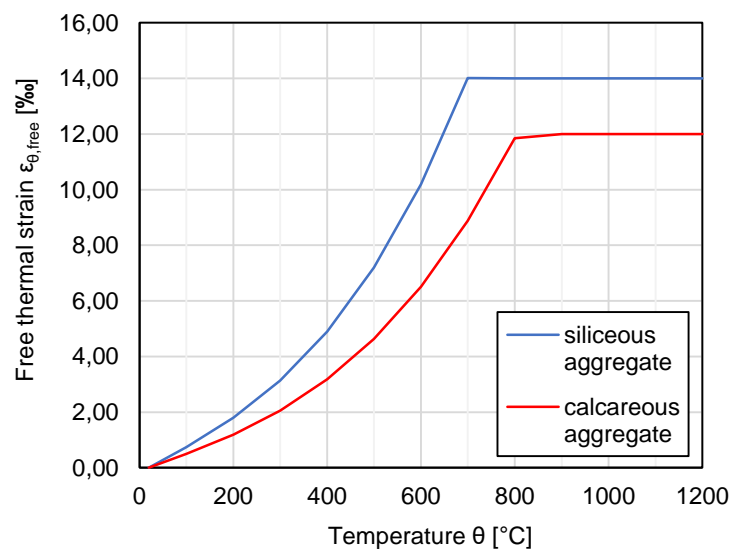


Fig. 2-11. Free thermal strain of concrete according to EC2 [16].





In general it is believed that coefficient of thermal expansion of concrete is equal to  $\alpha_c = 10 \cdot 10^{-6} K^{-1}$  which approximately agrees with the coefficient of thermal expansion of steel  $\alpha_s = 12 \cdot 10^{-6}$ . Both values are also suggested by Eurocode 1992-1-1 [25]. Although it is not said explicitly these values are valid only when speaking about common temperatures up to approximately 200 °C. If the basic equation of thermal elongation  $\Delta l/l_0$  (see Eq. (2-3)) is expressed with respect to coefficient of thermal expansion  $\alpha_c(\theta)$  (see Eq. (2-4)) the difference can be seen in Fig. 2-12. The value of  $\alpha_c(\theta)$  is getting bigger than the constant value after reaching 200 °C for siliceous aggregate concrete, where the curves cross. Whereas for calcareous aggregate concrete the curves cross at approximately 500 °C. Up to this temperature the  $\alpha_c(\theta)$  is lower than the constant value, then it is exceeded. As the temperature dependent coefficient of thermal expansion is derived from equations of free thermal strains, obviously  $\alpha_c(\theta)$  is related to thermal strains with no restraints as well.

$$\varepsilon_{th} = \frac{\Delta l}{l_0} = \alpha_c(\theta) * \Delta\theta \quad (2-3)$$

$$\alpha_c(\theta) = \frac{\varepsilon_{th}}{\Delta\theta} \quad (2-4)$$

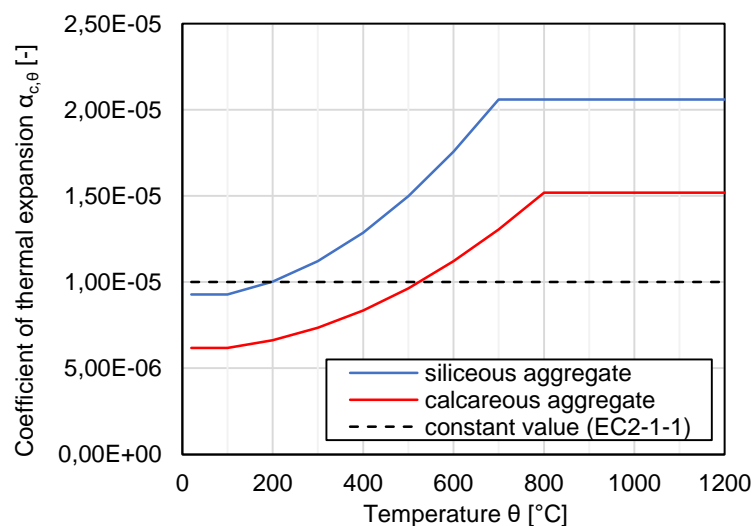


Fig. 2-12. Derived coefficient of thermal expansion of concrete.

To conclude with thermal properties of selected building materials are summed up in Tab. 2-2. Values are given primarily to see the major differences between individual materials and they correspond to the temperature 20 °C. From comparison of concrete and steel it can be stated the specific heat capacity of concrete is approximately twice as much as that of steel. Contrary, thermal conductivity of steel is about 50 times higher than that of concrete.

Tab. 2-2. Overview of thermal properties of building materials at 20 °C.

Material	Bulk density $\rho$ [kg/m <sup>3</sup> ]	Specific heat capacity $c$ [J/kgK]	Thermal conductivity $\lambda$ [W/mK]	Coefficient of thermal expansion $\alpha$ [1/K]
concrete	2300	900	1,3 - 1,9	$10 \cdot 10^{-6}$
steel	7850	440	50	$12 \cdot 10^{-6}$
aluminium	2700	870	204	$22,2 \cdot 10^{-6}$
ceramics	1400 - 1800	900	0,28 - 1,2	$5,5 \cdot 10^{-6}$
timber	450 - 700	2510	0,18 - 0,49	$5 \cdot 10^{-6}$
mineral wool	~ 40	800 - 1200	0,03 - 0,1	-





### 2.1.3 Effect of Aggregate Content

From previously written it is clear scientists as well as design codes distinguish the type of aggregate used in concrete mixture because of its crucial impact on damage mechanism of concrete exposed to elevated temperatures [26]. The most important property of aggregate is its thermal stability and coefficient of thermal expansion respectively. When concrete is being heated up, the cement paste tends to expand up to approximately 200 °C, but then it starts to shrink extensively. However, both natural and artificial aggregate expands in all temperature range. As a result, micro-cracks create in the concrete matrix because of the thermal incompatibility of its constituents. A screenshot of microscopic view on concrete matrix at ambient temperature and at 750 °C is shown in Fig. 2-13. It is evident the matrix of not heated concrete is dense and compact, whereas the one of heated concrete is weakened by cracks. The cracks creation and propagation is connected to strength and stiffness decay, as can be seen in Tab. 2-1.

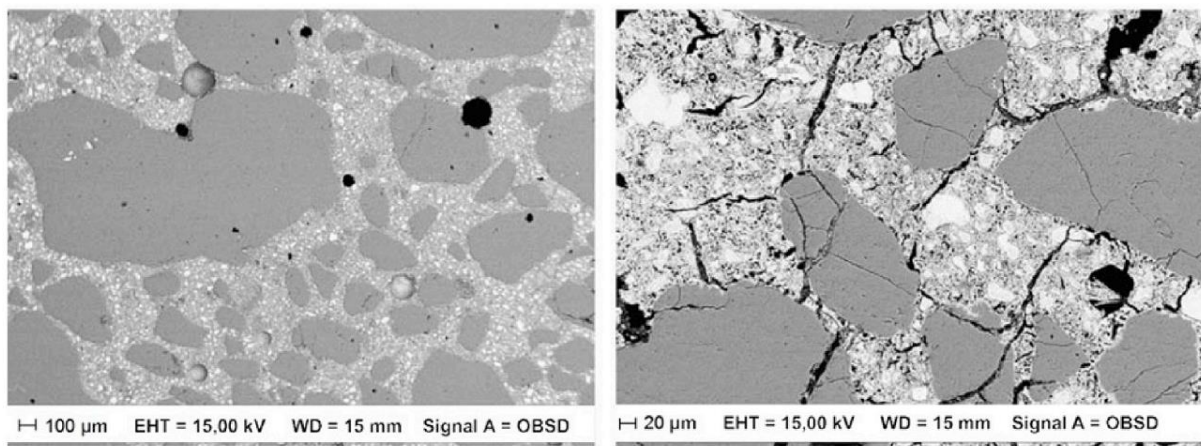


*Fig. 2-13. Microscopic images of concrete matrix at ambient temperature (left) and 750 °C (right) – taken over [27].*

There are several fundamental groups of aggregate which are being used in concrete production:

- siliceous aggregate (such as granite and sandstone – containing quartz),
- calcareous aggregate (such as limestone and dolomite),
- lightweight aggregate (artificially made of clay or slate),
- recycled aggregate (crushed old concrete, ceramic bricks, etc.).

Siliceous aggregate is known as thermal-sensitive which expands more than other types of aggregates when being heated up. Moreover, such aggregate contains quartz which expands even more greatly when temperature reaches 573 °C [28, 29, 30]. At this temperature a change of crystalline grid of quartz takes place (from  $\alpha$ -phase to  $\beta$ -phase). Contrary, calcareous aggregate is more thermal stable and therefore the difference between expansion of aggregate and shrinkage of cement stone is smaller [ref]. It is also connected to strength decay which tends to be slower (see Figs. 2-2 and 2-4). Another group of aggregate is the lightweight aggregate. Thanks to the nature of its production process which takes place under high temperatures the aggregate is very thermal stable and therefore its thermal expansion is much lower. Concrete with lightweight aggregate is not so common in engineering practice and EC2 does not provide instruction about its mechanical nor thermal properties so far (unlike ACI 216.1 which does provide them). New group of aggregate which is starting to be used in concrete production these days is the recycled aggregate gained mainly from crushed old concrete. This is happening due to environmental reasons and sustainable approach to building industry and because the world's supplies of quarries are getting smaller quickly. Thermal strains of different types of aggregate can be seen in Fig. 2-14.

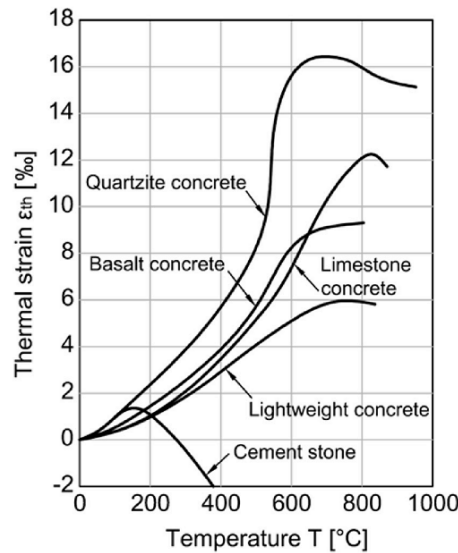


Fig. 2-14. Thermal strain of different types of aggregate – taken over [31].

A comprehensive overview of aggregate’s thermal stability and damage caused by high temperatures can be found in Fig. 2-15.

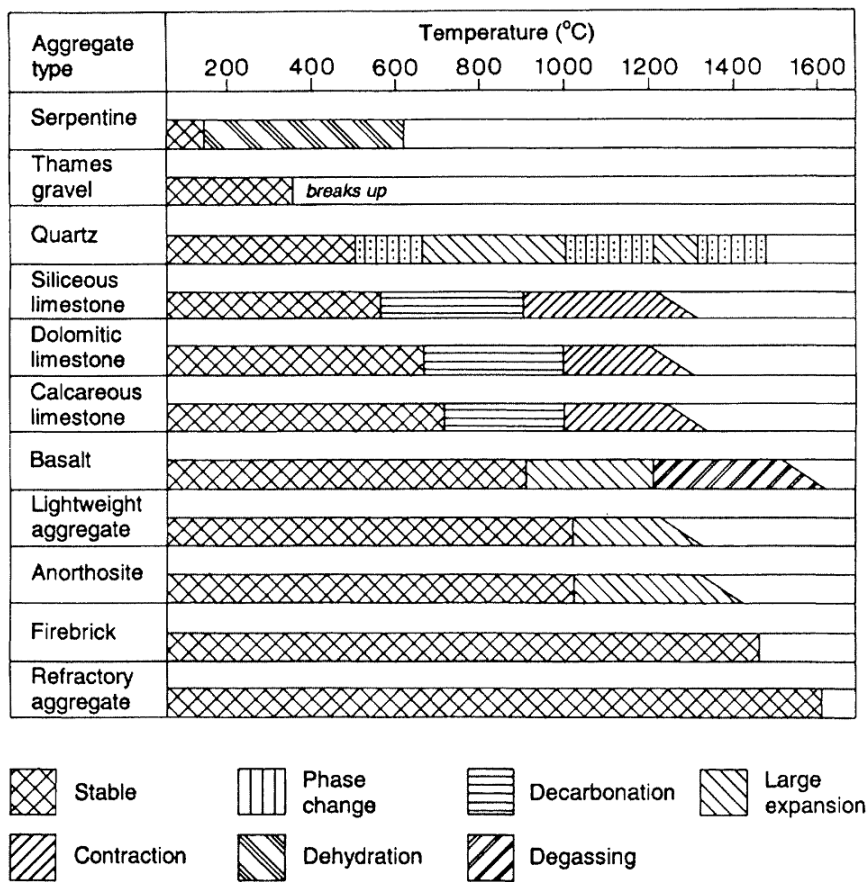


Fig. 2-15. Overview of aggregate types used in concrete production and their thermal stability, taken over [15].



#### 2.1.4 Effect of Moisture Content & Explosive Spalling

To start the process of hydration water has to be added to the concrete mixture. The optimal amount of water is given by the amount of cement and admixtures. The actual volume of added water is then expressed by so called water-cement ratio (ratio of weights) and usually it is equal to 0,4 – 0,6 and 0,25 – 0,4 for normal-strength concrete and high-strength concrete, respectively. If higher amount of water is added to the mixture, it is beneficial for fresh concrete workability, but contradictory for final strength of concrete, its shrinkage and creep. Lower strength and increasing creep are caused by evaporation of free water from the matrix and thus increasing porosity.

Higher water content also rises the risk of explosive spalling. Based on comprehensive research it is believed that spalling phenomena is caused by combination of these processes [32]:

- Growth of pore pressures as moisture evaporates from the matrix. Moisture migration is driven primarily in the direction of thermal gradient – it means towards the cold concrete core. In certain depth the pore system is filled completely with water – this is called the moisture clog in the literature [15]. From this moment pore pressure rises as the water is being compressed with another migrating molecules. So the pore pressure acts like internal load to the concrete matrix and if it rises above the tensile strength of concrete, a piece of concrete from surface layer spalls.
- Internal stress caused by thermal expansion. Surface concrete layers tend to expand which is restrained by ambient material, so the compressive stress develops. It is accompanied by transversal tension which if it is larger than concrete tensile strength cause spalling of pieces of concrete from surface layers.

The explosive spalling is then causing irreversible damage to the structure. The cross-sections are getting smaller, concrete cover of reinforcement is being damaged due to which reinforcement bars are exposed to high temperatures directly and thus losing strength quickly. Also reinforcement anchorage is being weakened as the part of interacting concrete is lost. All of this results in decrease of load-bearing capacity of structural element.

Structures exposed to severe fires with fast heating rate are extremely prone to the risk of explosive spalling, especially if the moisture content of concrete is high. Tunnel linings are an example of such structures. When designing such structures there is an effort to mitigate or even better totally eliminate the risk of spalling. This could be achieved by adding fibres to concrete mixture. Whereas steel fibres generally enhance mechanical properties of concrete and the tensile strength of concrete in particular, polypropylene (PP) fibres do not enhance the properties if not worsen them. But for a long time it is known it can help to mitigate the risk of explosive spalling [26]. The mechanism works on principle of reducing pore pressure. Because the melting temperature of PP fibres is relatively low (about 170 °C) once it is exceeded the fibres melt and therefore create additional space in concrete matrix where vapour can be release. Thereby the pore pressure decreases and the risk of spalling lowers.



## 2.2 Mechanical and Thermal Properties of Reinforcing Steel at Elevated Temperatures

Properties of reinforcement steel at elevated temperatures are dependent on the nature of production. Over the years, metallurgical processes have been developed in order to enhance the mechanical properties of steel. In case of reinforced concrete, the reinforcement is being produced either by hot-rolling or cold-working, moreover prestressing high-strength steel can be produced using quenching and tempering processes. Due to the nature of production process hot-rolled bars are the least sensitive to high temperatures, cold-worked reinforcement shows higher sensitivity, whereas prestressing steel is known for its significant thermal sensitivity and rapid deterioration when exposed to high temperatures [16].

EC2 introduces two classes of normal (not prestressing) reinforcement, class “N” and class “X”. Czech national annex recommends to work with class “N”, unless verified experimental data for class “X” are available [16]. The strength decay is expressed analogically to strength decay of concrete, using Eq. (2-5). Value of the reduction coefficient  $k_s(\theta)$  is given in Fig. 2-16.

$$f_{sy,k}(\theta) = k_s(\theta) * f_{yk,20} \quad (2-5)$$

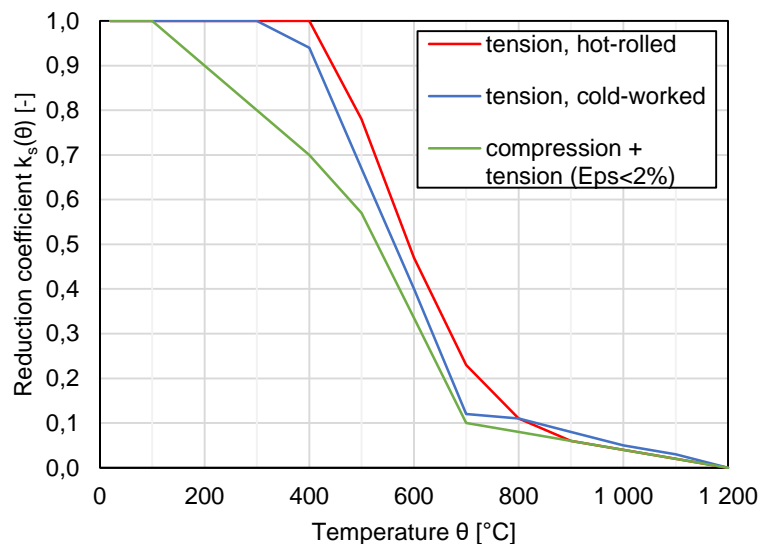


Fig. 2-16. Reduction coefficient of yield strength according to EC2 [16].

There can be seen the loss of yield strength of reinforcement steel is dependent not only on nature of steel production but also on reinforcement stress and strain. The hot-rolled steel bars in tension (red curve) keeps its initial tensile strength up to 400 °C which then decreases rapidly. Behaviour of cold-worked steel bars in tension (blue curve) is similar to hot-rolled steel, but the strength decay starts earlier about 300 °C, which corresponds to higher thermal sensitivity described in the previous paragraph. At the same time, it is assumed the strain of both types of steel is relatively high,  $\epsilon_s \geq 2\%$ , which is according to stress-strain diagram published in EC2 a value when stress in steel reaches a yield plateau. The green curve is related to reinforcement in compression and also tension when the yield plateau is not reached ( $\epsilon_s < 2\%$ ). It is also noted [28, 33] the marked yield plateau of hot-rolled steel clearly visible in stress-strain diagram at ambient temperature disappears when temperature reaches approximately 200-300 °C so the 0,2% proof stress has to be taken into account.

From above mentioned it is obvious that reinforcement does not suffer from exposure to elevated temperatures until it is heated to certain temperatures. Therefore, the concrete cover is that much important as it slows down heating of steel bars. Also because of this fact the explosive spalling is considered as a threat which may expose reinforcement directly to high temperature and thus cause



tremendous decay of load-bearing capacity. Tabular assessment given by EC2 and ACI is based on thickness of concrete cover as well.

The reduction diagram of steel tensile strength dependent on temperatures according to ACI 216.1 [17] can be seen in Fig. 2-17. The curves are similar to those suggested by EC2. The differences can be attributed to different experimental results database and different requirements for reinforcement steel production codes.

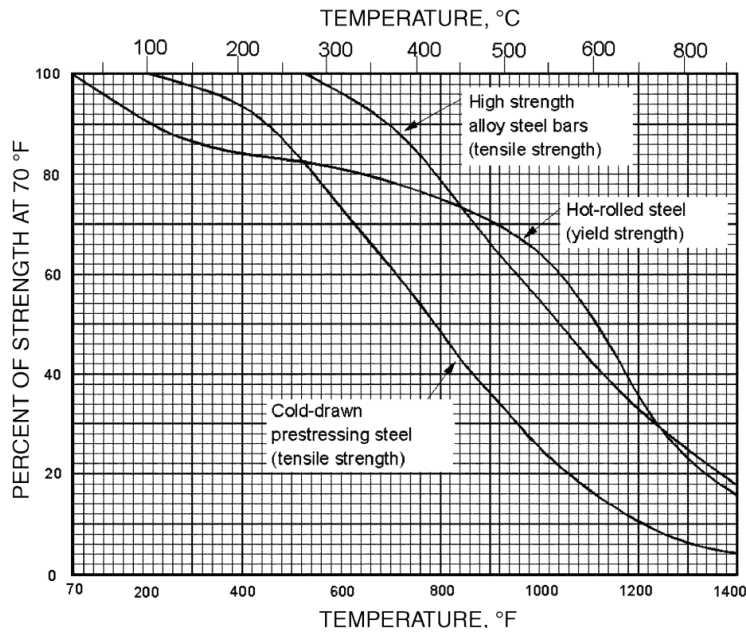


Fig. 2-17. Reduction diagram of tensile strength according to ACI 216.1, taken over [17].

High temperatures influence not only tensile strength of steel and its ductility (which grows with temperature, see stress-strain diagram in Chapter 2.1.2) but Young’s modulus of elasticity as well. In Fig. 2-16 it can be seen that yield strength of rebars in tension is reduced when temperatures reach 400 °C (300 °C respectively for cold-worked steel), up to these temperatures the initial yield strength is assumed to be fully preserved. The modulus of elasticity decay is then expressed using Eq. (2-6), where  $k_{s,E}$  is the reduction coefficient and it is a function of temperature. Its evolution with increasing temperatures can be seen in Fig. 2-18. Curves for hot-rolled and cold-worked steel are distinguished. From the diagram it can be stated the Young’s modulus decay starts right after reaching 100 °C. In case of hot-rolled steel the first branch of the curve up to 500 °C is less progressive, for higher temperatures the slope of the curve rises significantly. In case of cold-worked steel the drop is linear up to 700 °C and it is higher in whole temperature range, which corresponds with the assumption cold-worked steel is more sensitive to high temperatures.

$$E_s(\theta) = k_{s,E}(\theta) * E_{s,20} \quad (2-6)$$

The Young’s modulus decay does not influence directly load-bearing capacity, however similarly to concrete’s modulus of elasticity it effects serviceability of the structural member, its deflections and curvature and in general its stiffness, internal forces redistribution and in case of slender members also their sensitivity to buckling.



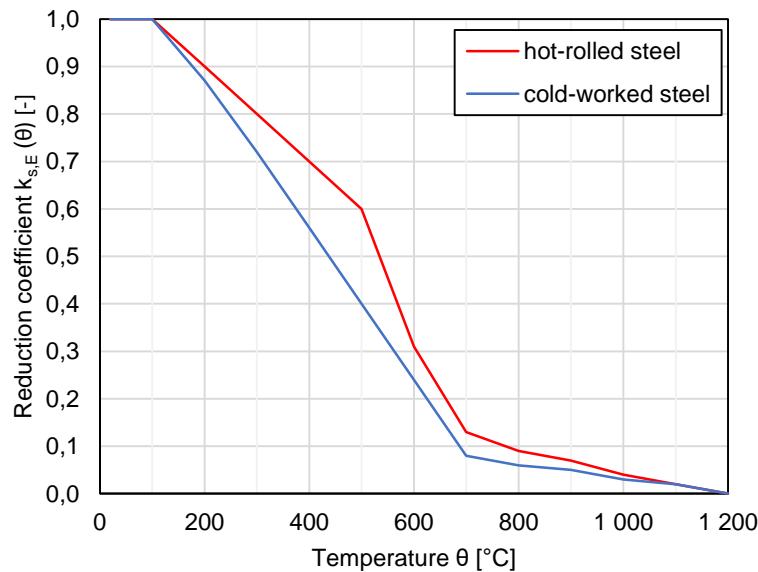
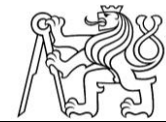


*Fig. 2-18. Reduction diagram of Young's modulus of reinforcing steel according to EC2 [16].*

Thermal properties of steel can be found in the overview in Tab. 2-2, but for conducting the thermal analysis of either cross-section or whole structural concrete element it is not necessary to use them directly. It is supposed that contribution of steel to the thermal field is minor [28]. Thus it is usually neglected to make the calculation simpler and so the cross-section is assumed to be made of concrete only. Reinforcement temperatures are then overtaken from the concrete temperatures at the very same positions in the cross-section.

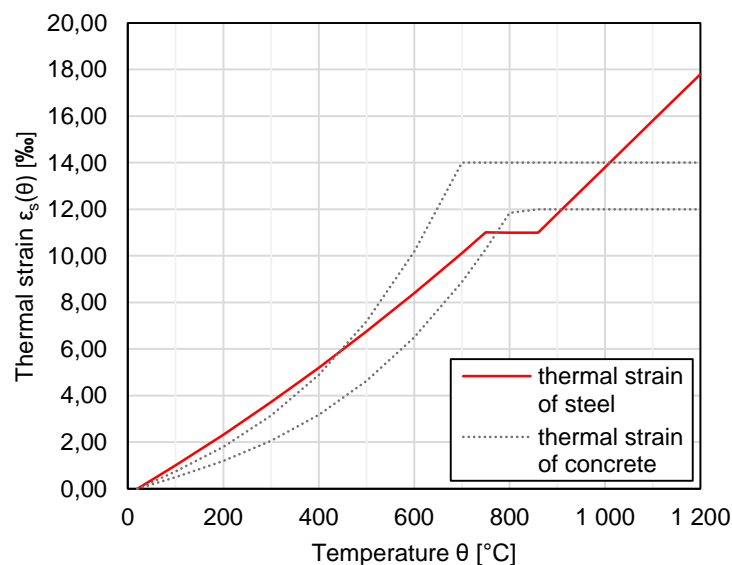


*Fig. 2-19. Free thermal strain of steel according to EC2 [16].*

The thermal property that is worth to mention is the thermal strain of steel depending on temperatures. The definition from EC2 is plotted in Fig. 2-19, where also free thermal strain curves of concrete are indicated. From the comparison it is clear the thermal strains of both materials are approximately equal at ambient temperatures ( $\alpha_c = \alpha_s \approx 10^{-5} K^{-1}$ ), but they do not correspond to each other at elevated temperatures. An equation (2-7)<sup>4</sup> can be written describing the induced stress

<sup>4</sup> The decay of elastic modulus  $E_c$  has been incorporated according to [23], concrete C25/30 is assumed.



between concrete and steel bars caused by thermal incompatibility. The induced bond stress is plotted in Fig. 2-20 and according to it the peak stress is induced around 500 °C for siliceous and calcareous aggregate concrete as well.

$$\Delta\sigma_{\theta} = \sigma_{c,\theta} - \sigma_{s,\theta} = \varepsilon_{c,\theta} * E_{c,\theta} - \varepsilon_{s,\theta} * E_{s,\theta} \quad (2-7)$$

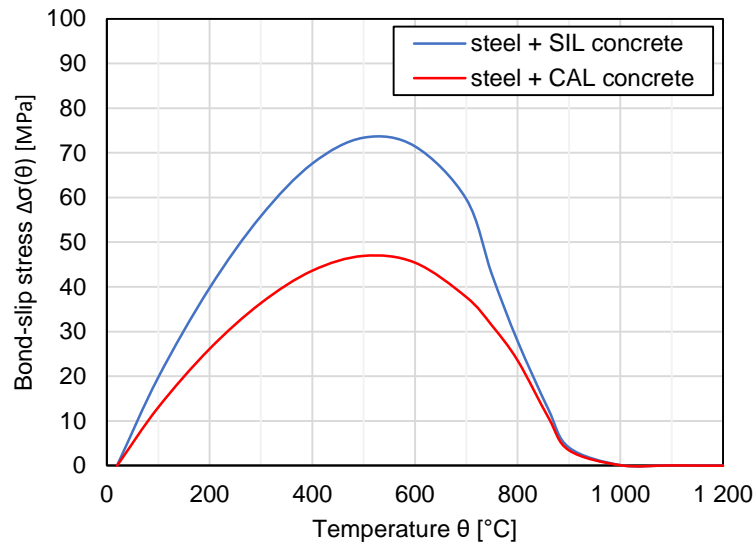


Fig. 2-20. Temperature induced bond stress between reinforcement and concrete.

### 2.3 Determination of Concrete Mechanical Properties at Elevated Temperatures by Laboratory Tests

Mechanical properties of concrete have been studied experimentally for many decades. Because the research lies on material level, it is principally conducted on specimens at laboratories. Since 1960s a comprehensive database of test results has been created. Based on the database design instructions were incorporated into design codes.

Such tests basically consist of a relatively small specimen made of concrete (usually without reinforcement bars, but it may contain fibres), which is heated. The heat treatment can be done in various ways [ref], but a special laboratory furnace is the most common one. The specimen is then tested to gain the compressive strength of concrete as it is the most important concrete material property. The compression test can be either destructive or non-destructive, but traditionally the destructive tests are considered as fundamental and non-destructive tests are considered only as additional and informational – therefore the destructive compression test will be discussed. More about testing methods can be found in Chapter 6. So the result of such test is the compressive strength of concrete damaged by high temperature. However, according to [26] it seems the results may be affected by various test arrangements to a considerable extent. Unfortunately unified test arrangement has not been adopted yet.

The main difference is whether the compression test is conducted on yet hot specimen or specimen cooled down to ambient temperature. Result from hot specimen represents compressive strength of concrete right at fire situation and may be used to calculate the fire resistance. On the other hand, result from specimen cooled down to ambient temperature represents residual compressive strength of concrete and may be used when calculating the residual load-bearing capacity. If both types of results are compared to each other, residual strength should be theoretically always lower than result at hot state according to [28, 34]. When the damage mechanism is repeated it sounds logical. Aggregate and cement paste expands and shrinks, respectively, when concrete is being heated up. As a result, the concrete matrix is damaged due to micro-cracks. After cooling to ambient temperature, aggregate shrinks back



to its initial volume, so the cracks in the matrix become even bigger. The matrix is therefore less compact and residual compressive strength lower. However, according to [26] it seems aforementioned may not be true in all range of temperatures. When moisture evaporates extensively from concrete matrix, migrating vapour causes rise of pore pressures. These together with stress from conventional external loads might reach ultimate compressive strength earlier than in case of residual strength. Because of nature of this mechanism it seems this might happen up to about 400 °C when moisture evaporation culminates. The second approach of testing is much more popular among scientists mainly because it is much less difficult to carry out. However, from the aforementioned it is clear test results from both options mean something different.

Another possible arrangement is whether the specimen is heated with or without any priory applied compressive stress. The difference is mainly a matter of thermal strains which are discussed in detail in Chapter 2.5. When a specimen is heated with no applied stress free thermal strains can propagate (as they are described in Chapter 2.1). As a result, the concrete matrix is significantly damaged due to micro-cracks caused by thermal incompatibility of aggregate and cement paste). However, when a compressive stress is applied to certain level of ultimate strength, thermal strain of concrete is considerably reduced [28], therefore the matrix is less damaged and the strength (either at hot state or residual) is higher. The arrangement with applied compression represents concrete strength of members with dominant axial compressive force, such as columns, walls and parts of slabs and beams that are in compression. Whereas the other arrangement represents concrete strength of members in tension or simply without prestressing force. Among researchers the approach without applied stress is more popular because of test difficulties. However, these two test options have to be distinguished carefully again. Comparison of residual compressive strength test results from different test arrangements can be seen in Fig. 2-21.

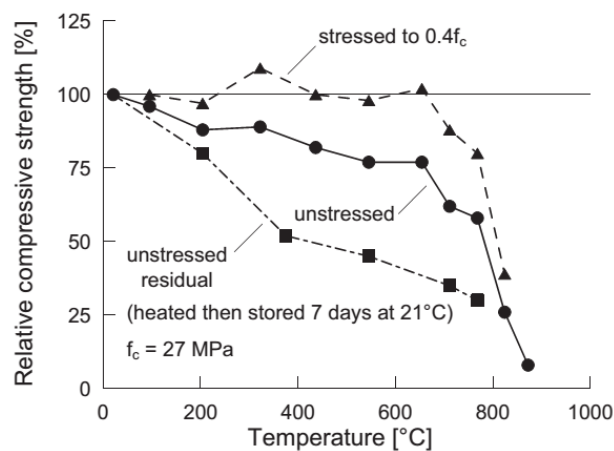


*Fig. 2-21. Comparison of relative compressive strength of concrete with calcareous aggregate according to test arrangement, taken over [28].*

To continue with, when testing the residual compressive strength, a type of specimens cooling regime after the end of heat treatment has to be distinguished carefully since it affects the results significantly. The most sensitive way to treat the specimens after heating is letting them to cool down back to ambient temperature naturally on air. As the concrete matrix is cooling down slowly, expanded volume of its constituents is gradually getting back to initial values and the matrix more probably accommodates the tensile stress induced by volumetric changes. Whereas when the specimens are cooled down rapidly in water, the volumetric changes happen faster and the matrix usually cannot withstand induced tensile stresses, which leads to another formation of tensile cracks. The matrix is then damaged additionally [28], therefore the residual strengths of such specimens are lower. The two types of cooling regime are ought to simulate real conditions of concrete structure after fire which can be





either let to cool down itself or can undergo the thermal shock by cold water from fire brigade intervention.

When conducting the specimen heat treatment, it is also important to think about the temperature distribution inside the specimen. The most common way is to set the length of heat treatment long enough to ensure uniform temperature in whole specimen, especially because then the test result can be attributed to a certain temperature. However, if the temperature differs inside the specimen, the test results interpretation is more complicated as it can only represent a mean value to a certain extent. This type of problems is typical when testing the real structure after fire. Ways how to work with such results can be found in [Chapter 6](#).

From the aforementioned it is obvious that testing specimens due to gaining mechanical properties of concrete either at hot state or cooled down state is very specific and it differs from regular testing of concrete. Therefore, it is necessary to distinguish all possible options of test arrangement because of different result meanings. General instructions to conducting such tests can be found e.g. in RILEM technical regulations.

To conclude with it is worth to mention that concrete strength decay suggested by EC2 is related to the hot state of material [16]. Moreover, it is assumed free thermal strains of concrete can propagate with no restraints and thus no beneficial compressive force is reducing the strength decay.

## 2.4 Residual Properties of Concrete and Reinforcing Steel after Exposure to Elevated Temperatures

### 2.4.1 Residual Properties of Concrete

It was already stated that mechanical properties of concrete affected by high temperatures have been studied for a long time already. Thanks to it a comprehensive database of test results was obtained. According to the most common test arrangement (see [Chapter 2.3](#)), most of the so far conducted tests was aimed at investigating residual properties of concrete (primarily the residual compressive strength) mainly because it is much easier for scientists to conduct such tests.

In the previous chapter the basic difference between properties at hot and residual state was described. The defined mechanism is dedicated to compressive strength decay, but it is very similar also when speaking about decay of tensile strength and modulus of elasticity, as the reason of decay of all mentioned mechanical properties is basically the same – deteriorated concrete matrix. During cooling period concrete matrix is additionally damaged due to volumetric changes of its constituents. Therefore, the residual mechanical properties are assumed to be always lower than properties at hot state. In [Chapter 2.3](#) it was mentioned that when conducting laboratory tests on hot specimens there is a range of temperatures up to approximately 400 °C when inner stress generated by moisture evaporation together with external load can cause earlier reaching of ultimate compressive strength than in case of testing after cooling down. However, the effect of additional inner stresses from vapour release is questionable in case of real-scale structures, especially slabs and walls. The vapour migration can cause spalling of concrete with all its consequences, but inducing a structural collapse seems to be rather unlikely.

In [28] it is stated that the residual compressive strength of thermally-damaged concrete is generally not constant after the end of fire event, but it can vary in a limited extent with time. Right after the end of fire the damaged matrix is either absolutely or nearly dry. At this moment the material starts to absorb air moisture (mainly surface layers) and some compounds start to hydrate secondarily. At the beginning of the hydration, compressive strength can lower a bit for few months as new compounds are created (due to their volumetric expansion), but in time range of next months and several years the compressive strength grows as the matrix heals itself. According to [28] the compressive strength can recover even up to the strength at hot state. Visual interpretation can be seen in [Fig. 2-22](#). Because other



mechanical properties depend basically on the same factors as compressive strength does, evolution of tensile strength and modulus of elasticity with time follow the same trend.

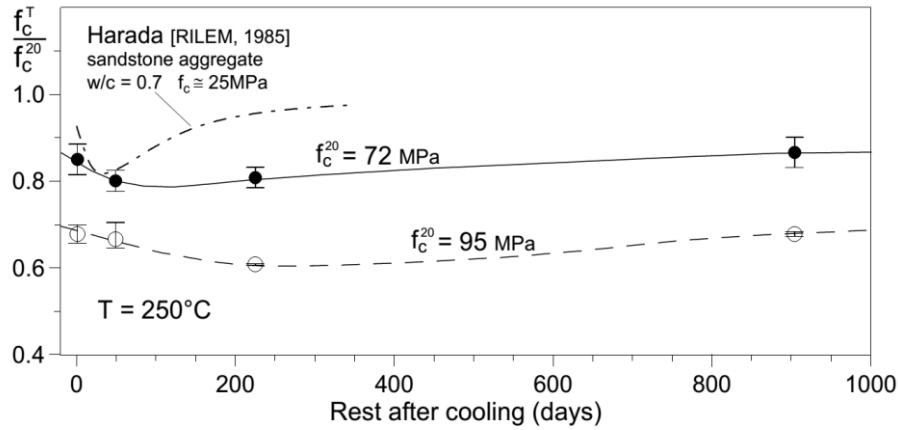


Fig. 2-22. Time-dependent residual compressive strength of concrete specimen after exposure to 250 °C, taken over [35].

Although previously mentioned knowledge about concrete after fire is available, it is still very hard to estimate the expected residual mechanical properties mathematically or using some empirical equations, as the residual parameters can vary significantly when compared to “hot” properties. As it was already mentioned in Chapter 2.3, the actual values are strongly dependent on several boundary conditions. Effects of high temperatures and stress-state in the structural members have been already discussed. The last important factor to mention is the cooling regime of structures. While high temperatures and stress-state influence decay of mechanical properties directly and can be expressed by equations, tables or charts, it is more complicated when speaking about possible cooling regimes. If a structural member after fire is cooled down naturally on air, the ultimate compressive strength should be reduced approximately by 15-20 % with respect to “hot” strength, while the stress-strain curve should be edited analogically [15]. The design code for composite concrete-steel structures [36] proposes in Annex C approach how to take into account the residual compressive strength of concrete and according to it the strength should be taken according to Eqs. (2-8) – (2-10). From the equations it is evident the strength is not lower than 90 % of the strength at “hot” state related to the peak temperature which is less conservative than values advised above. However, if the structure is cooled down very quickly by cold water, it undergoes thermal shock which usually causes another damage of the matrix (the damage mechanism is described in Chapter 2.3). According to test results, in [37] it is stated the residual mechanical properties can be additionally worsen up to 38 % when compared to residual properties of concrete cooled down slowly on air.

$$\text{– for } 20 \text{ } ^\circ\text{C} < \theta_{max} < 100 \text{ } ^\circ\text{C} \quad f_{ck,\theta,res} = k_{c,\theta,max} * f_{ck,20} \quad (2-8)$$

$$\text{– for } 100 \text{ } ^\circ\text{C} \leq \theta_{max} < 300 \text{ } ^\circ\text{C} \quad f_{ck,\theta,res} = 0,95 - \left(0,185 \frac{\theta_{max} - 100}{200}\right) * f_{ck,20} \quad (2-9)$$

$$\text{– for } \theta_{max} \geq 300 \text{ } ^\circ\text{C} \quad f_{ck,\theta,res} = 0,9 * k_{c,\theta,max} * f_{ck,20} \quad (2-10)$$

To continue with, even though quick cooling of concrete building which is on fire can be highly unfavourable from structural point of view, it is very often situation as extinguishing by water stream is the most common extinguishing technique which fire brigades use during interventions and it does not seem this will change in near future. The additional strength decay cited in the previous paragraph has to be understood as proved in laboratory tests on small specimens. During the test the specimen was firstly heated to a uniform temperature and then the whole specimen was cooled down to ambient temperature – the test result then proves the damage mechanism at a steady-state condition. However, in case of real structure the situation is different. The temperature distribution in member’s cross-



sections is generally non-uniform and highly nonlinear and also the extinguishing does not proceed until the whole structure exhibits uniform ambient temperature. Therefore, the effect of cooling influences mainly the surface layers of concrete, but the cross-section's core might not be affected at all. As a result of thermal shock, following consequences should be taken into account in the post-fire structural assessment:

- compressive strength reduction in those parts of cross-sections which are under compression – walls, columns and parts of slabs and beams under compression (the affected thickness of concrete can be investigated conducting reverse thermal analysis);
- risk that concrete cover will slough off and/or will not be cohesive with the reinforcement and the rest of cross-section (often seen during fire situations or after their ending [38]);
- tensile strength reduction – tensile strength of concrete is generally neglected according to common design approach of concrete structures [25]; however, it has to be taken into account when speaking about bond strength of reinforcement, its anchoring and rebars connecting via overlap lengths;
- temperature-induced structural effects similar but reversed to the effects when structure is being heated.

When speaking about residual bond strength of concrete, growing interest of scientists has been dedicated to this topic lately [39, 40]. According to the published experimental results it was proved the bond strength is sensitive to elevated temperatures to a no negligible extent. As the bond strength at ambient temperatures is directly dependent on compressive and tensile strength of concrete, the dependency at elevated temperatures sounds reasonable. Following the decay trend of residual compressive and tensile strength of concrete, the bond strength is reduced only minimally up to 200 °C. However, if rebars temperature 600 °C or 800 °C is reached, the bond strength might reduce up to 70-75 %, respectively. Because the tensile reinforcement is basically located close to the element's surface the cooling regime described in the previous paragraph affects the residual bond strength significantly as well. Beside the direct impact of high temperatures, the residual bond strength depends strongly on the concrete cover thickness and the type of used rebars (ribbed or plain bars). The cohesion between concrete and rebars can be damaged also due to the stress induced by differential thermal elongation, as described in Chapters 2.1 and 2.2 (partial slip of reinforcement can happen). Such deterioration has apparent effect on reinforcement anchorage and rebars connecting via overlap lengths. Therefore, it has to be investigated carefully due to direct impact on structural performance.

The last thing to discuss is the impact of exposure length of concrete structures to high temperatures and its effect on residual properties of concrete. In [22] it is stated the most important parameter of fire event is the maximal reached temperature, whereas the length of exposure to high temperature has only minor effect. This seems to be valid when speaking about fires of buildings, as the fire event usually lasts only several hours (several days in maximum) and it is very probable there will be maximally one fire event in given structure during its life-cycle. The situation might be different in case of special structures which are exposed to high temperatures due to the nature of industrial facility, power plant, etc. The long-term and cyclic exposure might influence the material in some additional way, however this is not in scope of this Thesis.

#### 2.4.2 Residual Properties of Reinforcing Steel

Over the years the main attention of scientists has been dedicated to testing and describing the behaviour of concrete, either at hot state or after cooling down. Less attention has been paid to behaviour of reinforcing steel. According to the test results [41] and also design code prescriptions [16] it is known that the strength decay of reinforcing steel depends on the production technique of rebars (hot-rolled steel is less temperature-sensitive, whereas cold-worked steel exhibits more significant and faster strength decay and the most temperature-sensitive type of steel is the high-strength steel for pre-stressed concrete structures). To continue, it was discovered that for temperatures up to 400 °C there is almost



no decay of tensile strength in case of hot-rolled reinforcement (300 °C for cold-worked reinforcement), while the Young's modulus starts to decrease gradually from 100 °C on for both types of rebars. Such properties are valid for hot state.

When compared to the amount of rebar tests at hot state, only very small attention has been dedicated to testing the residual properties of rebars after exposure to high temperatures. Therefore, only limited amount of test results is available. Generally, it is stated that after the exposure to elevated temperatures the yield strength recovers fully to the initial extent prior to heating, which is based on the fact no significant changes in microstructure nor crystalline grid happens in the steel rods when being heated. On the contrary, this is probably not true for whole range of temperatures. According to [38] the yield strength recovers fully when reinforcement is heated only up to 550-600 °C in maximum for hot-rolled steel and 450 °C for cold-worked steel, while these temperatures are called as *critical temperatures* [41]. After these temperatures are exceeded the residual yield strength cannot be restored fully as some changes at a microscopic level happened during heating. The residual strength decay can be seen in Fig. 2-23. The diagram is derived only to 700 °C based on the idea that a structure with reinforcement heated to more than 700 °C has to be damaged so heavily that another use or repair is not possible [38]. Nevertheless, if the information about residual yield strength of such rebar is still needed, an experimental tests have to be carried out using specimens taken out of the damaged structure. However, the heat treatment of reinforcement does not influence the residual Young's modulus of steel according to [41].

Similarly to concrete, also in case of reinforcing steel the structure cooling regime after end of fire event has an impact on residual properties of rebars, especially ductility. If very hot reinforcement is cooled down quickly with cold water, another changes in steel microstructure happen and *Martenic structures* form, which can improve the hardness of steel, but also worsen steel ductility [42]. Eventual collapse then might be brittle which is an unfavourable failure mode.

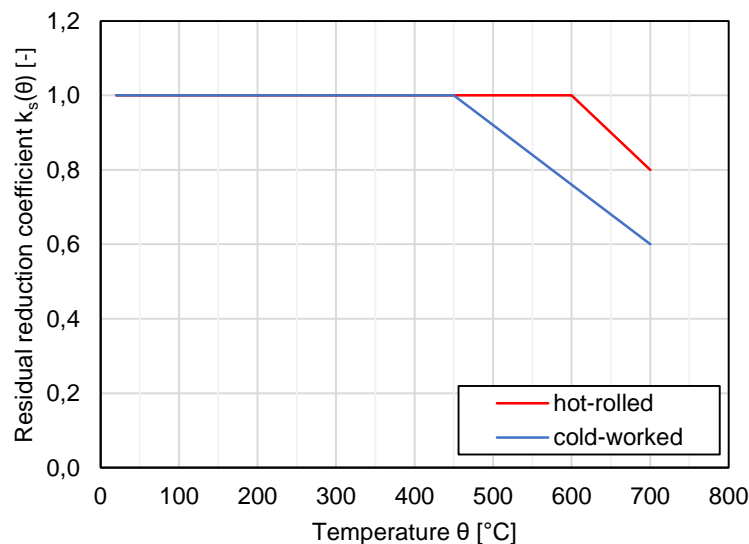


Fig. 2-23. Reduction coefficient of residual yield strength according to [38].



## 2.5 Stress-Strain Diagrams & Thermal Strains

### 2.5.1 Stress-Strain Diagram of Concrete

For many decades there has been effort from scientists all over the world to mathematically define stress-strain diagram of concrete which is exposed to high temperatures. Over the years it has shown it is very challenging task to derive such stress-strain constitutive model that would be as generic as possible (for most common usage) and at the same time it would correspond with experimental results. Aim of this chapter is not to bring exhaustive and deep overview of existing models and knowledge, it should lie in describing the thermal strains phenomenon, pointing out the most important facts and mentioning advantages and disadvantages of several constitutive models published in literature.

The conditions that constitutive stress-strain model should cover can vary significantly. Concrete can be either:

- under constant load while temperature is rising (transient conditions);
- under constant temperature while load is constant or rising (steady-state conditions);
- under changing load while temperature is changing as well;

To continue with, the constitutive model should consider correctly:

- not only ascending branch up to peak stress, but descending branch up to ultimate strain of concrete as well;
- the unloading branch of diagram with appropriate modulus of elasticity;
- not only heating but cooling phase as well.

The essential problem which is making aforementioned so difficult is the phenomenon of temperature-induced strains in concrete. Based on many experimental results it was found that elevated temperatures have significant effect on measured strains. They were already partially described in [Chapter 2.1](#) and [2.3](#). The mechanism is primarily dependent on thermal expansion of concrete matrix induced by high temperatures and also on the stress level in concrete and whether the stress is compressive or tensile. If concrete is being heated without any priory applied compressive stress, due to thermal expansion of aggregate the volume rises proportionally to the coefficient of thermal expansion (see [Chapter 2.1](#)). However, if concrete is being compressed and afterwards heated, the volumetric expansion is significantly reduced depending on the stress level (which is usually defined as a ratio of applied compressive stress to compressive strength of concrete at ambient temperature). If the stress level is higher than certain value, the volumetric change turns opposite and concrete shrinks instead. The thermal expansion is naturally reduced by the elastic strain induced by external load and in case of long-term loading also by creep of concrete. Beside these two there is another constituent called usually as *transient creep strain* (TCS) or *load-induced thermal strain* (LITS). Both names are used in the literature and both of them represent sum of partial strains developing in concrete subjected to compressive load and elevated temperature at the same time. Although they do not represent absolutely the same, they refer to the same phenomenon (actually TCS is by far the biggest part of LITS) (see e.g. [\[43\]](#)). Visual explanation of LITS can be seen in [Fig. 2-24](#) ( $\varepsilon_0$  represents free thermal strain of concrete,  $\varepsilon_{ela,0}$  represents the elastic mechanical strain of concrete,  $\varepsilon_{lits}$  represents the load-induced thermal strain causing strains relaxation and  $\varepsilon_{tot}$  represents the total sum of all strain constituents).

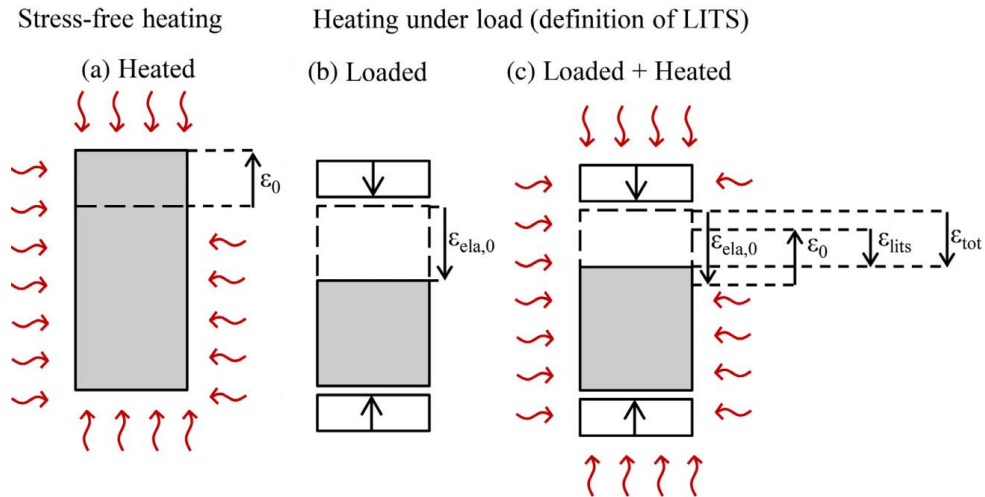


Fig. 2-24. Visual interpretation of LITS, taken over [44].

It was found LITS are induced mainly by chemical and physical changes in cement paste and with higher temperatures (from 400 °C above) they depend primarily on thermal incompatibility of aggregate used in concrete mixture and cement paste. Moreover, initial moisture level of matrix and also heating rate influences LITS to a limited extent. However, by far the biggest influence is connected to applied compressive stress and temperature level [44]. LITS are also considered to be irrecoverable after unloading and the end of heating phase as well, which has significant impact on the constitutive stress-strain models, as will be mentioned later on. Also because of irrecoverability and influence of moisture content, LITS develops only during first heating of concrete and only at unsealed conditions [24, 43, 44], it does not develop during cooling or repeated heating. Its extent can be reduced by preheating cycles [44].

Previously it was mentioned the total strain of concrete subjected to high temperatures consists from several components, mainly from free thermal strain (FTS), transient strain (TS), creep strain and mechanical elastic strain. Graphical interpretation of these constituents can be seen in Fig. 2-25.

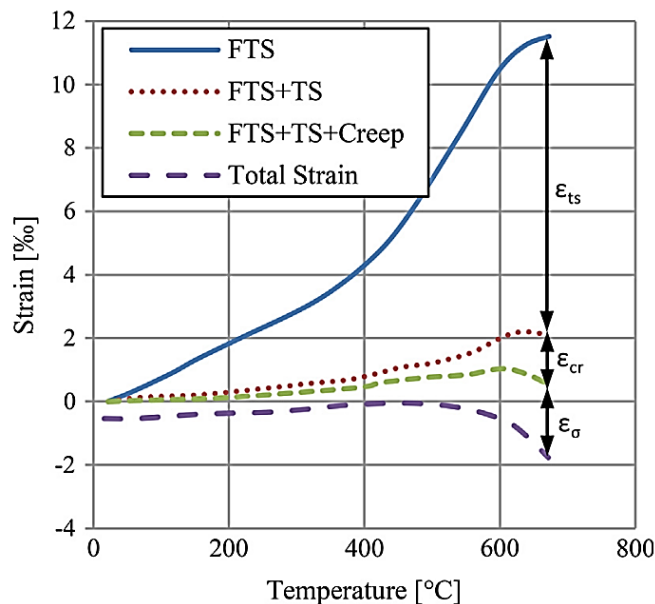
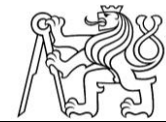


Fig. 2-25. Total strain decomposition and constituents interpretation, taken over [44].





The effect of LITS on reduction of thermal strains according to different compressive stress levels is demonstrated in Fig. 2-26. In the diagram the heating and cooling phase is drawn as well. It can be stated the cooling branch of FTS is almost identical but mirrored to the heating branch of the curve. The heating branches of other curves refer to significantly lower strains when compared to FTS curve, for curves of 20% and 30% applied load the strain even changes to shrinkage instead of expansion, as was already stated above. However, it can be noticed the cooling branches of these curves are approximately parallel to cooling branch of FTS curve which corresponds to the fact LITS does not develop during cooling phase.

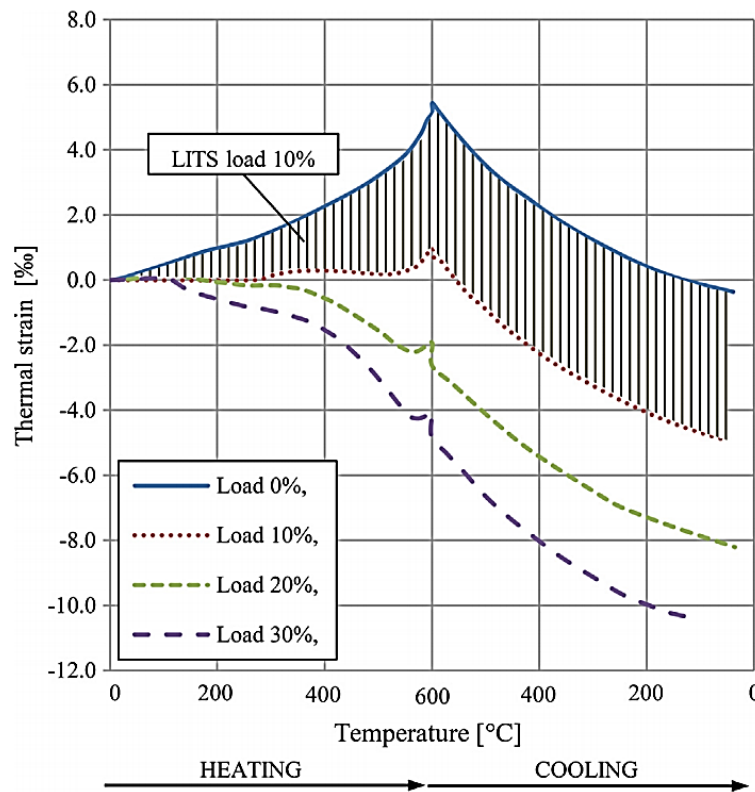


Fig. 2-26. Total thermal strain of concrete at high temperatures with different applied load levels, taken over [44].

The irrecoverability of LITS after unloading is visible in Fig. 2-27. Grey curve represents stress-strain diagram if concrete is not influenced by LITS (with appropriate modulus of elasticity according to actual temperature), whereas the black continuous-line curve represents the actual stress-strain diagram of concrete under compression and high temperature with effect of LITS. Significant decay of Young's modulus can be seen when curves are compared, which is the effect of LITS. Then the branches after unloading are displayed, where major difference between implicit and explicit constitutive models can be seen (it will be discussed in detail later on). Though it is worth to mention now that implicit models cannot consider stiffness of unloading branch of stress-strain diagram correctly as LITS are incorporated directly in the equations of stress dependency on strain, therefore they are permanently included during loading and unloading as well – which does not correspond to experimental results and the statement of its irrecoverability [44]. On contrary, in explicit constitutive models LITS can be excluded from the equations and stiffness in the unloading branch can be computed correctly. The unloading branch of the stress-strain curve therefore should not be parallel to the tangent of loading branch with LITS counted in, but parallel to the tangent of instantaneous stress-strain curve [43].

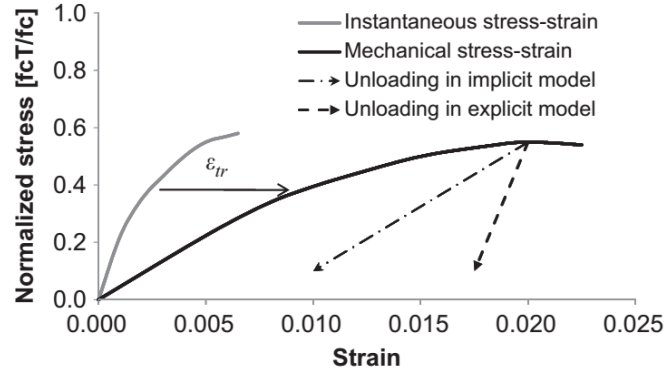


Fig. 2-27. Stress-strain diagram with unloading branch, taken over [43].

When speaking about constitutive models, there are basically two different approaches of their derivation. First approach is related to implicit constitutive models. The name *implicit* is based on the fact in such models the effect of LITS is incorporated directly in the equations of stress dependency on strain. It means LITS are counted in permanently, during loading and unloading, during heating and cooling. They also cannot be simply excluded. The total strain is then a sum of mechanical elastic strain (eventually with creep) with LITS already counted in and free thermal strain of concrete. Example of such approach is the constitutive model incorporated in EC2 [16], which is the most common model nowadays. In EC2 [16] Eq. (2-11) can be found describing the composition of concrete total strain.

$$\varepsilon_{c,\theta} = \varepsilon_{\sigma} + \varepsilon_{th} + \varepsilon_{creep} + \varepsilon_{tr} \quad (2-11)$$

where  $\varepsilon_{c,\theta}$  represents total strain of concrete at high temperatures,

$\varepsilon_{\sigma}$  represents instantaneous mechanical strain of concrete induced by external load,

$\varepsilon_{th}$  represents free thermal strain induced by thermal expansion (see Fig. 2-11),

$\varepsilon_{creep}$  represents long-term strain of concrete caused by creep, with respect to the usual length of fire event this constituent can be omitted [44],

$\varepsilon_{tr}$  represents transient strain induced by temperature and stress-state in concrete.

EC2 [16] also provides Eq. (2-12) to calculate stresses according to strains. Effect of LITS and related decay of stiffness is already incorporated, particularly in the increasing strains  $\varepsilon_{c1,\theta}$  and  $\varepsilon_{cu1,\theta}$ . The stress-strain diagram can be obtained for concrete with siliceous and calcareous aggregate as well, as the decay of ultimate compressive strength is distinguished according to used type of aggregate.

$$\text{– for } \varepsilon \leq \varepsilon_{c1,\theta}: \quad \sigma_{c,\theta} = \frac{3 * \varepsilon * f_{c,\theta}}{\varepsilon_{c1,\theta} * \left( 2 + \left( \frac{\varepsilon}{\varepsilon_{c1,\theta}} \right)^3 \right)} \quad (2-12)$$

– for  $\varepsilon_{c1,\theta} < \varepsilon \leq \varepsilon_{cu1,\theta}$ : linear or nonlinear descending branch is possible up to  $\varepsilon_{cu1,\theta}$

Another limitation of such constitutive model is that the stress-strain diagram can be obtained for a specific temperature, as the strength decay and strains are defined with respect to temperature level. It means steady-state conditions are assumed and transient state conditions cannot be described. An example of stress-strain diagrams of concrete for different temperatures according to EC2 [16] formulation can be seen in Fig. 2-28.



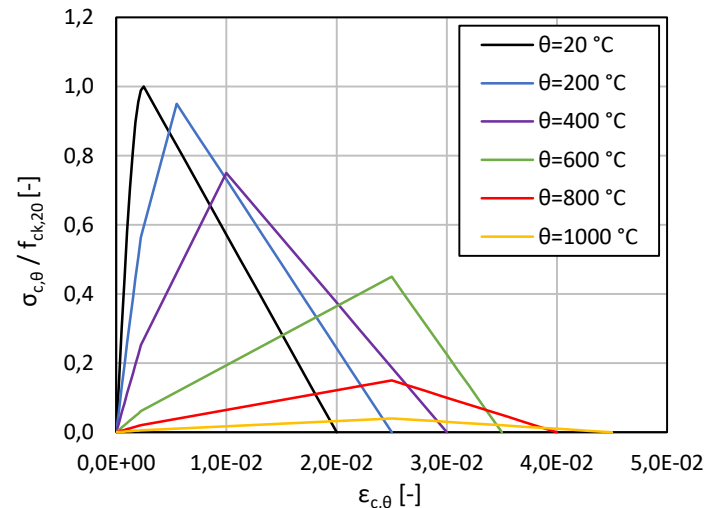


*Fig. 2-28. Stress-strain diagram of siliceous aggregate concrete at high temperatures with linear descending branch, according to EC2 [16].*

The second approach how to derive constitutive models of concrete subjected to high temperatures is related to explicit constitutive models. They are called *explicit* because the LITS part of total strain is calculated separately and it is not included in the mechanical strain. Therefore, total strain can be calculated correctly for different boundary conditions – steady-state and transient state, heating and cooling as well. If a situation when LITS does not develop occurs, it is simply not counted in the total strain calculation.

Over the years number of explicit constitutive models have been developed. Most of them is dedicated to uniaxial loading conditions which corresponds well with loading conditions of beams, frames and columns. Only few of them describes multiaxial (bi- and triaxial) loading conditions which would be more appropriate for some type of structures (nuclear vessels, spatial shells, but also two-way slabs) as stated in [44]. Only uniaxial models will be discussed. First model to mention is a transient strain (TS) model proposed by Anderberg and Thelandersson [45]. According to it TS is linearly proportional to FTS and load level. There is a calibration coefficient  $k_{tr}$  proposed, which is according to number of experimental tests expected to be equal to 1,8 – 2,35 [–]. The formula can be seen in Eq. (2-13). Although the model is simple and thus easy to use and according to [44] exhibits relatively good agreement with test results up to temperatures 500-550 °C, after exceeding these temperatures the model cannot estimate TS accurately enough due to linear proportionality with FTS which does not correspond with the trend seen in experiments (the dependency is not linear). Second explicit model is the LITS model proposed by Nielsen [46], which is considered as modified Anderberg and Thelandersson’s model. This model counts with linear proportionality of LITS with applied stress level and temperature difference. The formula can be seen in Eq. (2-14). Calibration coefficient  $a$  is proposed and based on test result is expected to be equal to  $3,8 * 10^{-5} \text{ } ^\circ\text{C}^{-1}$  (the calibration was conducted for temperatures up to 500 °C). The main advantage when compared to the previous model lies in the independency of FTS which is govern mainly by aggregate type, however LITS takes place mainly in cement paste. Similarly to Anderberg and Thelandersson’s model, due to linear proportionality the model cannot estimate LITS properly for temperatures above 500 °C. Another LITS constitutive model modifying Nielsen’s model was proposed by Diederichs [47]. It also uses dependency on applied stress and temperature difference, but it is defined using polynomial equation of third order (see Eq. (2-15)) instead of linear proportionality, which is more suitable for description of LITS evolution. Correlation coefficients are introduced and based on test results they are believed to be equal to  $a_1 = 0,0412 * 10^{-3} \text{ } ^\circ\text{C}^{-1}$ ,  $a_2 = -1,72 * 10^{-7} \text{ } ^\circ\text{C}^{-1}$  and  $a_3 = +3,3 * 10^{-10} \text{ } ^\circ\text{C}^{-1}$ . According to [44] this constitutive model is suitable especially for higher temperatures (500 °C and more).



$$\varepsilon_{ts} = k_{tr} * \frac{\sigma}{\sigma_{u0}} * \varepsilon_{th,free} \quad (2-13)$$

$$\varepsilon_{lits} = \frac{\sigma}{\sigma_{u0}} * a * (T - T_0) \quad (2-14)$$

$$\varepsilon_{lits} = \frac{\sigma}{\sigma_{u0}} [a_1(T - T_0) + a_2(T - T_0)^2 + a_3(T - T_0)^3] \quad (2-15)$$

Last constitutive model to mention is the *Explicit Transient Creep Eurocode model* proposed by Gernay and Franssen in [43]. In the article following interesting idea is written: the actual EC2 implicit model was derived to be as generic as possible and with satisfactory results when compared to experimental data. From the beginning it was more or less clear that this model is compromise solution, however it was incorporated in the design code. Now it seems that instead of replacing it with some of published explicit models it would be more appropriate to derive a new model (with transient strains expressed explicitly) which would correspond to actual EC2 implicit model at such boundary conditions where EC2 model exhibits good agreement with test results as much as possible. Such new explicit model might be then considered as a proper replacement of actual implicit model. This new explicit model has already been developed by authors and it was incorporated in the finite element code SAFIR [48], which is one of very few computational programmes dedicated to fire resistance of structures. Conciseness of the model was verified e.g. in an experiment [43], where concrete column was loaded with axial compressive force and then subjected to Japan standard fire test. The heat treatment was held for 180 min, then the cooling phase begun. Thermal elongation/shrinkage was observed during whole test. Along with the experiment three numerical calculations were conducted in SAFIR with different stress-strain models of concrete. Plotted results can be seen in Fig. 2-29. It is clearly visible up to 120 min new explicit EC2 model and actual implicit EC2 model follow experimental results and themselves as well, however after 120 min EC2 curves start to recede from themselves and the difference starts to be even more visible after cooling phase begun in 180 min. On the contrary, the curve representing new explicit EC2 model follows experimental results very well. Therefore, new *Explicit Transient Creep Eurocode model* could be a suitable replacement of the actual implicit EC2 constitutive model.

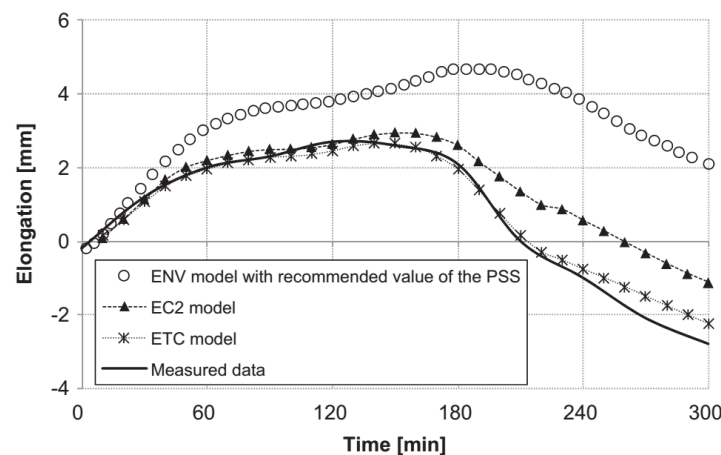


Fig. 2-29. Thermal deformation of concrete column axially compressed and subjected to Japanese standard fire according to different numerical models and test results, taken over [43].

## 2.5.2 Stress-Strain Diagram of Reinforcing Steel

When reinforcing steel is subjected to elevated temperature, the situation is simpler than in case of concrete, as its strain can be calculated directly as a sum of mechanical strain induced by external load and free thermal strain induced by high temperature, according to Eq. (2-16).

$$\varepsilon_{s,\theta} = \varepsilon_{\sigma} + \varepsilon_{th} \quad (2-16)$$



where  $\varepsilon_{s,\theta}$  represents total strain of reinforcing steel at high temperatures,  
 $\varepsilon_{\sigma}$  represents mechanical strain of reinforcing steel induced by external load,  
 $\varepsilon_{th}$  represents free thermal strain of reinforcing steel induced by high temperatures (see Chapter 2.2).

It is worth to point out free thermal strains usually cannot develop fully freely as rebars are restrained by ambient concrete to a significant extent. Due to cohesion between concrete and reinforcement both materials exhibit the same strain until bond strength is exceeded. If it is exceeded, rebars partially slip and the excessive stress is relieved (however the slip has direct impact on either hot and residual structural performance as well).

The generic constitutive stress-strain model of reinforcing steel subjected to high temperatures is proposed in EC2 [16]. The formulae can be seen in Eqs. (2-17) – (2-20). The design stress-strain diagram is parabolic-rectangular with linear descending branch. Stress-strain diagrams of reinforcement in tension and compression drawn for different temperatures according to EC2 model can be seen in Fig. 2-30 and 2-31.

$$\text{– for } \varepsilon_{s,\theta} < \varepsilon_{sp,\theta}: \quad \sigma_s(\theta) = \varepsilon_{s,\theta} * E_{s,\theta} \quad (2-17)$$

$$\text{– for } \varepsilon_{sp,\theta} \leq \varepsilon_{s,\theta} < \varepsilon_{sy,\theta}: \quad \sigma_s(\theta) = f_{sp,\theta} - c + \frac{b}{a} * \left[ a^2 - (\varepsilon_{sy,\theta} - \varepsilon_{s,\theta})^2 \right]^{0,5} \quad (2-18)$$

$$\text{– for } \varepsilon_{sy,\theta} \leq \varepsilon_{s,\theta} < \varepsilon_{st,\theta}: \quad \sigma_s(\theta) = f_{sy,\theta} \quad (2-19)$$

$$\text{– for } \varepsilon_{st,\theta} \leq \varepsilon_{s,\theta} < \varepsilon_{su,\theta}: \quad \sigma_s(\theta) = f_{sy,\theta} * \left[ 1 - \frac{\varepsilon_{s,\theta} - \varepsilon_{st,\theta}}{\varepsilon_{su,\theta} - \varepsilon_{st,\theta}} \right] \quad (2-20)$$

$$\text{– parameters:} \quad \varepsilon_{sp,\theta} = f_{sp,\theta}/E_{s,\theta}, \quad \varepsilon_{sy,\theta} = 0,02, \quad \varepsilon_{st,\theta} = 0,15, \quad \varepsilon_{su,\theta} = 0,20$$

$$\text{– functions:} \quad a^2 = (\varepsilon_{sy,\theta} - \varepsilon_{sp,\theta}) * \left( \varepsilon_{sy,\theta} - \varepsilon_{sp,\theta} + \frac{c}{E_{s,\theta}} \right)$$

$$b^2 = c * (\varepsilon_{sy,\theta} - \varepsilon_{sp,\theta}) * E_{s,\theta} + c^2$$

$$c = \frac{(f_{sy,\theta} - f_{sp,\theta})^2}{(\varepsilon_{sy,\theta} - \varepsilon_{sp,\theta}) * E_{s,\theta} - 2(f_{sy,\theta} - f_{sp,\theta})}$$

where  $\varepsilon_{sp,\theta}$  represents strain of reinforcement at high temperatures at proportionality limit,  
 $\varepsilon_{sy,\theta}$  represents strain of reinforcement at high temperatures when yield strength is reached,  
 $\varepsilon_{st,\theta}$  represents strain of reinforcement at high temperatures when tensile strength is reached,  
 $\varepsilon_{su,\theta}$  represents ultimate strain of reinforcement at high temperatures.

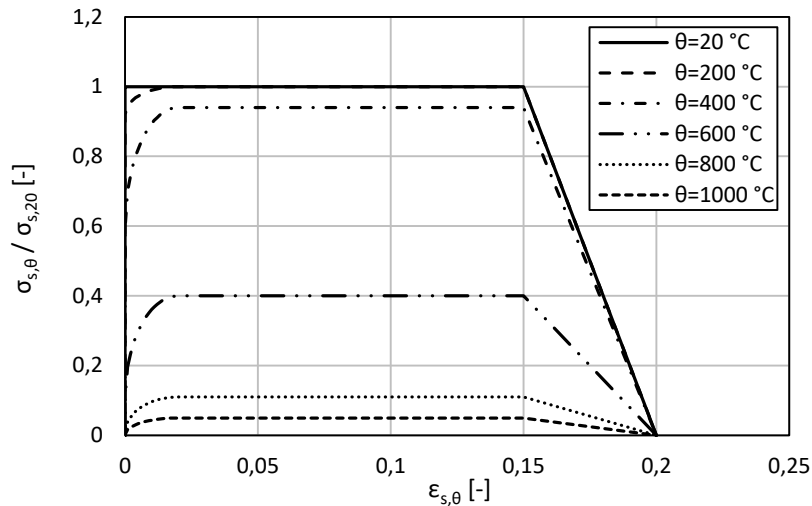
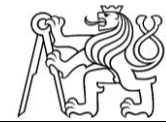


*Fig. 2-30. Stress-strain diagram of cold-worked reinforcing steel in tension at high temperatures, according to EC2 [16].*

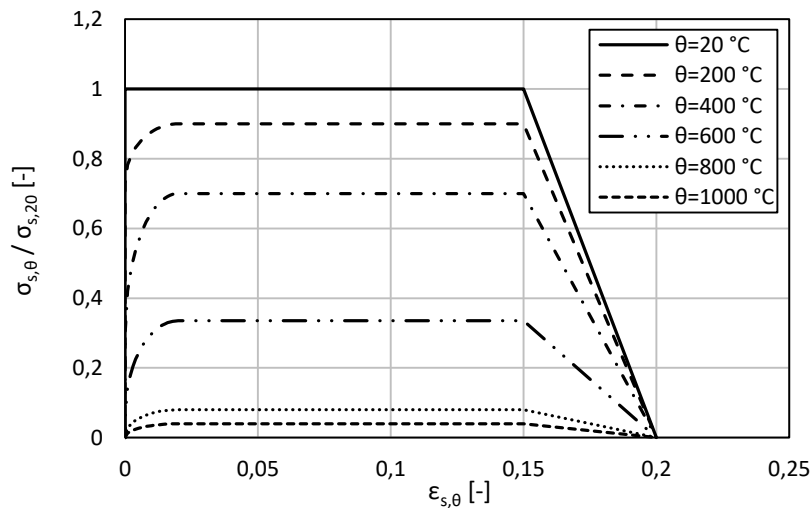


*Fig. 2-31. Stress-strain diagram of reinforcing steel in compression at high temperatures, according to EC2 [16].*

## 2.6 Approaches to Estimate Fire Resistance

In today's engineering practise a part of project documentation dedicated to fire safety is usually needed. This project part is elaborated by specialists that generally focus only on fire safety and consists from assessment of escape ways, used material's reaction on fire, options of fire extinguishing and many others, among them also assessment of structural fire resistance. In easier cases this assessment is carried out directly by mentioned fire safety specialist, in more complicated cases it is carried out with help of structural engineer.

In case of concrete structures, there are several possible approaches how to estimate the fire resistance. The easiest possible way is to use tabular method and to check dimensions of a structural member and concrete cover thickness using tables published in EC2 [16] or other valid regional design code, such as ACI 216.1 [17]. The method is based on number of test results as well as experience with real fires – therefore it is considered to be rather empirical than analytical – it means it does not follow real structural performance during fire. The method is easy-to-use and very fast, however, in some cases it could be very conservative, especially for longer fire durations. On contrary, in cases of less ordinary structures the results can be non-conservative and hence on the dangerous side. Such structures can be very slender structures with impact of second-order forces, spatially performing structures, multi-



statically indeterminate structures, dynamically loaded structures, etc. In case of tabular methods constitutive stress-strain model is not needed since no structural calculation is conducted.

According to EC2 [16] the second option to assess fire resistance is to use simplified calculation methods. In mentioned design code there are two methods proposed: (i) *isotherm 500 °C method* and (ii) *zone method*. Both calculation methods use similar principle – a simplified way to express material deterioration and strength decay of mechanical properties based on conducted thermal analysis:

- *Isotherm 500 °C method*: main idea of this method lies in assumption that concrete heated to the temperature over 500 °C exhibits no contribution to the load-bearing capacity of the cross-section, whereas concrete heated to the temperature under 500 °C preserves full strength. Tensile strength of reinforcement is reduced according to rebars temperature and reduction diagram (see Chapter 2.2).
- *Zone method*: this method enables to distinguish the extent of material deterioration by dividing cross-sectional area into zones. Part of cross-section is then excluded and for the rest mean strength reduction is calculated based on partial reduction coefficients for chosen zones. Reinforcement strength decay is determined in the same way as in *isotherm 500 °C method*.

These methods provide relatively simple way to estimate load-bearing capacity of cross-section which should be compared with internal forces based on accidental load case. Prescribed load combination for such situation is proposed in EN 1990 [49] and EC2 [16] and can be seen in Eq. (2-21). The load is reduced with respect to probability of live load occurrence in full extent during accidental situation. Also indirect loads induced by fire should be taken in account, however this is the only mention without any detailed advice how to estimate and include them in calculation.

$$f_{d,accident} = \Sigma G_{k,j} + P + A_d + \Sigma \psi_2 Q_k \quad (2-21)$$

where  $f_{d,accident}$  represents total sum of load constituents in accidental design situation,  
 $G_k$  represents characteristic dead load,  
 $P$  represents potential prestressing force,  
 $A_d$  represents design value of temperature-induced forces,  
 $Q_k$  represents characteristic live load.

The last possible way of fire resistance estimation is using advanced calculation methods. They are the most accurate but time-consuming at the same time. Generally, such method is based on finite element nonlinear numerical calculation, where thermal and mechanical analysis are coupled. Only thanks to such connection correct time evolution of thermal and mechanical strains and internal forces can be obtained. The assessment is basically conducted right in the nonlinear calculation and the fire resistance is assumed to correspond to the moment when ultimate strain or stress in one of used materials or maximum crack width is reached. It is obvious correct constitutive stress-strain model of both concrete and reinforcing steel is needed.

Special way of estimating fire resistance of structural member is conducting standardised fire experiments, which is suitable mainly in case of industrially produced members, such as reinforced-concrete (RC) or prestressed-concrete (PC) floor panels, ceramic hollow-core composite slabs or masonry walls. This way of estimating fire resistance is very expensive and time-consuming, nevertheless it is very popular since higher fire resistance can be usually obtained when compared to calculations and due to amount of produced members it is still beneficial for the producer. Result of such experiment is then the time within tested structural member can carry prescribed load.



In this chapter possible ways of fire resistance estimation of concrete structures were described. The tabular methods are still the most common way, but their limits were mentioned. In more complicated cases simplified calculation methods can be used. The calculation of load-bearing capacity of a cross-section is not complicated and thus can be conducted relatively easily. If concrete structure is statically determinate, the method seems to be accurate and reliable enough, as high temperatures do not induce any additional forces but only deformations (deflections, curvature and elongation).

However, if a structure is more or less statically indeterminate (which to be honest is by far the majority of concrete structures) the temperature-induced deformations are restrained to a certain extent (depends on stiffnesses) and thus additional internal forces develop (usually axial compressive force and negative bending moment). The flexural and axial stiffness of members and their joints subjected to fire basically evolves with time of fire event as mechanical parameters deteriorate, therefore redistribution of internal forces happens – loading moves from more damaged parts of structure with smaller stiffness to the less damaged part with higher stiffness. Such redistribution together with additional temperature-induced forces might very significantly change the stress-state of structure.

In [Eq. \(2-21\)](#) in this chapter it was stated the indirect effect of high temperatures has to be taken into account in the load combination but no hints how to do it are proposed. From above mentioned and [Chapter 7](#) it is obvious that correct estimation of additional temperature-induced internal forces is possible only when advanced numerical calculation with both thermal and mechanical analysis is carried out. Moreover, the results correctness is directly dependent on used constitutive stress-strain model with appropriate definition and incorporation of LITS. On the other hand, if only free thermal expansion of members is taken into account and LITS are omitted, unrealistic and very overestimated results of internal forces will be obtained. To conclude with, using either simplified or advanced calculation methods without proper consideration of mentioned mechanisms could lead to wrong findings on both very conservative and dangerous side. More about estimating fire resistance can be found in [Chapter 7](#).





## 3 Post-Fire Procedure

Usual process of post-fire procedure is described in this chapter. It contains approach and decisions of local authorities, findings and information about the fire event from fire brigade, witnesses, building owner or business operator. Later on generic flowchart of post-fire approach towards structural assessment is proposed (later on *Flowchart*, see [Fig. 3-2](#)) with commentary to each step. Several topics which are not discussed in detail later on are also mentioned in this chapter. Consequently, from this chapter on the Thesis is going to follow the *Flowchart*, where individual chapters are highlighted.

### 3.1 General Aspects of Post-Fire Procedure

When a building is on fire, two possible options may happen. If the fire event is reported to fire brigade, firefighting squad comes and starts with extinguishing and evacuation of inhabitants. In this case the building is already closed for public during fire brigade intervention and all involved people have to follow orders from commanding firefighter. If the fire event is not reported to fire brigade, fire spreads with no control and theoretically the building is not closed for public. After the end of fire event, representatives of local authorities together with commanding firefighter who lead the intervention and policemen officially declare the burned building as *closed for public*, which is important step from the legal point of view. The closure is usually highlighted with stripped police line around closed area. Eventual entrance into the area is then considered as a self-risk with all consequences (danger of injury or even death, etc.); the entrance can be also forbidden under the thread of fines.

Before anybody enters the burned building existing risk based on possible damage of load-bearing and other secondary structures has to be considered very carefully since theoretically the structural system can be deteriorated to such extent that it might not be safe and stable anymore. Priceless information can be provided by the firefighters who operated inside the building before. However, even though during fire and firefighting intervention no visible structural problems were witnessed, after cooling down severe structural problems might occur (because residual mechanical properties of concrete and steel after fire are generally worse than those at *hot state*, see [Chapter 2.4](#)). If there is a doubt about safety of people entering the damaged building there are some options how to obtain general information about the state and damage severity. The traditional option is to use specially trained dog. In such situations dogs are trained to search human victims that may still be inside building. In modern age a digital camera can be equipped to dog's back so his motion inside the building can be recorded. Another option lies in using drones or even special robots to explore the building in detail.

During such exploring heavily damaged structural members or eventual local collapses can be found. Such members are then suitable or even necessary to be propped before people enter the building and start the investigation process. The propping is generally considered and prescribed by a structural engineer who is usually invited to the analysis group at the beginning of investigation. Before propping selected members, the structural engineer has to have an idea about the structural system in order to choose the right spot where to erect the falsework. Sometimes and generally in structures with long spans the falsework might be necessary to be raised in every floor under the damaged member in order to be supported directly by foundations and not intermediate slabs or girders.



### Information about Fire Event & Firefighting Report

One of the main objectives to make post-fire structural assessment possible to be conducted is to gather information about the fire event. Based on such information effects of fire on structural members can be taken into account and subsequently thermal and mechanical analysis can be carried out. In special cases whole fire event can be remodelled in special computer software for detailed structural analysis (see [Chapter 5](#)).

This type of information can be obtained from different sources. The most important and biggest source is the experience of fire brigade which conducted the intervention, usually summed up in the *firefighting report*. This document contains the description of facts about the event, chosen way of extinguishing and estimated extent of damage. Visual overview of content of such firefighting report related to post-fire structural assessment can be seen in [Fig. 3-1](#). Special attention has to be paid to the maximal reached temperatures, duration of fire and description of cooling regime of structures due to their direct impact on residual structural performance (see [Chapter 2.4](#)).

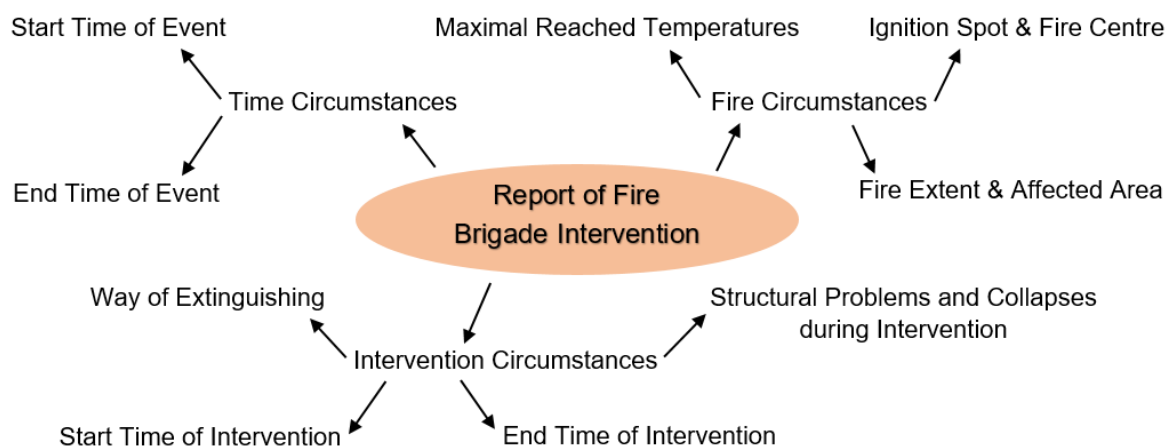


*Fig. 3-1. Content of firefighting report related to post-fire structural assessment.*

Information about fire event can be also provided by people who witnessed it (especially the man who reported the event to the fire brigade), more on by owner or operator who runs his business inside the building, neighbours, etc. In case the event was not reported to the fire brigade and the firefighting report does not exist, it represents considerable problem for conducting the post-fire assessment.

However, even in this case a basic idea about the event progress can be gained. During the preliminary or detailed inspection of burned building one can notice several clues that can describe the extent and severity of fire. Beside the state of load-bearing and secondary structures, which will be described in [Chapter 4](#), there are plenty of things in all types of buildings made of different materials. Each material reacts somehow to the exposure of high temperature. Therefore, according to their state maximal reached temperature can be approximately estimated for surrounding area. For instance, if pipes, ducts, bottles and toys made of polyethylene and polyvinylchloride are found melted and brown, temperature at such spot definitely was higher than 150-200 °C. If paper and wood are found charred and brown and at the same time aluminium parts are not melted, the temperature was probably somewhere between 200-400 °C. If window glazing is broken and the broken glass is melted and at the same time copper heating ducts are not melted, temperature was probably between 800-1000 °C. Comprehensive table of materials with example of household items and their reaction to high temperatures can be found in [Tab. 3-1](#).



**Tab. 3-1.** Overview of common household material's reactions on increasing temperatures [28, 38].

Material	Example of Items	Condition	Approximate Temperature [°C]
Paints	-	Deterioration	100
		Destruction	150-250
Polystyrene	Food containers, curtain hooks, window light shades,	Collapses	120
		Softens	120-140
		Melts and flows	150-180
Polyethylene	Bottles, bags and sacks, toys, electrical device casings, pipes	Shrivelling	120
		Softening and melting	120-140
Polyvinylchloride	Pipes, ducts, houseware, bottles, toys, handles and knobs	Degrades	100
		Smokes	150
		Browns	200
		Chars	400-500
Celluloses	Paper, cotton	Darkens, burns	200-300
Wood	Doors, window frames, furniture, toys	Burns	180-270
		Ash formation	
Lead	Pipes, sanitary installations	Melts	250
		Sharp edges rounds	300-350
		Drops formation	350-400
Aluminium	Small mechanical parts, parts of electronic devices, old wiring	Softens	400
		Melts	600
		Drops formation	650
Glass	Window and door glazing, dishes, glasses, bottles	Softening	500
		Sharp edges rounds	600
		Flows	800
Iron (steel)	Plumbing, radiators, workroom equipment	Softens	500-700
		Melts	1500-1550
Silver	Cutlery, jewellery	Melts	900
		Drops formation	950
Copper	Wiring, plumbing	Melts	1000-1100
Cast iron	Radiators, pipes	Melts	1100-1200
		Drops formation	1150-1250

Temperature rise ↓

Another interesting information related to fire duration can be seen on condition of timber structures. Due to high temperatures and flames wood catches on fire and since it is combustible material it burns. Outer layers of cross-section gradually get charred and the mechanically effective cross-sectional area is getting smaller with time of fire. The velocity of combustion depends on several aspects, mainly on moisture content of timber, its density, nature of origin (coniferous or deciduous trees) and nature of production (solid timber, glued laminated timber, etc.). For common structural built-in timber, the design code EN 1995-1-2 [50] proposes tables where can be read that solid and glued laminated timber burns approximately with velocity of 0,6 – 0,7 mm/min (the information is related to standard fire). Owing to this approximate time of fire can be estimated based on the thickness of charred layer. On the other hand, estimating the fire time according to charred thickness of plywood or OSB boards or even furniture is not a good idea since the boards are usually too thin and burn throughout. Moreover, their surface is often covered with flammable finishing which can accelerate the combustion velocity significantly.



## 3.2 Approach to Post-Fire Structural Assessment

A usual way of conducting post-fire process is described in the *Flowchart* in Fig. 3-2. It contains the most important steps and decisions in the process of post-fire structural assessment. Now it will be commented step-by-step.

The flowchart continues to the one proposed in Fig. 1-9 in Chapter 1. After the end of fire event first steps have to be done in order to ensure safety for public and to minimise risk of another economical and commercial harms or even human lives losses. It contains closing the building for public and preventing people from entering it, ensuring debris and parts of structure not to fall freely from the burned building to the surroundings (important mainly in dense development), and usually also cutting off the building from supplies of water, electricity, heat and gas to avoid danger of another accident. Among legal steps an *investigating group* is established which conducts forthcoming investigation and leads the post-fire process. In general, the members of such group are: building owner/administrator, member of fire brigade, civil engineer, diagnosis engineer and representative of the state administration.

One of the first decisions of investigating group is when to enter the building to conduct the preliminary inspection. It has to be considered carefully every time with respect to safety, it seems the right time is usually after a number of days from the end of fire event. The period of time is a result of several aspects and expected damage severity:

- The building should be cooled down completely to ambient temperature in order to avoid volumetric changes of structural members related to cooling phase and consequent structural effects;
- The building should go through one or two day-night cycles in order to withstand the temperature changes (the number of day-night cycles might be raised in case of significant weather changes);
- The building should be completely cut off energy supplies in order to avoid water or gas leakage from damaged ducts and pipes, electricity harms by uncovered wiring, etc.;
- The building should be let for some time just to see it is still stable and safe and no collapses are happening inside. It should not be entered during bad weather conditions (storm, strong wind, heavy snow blanket, earthquake).

During the step of preliminary inspection gathering as much information about the fire event as possible proceeds and rough idea about the fire severity and its extent is assembled. Based on visual assessment and first on-site material tests (see Chapter 4) structural members are classified into the damage classes which helps to estimate the overall damage extent and affected area. This step should provide an answer to essential question whether the fire event caused so serious damage that after conducting the preliminary inspection inside the burned building it can be stated with no doubts that the load-bearing structural system is clearly critically damaged, it is not safe anymore and the refurbishment is with high probability neither possible or valuable. If the answer to this question is *no*, the post-fire process continues with detailed inspection, structural diagnosis and estimating the residual load-bearing capacity with options of possible ways of refurbishment. Contrary, if the answer is *yes*, it seems the best way is to pull the building down. The demolition has to be proved by local building bureau and building demolition project has to be elaborated for this purpose. Hence, it is evident this decision is substantial in the post-fire process not only because it directly influences future of the building but also because it is related to enormous forthcoming effort and labour for a number of people not speaking about financial demands.

If the answer to the previously written question is *no*, it can mean there is high probability the building can serve to its purpose in the future as well (with or without refurbishment) because the damage extent and severity is not critical, or it is not evident that opposite is truth. In both cases more information about the building state has to be obtained. Therefore, another detailed inspection of the



building is conducted (which will be discussed in [Chapter 5](#)). During it *damage level* of structural members is investigated in detail. Material on-site tests are conducted and specimens for laboratory tests are cut off from selected elements. Both types of tests are done in order to obtain residual material mechanical properties which are necessary for calculating residual load-bearing capacity. For this purpose, not only material properties are needed, the indirect structural effects caused by high temperatures have to be taken into account as well (see [Chapter 7](#)). Therefore, the fire event has to be remodelled, at least in (very) simplified way. Based on it thermal analysis of the structure (together with mechanical analysis) can be conducted. Theoretical results are then compared to those gained from material tests. After calibrating results the calculation can be used for whole structure or its part while amount of material tests can be reduced which saves time, money and labour.

[Chapter 6](#) follows previously mentioned while post-fire structural diagnosis is discussed. Different on-site and laboratory material test options suitable for investigating mechanical properties of concrete structures after fire are proposed with advantages and disadvantages highlighted. Results of such tests and their correct interpretation are essential for estimating the damage severity and calibration of theoretical calculations. [Chapter 7](#) deals with the phenomenon of indirect structural effects of high temperatures on structural systems and also the effects of load history during fire event. Both phenomena affect structural performance during fire event and after its end and thus have to be taken into account when conducting global analysis. In this step, based on the global analysis possible irrecoverable changes in structural system must be considered due to overloading of some cross-sections and propagation of plastic deformations. Such theoretical assumptions have to be validated on the real structure since eventual change of structural system has obvious impact on internal forces distribution and residual structural performance. Based on previous steps now there is enough information to conduct the calculation of residual load-bearing capacity of structural elements and whole structural system, respectively. [Chapter 8](#) is dedicated to this topic.

When the calculation of residual structural performance is done, another substantial question is about to be answered: is the calculated residual load-bearing capacity sufficient with respect to the purpose of future use and its adequate load level? If the answer is *yes*, the structure was not significantly damaged or there was some extra load-bearing capacity prior to fire event, and thus no strengthening or refurbishment is needed. After surface repairs and clean-up, the structure can be used and fully loaded again. However, in case the answer is *no*, the structure cannot be used again without repair works containing deep refurbishment and/or structural strengthening. According to the damage extent and damage level of structural members it must be considered carefully whether the refurbishment is realistic, the strengthening will be sufficient with respect to design load level and it will be still worth from financial and other points of view. If so, the repair works are conducted after which the structure is ready-to-use again. In case the repair works are not possible or worth to be done for some reasons and if the problem lies in insufficient load-bearing capacity, making it sufficient can also be achieved from the opposite side by lowering the acting load level. This can be reached for instance by using lighter layers of flooring and other dead load, changing purpose of building use (e.g. from warehouse to offices, from offices to apartments, etc.) which basically represents reduction of live load or preventing people from entering specific areas. If load reduction is not possible or is not sufficient, the damaged building should be demolished and replaced.

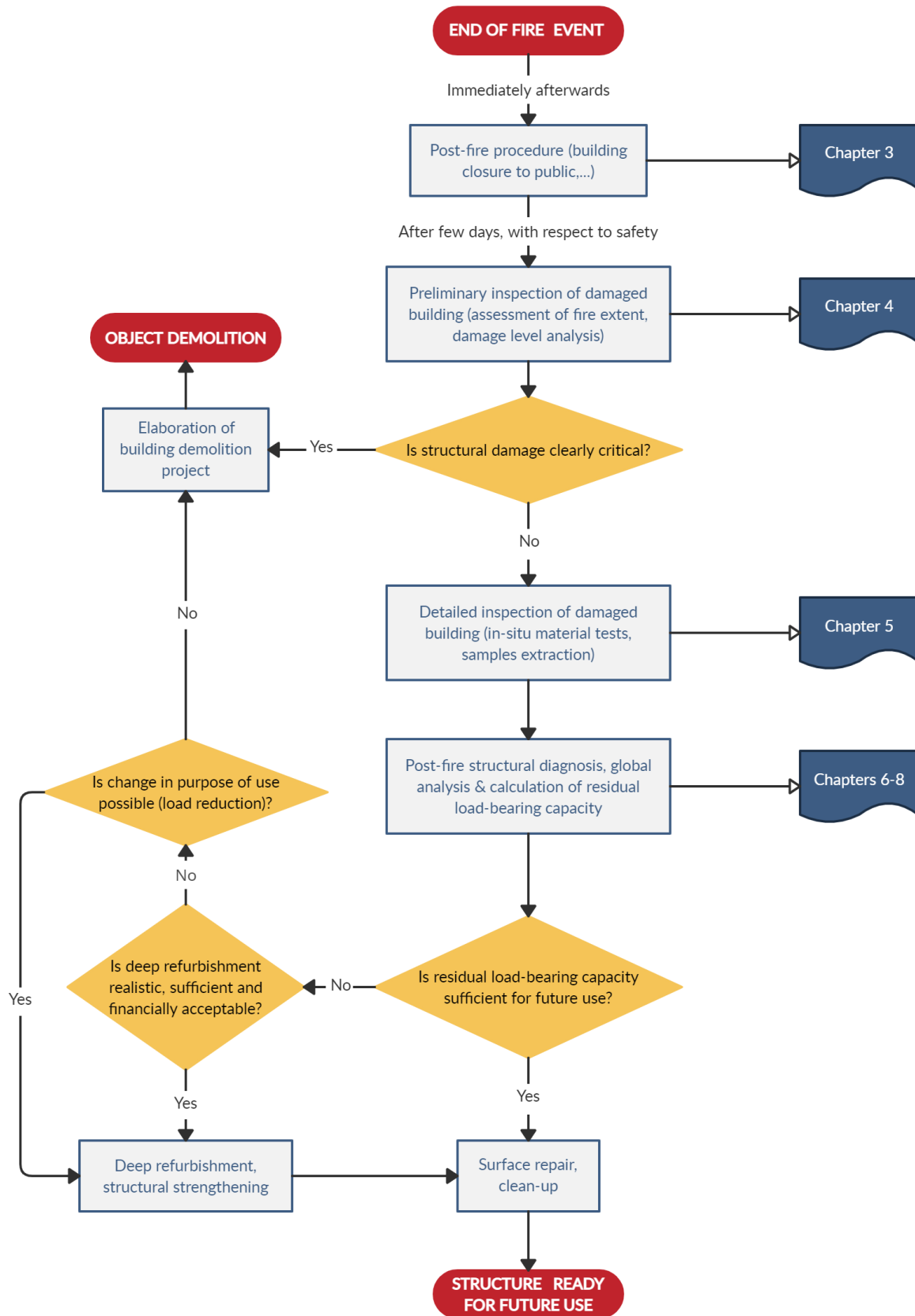
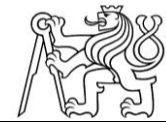


Fig. 3-2. Flowchart of the structural assessment after fire.





## Refurbishment of Load-Bearing Structures

Almost every building where fire event took place needs certain way of refurbishment, load-bearing structures not excluding. According to damage severity and its extent the refurbishment can contain only surface or shallow repairs in case of low damage levels, however in case of intermediate and significant damages the needed refurbishment may contain deep repairs and structural strengthening as well. In general, the refurbishment can be conducted from different reasons:

- To make the structure clean and good looking again;
- To renew visible surface layers (e.g. plaster or coating);
- To restore its original shape and volume;
- To strengthen or stiffen it in order to enhance its structural performance;
- To achieve sufficient fire resistance for future use;
- To ensure appropriate durability for future use.

Ways of refurbishment and structural strengthening are not in scope of this Thesis and therefore they will be mentioned only briefly. According to [38] it seems the nature of structural damage caused by fire is not so unique and thus usual ways of concrete structures refurbishment are applicable. Nevertheless, it is worth to mention the specific aspects of concrete structures damaged by fire as they influence the design of structural strengthening:

- Concrete is usually not damaged uniformly throughout the cross-section;
- Residual strength of concrete can vary significantly due to heating and cooling regime;
- Residual yield strength of reinforcement is usually expected to be equal to initial values, however in case of severe and longer fires it can be reduced (see [Chapter 2.4.2](#)); in such cases the reduction is strongly dependent on maximal reached temperatures which are directly connected to concrete cover thickness – the reduction can vary from rebar to rebar;
- Surface layers of concrete are expected to be the most damaged, somewhere spalled and overall with possible deteriorated cohesion to reinforcement;
- Due to damage of concrete cover layers and drop in its tensile strength the bond strength between concrete and reinforcement is generally affected and reduced;
- Structural system of structure might be changed after fire event due to overloading of some cross-sections and propagation of plastic deformations.

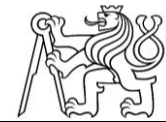
Based on specific conditions, type and extent of damage and number of other aspects (financial demands of refurbishment, possibility of enlarging elements, difficulties of conducting the strengthening, structural engineer's experience with strengthening design, etc.) the structural strengthening can be realised by enlarging cross-sectional area (using concrete, mortar or shotcrete jacketing), steel jacketing, applying external post-tensioning, adding reinforcement (conventional or high-strength reinforcement or fibre-reinforced polymer (FRP) reinforcement) or by combination of previously mentioned options. Adding new support to the damaged member can also solve the problem with insufficient load-bearing capacity, however it is not enhanced directly, but due to new support the distribution of internal forces changes (new support is placed to such spot that internal forces decreases in selected critical cross-section). This should be done carefully as in case of concrete structures adding new support can result in creation of hogging bending moment in part of element with no or only weak top reinforcement. Nevertheless, general principle of structural strengthening lies in the activation of strengthened elements and new parts of their cross-sections respectively. To achieve the highest effectivity of strengthening, the strengthened member has to be unloaded as much as possible since the strengthening action contributes to the total load-bearing capacity only to the part of loads that act on both old and new parts of cross-section. In real it means the element that is about to be strengthened should be loaded only with self-weight and necessary other dead load, however with no live load.



One of the most important aspects of structural strengthening is to provide sufficient cohesion between old and new part of cross-section to ensure mutual behaviour and deformation of coupled cross-section, to eliminate slip between both parts and to exploit the synergic effect of strengthening as much as possible. Ensuring cohesion can be achieved by special shear reinforcement or steel dowels connecting both parts or by roughened interfacial surface. The option with shear reinforcement is typical for precast concrete-on site concrete composite elements, steel dowels are typical for steel-concrete composite elements. However, in case of additional strengthening using shear reinforcement or dowels is usually not possible and the needed cohesion has to be achieved by friction between rough surfaces. The friction coefficient can be also increased by transverse confinement generated by steel jacketing or post-tensioning. Achieving selected cohesion between old concrete and new one can be tricky. New layers of concrete are applied or shot directly to the old concrete cover layers which are the most damaged as it was already mentioned in this chapter. Such damaged concrete layers can have deteriorated its cohesion to reinforcement significantly and could split from it or the rebars could slip. Typical example of such case is a floor slab. In general, it is exposed to fire from the bottom which results in damaging the concrete cover the most. Due to volumetric changes, drop of tensile strength and differential thermal expansion of concrete and reinforcement the bond strength and cohesion between both materials decrease. In case of shotcreting new layers to the bottom of the slab cohesion between old and new concrete could be sufficient but the weakest part might be the interfacial zone between old concrete cover and bottom reinforcement which could control the overall load-bearing capacity. To avoid such risk, the old deteriorated concrete cover is often removed from the element usually up to the reinforcement and to such surface new concrete is attached. Old concrete layers are removed using jackhammering, sand blasting or hydro blasting [38]. After such steps the surface of old concrete is usually rough enough and therefore suitable to be jacketed by new concrete.

Beside ensuring activation of coupled composite cross-sections and sufficient cohesion between old and new parts of cross-sections there are two more important aspects that have to be taken into account. The designed way of structural strengthening has to be carried out with respect to the target fire resistance of selected members according to the requirements of building's future use. If the fire resistance is not fulfilled, appropriate fire protection has to be designed and conducted. The second important aspect is related to the process of concrete carbonation. Said in simplified way, carbonation is a natural degradation process when carbon dioxide ( $\text{CO}_2$ ) permeates into the concrete matrix and reacts with portlandite  $\text{Ca}(\text{OH})_2$  when water  $\text{H}_2\text{O}$  and calcium carbonate  $\text{CaCO}_3$  is created. Environment in young concrete is strongly alkaline with pH somewhere in between 12-13 and thanks to it the reinforcement is naturally protected against corrosion. However, change of  $\text{Ca}(\text{OH})_2$  to  $\text{CaCO}_3$  gradually lowers inner pH level. When pH is around 9, the reinforcement ceases to be protected and is prone to start corrode (due to water and oxygen exposure). In general, the carbonation is slow process that takes place during whole life cycle of concrete structure affecting surface layers at first but gradually penetrating inner layers as well. However, when concrete structure is exposed to fire, the process is much more accelerated due to fumes and smoke produced by combustion [51]. Thus the structure after fire exposure should be treated with respect to this phenomenon and higher risk of reinforcement corrosion during future use. To lower the risk uncovered rebars should be preserved with anti-corrosion coating before being covered with new concrete or mortar again and the exposed concrete surface should be deeply penetrated with special anti-carbonation solution.

It is also worth to mention that ensuring sufficient load-bearing capacity of damaged structural member might not be the biggest problem. Due to high temperatures exposure Young's modulus of both concrete and steel decreases (partly irreversibly) and therefore the bending stiffness drops. As a result, deflection of an element rises during fire, however it does not come back completely after the end of fire and stays as residual (see Chapter 2.4). Structural strengthening conducted afterwards is related primarily to the ultimate load-bearing capacity, not serviceability. Reducing deflections is very tough problem even in case of new or undamaged structures and there are not many ways how to achieve it.



Therefore, in some cases the exceeded deflections (vertical and horizontal as well) might be the reason to replace the element, or in case of bigger extent to pull the building down even though reaching the needed load-bearing capacity might not be unachievable problem.

### Cost-Effectiveness Analysis (CEA)

The decision whether to conduct refurbishment, repair the structure and ensure its adequate load-bearing capacity, serviceability, fire protection and durability for future use, or contrary pull the building down and build a new one, can be very difficult. At the same time, it has to be made in every case of post-fire process investigating fire damaged building. Such decision has to be made together by a group of involved and competent people (owner of the building, local authorities, civil and structural engineer, fire brigade representatives).

Making the decision gets even more difficult with increasing damage level of the structure. Investigating the residual material parameters and conducting material tests (which are essential and necessary for post-fire structural assessment), designing refurbishment and eventual structural strengthening, but primarily carrying out the refurbishment and strengthening cost all together enormous amount of time, money and human labour. Therefore, the decision has to be considered very carefully and should be made as objectively as possible. For this purposes these assessments are recommended to be made to help with making the decision (some of them are even obligatory in the legal process):

- To know what part of nonload-bearing and complementary structures (windows, doors, floors, partitions, thermal insulation, sanitary equipment, ducts, pipes and wiring, etc.) are damaged and have to be replaced or renewed a visual interior and exterior assessment is conducted by civil engineer and other specialists;
- To know what is the residual structural performance, whether the building is safe and stable and whether the deep refurbishment and structural strengthening is necessary a post-fire structural assessment is elaborated by specialist-structural engineer;
- To know how important from social, cultural and historical point of view the damaged building is and how big public interest in preserving the building an official statement of local authorities is made;
- To know what impact on nature and sustainable approach to building industry possible options have a statement of local municipal environmental department is made. If legally binding statement is needed an environmental impact assessment (EIA) is elaborated.

Based on aforementioned assessments and statements an analysis, which is usually the most important document for the building's owner in the environment of western society, can be conducted. The analysis is obviously related to money and is called *cost-effectiveness analysis* (CEA). Its task is to consider all actions and steps that have to be done on the way towards using the building again (either repaired old one or built new one instead of damaged old building), estimate the needed time for carrying the chosen process out and mainly appraise the financial demands for conducting such process. In the appraisal there should be incorporated a sort of weight system to make possible taking into account owners preferences for individual items. The time when building is unable to be used has to be taken into account as well. Possible financial risks and threats should be added to make the analysis more accurate. When all aspects are considered and the final assumed amount of time and money is estimated, results of possible solutions are compared. Based on such comparison it is easier for building's owner to decide whether preserve the old building and conduct the refurbishment or pull the old building down and build a new one instead. The comparison of both ways can be seen in Fig. 3-3. The final comparison can be expressed in simplified way using Eq. (3-1).

$$\Sigma(\text{financial demands})_A \cong \Sigma(\text{financial demands})_B \quad (3-1)$$

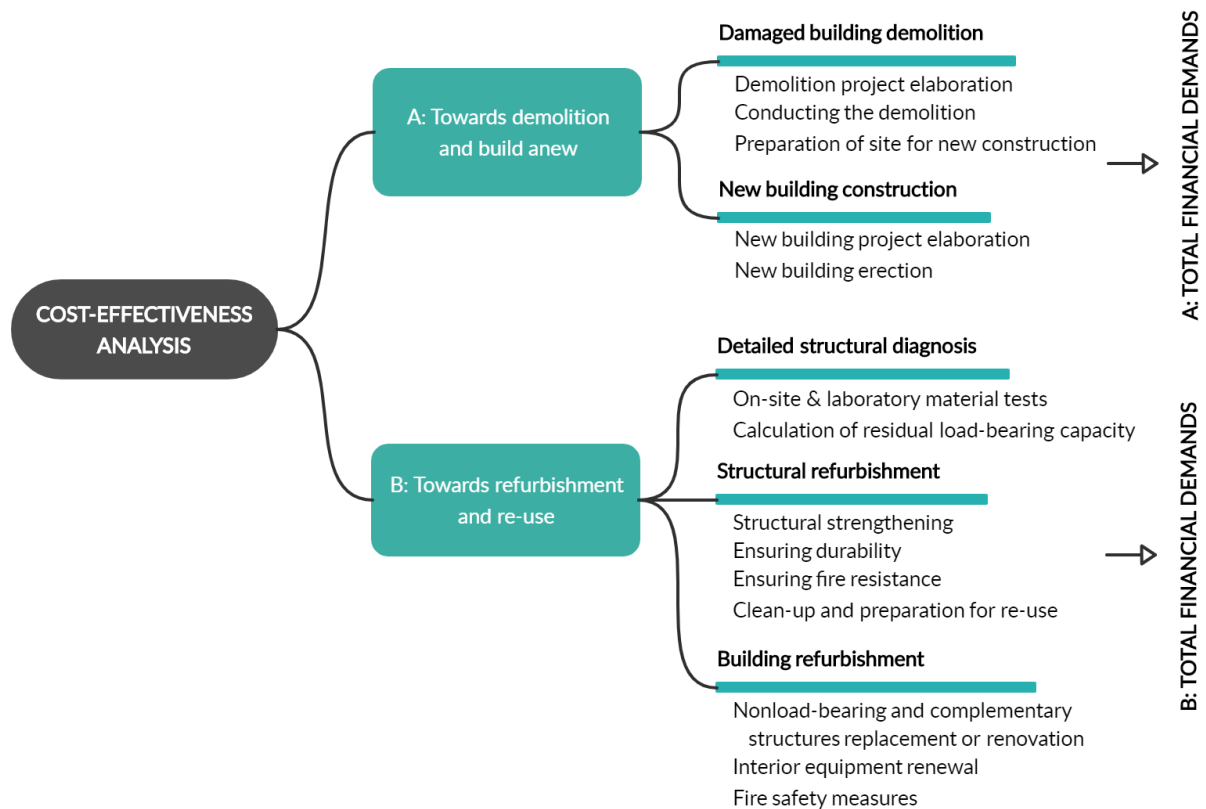


Fig. 3-3. Simplified interpretation of possible ways of fire damaged building treatment related to CEA.

### Object Demolition

Building demolition is an extreme option how to treat a building after exposure to fire event. It is usually chosen because no other option is either possible or (financially or socially) valuable due to excessive damage level, poor residual structural performance, financial and time demands of eventual refurbishment and social or cultural substitutability of the building. The demolition has to be approved in advance by local authorities and owner of the building, while assessment made by structural engineer is usually needed.

In the legal process of authorities' approval, a project of demolition works has to be elaborated. One part of the project is dedicated to structural aspects of demolition and contains description of approach how to conduct the demolition, order of dismantled elements, appropriate tools and mechanization which should be used for demolition. All of it is related to preserving stability of the building which is being demolished and ensuring safety for workers on site as well as for people, animals, other buildings and properties in surroundings. The Thesis is not aimed at problematics of building demolitions and hence it will not be discussed further on.



## 4 Preliminary Inspection of Damaged Building

### 4.1 General Aspects of Preliminary Inspection

After the end of fire event the subjected building is let for some time to cool back to ambient temperature and to see if it is still stable and safe enough to be entered, as it is described in [Chapter 3.2](#). In case the building does not show any evolving structural problems and continuing processes and seems to be in steady-state at the same time, then the preliminary post-fire inspection is about to be conducted. It is important to mention all actions and steps of preliminary inspection have to be done primarily with respect to safety of investigators and other involved people. If the structure is damaged to bigger extent there should be an option to operatively prop selected elements to ensure safety of motion in interiors at least for limited amount of time, for instance by using timber struts and falsework. Such action is usually prescribed by structural engineer. If the safety is ensured the inspection can proceed and is usually carried out to obtain more specific idea about the fire event, particularly:

- Area and number of floors affected by fire;
- Probable ignition spot of fire;
- Duration of fire measured from flashover effect;
- Maximal reached temperatures in individual compartments or regions;
- Damage severity of structural elements caused by fire;
- Overall ratio of damaged and undamaged structural elements.

At this stage of post-fire investigation only visual assessment is usually carried out. So far known information about fire event is essential and helps with conducting the assessment. This information is then amended by information gained on-site, usually according to the state of various items and their reaction on high temperatures (see [Tab. 3-1](#) in [Chapter 3.1](#)). According to the available evidence maximal reached temperatures in compartments can be approximately estimated and together with fire duration gained from firefighting report the idea about structural damage is obtained. The evidence about structural damage can be also provided by visible signs. If the damage is rather lower, no special signs may be visible. However, if the damage is more significant, specific types of failures usually develop and these help to select more damaged members and focus on them in the forthcoming investigation. Overview of signs that are often related to more serious structural damage can be seen in [Fig. 4-1](#).

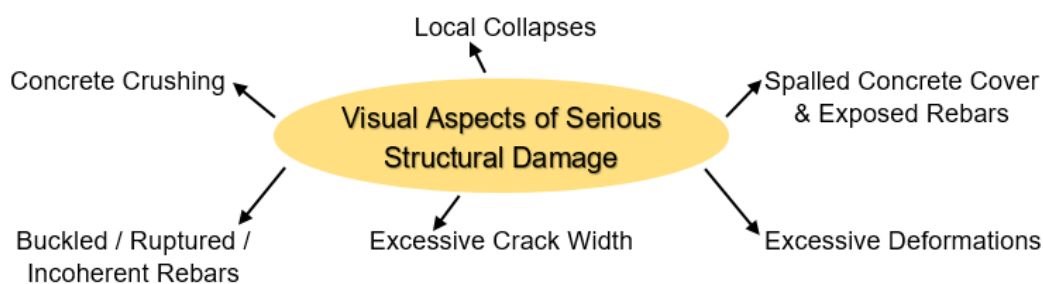


*Fig. 4-1. Visual aspects of possible serious damage of concrete structure caused by fire event.*

If some of the mentioned information is missing different investigation approach may be needed. Lack of information about maximal temperatures and their duration can be substituted by material tests, however simple and fast on-site tests can provide elementary idea about the damage severity. *Rebound hammer test* measures the hardness of surface concrete and can give the idea about maximal temperatures in surface layers and therefore approximately temperature profile of the whole cross-section. *Hammer and chisel test* can (based on sound) then give information about compactness of concrete and cohesion of its surface layers to inner concrete layers and reinforcement. Both methods are necessary to be conducted also on the undamaged part of concrete structure in order to compare both results and get relative conclusions. More about testing methods can be found later on in [Chapter 6](#).





## 4.2 Classification to Damage Classes

During the preliminary inspection a general idea about fire event, its extent and time duration is obtained based on the firefighting report and evidence revealed on-site. Moreover, visual assessment of structural elements is carried out which provides basic overview of damage severity. Based on the sum of gained information the structural members located inside the area and floor affected by fire can be classified into *damage classes* according to amount of signs and evidence. Such classification helps to estimate the overall state of structural performance, roughly estimate the costs of potential refurbishment and select the most damaged elements which may represent the weakest part of the structural system. Several classification approaches have been published in the literature so far (e.g. [28]), though approach proposed by British Concrete Society [38] seems to be the most comprehensive one. The classification key is summed up in the [Tab. 4-1](#).

The published algorithm deals only with reinforced concrete structures and introduces 5 damage classes in total (0-4), where structure not influenced by fire is marked as “class 0” and structure very much damaged by fire is marked as “class 4”. The elements are then distinguished according to their type – whether it is plain- or linear-like element and whether it works mainly as flexural or compressive element. The classification aspects are divided into two groups – (i) appearance of concrete surface, and (ii) structural conditions. Both groups have number of more particular classification aspects. In case of “appearance of concrete surface” group state of element’s finishing (either plastering or coating) is assessed, then the colouring of visible concrete surface is described and the last aspect is related to possible crazing of concrete surface. These aspects thus describe primarily the extent of element’s exposure to high temperatures according to condition of its surface layers. On contrary, in case of “structural condition” group the investigated aspects are directly connected to the load-bearing capacity of a structural member and its decrease, respectively. Phenomena like spalling of concrete surface layers and related exposure of reinforcement, conditions of reinforcement (cohesion with concrete, potential buckling or rupture of bars), crack propagation together with their width and finally deformation of elements are considered and classified. Logically, the less of mentioned signs are found on elements, the less the members are assumed to be damaged and the lower damage class mark they obtain – and vice versa.

From the non-structural aspects group, the damage of finishing on elements as well as its crazing or crazing of the concrete surface layers are mostly induced by fast dehydration of the material and consequent shrinkage. Thus tensile cracks propagate and in case of plastering or coating the cohesion to the base decreases and may end in sloughing the finishing layer off. Concrete colouring is caused by chemical changes in the matrix and is usually connected to the aggregate compound. More about this phenomenon and related testing technique can be found in [Chapter 6](#). From the structural aspects group, the risk of spalling is basically driven by elements moisture content and the heating rate caused by fire. Beside lowering the cross-sectional area, the most dangerous impact of spalling is making the reinforcing bars directly exposed to fire and high temperatures. Both of mentioned results directly influence the load-bearing capacity. Cracks that create and propagate due to fire are basically caused either by stiffness or tensile strength decrease, considerable strains of both concrete and steel, by thermal effects or by excessive deformations in vertical or horizontal direction. Such cracks influence mainly serviceability and durability of the structure, however moment of inertia is also affected and thus crack creation and propagation contribute to the redistribution of internal forces. Assessing structural damage according to the deformation and mainly deflection is very important and frequent diagnosis technique used commonly even in case of non-fire damaged structures, mainly because the deformation is usually directly visible and is proportional to the structural performance. According to measured residual deflections fire severity and structural damage can also be approximately estimated.





Tab. 4-1. Classification of structural damage caused by fire according to [38].

Damage class	Element	Surface appearance of concrete			Structural condition			Cracks	Deflection/ distortion	
		Condition of finishing	Colour	Crazing	Spalling	Exposure and condition of main reinforcement*				
0	Any	Unaffected or beyond extent of fire								
1	Column	Some peeling	Normal	Slight	Minor	None exposed	None	None	None	
	Wall									
	Floor slab									
	Beam									
2	Column	Substantial loss	Pink/red**	Moderate	Localised to corners	Up to 25 % exposed, none buckled	None	None	None	
	Wall									
	Floor slab									
	Beam									
3	Column	Total loss	Pink/red** Whitish grey***	Extensive	Considerable to corners	Up to 50 % exposed, not more than one bar buckled	Minor	None	None	
	Wall									
	Floor slab									
	Beam									
4	Column	Destroyed	Whitish grey***	Surface lost	Almost all surface spalled	Over 50 % exposed, more than one bar buckled	Major	Any distortion	Severe and significant	
	Wall									
	Floor slab									
	Beam									

Notes:

\* In the case of beams and columns the main reinforcement should be presumed to be in the corners unless other information exists.

\*\* Pink/red discolouration is due to oxidation of ferric salts in aggregates and is not always present and seldom in calcareous aggregate.

\*\*\* White-grey discolouration is due to calcination of calcareous components of cement matrix and (where present) calcareous or flint aggregate.



### 4.3 Output of Preliminary Inspection

If the preliminary post-fire inspection is done and the idea about extent and severity of the structural damage caused by fire is obtained, it is appropriate to mark graphically all gained information to a drawing in order to make it clear and organized. For such purposes it is favourable to get the project documentation. In case of older building with drawings only in paper form a photocopy of selected drawing is made and notes from the inspection is made by hand. In case the subjected building is rather new, project documentation in digital version might be available – then it is suitable and easy to make the notes on computer using some of available CAD software. According to author's opinion it is suitable to work with both civil engineer and structural drawings at the same time. The structural drawings are necessary because the shape and specification of structural elements have to be visible and are about to be classified. The civil engineer drawings are then useful since partitions, soffits and other complementary constructions are visible. Especially the partitions are important since they divide the inner space and may also serve as outer boundary of fire compartment and therefore influence the fire spread. To continue with, it is useful to treat both types of drawings as external references with possible partially hidden visibility. Then the newly drawn lines and notes will be clearly visible.

An example of such graphical output was elaborated. The virtually subjected object is a Harfa residential building<sup>5</sup>, twelve-storey residential building made primarily of concrete and masonry. It is located in Prague, Czech Republic, in district called Vysočany. Floors 2-12 are dedicated to apartments whereas the parterre is meant to serve as commercial space. For example purposes a part of first above-ground floor is used. The fictitious fire could start by a short circuit in an electrical device in restrooms for employees of the shop. The spot is marked with sign *ignition spot* with approximate time of fire start. From there the fire would spread to the surrounding compartments, for instance through opened door. The overall area affected by fire is highlighted in the plan and it is divided into several smaller areas (*damage zones*) according to approximately estimated maximal reached temperatures and duration of fire exposure – both information is mentioned in the drawing. Within the highlighted area every structural member has its mark with evaluated damage class and mentioned element type. If a floor slab or wall would not be damaged uniformly in the damaged zone, there should be drawn another classification mark with indicated extent. Elaborated graphical report of the preliminary inspection can be seen in Fig. 4-2.

At the very end of the preliminary post-fire inspection decision about future steps and forthcoming investigation approach have to be done. At this moment it is neither necessary nor useful to make the decision very detailed with specific steps what to do with the structure afterwards. The decision should only deal with the question whether it is either probable that refurbishment and rehabilitation of the structure is possible and economically, socially and culturally favourable. In this case the investigation process continues with detailed inspection and structural diagnosis. Or on the other hand whether the damage level and extent, which were investigated briefly within the preliminary inspection, are so large that it can be stated with high probability that rehabilitation is either not possible or would not be valuable. In such case the process continues towards building demolition. Answering to this question is the key aspect of the preliminary post-fire inspection.

---

<sup>5</sup> Harfa residential building is real object under construction (year 2020). It is a project of the Czech biggest residential developing company CENTRAL GROUP, a.s. Structural part of the project was made by structural office STATIKON Solutions s.r.o. For more information, see [52].

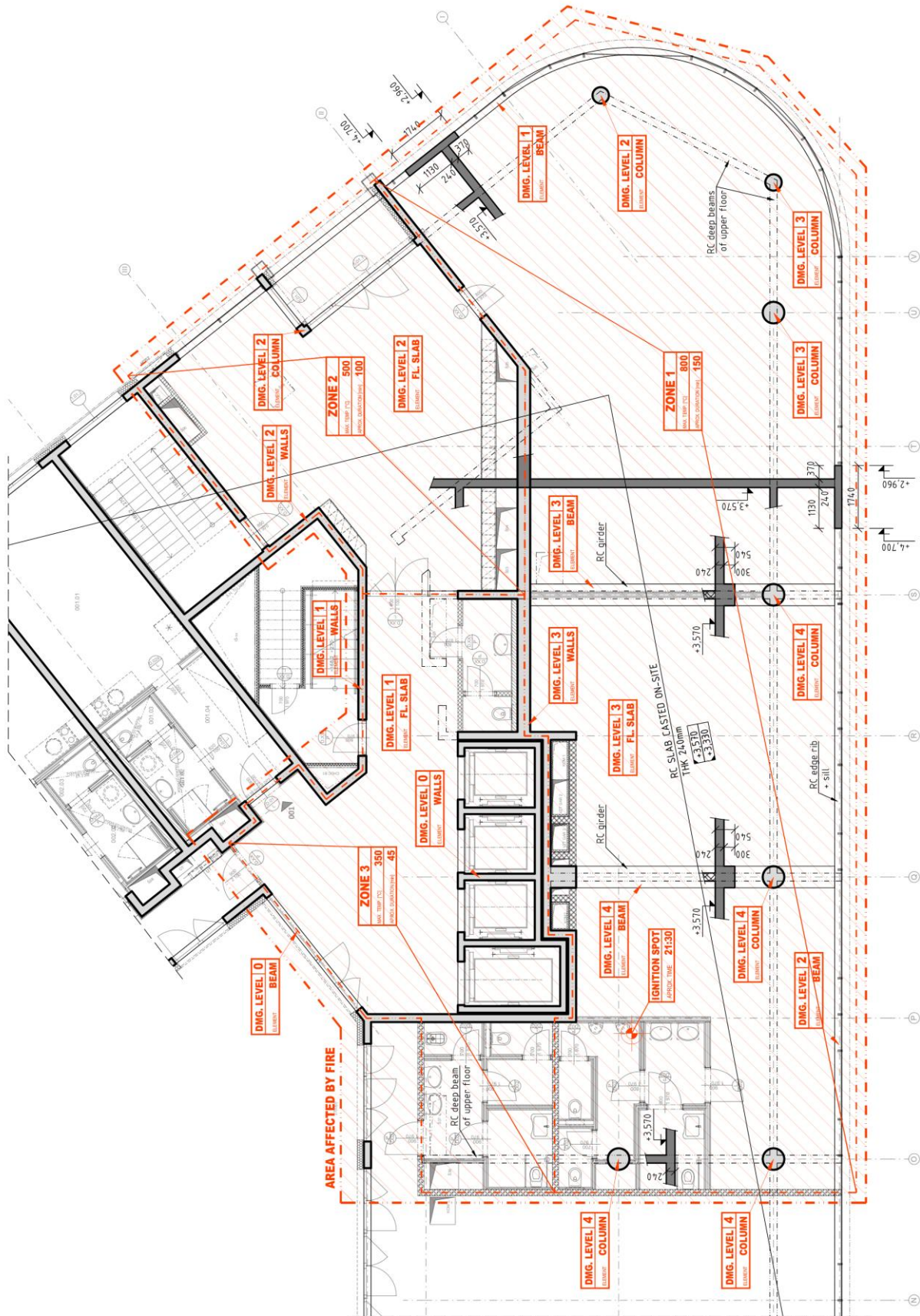


Fig. 4-2. Example of graphical output based on preliminary post-fire inspection drawn into the shape of ground floor.





## 5 Detailed Inspection of Damaged Building

### 5.1 Amending Information from Detailed Post-Fire Inspection

If the investigation process gets to this point and the detailed post-fire structural inspection is about to be conducted, it means the subjected building is not in a critical state and there is a need to get more detailed information about the structural damage caused by fire in order to estimate the residual structural performance, design eventual refurbishment and to return the building back to its using. At this point fundamental information about the fire event, its extent and probable severity and also the damage level of structural elements are known based on the preliminary inspection carried out earlier. Aim of the detailed inspection is to amend information necessary to conduct post-fire structural diagnosis and to carry out the calculation of residual structural performance.

First of all, it is essential to obtain the original building's project documentation from building owner or local building bureau – if the documentation is not available, it represents considerable problem. The more actual and detailed the documentation will be, the better. For instance, it should contain eventual refurbishment and (mainly but not only) structural changes realized in the building over the years so far. Beside structural and also civil engineering drawings, the documentation should also contain detailed technical and structural report, reinforcement drawings with details and sections in case of concrete structures and drawings of details and joints in case of steel and timber structures. The documentation should be related to the whole structure (and not only floor(s) subjected to fire) because of possible mutual affecting of whole structural system. Generally, before carrying out the detailed inspection these aspects about the building's structure should be known from the documentation:

- Construction system of the building (at least its wider part including the fire affected one);
- The way how vertical loads are transferred from floor slabs to foundations;
- The way how spatial stability is ensured, bracing is done and how horizontal loads are transferred from façade and roof to foundations;
- Positions and continuity of vertical load-bearing elements over all floors;
- Special and uncommon structural solutions, particularly in transition floors;
- The type of building's foundations;
- Eventual structural fire protection prescribed in the project.

After gaining comprehensive idea about the subjected structure the detailed inspection is carried out. During it the main attention is paid to structural members marked as more significantly damaged, which would correspond to damage classes 2-4 (see [Tab. 4-1](#)). In order to assess their damage precisely, information about material deterioration are needed. These elements are thus about to be inspected by particular on-site and laboratory tests. In case of laboratory tests concrete and steel specimens are needed, therefore number of spots suitable for samples extraction are chosen. Conducting material test should provide as much information as possible, in ideal case not only about the particular element but also about its surroundings, maximal reached temperatures and estimated fire duration. Fire scenario approximation and particularly fire event remodelling based on available information can significantly help with choosing the most cogent elements for inspection (see [Chapter 5.2](#)). After picking up the structural elements that are about to be inspected by material tests and choosing suitable spots for extraction of concrete and rebars samples, all of such information and guidelines have to be written somewhere – it is beneficial to do it in the same graphical output as was elaborated as a result of preliminary inspection (see [Fig. 4-2](#)); then all results of both preliminary and detailed inspections will be recorded in the same source. It is also necessary to specify the exact position of non-destructive testing and extraction of samples (e.g. in the middle of the elements height, 0,5 m below soffit, etc.). Example of such graphical output is presented in [Fig. 5-1](#), which would be then the basic document and guideline for the company conducting structural diagnosis.







## 5.2 Fire Scenario Approximation

### Effect of Fire Scenario Assumption

One of the classification aspects proposed in [Tab. 4-1](#) is assessing the surface condition and colouring. Changes of such states are related to high temperatures exposure and its duration and severity. If it is possible to estimate the maximal surface temperature based on the visual assessment and results of various material tests (see [Chapter 6](#)), together with presumed fire scenario the temperature-time curve can be roughly approximated. Then, based on the curve thermal analysis of selected members can be conducted which can provide very useful and more detailed information about material deterioration.

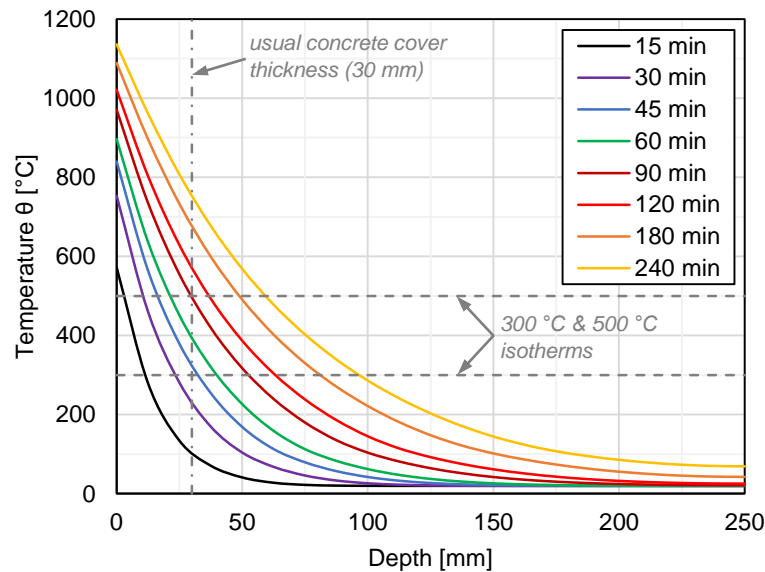
However, approximation of temperature-time curve according to assumed fire scenario seems to be the crucial step in this investigation technique. The process of natural fire is unique every time and is influenced by number of boundary conditions and input parameters. Therefore, it is hard to describe it mathematically, nevertheless such description is necessary when thermal analysis of structural members is about to be conducted. Design code EN 1991-1-2 [[16](#)] proposes several options how to take the effect of fire into account. The simplest way is to use some of the nominal temperature-time curves – the most common and generic one is the standard temperature-time curve (also called as *ISO834 temperature-time curve*). These curves are defined using simple logarithm-like equations according to which the gas temperature still increases until the end of considered time period; it means no cooling phase takes place. Moreover, uniform gas temperature in whole compartment is assumed. They are very easy to use, but due to their simplicity and versatility these curves cannot describe the process of fire and combustion precisely. In some cases, the reality and mathematical assumptions can differ greatly. More sophisticated models of fire are available as well (parametric curves, local fires, zone models, computational fluid dynamics). These approaches are more cogent and precise but more time demanding and laborious at the same time. In the stage of fire safety project elaboration, the usual way when selecting the fire scenario is to find a compromise between desired conciseness and precision on one hand and demands of labour, time and energy on the other. For design purposes often rather simple fire scenarios and temperature-time curves are used. However, if approximation of temperature-time curve based on post-fire structural assessment is about to be done, it is probable that more precise models suitable for the specific compartment and other boundary conditions will be needed.

### Case Study: Thermal Analysis according to Selected Fire Scenario

In order to show the differences between selected fire scenario and subsequent thermal analysis with its impact on structural performance a case study was conducted. At first thermal analysis of 250 mm thick concrete slab was carried out, when one-sided exposure to standard fire according to ISO834 temperature-time curve was presumed. Temperature profiles of the slab can be seen in [Fig. 5-2](#). The curves are proposed for various fire durations, from 15 to 240 minutes. Isotherms 300 °C and 500 °C and usual concrete cover thickness are also highlighted in the diagram. Based on the selected fire scenario and thermal analysis following statements can be made:

- Fire durations up to 60 minutes are usually not a problem for concrete structural elements as temperature in tensile reinforcement is still below or equal to 400 °C which represents sort of borderline in its mechanical parameters decay and concrete heated over 500 °C is less than 25 mm thick.
- Fire duration longer than 60 minutes should be considered as potentially dangerous since more significant decay of load-bearing capacity can be expected.
- Fire durations longer than 90 minutes causes rapid drop of reinforcement yield strength and concrete cover in its whole thickness is very much damaged since it is heated to more than 500 °C.
- Fire duration of 120 minutes and more represents big threat to the structural performance because of critical deterioration of both concrete and reinforcement.

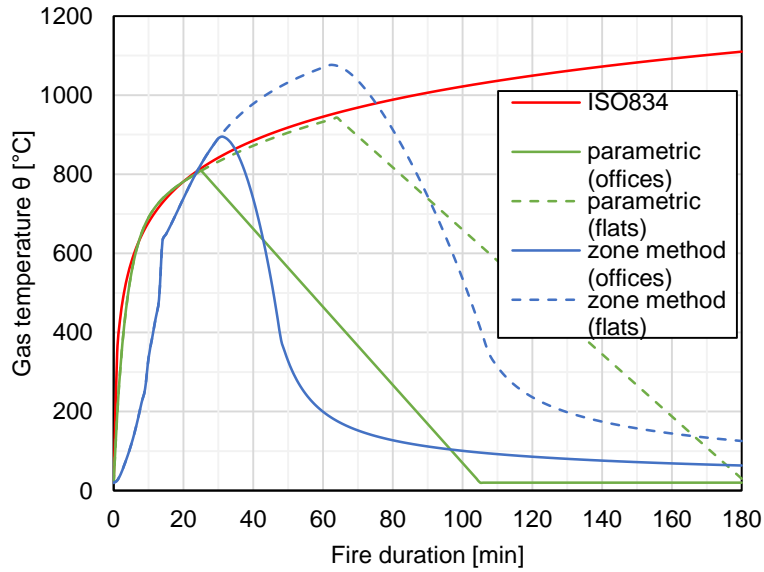




*Fig. 5-2. Temperature profiles of 250 mm thick concrete slab, subjected to one-sided standard fire exposure for various durations; thermal analysis conducted in TempAnalysis software [53].*

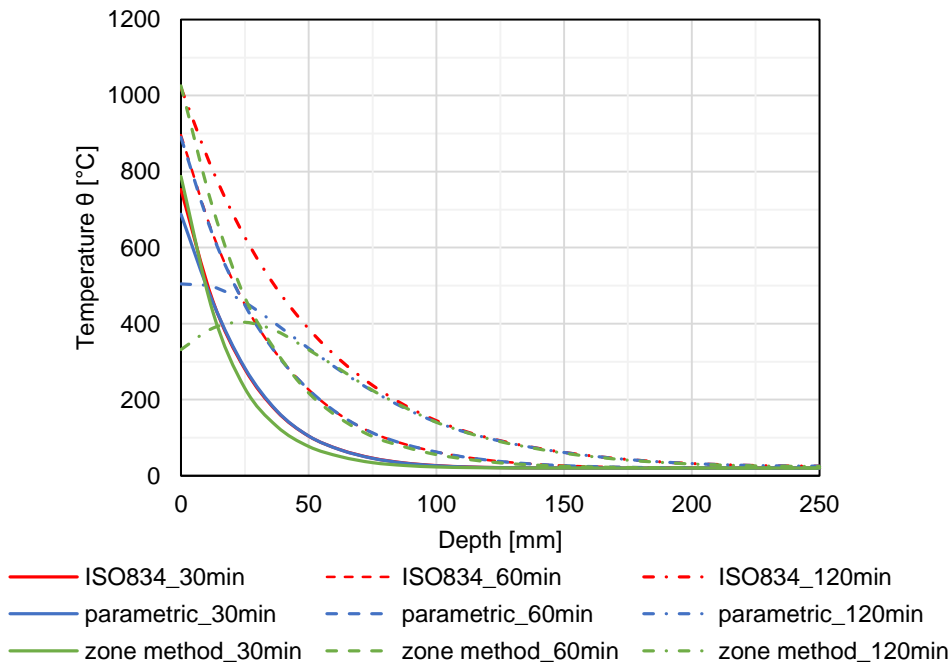
Conclusions mentioned above are thus directly influenced by selected fire scenario and temperature-time curve. Let's say different fire scenario would be chosen. The example compartment is 10 m long and 5 m wide, 3 m high with 2 windows in perimeter walls. Floor and ceiling are made of concrete; walls are made of standard masonry. At first it is presumed the room serves as an office, later on it is presumed to be a flat. In case of office usual fire safety active measures are assumed (automatic fire detection by heat and smoke, safe access routes, firefighting devices and smoke exhaust system), in case of flat automatic fire detection devices are not considered. With such boundary conditions parametric temperature-time curve according to Annex A [54] and zone method temperature-time curve according to *Ozone* fire software [55] are calculated. Diagram with all mentioned curves can be found in Fig. 5-3.

Based on the diagram it can be stated that the curves are either identical or very close to each other up to approximately 30 minutes (in case of assuming the compartment is office) or 60 minutes (in case of assuming the compartment is a flat). After reaching mentioned times the curves start to differ dramatically as in case of parametric and zone method curves the cooling phase takes place which is a phenomenon that ISO834 curve cannot consider. Due to it, according to the two mentioned curves gas temperature starts to decrease gradually, whereas gas temperature according to ISO834 curve still increases. Difference in gas temperature based on selected temperature-time curve is thus getting bigger until the end of selected time. For example, at time  $t = 120 \text{ min}$  the temperature difference is tremendous.

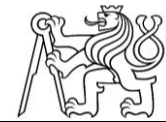


*Fig. 5-3. Temperature-time curves according to different fire scenarios and compartment parameters.*

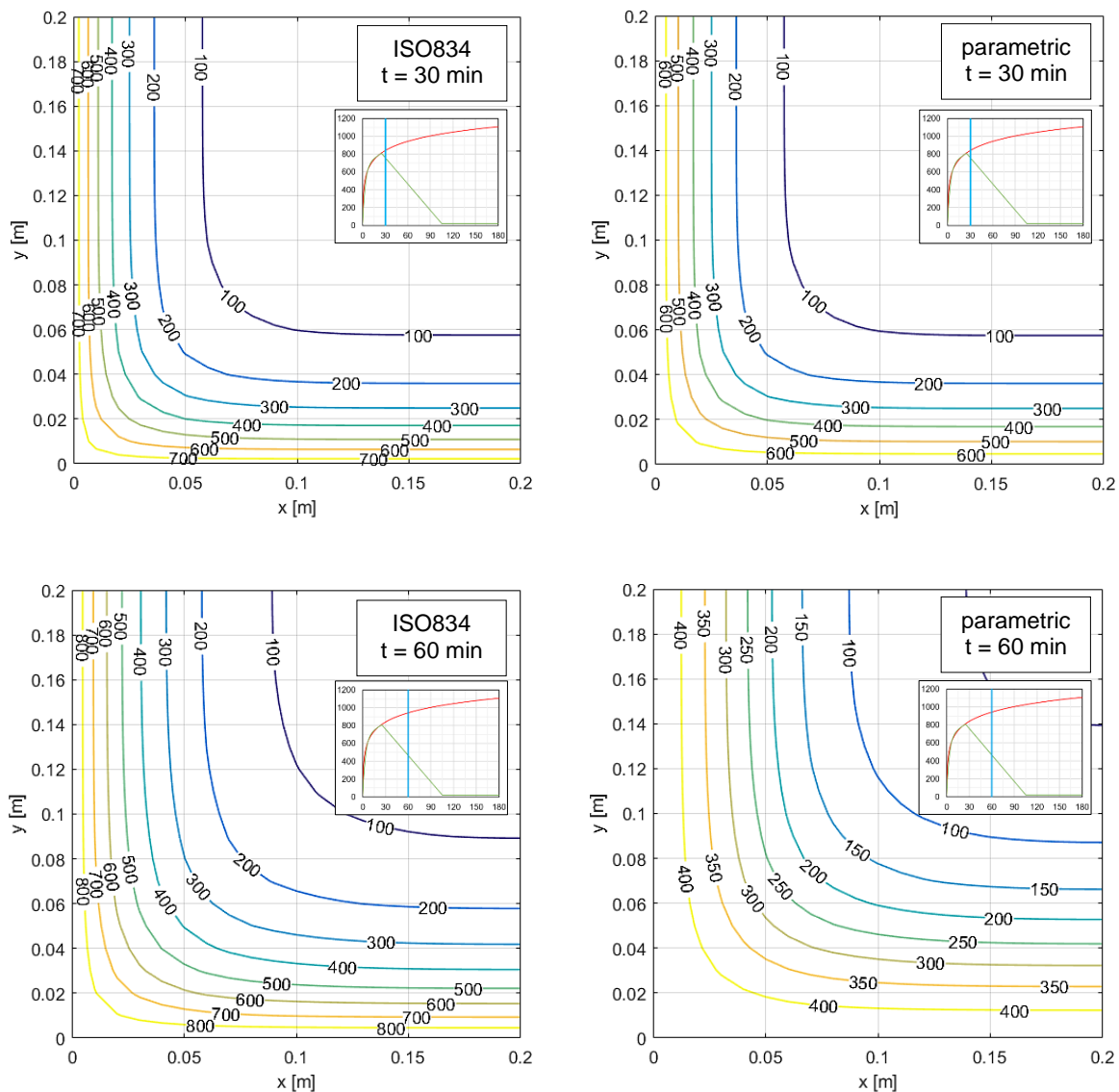
When thermal analysis of the mentioned 250 mm thick concrete slab is carried out based on the temperature-time curves proposed in Fig. 5-3, temperature profiles shown in Fig. 5-4 are obtained. In case of parametric and zone method temperature-time curves, only flat compartment is considered. From the temperature profiles it can be stated, that up to time  $t = 30 \text{ min}$  and  $t = 60 \text{ min}$  all curves are practically identical which corresponds well with the temperature-time curves. However, in case of long fire duration ( $t = 120 \text{ min}$ ) different temperature profiles can be seen. In parametric and zone method curves the cooling phase already begun which causes decay of surface temperature, the curves start to correspond again with the curve based on ISO834 fire scenario in depth approximately equal to 75 mm. This fact is very important since temperatures in reinforcement and surface concrete layers are very different and thus conclusions about material deterioration will differ as well.



*Fig. 5-4. Temperature profiles of 250 mm thick concrete slab, subjected to one-sided fire exposure according to different fire scenarios and durations; thermal analysis conducted in TempAnalysis [53].*



Another example of the impact of temperature-time curve approximation can be seen in series of diagrams in Fig. 5-5. Thermal analysis of square-shaped cross-section exposed to fire from all sides is proposed (one quarter of cross-section is displayed) for various fire durations and based on ISO834 temperature-time curve (diagrams in left column) and parametric curve (diagrams in right column). In case of parametric curve, the compartment used as flat is considered (other boundary conditions are preserved). Based on the results it can be stated that until fire exposure up to 30 minutes the temperature profiles are very similar, layer of concrete heated to 500 °C or more is approximately 10 mm thick and reinforcement temperature is approximately equal to 300 °C (one corner bar is assumed). Since cooling phase starts after 30 minutes in case of parametric temperature-time curve both temperature profiles differ from this point on. According to standard fire curve concrete layer beyond 500°C isotherm is 30 and 50 mm thick for 60 and 120 min duration of fire, respectively. Rebar temperature is then approximately 450 and 700 °C, respectively. Based on such information it seems the cross-section is significantly damaged. On contrary, in case of parametric curve due to cooling phase the temperature distribution along cross-section at 60 and 120 min fire duration is more favourable than at 30 min fire duration with consequent positive effect on load-bearing capacity.



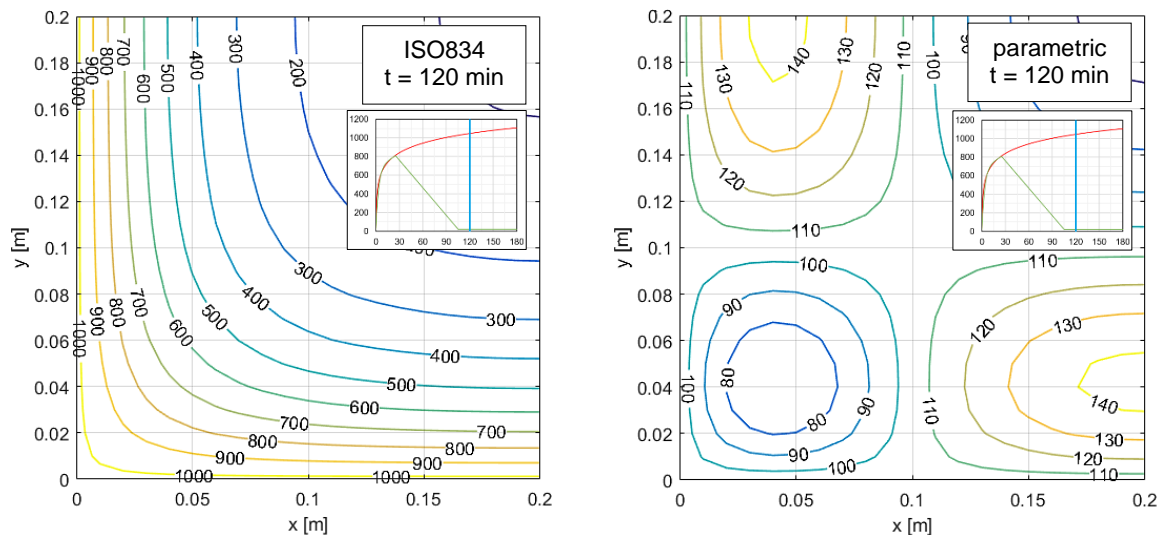


*Fig. 5-5. Temperature profiles of 400x400 mm concrete cross-section, subjected to four-sided fire exposure for different fire scenarios and durations (one quarter of cross-section displayed); thermal analysis conducted in TempAnalysis software [53].*

### Advanced Modelling Methods of Natural Fires and their Use in Post-Fire Investigation

Options of fire effects mathematical modelling were mentioned in the previous chapter and the effects on subsequent thermal analysis of the structural elements subjected to fire were shown as well. In the real post-fire investigation, a cogent fire scenario is searched mainly because it could provide priceless information to the forthcoming investigation, ensure more effective approach, reduce the amount of material tests and thus save a lot of time, money and labour. However, all these benefits are directly dependent on the accuracy of approximated fire scenario.

The simplest way is to use some of the nominal temperature-time curves. However, it is very probable that such fire scenario will be considerably different from the real fire event because neither specific boundary conditions nor cooling phase can be taken into account. Therefore, according to author's opinion it is believed that at least parametric temperature-time curve should be always used. In simplified way, it could take into account the specific boundary conditions of the compartment, fire load according to the purpose of use, conditions of ventilation and the cooling phase. Without by-hand calculations the parametric temperature-time curve can be easily obtained using some of the available software, e.g. *FINE Parametrická teplotní křivka* [56]. If the parametric temperature-time curve cannot be used because the conditions specified in [16] are not fulfilled, or more precise fire scenario is needed, localised fire or zone method models should be used. These approaches are still relatively easy and not time-demanding and can take into account even more input parameters on one hand and provide more detailed information about the fire event on the other. In case of zone method, the calculation can provide information about evolution of temperatures in both hot and cold zones, rate of heat release, height of the zones interface and time when fuel is burned out and cooling phase begins. The fire load can be assumed either according to purpose of compartment use which is well defined in [16] or can be defined completely by user – number of items, their position, material together with thermal properties, time or temperature when they catch on fire, detailed specification of ventilation, effects of sprinklers, etc. In case of fire load defined according to design code *Ozone* fire software [55]. In case of user defined conditions the *CFAST* fire software [57] is more appropriate due to high number of possibilities and options. Figs. 5-6 to 5-8 are results from it and are related to the same example compartment.

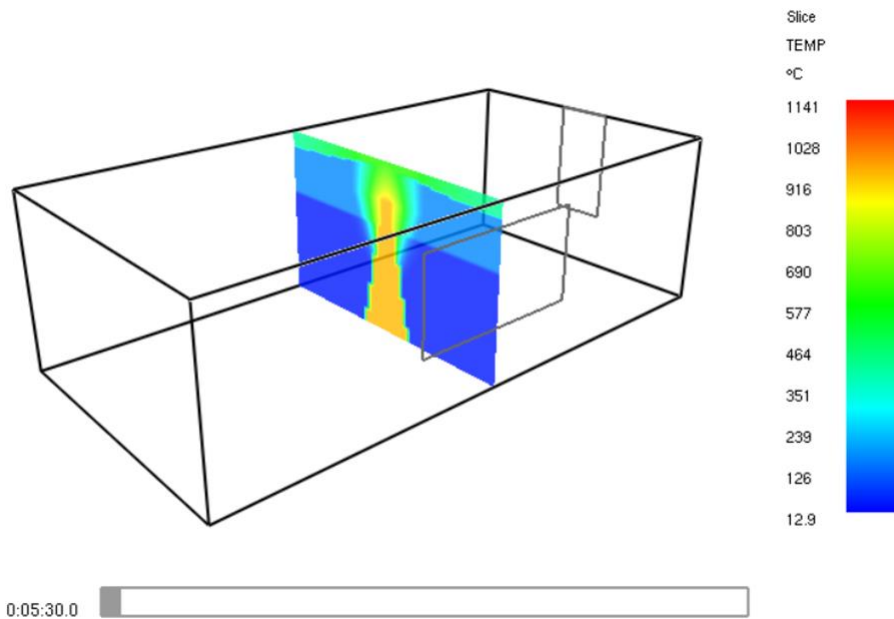


*Fig. 5-6. Simulation of temperature evolution in  $T=5$  min displayed on the transverse plane section, CFAST fire software [57].*

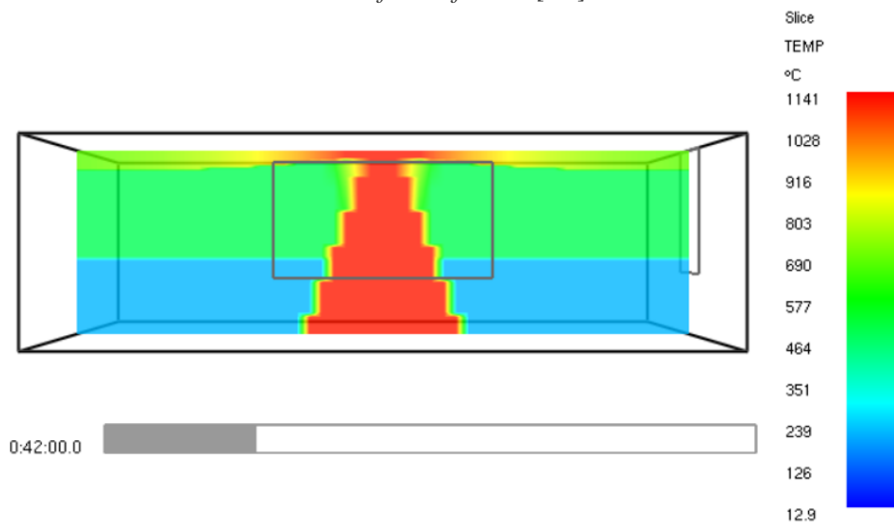


*Fig. 5-7. Simulation of temperature evolution in  $T=42$  min displayed on the longitudinal plane section, CFAST fire software [57].*

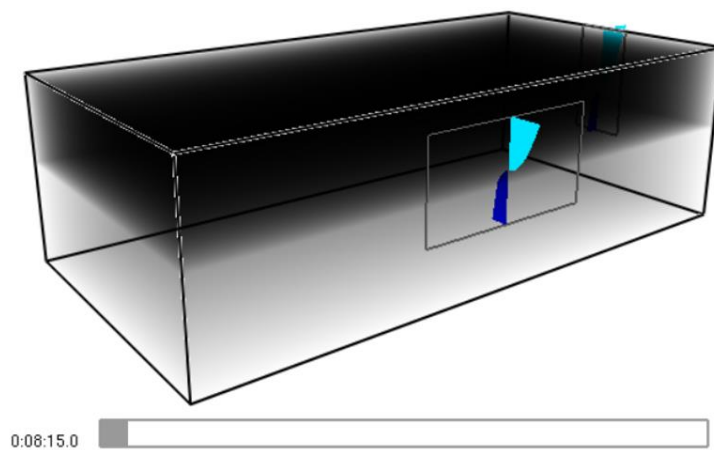
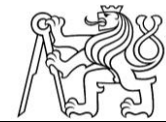


*Fig. 5-8. Simulation of smoke production in  $T=8$  min, CFAST fire software [57].*





Even more advanced way of modelling fire events is using *computational fluid dynamics* (CFD) technique, which represents very sophisticated and detailed approach. It consists of numerical solving differential equations of heat transfers and is based on the physic laws of energy and momentum conservations. A spatial mesh of finite elements is created in the 3D model and the thermodynamic and aerodynamic variables are calculated in discretized time steps. As a result, evolution of gas and surface temperatures, production of smoke and vector field of fluids convection in time are obtained. Generic fire events can be thus remodelled using such technique, including very specific situations. The technique requires high number of input parameters and is computationally very demanding. Moreover, the results are sensitive to the accuracy of input parameters. Nevertheless, when used properly it can provide useful and cogent information about the fire event and subsequent structural damage, even in cases other models cannot describe the event accurately enough.

CFD modelling is difficult and wide topic and is very actual, mainly in last years thanks to still increasing capabilities of computers and therefore it will not be discussed in this Thesis in detail. More about CFD can be found in the literature, e.g. [58]. The examples of CFD outputs can be seen in Figs. 5-9 and 5-10, which are taken over from [59] and are created in *Fire Dynamic Simulator* (FDS) [57].

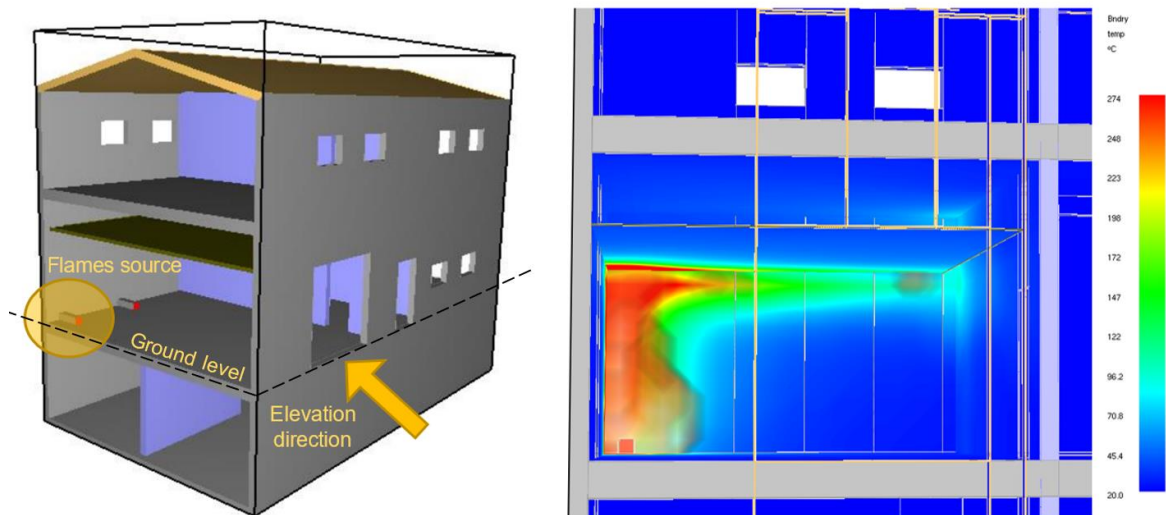


Fig. 5-9. CFD simulation; left: overall 3D model, right: surface temperatures at time  $T=3$  min [59].

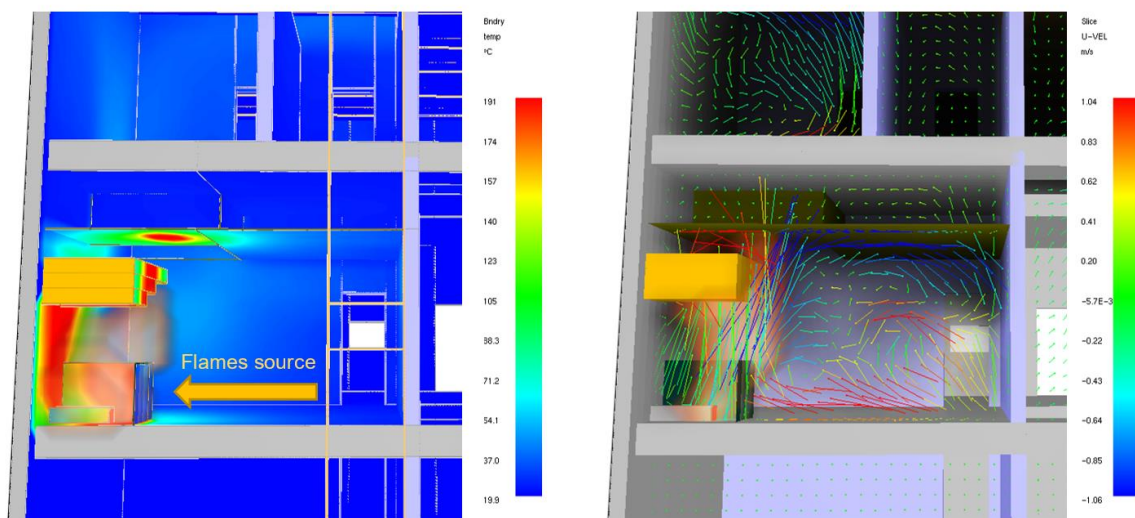


Fig. 5-10. CFD simulation; left: surface temperatures at time  $T=3$  min with obstacle above flames source, right: smoke visualisation with vectors of convection [59].





Within Chapter 5.2 it was shown that approximating the fire scenario and subsequent temperature-time curve after the fire event together with forthcoming thermal analysis can be a mighty tool used in the investigation process. According to the author's opinion this approach should be a part of the investigation in every case except of cases where based on the visual inspection it can be said with very high probability that only negligible damage occurs on the load-bearing structures. Idea about maximal temperatures in selected elements together with temperature distribution along their cross-sections and length can help with the investigation, diagnosis and structural assessment very much and can save time, money and human labour. Choosing the appropriate fire scenario is very actual and discussed topic, especially as a part of fire safety engineering [58].

The output of the fire scenario approximation is the temperature-time curve. Even if a simple model is adopted, it should always reflect reality as much as possible. Beside the heating rate and temperature distribution inside the compartment (and sometimes also the spread of fire in case of CFD simulations) it should contain the effect of extinguishing by fire brigade and, if it is possible, eventual secondary growth of temperature caused by another released or leaked fuel. In the end, the curve can look differently from those proposed in design code [16] or just from the usual shape. Taking into account the cooling phase is important mainly because of the global analysis and consequent structural effects, as will be discussed later in Chapter 7.

Another interesting fact that has to be taken into account is related to the comparison of temperature evolution of gas in the compartment and in the structure. When temperature-time curve is approximated, at certain time there is a temperature peak. After this time the gas temperature starts to decrease. However, when speaking about temperature in the cross-section of selected structural element, due to thermal inertia the temperature peak takes place a while after the temperature peak of ambient gas. An example was created with already proposed temperature-time curves and can be seen in Fig. 5-11. Because surface temperature is not as relevant, temperature in concrete depth  $x = 30 \text{ mm}$  is assumed since it is related to structural damage better. From the diagram it can be seen that whereas peak of gas temperature takes place approximately in time  $t = 60 \text{ min}$ , the peak of concrete temperature in case of parametric and zone method temperature-time curves comes approximately after next 30 minutes ( $t = 90 \text{ min}$ ). Whereas at this time the gas temperature according to parametric and zone method curves is already decreasing quickly. This effect should be thus always on mind of the investigators.

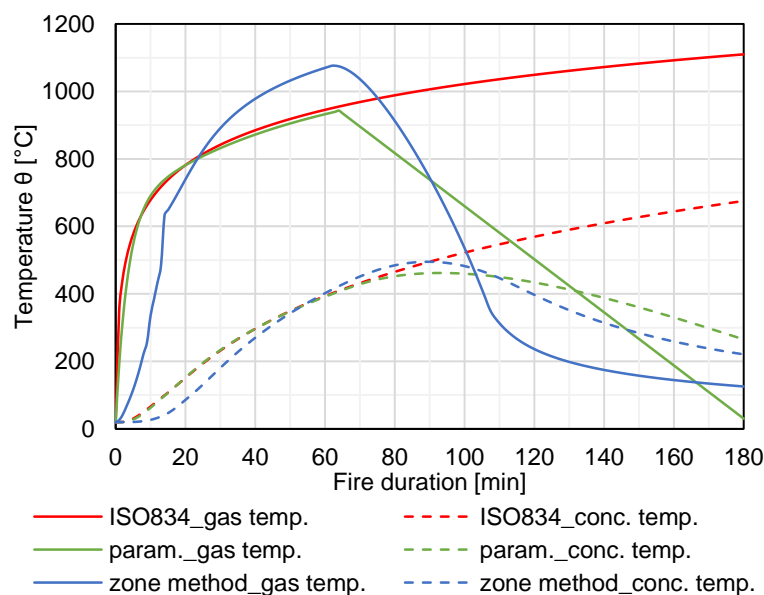


Fig. 5-11. Temperature evolution of gas and concrete (depth 30 mm from heated surface) according to various fire scenarios; thermal analysis conducted in TempAnalysis software [53].



To describe the fire event precisely enough it is probable temperature-time curve different to the ISO834 curve will be approximated. However, this curve is the most usual one and therefore it is used as reference in proposed tables of fire resistance and calculation methods [16]. The simplified calculation methods proposed by EC2 [16] are also meant to be used primarily with the ISO834 curve. In case of isotherm 500 °C method the parametric temperature-time curve is allowed at certain conditions, but the zone method should not be used with it. Even fire tests of industrially produced structural elements are being basically conducted according to ISO834 curve. Then, the estimated fire resistance is related to this curve only and must not be interpreted in any other way. Also some software applications suitable for conducting the thermal analysis can calculate only with ISO834 fire curve. Hence, a situation when effects of different temperature-time curve need to be converted to the effect of ISO834 curve might occur.

Such approach is proposed in the Annex F [54]. Because the only variable in the equation of ISO834 curve is the time, according to several input parameters characterizing fire load, geometry and thermal properties of the compartment and its ventilation conditions, the equivalent duration of standard fire based on ISO834 curve is calculated. An example was developed to show the results. A compartment with the same geometry as in previous chapter is presumed. The only change is that it is used as a library (to make the fire load big enough). Two different situations are prepared differing in used active firefighting measures – case A:  $q_{f,d} = 1190 \text{ MJ/m}^2$ , case B:  $q_{f,d} = 1980 \text{ MJ/m}^2$ . Temperature-time curves can be seen in Fig. 5-12. The zone method curves are obtained using Ozone software [55].

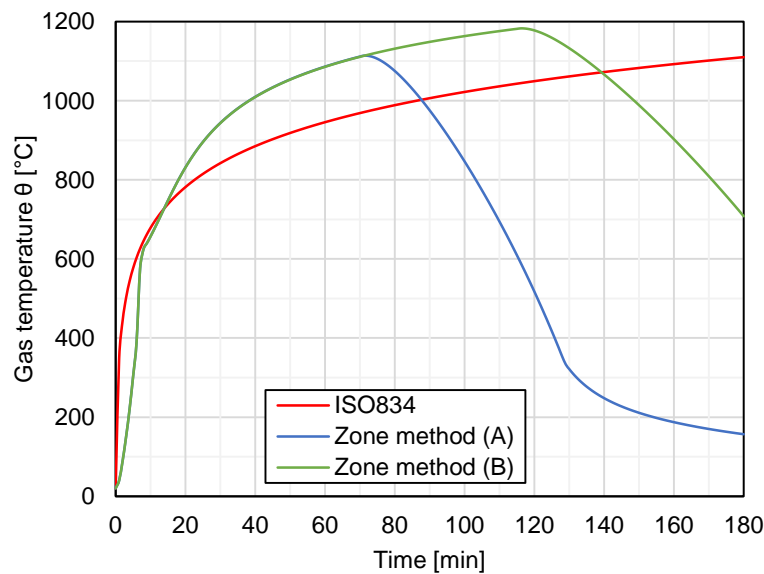
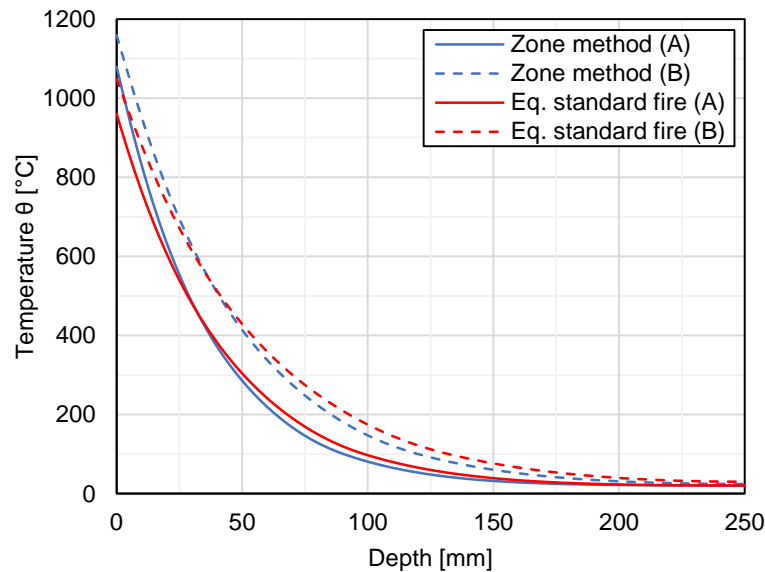


Fig. 5-12. Temperature-time curves according to different fire scenarios.

In case A the temperature peak takes place in time  $t = 72 \text{ min}$  when temperature is equal to  $\theta = 1113 \text{ }^\circ\text{C}$ . In case B the highest temperature  $\theta = 1183 \text{ }^\circ\text{C}$  is reached in time  $t = 116 \text{ min}$ . To simplify the example, the thermal analysis of 250 mm thick concrete slab subjected to the described curves from one side is carried out at the times of maximal gas temperatures. After conducting the calculation according to Annex F [54], the equivalent time of exposure to ISO834 fire is equal to  $t_{eq}(A) = 85 \text{ min}$  and  $t_{eq}(B) = 142 \text{ min}$  in case A and B, respectively. Temperature profiles based on zone method temperature-time curves and equivalent ISO834 curves can be seen in Fig. 5-13 from which can be stated that the equivalent curves follow the curves based on zone method very well. Hence, various temperature-time curves obtained from fire scenario approximation can be transferred to the effect of ISO834 curve using this method. Then the equivalent time of ISO834 exposition can be used for thermal analysis or use of tables and simplified calculation methods.



*Fig. 5-13. Temperature profiles of 250 mm thick concrete slab according to zone method temperature-time curves and their equivalent standard fire curves; thermal analysis conducted in TempAnalysis software [53].*

The method of transferring the effect of different temperature-time curves to the equivalent ISO834 curve can be used in one more way. On the previous page and in [Chapter 2.6](#) it was mentioned the fire resistance of industrially produced structural elements is generally tested experimentally since it usually provides the producer higher time of fire resistance than it would be obtained from calculations. The tested elements are then heated according to ISO834 curve. Because the producers generally want to design their products efficiently, the estimated and experimentally proved fire resistances will not be significantly lower than the actual structural performance. This presumption can be used in the post-fire investigation. Contrary, this method would not be beneficial very much in case of concrete structural elements casted on site because in the design stage their fire resistance is usually estimated using tables which represent rather prescriptive approach and not performance-based, therefore the estimated time of their fire resistance is not directly related to the actual structural performance.

Let's have an example: a precast hollow-core floor panel with guaranteed fire resistance of 60 minutes was subjected to a fire event within the building. The fire scenario was approximated and temperature-time curve using zone method was derived. After conversion to standard fire the equivalent fire duration was calculated as approximately 70 minutes. Then it can be stated the floor panel was very close to its collapse and therefore it can be expected to be considerably damaged. The residual parameters are about to be inspected carefully while material tests should be carried out. However, if the equivalent fire duration would be only 20 minutes instead, it can be stated the structural performance of the element was not lowered to higher extent and therefore there is quite a big chance the residual load-bearing capacity will be high enough. To such member smaller attention can be paid only to prove the assumptions and the effort can be paid to more damaged parts of structure instead.

To conclude with, since the temperature-time curve derived from the fire scenario approximation is still only a presumption and definitely will differ from the real fire event, it is strongly recommended to confirm the assumptions and validate the expected temperature profiles by conducting and evaluating material tests on reasonable number of cogent spots. For more about suitable material tests, see [Chapter 6](#).



### 5.3 Approach to Damaged Structural Elements

At this stage of post-fire investigation relatively detailed idea about damage level of structural elements exposed to high temperatures is gained based on the preliminary and detailed inspections. To continue in the post-fire process, an attitude to treatment of damaged members have to be assembled. Structural elements which are classified into damage classes “0” and “1” do not have to be investigated anymore because the damage caused by fire is minor, affects only surface layers and therefore can be neglected. Elements classified into damage classes “2” and “3” are damaged more significantly and attention should be paid on them. Such elements ought to be inspected with material tests and detailed calculation of residual load-bearing capacity. Elements classified into damage class “4” are damaged to considerably big extent and decrease of their structural performance is expected to be critical. For such members the same as for classes “2” and “3” is valid. Moreover, they have to be treated with special care to ensure their stability during inspection and refurbishment works – propping such members or adding supports might be necessary. It is also probable deep refurbishment, strengthening or even replacement will be needed.

The previously mentioned approach is dependent on the classification to damage classes, which is usually conducted during the preliminary inspection based on the visual assessment and so far known information. Because new important information about the decay of structural performance may be revealed during the detailed inspection the classification mark of such elements should be revised and elements should be then treated according to the key described above. It is also appropriate to analyse whole structural system and recognize key elements, such as massive girders, columns, deep beams and bracing. To those elements special attention should be dedicated and in case of any doubts about their condition the damage class mark can be artificially increased to ensure adequate care. Higher attention should be also given to all uncommon structures solving long spans, cantilevers with high slenderness ratio, vertically not continuing columns and walls, deep beams, etc. – especially in transition floors. The detailed inspection should be focused also on the details – joints of members (especially to those where different materials occur, most commonly concrete and steel), both mechanical and chemical anchoring, joist steel plates, etc.

The last phenomenon which is necessary to be taken into account is the effect of elements concurrence within given structural system. In case of statically indeterminate structures the elements influence each other considerably and hence the damage caused by fire on one element can affect the adjacent one even though this one was not exposed to fire directly and therefore probably obtained low damage class mark, if it was even inspected. The drop of stiffness, crack propagation and possible creation of plastic hinges together can irreversibly change the structural system and consequent redistribution of internal forces can load some cross-sections (typically the mid-span ones) more than they were prior to fire – as it is shown in Fig. 5-14. The load-bearing capacity then has to be checked due to increase of acting forces. Therefore, the global analysis always has to be done and its results taken into account. For more about global analysis, see Chapter 7.

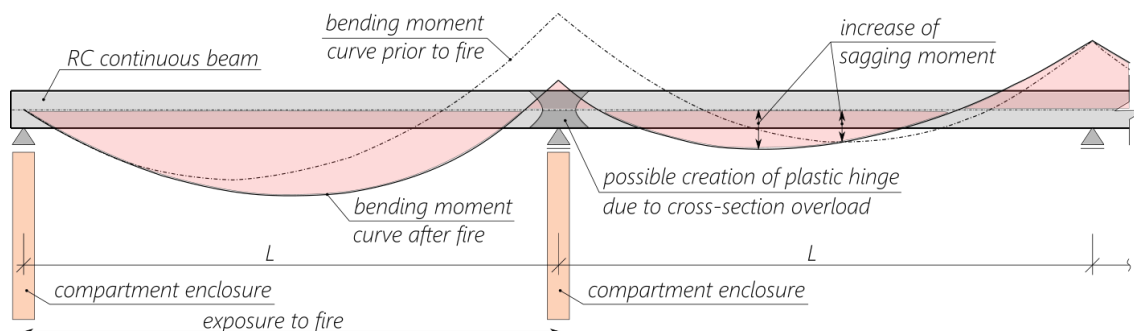


Fig. 5-14. Possible effect of internal forces redistribution on element not directly affected by fire.



## 6 Post-Fire Structural Diagnosis

### 6.1 General Aspects of Post-Fire Structural Diagnosis

The next step of the post-fire investigation process which is about to be carried out according to the *Flowchart* (see [Fig. 3-2](#)) is the structural diagnosis. It is a common process of investigating mainly (but not only) elderly buildings and other kinds of construction (typically bridges) to reveal their actual structural performance when:

- Serious structural malfunctions evidently exist on the structure;
- There is a suspicion and doubt about material quality used in the structure;
- Progressed stage of corrosion is expected;
- Structure withstood some kind of extraordinary loading situation (flood, windstorm, earthquake, fire, etc.);
- General refurbishment is about to be done and actual information are needed for design and budget purposes;
- Load level is about to be raised and real load-bearing capacity has to be proved.

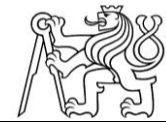
Then, based on the diagnosis results actual material properties, corrosion level and overall structural performance are estimated, which are then used in another step of the process. Hence, performing structural diagnosis is very often necessary and cannot be substituted or skipped. Main aspects of concrete structures that are generally inspected during structural diagnosis are proposed in [Tab. 6-1](#).

*Tab. 6-1. Overview of structural aspects investigated during diagnosis of concrete structures.*

Assessment of concrete	Assessment of reinforcing steel	Assessment of structure	Malfunctions and defects of the structure
Concrete homogeneity	Diameters, spacing and positions of rebars	Load-bearing capacity and stiffness of the structure (static load test)	Excessive cracks
Strength (compressive, tensile)	Thickness of concrete cover	Record of oscillation with its peaks, eigenvalue frequency (dynamic load test)	Crushing of concrete
Young's modulus of elasticity	Strength (tensile and yield)		Buckled or ruptured rebars
Bulk density	Ductility		Excessive deformations
Carbonation depth	Corrosion level		State of concrete cover

Conducting structural diagnosis and evaluating its results is generally challenging task, therefore it has to be conducted by special company with appropriate equipment, knowledge and experience. There is a following list of valid international (and primarily European) codes that are meant to be the basis for conducting the diagnosis of concrete structures [[60](#), [61](#), [62](#), [63](#), [64](#)]:

- ISO 13 822: Bases for design structures – Assessment of existing structures.
- EN 13 791: Assessment of in-situ compressive strength in structures and precast concrete.
- EN 12 504-part 1 to 4: Testing concrete in structures.
- EN 12 390-3: Testing hardened concrete – Part 3: Compressive strength of test specimen.
- EN 206 + A1 Concrete – Part 1: Specification, performance, production and conformity.



One of the situations when structural diagnosis is undoubtedly needed is when a structure was exposed to fire event. To make the calculation of residual structural performance possible, material properties of both concrete and reinforcing steel of selected structural members are needed, as well as overall assessment of the structural system and its possible changes. Evaluating results from diagnosis is even more difficult in case of concrete structures after fire exposure since the nature of such damage is specific and differs from the usual situations. Common test methods thus have to be modified and special kind of tests may be used as well. The most important fact that makes the evaluation so difficult and ambiguous is that the damage level of concrete is not uniform through the cross-section due to nonlinear temperature distribution during fire which is a result of concrete thermal inertia. For example, it means the investigated strength of surface layers is expected to be significantly lower than strength of inner part of the cross-section. This fact also considerably complicates the evaluation of compressive strength based on the destructive test of a core drilled from the selected element. Moreover, the state of (primarily) surface layers and consequently their mechanical properties are dependent on the conditions of cooling after end of fire event. To end with, residual properties of reinforcement are directly dependant on the maximal reached temperatures which can differ either along the investigated element (effect of localised fire or position of plumes) but also in a range of cross-section (corner versus inner bars).

Beside testing the selected damaged part of structure it is always useful to carry out the same tests also on undamaged (i.e. unaffected by fire) parts of the structure, which is as close and as similar to the damaged one in order to obtain reference results [28]. The material tests which are suitable for inspecting concrete building after fire can be either direct, when result of such test is directly the searched property (typically destructive strength test) or indirect when some other mechanical property is tested and which can be then recalculated or transferred to the searched property (e.g. rebound hammer or ultrasonic pulse velocity test). In such case it is often advantageous and sometimes even necessary to compare the obtained result with the reference values as was mentioned earlier. The testing methods can be also divided according to the damage on structure which is caused by their performing. In general, destructive and non-destructive tests (NDT) are usually used. Some methods are then referred as semi-destructive due to small extent of damage caused on structure.

In general, when testing the state of concrete, the most important mechanical property is the residual compressive strength related to certain range of temperatures and depth (this can be assembled together using estimated temperature profile based on other performed tests and calculations). In case of reinforcement the most important parameter is the residual yield strength. Because possible (and very probable) scatter of gained results it is also important to conduct statistical analysis in order to get reliable characteristic values that can be used in forthcoming calculations. More about evaluation of results and statistical analysis, see [Chapter 6.3](#).





## 6.2 Overview of Post-Fire Diagnosis Methods

The methods available for concrete and steel post-fire inspection can be conducted either right at the place of building's location (then they are referred to as *on-site*, *in-situ* or *field tests*) or at the laboratory which is a part of some kind of testing facility (*laboratory tests*). In most cases the on-site tests are considered to be indirect and non- or semi-destructive. Their conduction is rather fast and can be repeated many times. However, the methods are often based on the response of concrete's surface layers or average response of whole cross-section. The measurement of concrete properties is also often disrupted by presence of rebars. Therefore, results of such tests are less accurate and reliable. On the other hand, these aspects can be mitigated by means of statistical analysis and higher number of performed tests. The other type of tests, that are being carried out inside laboratories, can be characterized oppositely to field tests. Laboratory tests are time- and financially-demanding and they are laborious, while special equipment is usually needed. Nevertheless, they can provide much more accurate results and because they are conducted on samples extracted out of the investigated structure, properties from different depths of the cross-section can be tested. As a result, detailed idea about overall damage of the cross-section can be gained. The methods can be either destructive or non-destructive and direct or indirect as well.

Visual overview of testing approach can be seen in Fig. 6-1. According to the methodology of actual codes of practise the destructive tests are considered to be the main source of information while results of non-destructive tests are considered to be rather informative and additional [62]. Thus, conducting destructive tests on samples extracted from the subjected structure is generally necessary and cannot be substituted. However, using non-destructive tests together with the approach and calculations described in Chapter 5 can ensure effective diagnosis and reduction of extracted samples number at the same time.

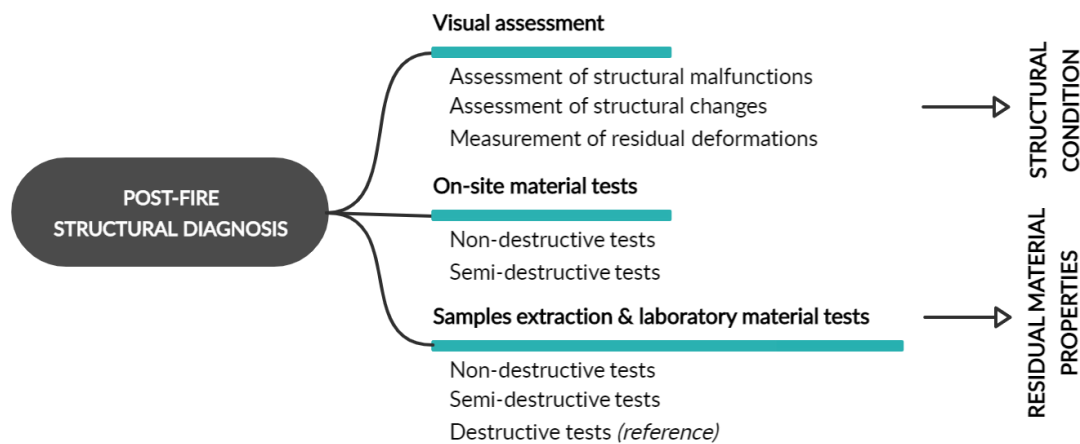


Fig. 6-1. Visual overview of post-fire diagnosis methods.

The non-destructive testing methods are based on measuring some kind of auxiliary property which is more or less directly related to concrete's compressive strength. In case of *rebound hammer test* hardness of element's surface layer is investigated. *Windsor probe test* is based on shooting metal projectile against concrete. According to its penetration depth (and consequent surface hardness) the compressive strength is correlated. *CAPO test* and *BRE internal fracture test* are based on measuring resistance against pull-out of mechanical anchor, which is then also correlated with the concrete compressive strength. When conducting *drilling resistance test* the amount of energy needed for drilling a hole inside damaged concrete element is recorded. *Ultrasonic pulse velocity test* (UPV) deals with the velocity of ultrasonic waves that are transmitted through the concrete, which is then transformed to the concrete's dynamic elastic modulus. All of mentioned properties are affected by fire exposure as well and thus can be used to investigate the damage level of concrete.



Comprehensive overview of existing testing methods suitable for inspecting concrete structures after fire is proposed in **Tab. 6-2**. To name some of the other methods [22, 28]:

- *Chemical analysis* – method based on analysing content of residual water within concrete matrix, which can be then transferred to approximate temperature profile; cement powder is used for analysis;
- *Colorimetry* – method for estimating temperature profile, based on aggregate colouring due to high temperatures exposure;

**Tab. 6-2.** Overview of non-destructive diagnosis methods usable for investigation of concrete structures damaged by fire, according to [28].

<b>Average response of the concrete cover</b>	<b>Point by point response of small samples</b>	<b>Special interpretation techniques</b>
Schmidt rebound hammer	Small-scale mechanical tests	Ultrasonic pulse velocity, indirect method
Windsor probe	Differential thermal analysis (DTA)	Impact echo
CAPO test	Dilatometry (TMA)	Sonic tomography
BRE internal fracture	Thermoluminescence	Modal analysis of surface waves
Drilling resistance	Porosimetry	Electric resistivity
Ultrasonic pulse velocity	Colorimetry	
	Microcrack-density analysis	
	Chemical analysis	

From the available testing methods summed up in **Tab. 6-2**, the most popular ones are the on-site methods inspecting response of concrete cover layer. These methods are relatively easy to execute, however evaluation of the obtained results is not always trivial, as will be discussed later on in this chapter. Also individual testing methods differ from each other when each method is suitable for slightly different situation. Advantages and disadvantages specifying their application are summed in **Tab. 6-3**.

**Tab. 6-3.** Advantages and disadvantages of on-site NDT techniques, according to [22].

<b>Testing method</b>	<b>Advantages</b>	<b>Disadvantages</b>
Hammer & chisel	Good as an assessment of the surface.	The surface properties are dominant.
Rebound hammer	Good as an assessment of the surface.	The surface properties are dominant.
Drilling resistance	Unaffected regions are used as reference.	Can only make safe assessments of the depth that correspond to a decay of 50-70 % of the virgin compressive strength. Require repair afterwards. No commercial equipment.
Pull-out test	Good relation with compressive strength.	Measures an average response only of the outer layer of concrete.
UPV test	Truly NDT method, 3 different configurations are possible.	An indirect method. Relative measurements are necessarily to achieve reliable results.
Windsor probe	Can be used to determine the strength profile of a cross-section	Measures response only of the outer layer of concrete.



## 6.2.1 Non-Destructive Diagnosis Methods

### Visual Assessment

Visual assessment is usually the first step to be carried out within structural diagnosis. As it was already mentioned in [Chapter 5.1](#), the original and most actual project documentation is necessary to be obtained before start of the diagnosis. In case of concrete structures also drawings of reinforcement with all detailing are needed since they represent valuable source of information. Based on it experts who conduct the diagnosis get to know the structure and can lead the investigation more efficiently. If structural drawings are not available, all information important for evaluating the residual structural performance has to be revealed and measured on-site. Nevertheless, even if such drawings are available, it is recommended to verify the basic things: main dimensions of elements, concrete cover thickness, rebars diameters, positions, spacing and orientation of reinforcement layers. Information about reinforcement can be gained e.g. by chiselling shallow groove perpendicular to the expected direction of the first layer inside the concrete cover up to rebars, or using special equipment *profometer* which can scan the concrete surface based on the ferritic properties of reinforcement.

One of the basic and very easy tests which is worth to conduct within the visual assessment is the *hammer and chisel test*. By this method delamination of surface concrete layers can be discovered [22, 38]. The test is based on the idea of propagation of mechanical waves induced by the impact of chisel and its consequent sound (the principle is similar to the UPV test). If the sound immediately after the impact lasts for longer time, is rather low and disappears gradually, the waves propagate inside the cross-section and the material seems to be compact. However, if the sound is high and hollow, there is high probability the surface layers are delaminated to certain extent and therefore not coherent. The prone depth of delamination is the interface between concrete cover and reinforcement, mainly due to incompatibility of thermal strains of concrete and steel at high temperatures. The incoherency of tensile reinforcement influences the load-bearing capacity of subjected element, mainly in anchoring zones. Therefore, if such situation occurs after conducting hammer and chisel test, such elements should be treated with higher attention and inspected in detail with other diagnosis methods. The test can also provide information about hardness of surface layers. If the structural concrete of ordinary compressive strengths is “healthy”, the chisel banged with hammer by human hand should cause only minor damage with negligible penetration depth. However, if the surface layers are significantly damaged by fire, their hardness is very much reduced and therefore the chisel is able to penetrate to bigger depths and might even cause sloughing off bigger piece of concrete due to delamination and incoherency.

Probably the most important step of visual assessment is measurement of residual plastic deformations of structural elements. The deformations during fire event propagate significantly due to deterioration of mechanical properties of both concrete and steel, decay of stiffness, damage of cross-sections, thermal effects (elongation and bowing) and also due to softening of stress-strains diagrams and rise of ultimate strains. After the end of fire event certain part of it goes back to the state prior to fire as structure cools down to ambient temperature. This part can be attributed to the elastic behaviour of materials which is in case of structures subjected to high temperatures related mainly to the volumetric changes and particularly their expansion and consequent shrinkage. However, in most cases the deformation does not disappear totally and some part of it remains as residual, because some changes that take place during fire cause irreversible damage to the material (e.g. cracking of concrete, yield of reinforcement). Such part of deformation can be then referred to as plastic since it is out of the region of material’s elastic behaviour. The residual deformations can be distinguished in following way:

- The deflection takes place along the subjected element and is caused by combination of natural deflection under dead and live load increased by decay of stiffness, and thermal bowing as the elements are very often heated only from one side. This type of deflection can be seen by both horizontal and vertical members. In case of vertical members, the enhanced deflection can rise bending moments and eventual second-order forces as well.



- The deformation is induced by movement of joints of two or more members. The movement is usually a result of element's thermal elongation and/or curvature. To preserve structural integrity and continuity the joint movement has to be followed by all involved elements, which can induce very high additional inner forces (usually shear force) already during fire; after its end according to the extent of residual deformation the additional forces are still acting. In case of compression elements, the movement of joints rises the eccentricity and subsequent bending moment. Moreover, in case of slender elements such joints movement can induce higher contribution of second-order forces. Joints movements thus have to be always measured and taken into account carefully within the post-fire assessment.

Both types of deformations are important not only because of impact on residual structural performance, but because of fulfilling the requirements of serviceability limit state (SLS) in the post-fire lifetime and maximal deflections in particular. There is often a situation when structure after fire has the residual load-bearing capacity high enough, but the residual deflections are beyond the limits of SLS. Since reducing residual deflections of concrete elements is very hard if not impossible, in some cases it can be the reason for decision of removing the subjected element. Besides that, measuring residual deflections can provide useful information to the forthcoming calculations, either as the evidence of stiffness decay or cross-check of calculations results. To make the information more reliable, comparison with measured deflection of identical non-damaged structural element (e.g. in different floor) is always beneficial.

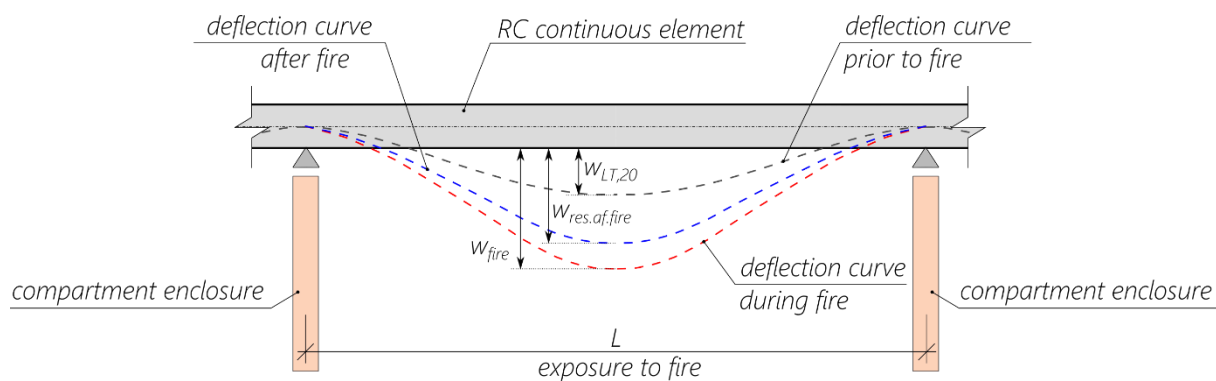


**Fig. 6-2.** Evolution of deflections due to fire exposure.

where  $w_{LT,20}$  represents long-term deflection prior to fire at ambient temperature,  
 $w_{fire}$  represents deflection during fire event,  
 $w_{res.of.fire}$  represents residual deflection after the end of fire event.

When carrying out the visual assessment within the post-fire structural diagnosis, one has to think about the state and degradation level of whole structure prior to fire. If the building has been already serving for decades, it is very probable some corrosion processes are in more or less progressed stage and hence the actual load-bearing capacity might be reduced when compared to the calculated values or the actual values of brand-new building. Also the deflections of slabs and beams might be higher than one would expect, typically due to creep or overloading. Then it is necessary to think about what part of measured deflection on fire-damaged element can be attributed to the effect of high temperatures and what part was already there prior to fire – priceless information can be again obtained from comparison with similar or even better identical non-damaged structural member from the same building.





### Rebound Hammer Test

Rebound hammer was developed for measuring surface hardness of various materials many decades ago and since then it has become very popular among civil engineers. Various types of the hammer are being used for measuring hardness of concrete, bricks or rocks. Carrying out the test is very easy and fast and beside the hammer no special equipment is needed. In case of testing concrete it is often used for testing young concrete to control material quality or the rise of strength, in case of elderly buildings it is used for checking material quality as well or corrosion level for assessment or refurbishment purposes. The test is based on hitting the surface of tested element with metal plunger which was previously pushed inside the body of the hammer while the impact spring was loaded. After the surface has been hit, the mass inside the body is pushed by released spring. According to the distance where it travels the *rebound number* is displayed. The harder the surface is, the further the mass travels and higher rebound number is recorded. The world's leading manufacturer of Schmidt rebound hammer, company called Proceq from Switzerland, offers several types of hammer according to needed accuracy of the device and also according to convenience of use (analogue or digital devices). The basic rebound hammer by Proceq can be seen in Fig. 6-3.



Fig. 6-3. Classic Schmidt rebound hammer, Proceq model N.

Although there is not any revealed analytical relationship between concrete surface hardness and its compressive strength so far, experience with the testing device show that some kind of dependency exists and hence the compressive strength of concrete also influences its hardness. The expected quality of concrete based on rebound hammer test is proposed in Tab. 6-4. Based on very big number of tests and subsequent regression analysis conversion diagrams were assembled by hammer manufacturers. Diagrams based on the data proposed by Proceq can be seen in Fig. 6-4, which contains also the equations obtained from regression analysis conducted in MS Excel. Because of the device testing principle, presence of the mass inside hammer's body and influence of gravity force, the device's direction during test has to be distinguished. Therefore, three conversion curves exist according to the position of hammer: (i) downward, (ii) horizontal direction and (iii) upward. As the hammer measures the hardness surface, it is believed the obtained value is related to the depth approximately equal to 30 mm [28, 65], which is basically the concrete cover layer. Due to the natural scatter of results manufacturers propose values of dispersion which has to be taken in account. The deviations are not constant since they are dependent on the concrete strength – from nearly 40 % for  $f_{c,cyl} = 10 \text{ MPa}$  up to 15 % for  $f_{c,cyl} = 60 \text{ MPa}$ . The value measured by original analogue Schmidt hammer is called *rebound value (R-value)*, while the new digital *Silverschmidt* by Proceq can measure either *R-value* or *Q-value*, which differs in the principle of record and thus the values and conversion to strength are different.



Tab. 6-4. Expected concrete quality according to rebound hammer test [66].

R-value [-]	Concrete quality assessment
over 40	Excellent
30 – 40	Good
20 – 30	Doubtful
under 20	Poor
0	Delaminated

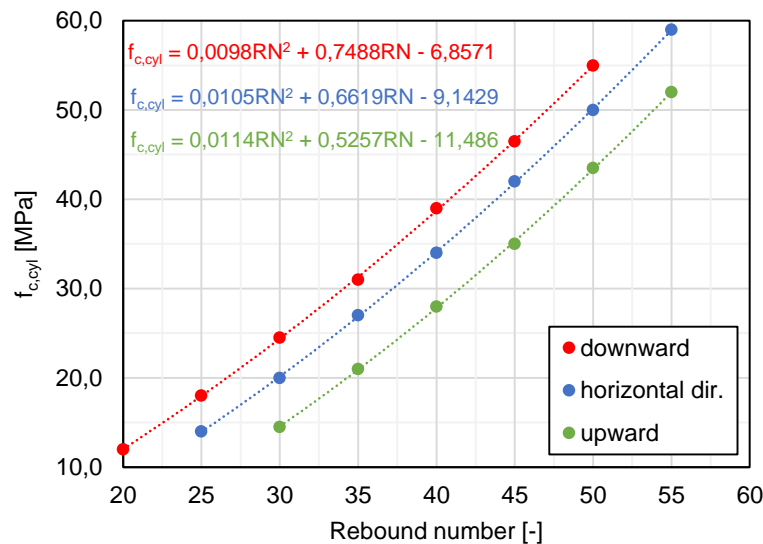


Fig. 6-4. Conversion diagram of classic rebound number to compressive strength according to [67].

When concrete is exposed to high temperatures, the compressive strength decreases due to many chemical and physical processes, as was discussed in detail in Chapter 2. Since compressive strength influences concrete hardness, it decreases as well when exposed to high temperatures – which is the principle of the rebound hammer test. Although this test method is so popular and easy to conduct, there is number of aspects which makes the usability of this method limited for purposes of testing thermally damaged concrete structures. The first thing is that the result of rebound hammer test is related only to the surface layers which is in case of exposure to fire always the most damaged – but it does not say anything about condition of concrete inside the cross-section. Also due to thermal inertia of concrete, which is so beneficial when speaking about fire resistance, the surface layers are heated quite quickly while inner part of cross-section remains cold – based on this test it is complicated if not impossible to estimate the duration of fire or the damage depth. Moreover, carbonation of concrete influence the results as well and limits the range of temperatures where test results exhibit satisfying accuracy (this phenomenon will be discussed later on). Due to the mentioned aspects this test method is generally considered as indicative and approximate and should not be used directly for estimating the compressive strength [22, 28]. It is suitable for recognizing spots and surfaces where compressive strength was reduced by 30-50 % [28]. The indicative way of use is meant by comparing the rebound number from damaged element to the rebound number from undamaged element with concrete of the same age, strength class and impact of surrounding exposure. Then the *relative rebound number* is obtained, which describes the damage level better than absolute values.

In the literature [26, 65] it is also stated the rebound hammer test can provide acceptably accurate results in the temperatures range of approximately 300-800 °C. The hammer is not able to measure relatively small decays of surface hardness due to skin hardening effect, which was often observed during experiments and which is most probably caused by progressed concrete carbonation [22, 38]. When testing such surface, the R-number does not seem to be reduced even though there is already not negligible decay of strength and only after the strength decay is high enough the R-number starts to decrease as well. This is why the hammer test can provide usable results from the moment strength





decay becomes more significant. On the other hand, in case of very much damaged surface of concrete, which can be attributed to higher temperatures (approx. 800 °C and more), the basic type of hammer is not sensitive enough and thus very low if not zero strengths are measured. The micro-cracking of concrete matrix can be so high and coherency of the surface layers to the rest of cross-section can be damaged to the extent that the hammer energy dissipates in the material instead of rebounding the plunger – therefore such low R-numbers and consequent strengths are gained.

When speaking about phenomenon of concrete carbonation, its main result lies in decrease of concrete inner pH (as was already mentioned in [Chapter 3.2](#)) and weakening natural protection of reinforcement which gradually starts to be prone to corrode. Side effect of the process is fact that carbonated concrete becomes harder and more brittle at the same time. Hence, this stands for affecting the results of rebound hammer test. The carbonation depth is thus need to be measured or at least empirically estimated every time. It can be neglected only in case of testing young concrete in new building which was not affected by fire. In every other situation one can expect that the carbonation process more or less takes place and thus the rebound hammer test results will be skewed. This is even more pronounced in case of fire-damaged concrete structures as the carbonation process is greatly accelerated by smoke and other products of fire, hence the surface layers of concrete will be very likely carbonated. In general, hammer manufacturers deal with the problem in two ways:

- After measuring carbonation depth using standard phenolphthalein solution it is advised to mechanically remove the carbonated layers, make the testing area smooth and flat and test the unaffected concrete. The actual not skewed R-number is obtained using this approach.
- Test both carbonated and noncarbonated concrete from the same structure and calculate the correlation coefficient. Then, only carbonated concrete can be tested which is much more convenient and much less laborious while actual R-numbers are obtained after results correlation. Beside this “manual” calculation some evaluation software (e.g. *Hammerlink* by Proceq) can deal with the carbonation depth and correlates the R-numbers and strengths, respectively, on its own based on the empirical know-how of the manufacturer.

Beside testing thermally-damaged concrete, following advices and requirements on testing concrete with rebound hammer are proposed either by hammer manufacturers [67] or standards [62, 68]:

- The hammer should be perpendicular to the tested surface.
- The tested surface should be smooth and flat. To reduce scatter of results it is advised to be smoothed with abrasive stone. Particularly this point is often a problem in case of testing fire-damaged concrete due to spalled surfaces – then the test is not able to be used.
- The hammer should be regularly calibrated in accredited testing laboratory.
- The plunger should hit cement paste and not aggregate particle – in such case the result is heavily affected by hardness of stone only.
- If a concrete specimen is tested, it should be strongly clamped to ensure it will not move during the test which could reduce the obtained R-number.
- Only dry concrete should be tested. If wet concrete is tested it was proved the results can be up to 20 % lower than in case of dry concrete [65]. This can be attributed to the migration of water molecules inside the pore system after the impact which probably absorbs the impact energy – the plunger hence rebounds less and the R-number is reduced. This might represent problem during preliminary inspections when rebound hammer test can help to reveal significantly damaged elements, however the structure is still water-saturated after the fire brigade intervention.



- Because of natural results scatter at least 8-10 impacts should be made when inspecting one spot. Then the highest and lowest value are excluded and a mean value of R-number is calculated from the rest of results. Finally, the adequate compressive strength is obtained using conversion curve or equation according to the hammer test position.
- The conversion curves were assembled years ago by the hammer manufacturers based on very many experimental results. Although they are considered as acceptably reliable, they were derived based on usual concrete mixes of that time which can differ from the modern concrete mixes of these days. Therefore, in order to achieve better result compliance, it is advised to derive own conversion curve based on correlation of rebound hammer test results and destructive compressive test results made on test specimens or concrete cores taken from the inspected structure in the means of regression analysis – then the correlation is made exactly for the concrete mixture used in the diagnosed structure.
  - In case of fire-damages structures deriving own conversion curve is even more important since the results needs to be correlated also due to carbonation, as was discussed earlier. Using own conversion curve makes possible to keep both influences separated.
- As it was already said, rebound hammer test is very popular due to its simplicity, low costs and quickness. Over the years testing standards have been implemented in the codes system. Nowadays following standards are available: European EN 12 504-2, American ASTM C805 or Czech national ČSN 73 1373.

In this chapter it was described how the rebound hammer test can be useful when inspecting concrete structure after fire. Limitations of the method were mentioned as well. It was stated the method refers to the state of concrete within cover layer of approximately 30 mm thick. Besides the usual way of estimating the residual compressive strength of concrete or its relative value respectively, it can also be used in following way. If decay of relative R-number according to temperature of cover layer is assumed to follow the decay of compressive strength proposed by EC2 [16] and possible influence of carbonation is omitted, simple diagram which can be seen in Fig. 6-5 can be assembled. Based on it one can roughly estimate the probable duration of standard fire exposure and subsequent average temperature of cover layer. If more exact data about R-number decay and its dependency on temperatures are available, the accuracy of the diagram can be raised.

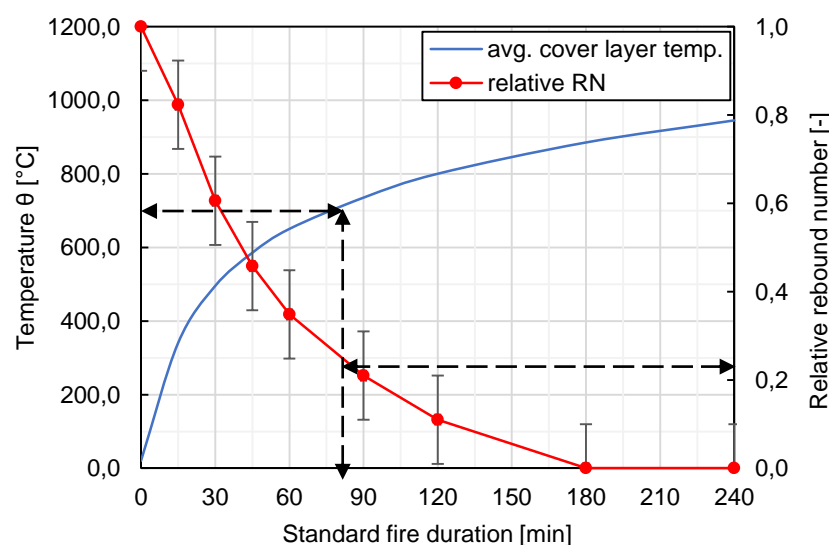


Fig. 6-5. Diagram of average concrete cover temperature (30 mm thick) and corresponding decay of compressive strength and related measured rebound index.



### Ultrasonic Pulse Velocity Test

The ultrasonic pulse velocity (UPV) test is one of the non-destructive tests working on the principle of mechanical waving propagation through solid medium. It is truly non-destructive test method as it can be repeated many times on the very same spot without inducing any damage to the material. The test principle lies in transmitting ultrasonic pulses to the material from one probe and receiving them by the other while travel time of the pulse  $t$  is measured. Based on the pulse travel time and known pulse path  $L$ , its velocity can be easily calculated according to Eq. (6-1).

$$V_p = \frac{L}{t} \quad (6-1)$$

The method was invented back in 1940s [69] and since then it has become well-established NDT technique for inspecting the condition and mechanical properties of various materials including concrete. When ultrasonic pulses are transmitted through concrete it was found three different types of waves propagate: (i) *longitudinal* (also pressure, P-waves), (ii) *transverse* (also shear, S-waves) and (iii) *Rayleigh* (R-waves) [70]. The P-waves are then referred to be propagating along the shortest possible way being thus the fastest, therefore they are used for calculation of pulse travel times and used in the diagnosis calculations. Basically there are three possible test arrangements according to the mutual position of probes: (i) *direct* – when probes are right against each other, (ii) *semi-direct* – when probes are in diagonal position around tested element's corner, and (iii) *indirect* – when both probes are placed on the same side of tested element. Graphical interpretation of possible test arrangements can be seen in Fig. 6-6. It is advised to use direct position whenever it is possible due to best results accuracy [28]. Usually it can be used when testing columns, pillars, short walls or webs and flanges of T- and I-beams. When this configuration is not possible or heavily-reinforced spot occurs (which disrupts the measurement, as will be discussed later in this chapter), the semi-direct arrangement might be beneficial, however lower accuracy has to be expected [22]. Usually it is used in case of beams or columns. The last option is the indirect method which often has to be used as it is impossible to place probes against each other – typically slabs or walls. The measurement is different and difficult to evaluate, nonetheless thickness of damaged layer can be estimated based on the test results [28, 70].

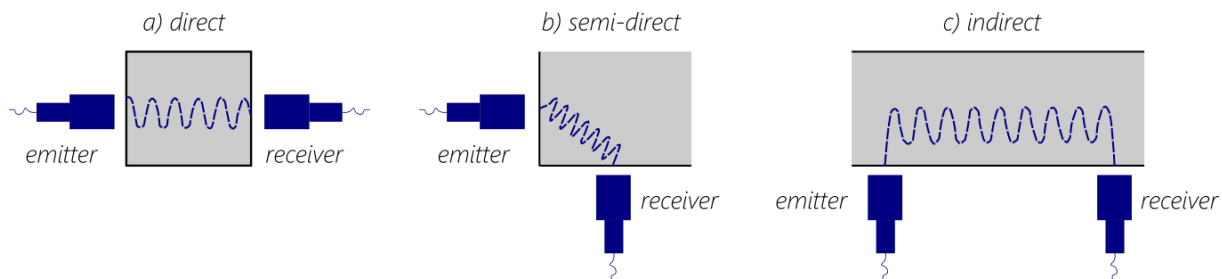


Fig. 6-6. Options of UPV test arrangement.

The measured pulse travel times are sensitive to material density and porosity, therefore it is usually used to investigate the compactness of concrete matrix and its overall quality, eventual occurrence of inner honeycombs, cavities or basically damage induced e.g. by freeze-thaw cycles or other corrosion processes. Such material quality decay can be revealed either by empirical evaluation of measured pulse velocities or mainly by relative comparison of pulse velocities from different spots on the structure. Rough assessment of concrete quality can be done e.g. according to the Tab. 6-5. The method is also being used in order to calculate the dynamic modulus of elasticity  $E_{c,dyn}$ , see Eq. (6-2), which can be afterwards easily transformed to static modulus of elasticity  $E_{c,stat}$  using Eq. (6-3) and conversion coefficient  $\kappa_u$ , see Tab. 6-6. Since exposure of concrete to high temperatures induces irreversible changes in material microstructure, which can be characterized foremost by its micro-cracking and consequent decay of mechanical properties, the method can be used when diagnosing concrete structures damaged by fire event as well [22, 28].



**Tab. 6-5.** Expected concrete quality according to UPV test, based on [71, 72].

Pulse velocity [km/s]	Concrete quality assessment	Note
over 4,5	Excellent	-
3,5 – 4,5	Good	Structural concrete ( $\geq$ C16/20)
3,0 – 3,5	Doubtful	-
2,0 – 3,0	Poor	Non-structural concrete ( $<$ C12/15)
under 2,0	Very poor	Non-structural concrete ( $<$ C8/10)

$$E_{c,dyn} = \rho_c * V_p^2 * \frac{1}{k^2} \quad (6-2)$$

$$E_{c,stat} = \kappa_u * E_{c,dyn} \quad (6-3)$$

where  $\rho_c$  represents bulk density of concrete,  
 $V_p$  represents measured pulse velocity,  
 $k$  represents dimension coefficient,  
 $\kappa_u$  represents conversion coefficient from dynamic to static modulus of elasticity.

**Tab. 6-6.** Conversion coefficient to static modulus of elasticity according to ČSN 73 2011 [73].

Conversion coefficient	Concrete strength class								
	C8/10	C12/15	C16/20	C20/25	C25/30	C30/37	C35/45	C40/50	C45/55
$\kappa_u$	0,62	0,71	0,76	0,78	0,81	0,83	0,86	0,88	0,90

When conducting UPV test, the pulse frequency has to be set prior to testing. In civil engineering applications the common range of pulse frequencies is equal to 20-150 kHz with maximum equal to 500 kHz [70, 71], while range of 40-60 kHz is the most usual. It is also stated the testing devices often has the initial frequency set to be 54 kHz. The frequency should be also in accordance with thickness of tested member. More about setting the frequency can be found in testing standard EN 12 504-4 [62]. The same document also advices that the material thickness should be at least 100 mm if the maximum size of aggregate particle is 20 mm or less and 150 mm if it is in a range of 20-40 mm. The emitting and receiving probes have to be in perfect contact with tested surfaces with whole area of the probe's head. To ensure such conditions, various coupling agents are usually used (medical jelly, grease, plasticine) [28, 62, 74]. If air pockets are present between probe and concrete surface, the measured result is skewed. This might be a problem in case of rough surfaces, especially in case of fire-damaged structures if the surface has been spalled. Smaller roughnesses can be mitigated by thicker layer of coupling agent or quick-setting mortar, in case of significant roughnesses grinding them down might be necessary.

The principle of testing method sensitivity lies in the fact that the ultrasonic pulses propagate through solid medium much faster than through air. It means that if the pulse comes to a crack or honeycomb inside the concrete it continues by going round still through concrete rather than through the crack or cavity, which results in longer travel time and thus lower pulse velocity. On the other hand, this feature is valid in case of reinforcement presence as well. If the pulse comes to longitudinal rebars it continues going through it rather than through concrete as the propagation velocity in steel is 1,4-1,7x faster than in concrete [22]. As a result, the measurement is skewed again – therefore it is advised to avoid measuring at places with reinforcement as much as possible. Measuring at heavily reinforced places might even end in unusable results. Similarly to rebound hammer test, it is advised not to measure moist concrete. Water content in the concrete matrix fills in the cracks which results in apparent higher density and compactness in which the ultrasonic pulses propagate faster. Effect of mentioned aspects on pulse propagation can be seen in Fig. 6-7.

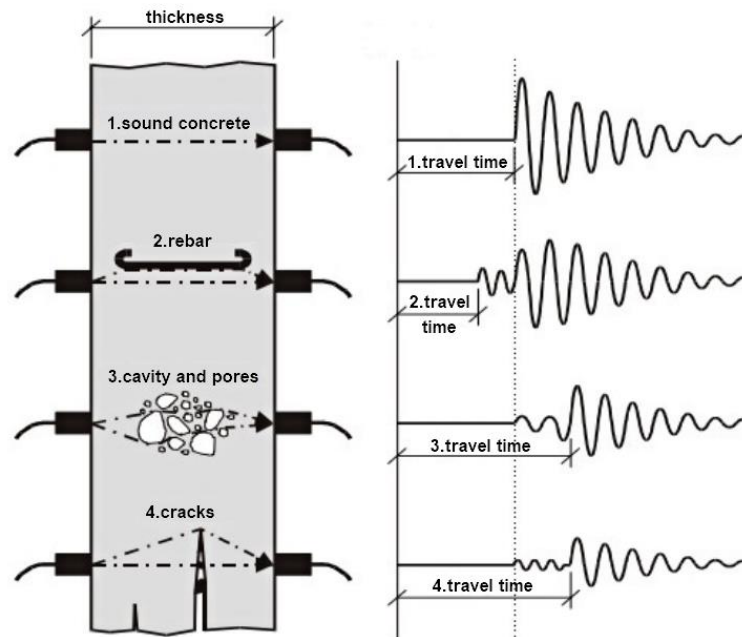


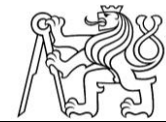
*Fig. 6-7. Aspects inside concrete element affecting pulse travel time, taken over [75].*

When UPV tests are used within the structural diagnosis, the results should be used mainly to roughly assess the mechanical condition of concrete or to get an idea about it based on the relative comparison of results from various spots on the structure. Estimating modulus of elasticity and especially compressive strength of concrete based on the measured pulse velocities only is questionable. During last decades, enormous effort has been dedicated to assembling versatile relationship between pulse velocity and compressive strength. Since no analytical relationship exists, all proposed equations were obtained based on the regression analysis of experimental results set, while some of them were also implemented into (inter)national standards. However, due to too many uncertainties and variables these equations cannot be used universally [76]. If it was done so, totally wrong results might be obtained. Therefore, EN 13 791 [61] proposes an approach where two options are available (the approach is identical for all indirect test methods):

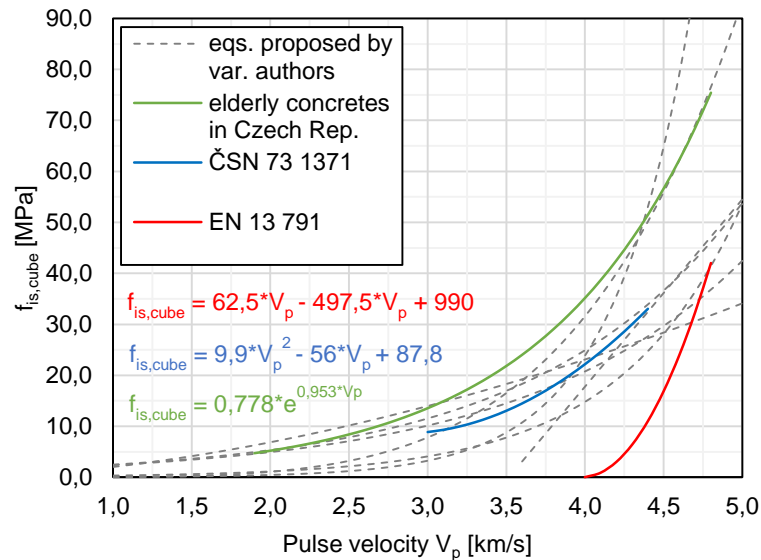
- Alternative 1 – to create own calibration curve based on the regression analysis of at least 18 pairs of measurement (UPV and compressive strength obtained from destructive test on cores extracted from subjected structure).
- Alternative 2 – to use basic calibration curve proposed in the standard [61] and to shift it based on the results of at least 9 pairs of measurement (UPV and compressive strength from cores).

Diagram with calibration curves taken over standards [61, 74] and gathered in the literature [71, 77, 78, 79] can be found in Fig. 6-8. The calibration curve from ČSN 73 1371 [74] is referred to be underestimating the actual strengths as it was derived on concrete mixes older than 30 years. The curve proposed by EN 13 791 [61] is the basic curve which should be shifted according to test results. Its disadvantage is the very limited range of pulse velocities where it can be used, which practically exclude all cases of elderly concretes. The curve referring to old concrete mixes used in Czech Republic was derived based on the comprehensive analysis of data set of more than 700 measurements gained within conducted structural diagnoses [71].





For conducting UPV test several valid testing standards have been introduced in the past. It is the European EN 12 504-4 [62], EN 13 791 [61], American ACI 228.1R [80] and ASTM C597 [81] or Czech national ČSN 73 1371 [74]. According to ACI 228.1R the UPV measurement should be repeated on the same spot at least 5x in case of old structure and 3x in case of new structure in order to mitigate possible measurement errors.



*Fig. 6-8. Calibration diagrams of concrete compressive strength based on UPV tests according to various standards and experimental results.*

With respect to the nature of concrete damage caused by fire, the deterioration level is not distributed uniformly through the cross-sections (excluding the cases of very long fires). Due to thermal inertia the surface layers are usually much more damaged than the inner core. Therefore, it is not beneficial to conduct UPV test through the whole cross-sections as usual. The measured pulse velocity will be affected by the deterioration caused by fire, however it will reflect the smaller extent of damage from the rest of the cross section as well – the result will be some kind of average. Then it is difficult if not impossible to distinguish both contributions and get accurate idea about the decay of concrete mechanical properties. Much more appropriate strategy is to conduct the UPV test on the core extracted from the subjected structure in the transverse direction in various depths. Based on the thermal analysis an approximate idea about the temperature distribution is gained, then the reference UPV values can be measured on the non-damaged part of core (e.g. on the upper layers of core extracted from slab exposed to fire only from bottom). If the whole core is supposed to be influenced by fire, the reference measurement is carried out on extra core cut from non-exposed part of structure. After obtaining reference values, standard destructive tests of compressive strength on drilled non-damaged cores are conducted, after which the calibration curve can be derived, as was described earlier. Then it is possible to compare measured UPV values from damaged depths of cores with the reference values and get the relative decays of pulse velocity and compressive strength, respectively, which can be assigned with assumed ranges of temperature as well.



## Colorimetry

Colorimetry is NDT diagnosis technique based on inspection of irreversible concrete colour alteration, which is induced by exposure to high temperatures and fire events, respectively. Basically it is being observed that when concrete is heated to elevated temperatures, specific compounds of concrete matrix gradually change their colour as the temperature rises. It is believed the colouring process is mostly governed by oxidation or dehydration of iron compounds in both coarse and fine aggregate [28]. The colour variation can be seen either by individual particles (coarse aggregate), however the overall concrete hue changes as well (induced by fine aggregate and cement paste). The siliceous aggregate seems to be more sensitive to such colour changes, while calcareous or artificial aggregate exhibits significantly less sensitivity [38].

As it was stated, the colouring of concrete is induced by changes of iron compounds. Because the fraction of iron in specific aggregates is generally variable, the extent and intensity of concrete colour change is variable as well. On the other hand, hue of undamaged concrete is not exactly the same every time as well, it is affected by number of parameters (cement type, aggregate, admixtures, etc.). Thus, unfortunately, it is not possible to create static hues scale which would serve to estimating the concrete temperature history. Nonetheless, the colour change can be assigned to several temperature ranges. The concrete colour gradually changes to pink and red (corresponding to temperatures 300-600 °C), whitish grey (600-900 °C) and finally buff (900-1000 °C) [28, 38, 82]. Example of typical colour alterations (visible on surface and inside the matrix) assigned to specific temperatures can be seen in Fig. 6-9.

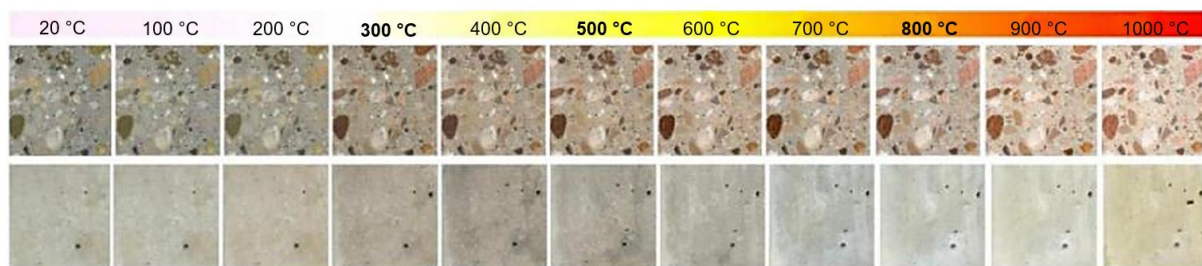


*Fig. 6-9. Varying colour profile of concrete according to exposure temperatures, taken over [83].*

The investigation is usually performed either by inspection of element's surface (when the colour changes are visible and the surface is not hidden by soot – this can provide information about maximal surface temperature) or by inspection of drilled core (when whole element's depth is visible – temperatures along the cross-section can be roughly estimated). However, situation when core cannot be cut out of the element may occur. Then different approach can be used – small-diameter hole is drilled into the element and after its clean an endoscope with camera is put inside. The colour profile can be thus observed right on-site. The endoscope can be nowadays connected to mobile phone, tablet or other portable device, making the inspection easier and more affordable.

Based on the colorimetry, it is possible to approximately estimate the temperature profile of concrete element after fire exposure. According to [38] it can be also used in order to gain an idea about position of 300°C isotherm (whenever colouring to pink or red hues can be observed, it means the material was heated to 300 °C or more), which is assumed to be the temperature when mechanical properties of concrete start to decrease more pronouncedly. In the mentioned document the position of 300°C isotherm is directly used in the forthcoming calculations of residual load-bearing capacity, however according to this Thesis author's opinion such assumption is too rough and more effort should be dedicated when assembling the probable temperature profile, e.g. by comparing the temperature profile estimated in the means of colorimetry with the calculated temperature profile based on conducted thermal analysis. In Tab. 6-7 the expected state of concrete and whole structure based on colour profile and temperature ranges is proposed.



**Tab. 6-7.** Assignment of temperature ranges to colouring and structural damage, based on [38].

Temperature [°C]	Colouring	Structural deterioration	State of concrete
20-300	None	None	Almost without damage
300-600	To pink and red	Surface cracks (~ 300 °C) Deep cracks (~ 500 °C)	Considerable strength decay
600-900	To whitish grey	Spalling, up to 25 % of reinforcement directly exposed (~ 800 °C)	Crumbly with poor strength
900 and more	To buff	Extensive spalling	Crumbly with poor strength

There are several options how to evaluate the colorimetry test. The most common one is by simple assessment made by human vision – the evaluation is fast and easy, however it cannot be really objective and the results may be affected by illumination conditions. Therefore, more objective ways of evaluation have been searched. More appropriate approach might lie in using special optical devices (colorimeters) which can analyse given surface point-by-point excluding the influence of illumination [82] and provide exact information about concrete colour. However, using this approach is rather time-demanding and laborious, while special laboratory equipment is needed – all mentioned aspects worsen the practical usability. Nonetheless, as the extent of concrete colouring is strongly dependent on used aggregate and thus varying in every case, the results should be treated as indicative and relative only rather than absolute and exact – then the usage of sophisticated testing machine is questionable.

The compromise might lie in using *digital camera colorimetry* method [82, 84]. In the cited literature the authors claim that it is possible to conduct and evaluate the colorimetry only by taking pictures of the coloured concrete with low-cost digital camera and analysing the colours alteration by pictures post-processing. There are several widely accepted colour systems defining every possible colour in different ways, among them the *hue-saturation-intensity* (HSI) system, the *red-green-blue* (RGB) system and XYZ system (see Fig. 6-10).

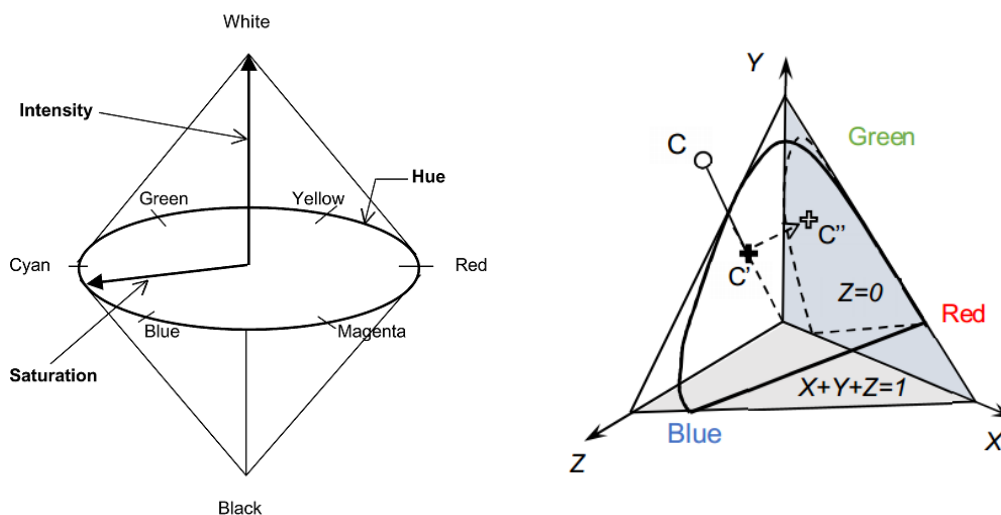
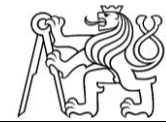


**Fig. 6-10.** Different colour systems – left: HSI [85], right: XYZ after RGB transformation [84].



Computer monitors, digital cameras and other electronic devices work with the RGB system as it is the most suitable option for them. In [82] an approach of colour transformation to different colour system is proposed, where the colour changes can be observed almost excluding the effect of illumination conditions. In particular, specific colour coordinates are transformed from RGB to *sRGB* colour system due to limited sensitivity of electronic devices. Then they are transformed to XYZ colour system and finally normalized to *x-y chromaticity diagram* (see Fig. 6-11). If characteristic colours information gained from concrete samples exposed to different temperatures are transformed according to the described approach and drawn into the chromaticity diagram, visible trend of points movement can be observed – first in the right bottom direction (towards “red point” – up to temperatures 400 °C) continuing in the left and bottom direction (towards “white point” – up to temperatures 800 °C). The overall trend of colour change in the diagram is highlighted with the red arrow. Similar trend can be expected when inspecting real structure after fire. According to conducted experiments, the method provides results with acceptable accuracy [84]. However, they should be interpreted in relative way to each other and one should critically think about them.

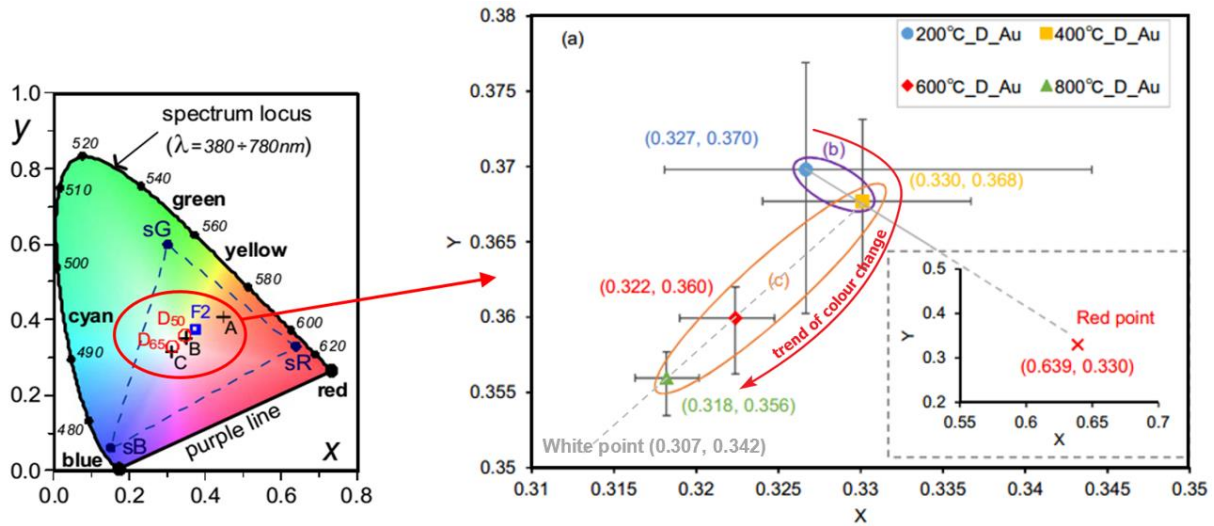
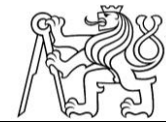


Fig. 6-11. Left: Whole chromaticity diagram in XY plane [82], right: concrete colour alteration caused by exposure to high temperatures put down into XY chromaticity diagram [84].



## Carbonation Test

The mechanism of the carbonation process is briefly described in Chapter 3.2. Generally, carbonation is considered to be a natural degradation process that takes place in every concrete structure. The velocity of its propagation can differ greatly as it depends on number of aspects – e.g. water/cement ratio and matrix porosity (indirectly concrete strength class), CO<sub>2</sub> concentration in the air, humidity of the environment, presence of plastering or other finishing layers, possible flexural cracks together with their width, etc. Therefore, whenever structural diagnosis is conducted, it should be expected the surface layers of the subjected structure will be carbonated to certain extent and thus it should be inspected in order to take appropriate measures. The expected carbonation velocity<sup>6</sup> at different boundary conditions for one specific concrete mixture without effect of fire is shown in Fig. 6-12.

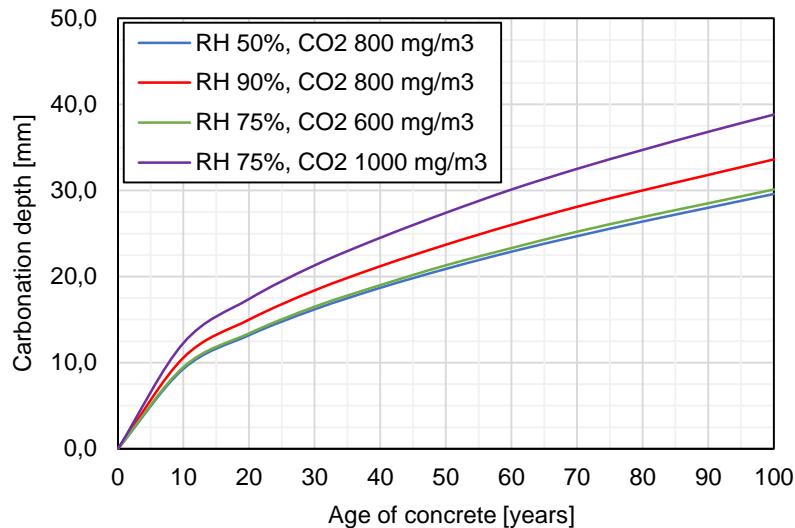


Fig. 6-12. Expected velocity of concrete carbonation, based on [86].

In case of concrete structures that have been subjected to fire event it is necessary to expect even more propagated carbonation and thus bigger depth of carbonated concrete as the products of combustion that are produced during fire generally accelerate the carbonation process [28]. In this particular case, the carbonation depth should be inspected not only because its effect on load-bearing capacity, but because it significantly influences the results of rebound hammer test as well. The carbonation depth can be estimated by conducting standard test when freshly broken surface of concrete is sprayed with 1% phenolphthalein solution – the carbonated layer does not change visually, however colour of the non-carbonated layers change to pink or purple, as can be seen in Fig. 6-13.

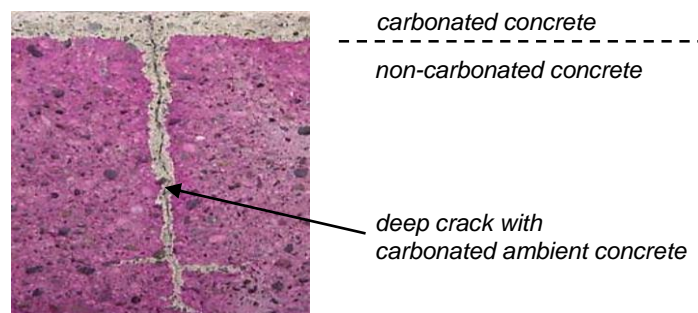


Fig. 6-13. Visual result of concrete carbonation test, taken over [87].

<sup>6</sup> Models for predicting velocity of carbonation propagation published in literature differs greatly taking into account more or less input parameters. The diagram proposed herein is based on software *RCLifeTime* developed at Brno University of Technology [86].





## 6.2.2 Destructive Diagnosis Methods

### Compressive Strength Destructive Test of Concrete

Testing compressive strength of concrete destructively in a laboratory testing machine represents the traditional way of inspecting concrete quality and according to valid testing standards it is considered to be the main source of information about the material. Contrary, the indirect non-destructive tests are considered to be additional and informative only. It means the results of destructive compressive strength test are assumed to be more reliable and should be taken as referential. In the previous chapters it was also described that according to results of destructive test calibration of indirect tests are made and thus amount of destructive tests and cores drilled out of the inspected structure can be reduced. To conduct the destructive compressive strength test, it is necessary to cut out a testing specimen out of the structure. In case of concrete structures, a method when round cylinder-shaped core is drilled out of the element is well-established. The core has to be drilled through whole cross-section depth and according to [62, 63, 88, 89] following general requirements have to be fulfilled:

- The diameter of core has to be at least 3,5x bigger than the biggest particle in the concrete matrix (if maximal aggregate size is assumed to be 22 mm, the least core diameter is theoretically equal to 77 mm) due to affecting test results.
- The core must not contain a rebar in the longitudinal direction, nor honeycombs or cracks due to affecting test results.
- The core has to fulfil specific length-to-diameter ratio ( $\lambda = l/a$ ) in order to obtain test results corresponding either to cylinder or cube strength. If the core shape is different it has to be modified and cut off. The effect of specimen shape on test results can be seen in Fig. 6-14.
- Core end planes that are pressured by the testing machine have to be perfectly smooth without any peaks or bumps, perpendicular to core's longitudinal axis and parallel to each other at the same time in order to achieve the desired failure mode. To ensure such conditions the core is usually modified and its ends aligned.

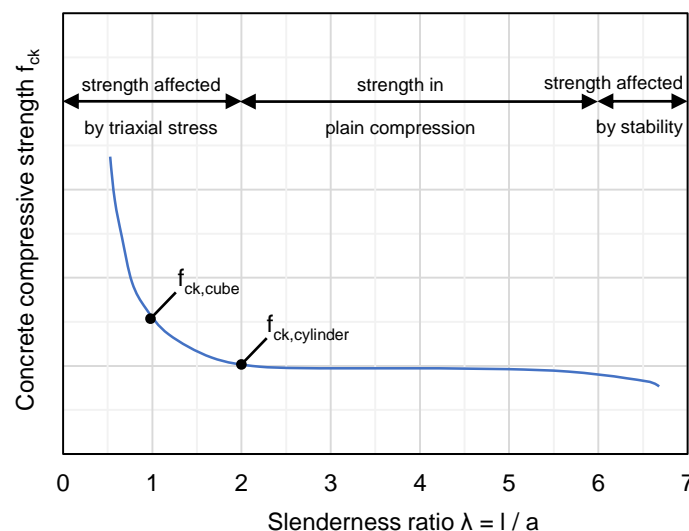


Fig. 6-14. Effect of slenderness ratio on compressive strength, based on [90].

Before the cores are drilled out of the inspected structure, one has to think about the structural damage caused by drilling cores. Even though the holes after drilling are casted with concrete or mortar right afterwards, it usually does not repair the cross-section completely, especially when rebars are interrupted. Usually drilling cores from slabs and walls does not represent problem, however drilling into columns or beams has to be considered thoroughly and in many cases cannot be used at all. Then some kind of alternative approach has to be found.



The most common core diameters are 50, 100 and 200 mm. Diameter 200 mm can be usually used only in slabs or walls since it represents relatively big weakening of the cross-section. On the other hand, diameter 50 mm is used when drilling into small cross-sections, however problems with not fulfilling the minimal diameter with respect to maximal size of particle in the matrix can occur. If a core of slenderness ratio  $\lambda$  different from 1,0 and 2,0 occurs, the test result can be recalculated to cylinder strength according to Eqs. (6-4) and (6-5) based on [89]. Specimens with slenderness ratio  $\lambda < 1,0$  and  $\lambda > 2,0$  should not be used due to results influence, see Fig. 6-14. The most common and practical core diameter is equal to 100 mm. Then it is beneficial to cut off the drilled core that its length is equal to 100 mm as well – based on the destructive test result the cube compressive strength is obtained.

$$f_{ck,cyl} = \kappa_{c,cyl} * f_{ck} \quad (6-4)$$

$$\text{– for } 1,0 \leq \lambda \leq 2,0: \quad \kappa_{c,cyl} = 0,8 + \sqrt{\frac{\lambda - 0,933}{26,667}} \quad (6-5)$$

where  $f_{ck,cyl}$  represents cylinder compressive strength of concrete,

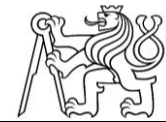
$\kappa_{c,cyl}$  represents correcting coefficient to cylinder compressive strength,

$f_{ck}$  represents compressive strength of concrete gained from specimen with different slenderness ratio.

When testing concrete core taken out of the structure damaged by fire, there are several differences that has to be taken in account. The biggest one is related to the nature of core damage, which usually takes place in the surface layers (thickness of such layer depends on the fire severity and duration) while the inner part of the core is not damaged. In case of core that has been subjected to elevated temperatures from one side only (typically slab or outer compartment wall) the damaged layer is logically located only by the exposed surface and the rest of core is not influenced; in case of cores subjected to fire from both sides (columns, walls inside one fire compartment) the damaged layers are located by both ends while the inner part is unaffected. Only in special cases (very long fires) the core is damaged similarly along its length due to uniform temperature distribution.

When a core damaged in such way would be tested as usual, the result cannot reflect the damage correctly and the obtained strength would represent some kind of average value. Strut & tie model in Fig. 6-15 represents the flow of inner forces inside the specimen during strength test and there it can be seen that approximately inner third of specimen height governs the test result as transverse tensile stress triggers the failure – the thermally-damaged surface layers influence the results in very limited extent, if ever. Therefore, it is necessary to work with such boundary conditions somehow:

- Thermal analysis of tested cross-section should be definitely conducted prior to destructive strength test. Even though the temperature distribution would be estimated only roughly, it provides an idea about the damage depth and based on it some kind of measures can be taken.
- Based on the theoretical temperature distribution along the core, the test result can be approximately attributed to particular temperature range of specimen's inner third.
- If the core is long enough, it can be divided into more specimens that will be tested separately and attributed to different temperature ranges and damage level. Typically, a core taken from a slab (e.g. 250 mm thick) can be divided into specimen by the damaged surface and specimen by the opposite one. The undamaged specimen provides referential result of undamaged concrete strength which should be also used to calibration of NDT tests. Result from damaged specimen provides then a kind of average value which can be then used in following considerations.



- Based on test results, not only compressive strength but static modulus of elasticity of concrete attributed to certain temperature range can be gained as well.
- Prior to conducting destructive test, it is beneficial to carry out the UPV test in the transverse direction along the core in different depths. After calibration of UPV test method based on the destructive test results a theoretical reduction curve of compressive strength related to certain temperatures gained from thermal analysis can be derived. Hence, more realistic idea about strength decay can be obtained than it is provided by design codes, e.g. EC2 [16]. Such reduction curve should be then used in forthcoming calculations.

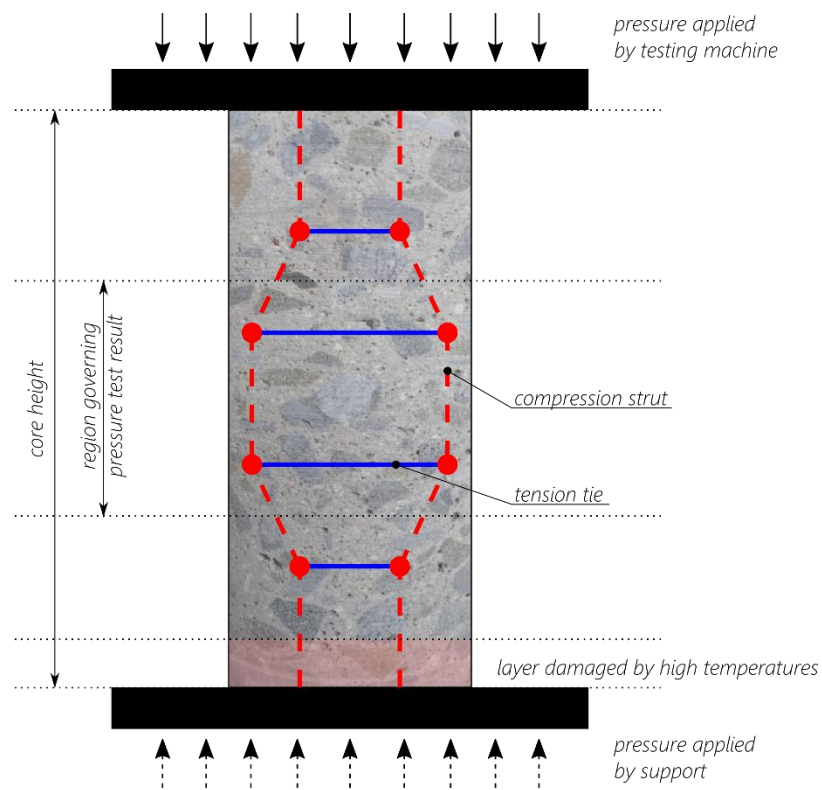


*Fig. 6-15. Strut & tie model in concrete specimen during destructive compressive strength test.*

For conducting destructive compressive strength test there are several testing standards providing general requirements: European EN 12 504-1 [62], EN 12 390 parts 1 and 3 [63], American ASTM C39 [88] and Czech national ČSN 73 1317 [89].



### Drilling Resistance Test of Concrete

Another test method suitable for inspecting thermally damaged concrete is the drilling resistance test. The testing method has been proposed in [91, 92] as an analogy to the approach of testing the hardness and subsequent strength of mortar in masonry structures, which was already standardized (see [93]). During the test an electric energy needed for drilling a unit of depth into concrete is measured by special gadget equipped on electric drilling-machine. Then, two assumptions are made: (i) the energy needed for drilling into concrete is proportional to its hardness and compressive strength, respectively, and (ii) hardness of thermally damaged concrete gradually decreases, which can be found by reduction of needed drilling energy and subjective feeling the drilling goes easier (if the thrust on the drill is maintained). The method is considered to be semi-destructive due to the local damage of inspected structure caused by its conduction. Because it is hardness-based method, its principle is similar to the one of the rebound hammer test. However, contrary to rebound hammer test not only surface layers are inspected since the hammer drill penetrates into deeper layers as well – then the hardness can be monitored along the elements thickness. The testing device together with measured and calculated parameters can be seen in Fig. 6-16.

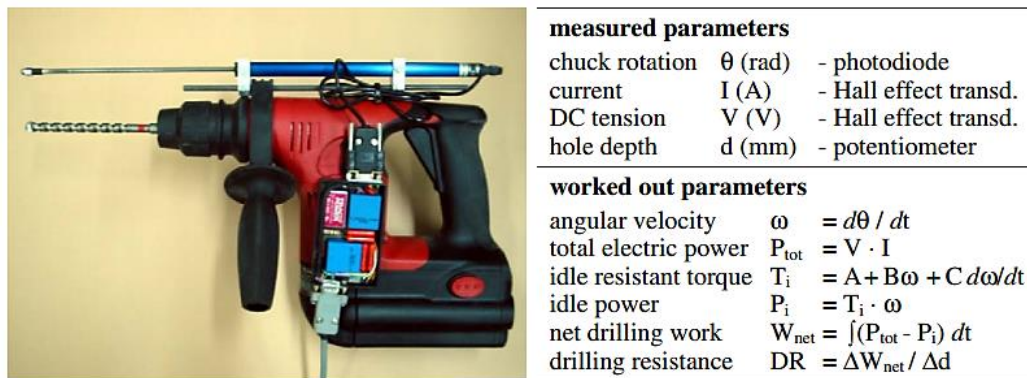


Fig. 6-16. Left: electric drilling-machine equipped with measuring gadget; right: measured and calculated parameters needed for test evaluation, taken over [91].

As a result of the test, depth-to-drilling resistance diagram is obtained (see Fig. 6-17), from which an idea about hardness decay and damage depth can be gained. The evolution of drilling energy and its relative comparison from both damaged and undamaged elements seems to be quite responsible evidence of damage caused by fire [28]. However, it can be expected the test results will be affected by concrete carbonation in the same way as results of rebound hammer test (the skin-hardening effect), therefore the carbonation depth has to be estimated in order to work with the results properly. Moreover, usability of this testing method is limited since no commercial equipment exists.

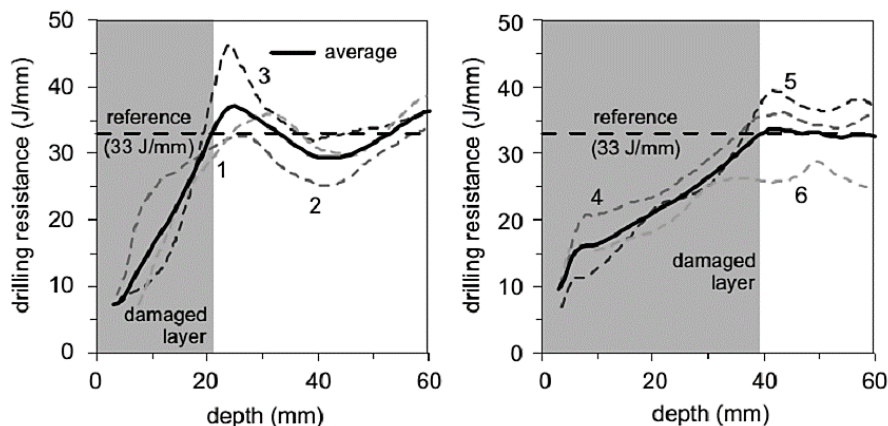


Fig. 6-17. Visual evaluation of drilling resistance test, taken over [91].



## Yield Strength Test of Reinforcement

Testing the residual yield strength of reinforcement after exposure to fire event is not so common, because usually it is assumed the yield strength recovers fully to the initial values prior to fire. However, as it was stated in [Chapter 2.4.2](#), this is not true for whole range of temperatures, especially for higher ones. Based on [Fig. 2-23](#) proposed in the mentioned chapter it seems reasonable to test the residual yield strength destructively in laboratory every time when there is a suspicion the maximal temperature in rebars reached 450-500 °C (these temperatures can be considered to be the critical values which when are exceeded the residual yield strength does not recover fully) and more. The idea about temperature distribution along the cross-section and in rebars, in particular, can be obtained based on conducted thermal analysis of assumed fire scenario and other material tests carried out within the structural diagnosis (especially the colorimetry test), while one has to think about the corner bars in columns and beams were exposed to higher temperatures than inner bars. If it is not possible to gain idea about temperature distribution the yield strength should rather be tested every time. To conduct this test, some specimens have to be cut out of the inspected structure. According to EN 1990, Annex D [49] the minimal amount of testing specimens is equal to 3 while bigger amount of specimens is recommended due to possible test errors and deviated results. However, taking samples of rebars out of the structure (especially bigger amount) might be a problem due to several reasons:

- Cutting the specimen out induces more or less irreversible damage to the structure with impact on load-bearing capacity.
  - In case of slabs and walls it is usually not a problem due to bigger amount of bars uniformly distributed close to each other and possible forces redistribution.
  - In case of columns and beams it is often not possible to cut pieces of rebars out of the structure at all due to concentration of load to the elements and much less amount of rebars (subsequently the rebars are bigger diameters).
- During the diagnosis the structure is usually still under load (at least dead load) and the decay of load-bearing capacity caused by cutting the rebars out might induce some problems – it may be necessary to take special measures for the period of inspecting the structure (e.g. propping the elements, forbidding the entrance of any people, etc.)

After cutting the rebar specimens out it is appropriate to repair the structure, analogically to the repair after core drilling. If the load-bearing capacity has been reduced significantly and has to be restored, concrete around the interrupted rebar is about to be removed, new piece of rebar of the same diameter and at least same strength is attached closely and welded to the both ends of interrupted bar; the welds must provide full strength connection. Then the whole spot is casted with special repair mortar again to ensure adequate concrete cover and thus cohesion, durability and fire resistance.

Generally, testing yield strength of steel should be performed in accordance with valid testing standard EN ISO 6892-1 [94]. Based on the standard the testing specimen has to meet required dimensions. Its cross-section should be either rectangular or circular and approximately in the middle third of specimen's length a necking should be done in order to control the spot of rupture. The required dimensions are specified in detail in mentioned standard. However, when conducting structural diagnosis and testing specimens are cut out of the structure on-site, it is often complicated if not impossible to meet all the requirements. Then the obtained yield and ultimate strength are valid, whereas ductility can be skewed and thus should be considered as informative only. Although all specimen dimension requirements might not be reached, they should be as close as possible. From practical point of view, the specimen's length should be such that the distance of clamps is equal to at least 100 mm. Prior to test, the actual cross-sectional area is about to be measured while every piece of adjacent concrete or rust has to be removed. It is also worth to note that due to the effect of high temperatures exposure the well-defined and visible yield plateau disappears which results in need of using the 0,2% proof stress.





## 6.3 Evaluation of Results

### Statistical Analysis

After conducting structural diagnosis and carrying out all sorts of both on-site and laboratory tests, big amount of data is obtained. Such data cannot be taken directly and used in calculations, but it has to be evaluated carefully in order to get correct, reliable and realistic information. The obtained data will surely be scattered to certain extent which is a natural phenomenon and happens due to number of various reasons, which can be generally divided as follows:

- Random errors – such errors cannot be completely mitigated, however they can be approximately estimated by repeating the measurement and statistical evaluation. Changes of temperature, vibrations, atmospheric pressure, etc. are considered to cause random errors.
- Systematic errors – such errors are caused by inaccuracies of testing device and testing method. They cannot be mitigated by repeating the measurement. Testing device manufacturers usually provide information about the expected device inaccuracy.
- Gross errors – such errors are usually caused by human faults, testing device malfunctions or use of inappropriate testing method. Gross errors can usually be eliminated by repeating the measurement, change of testing device or use of more appropriate testing method.

Beside the measurement errors described above the results scatter is also caused by natural variability of the measured property. This particular aspect depends on the homogeneity of tested material very much. Thus, it can be expected the measurement of steel properties will differ much less than measurement of concrete properties (assuming steel from one element and concrete of the same mixture is tested). Then there is another aspect – it is absolutely common that due to construction reasons the structural elements of the same strength class exhibit slightly different mechanical properties. Concrete structure consists of many concrete mixtures which has similar, but not exactly same mechanical properties. Steel members used in certain structure are not made from the very same steel, they might be differently old and produced by various producers - its steel is thus very similar but not exactly the same. Such differences in material quality of various elements are limited (basically from bottom by the characteristic value of certain property) according to the requirements of production standards and also because producers generally do not want to produce higher quality material and sell it cheaper.

Due to all mentioned factors a statistical analysis of the obtained data sets is needed. A general code of practise EN 1990 [49] proposes an approach how to design structures based on experimental results – this approach can be used when evaluating results of existing structure diagnosis as well. In most cases it is assumed the obtained data about material properties follows the standard distribution, (which is defined by Gauss function, see Eq. (6-6)), however this assumption should be yet verified by elaborating histogram of measured data – it should follow the curve of Gauss function. If it does not, more effort should be dedicated to the analysis why it is so and modification of original data set or choose of more appropriate probability distribution might be necessary. In case the data approximately follows the standard distribution, the mean value  $\mu_X$ , standard deviation  $\sigma_X$  and coefficient of variation  $V_X$  is calculated according to Eqs. (6-7) – (6-8). Then, using coefficient  $k_n$  taking into account the number of test results which are statistically analysed (see Tab. 6-8) a characteristic value of the desired property  $X_k$  can be calculated according to Eq. (6-9).

*Tab. 6-8. Values of  $k_n$  for 5% characteristic value, based on [49].*

n	1	2	3	4	5	6	8	10	20	30	$\infty$
$V_X$ previously known	2,31	2,01	1,89	1,83	1,8	1,77	1,74	1,72	1,68	1,67	1,64
$V_X$ previously not known	-	-	3,37	2,63	2,33	2,18	2,00	1,92	1,76	1,73	1,64



$$P(X) = \frac{1}{\sigma_X * \sqrt{2\pi}} * e^{-\frac{(X-\mu_X)^2}{2\sigma_X^2}} \quad (6-6)$$

$$\mu_X = \frac{1}{n} * \sum_{i=1}^n X_i \quad (6-7)$$

$$\sigma_X = \sqrt{\frac{1}{n-1} \sum_{i=1}^n (X_i - \mu_X)^2} \quad (6-8)$$

$$X_k = \mu_X * (1 - k_n * V_X) \quad (6-9)$$

To demonstrate the process of data evaluation and statistical analysis an example has been elaborated. Let's say concrete compressive strength was tested. Based on the conducted tests data set "A" containing 20 results was obtained, see Tab. 6-9. To see the trend of data distribution a histogram of results was created, see Fig. 6-18. Because the overall shape of the histogram relatively follows the Gauss curve it is assumed the values are distributed standardly. However, in Tab. 6-9 it can be seen the data set "A" exhibits quite big standard deviation, which induces big reduction of characteristic value. Suspicious values, which are too far from the mean value, are highlighted in the table. Second data set "B" is then created containing the same values as data set "A" while the highlighted suspicious values are excluded. All of needed statistical parameters is calculated for data set "B" as well. From the results it can be stated that even though less values were used, the standard deviation is much smaller and thus the characteristic value of compressive strength higher. Hence, only by careful data analysis much higher and thus more favourable material parameters can be obtained. The probability density with marked results and characteristic values for both data sets can be seen in Fig. 6-19.

*Tab. 6-9. Example of data set gained experimentally and its evaluation according to EN 1990 [49].*

Measurement number	Data set A - $f_c$ [MPa]	Data set B – $f_c$ [MPa]
01	30	30
02	28	28
03	23	23
04	31	31
05	16	excluded
06	22	22
07	35	35
08	19	excluded
09	31	31
10	27	27
11	39	excluded
12	36	36
13	26	26
14	25	25
15	34	34
16	30	30
17	36	36
18	33	33
19	42	excluded
20	26	26
<b>mean value <math>\mu</math></b>	<b>28,10 MPa</b>	<b>30,36 MPa</b>
<b>standard deviation <math>\sigma</math></b>	<b>6,59 MPa</b>	<b>4,22 MPa</b>
<b>coefficient of variation V</b>	<b>0,23 [-] (<math>k_n = 1,76</math>)</b>	<b>0,15 [-] (<math>k_n = 1,82</math>)</b>
<b>characteristic value <math>f_{ck}</math></b>	<b>16,50 MPa</b>	<b>22,51 MPa</b>

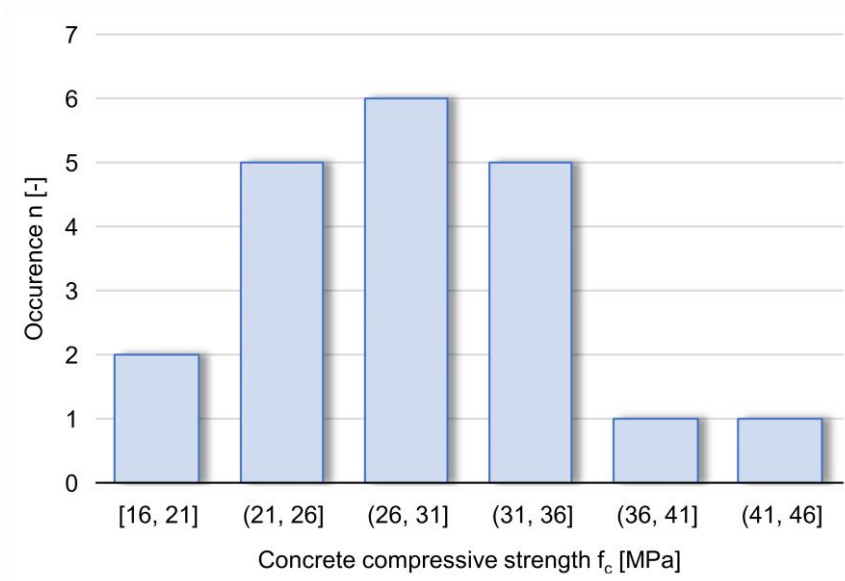


**Fig. 6-18.** Histogram of data set A.

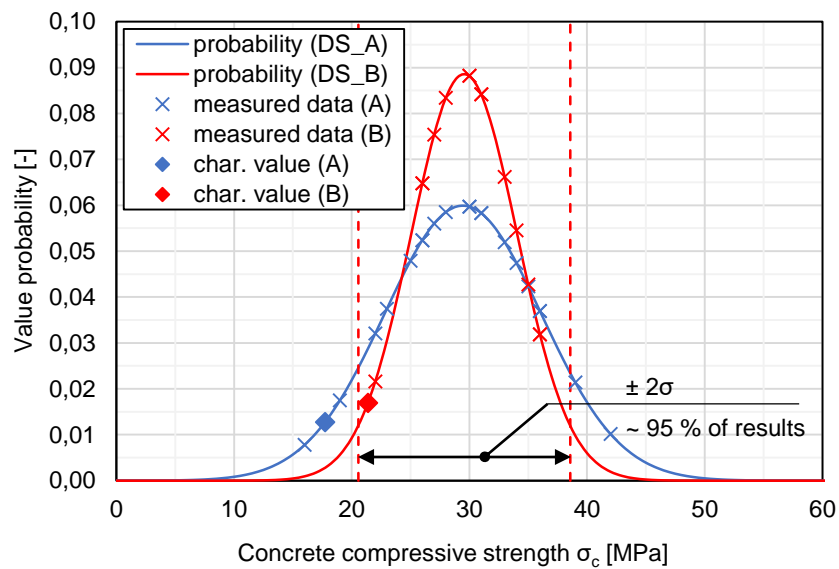


**Fig. 6-19.** Standard probability distribution of two data sets.



### Using the Diagnosis Results to Get an Overall Idea about Structural Damage

When assessment of existing structure is about to be done, usually structural diagnosis is needed. Based on its results an idea about actual material properties, damage or corrosion level and overall structural performance is obtained. It is not a trivial process and hence has to be always conducted and evaluated by company or people with adequate know-how and experiences. The importance of structural diagnosis is even more pronounced in case of structures damaged by fire. The residual mechanical properties of concrete and steel can be decreased either by: (i) corrosion processes (which can but do not have to be related to the effect of fire), (ii) directly by the effect of high temperatures exposure or (iii) by conditions during cooling period. They can differ in certain (but relatively wide) range every time due to mentioned aspects and thus it is impossible to describe their evolution generically by mathematical equations. Even though there are some relations, equations or reduction diagrams of residual mechanical parameters (which can be seen in [Chapter 2.4](#)), they should be considered only as informative and used for the first step of analysis and specified more precisely afterwards in the iteration process based on the diagnosis results – this is valid especially for concrete properties. At the same time, one has to keep on mind that during the diagnosis it is often not possible to fulfil all requirements and recommendations – then some compromises have to be made while the essentials must be done correctly. Also *engineering thinking* and improvisation are needed during the diagnosis.

Testing methods suitable for inspection of thermally-damaged concrete and reinforcing steel with their specifics were mentioned and described in this chapter. Based on the proposed overview of available testing methods it can be stated that by conducting:

- Visual assessment – serious structural damage and overloaded cross-sections can be detected as well as probable spots of the highest reached temperatures. By measuring residual deflections and joints movement valuable information to the calculations can be gained about the stiffness decay and thermal loads.
- Rebound hammer test – spots highly influenced by fire can be detected and approximate concrete compressive strength of surface layers can be obtained (after correlation).
- Ultrasonic pulse velocity test – internal heterogeneity, cracks, delamination or honeycombs can be detected and approximate decay of concrete compressive strength and modulus of elasticity related to certain temperatures can be obtained (after correlation).
- Colorimetry – approximate temperature profile (depths of important isotherms, respectively) can be gained by analysing colour changes of concrete matrix.
- Carbonation test – needs to be conducted in order to ensure adequate durability of subjected structure and lower the risk of reinforcement corrosion and to evaluate rebound hammer test correctly.
- Destructive compressive test of concrete – referential strength of concrete can be gained for calculations and correlation of NDT methods.
- Destructive yield strength test of reinforcement – residual yield and tensile strength of reinforcing steel can be gained (so far it is the only existing method for such purposes).
- Thermal analysis – although it is not directly diagnosis method it should be done within every post-fire investigation process. It can help with getting idea about fire severity and duration. By comparison with test results more confidence about obtained information can be reached.

Hence, it is evident that the overall idea about structural damage caused by fire is assembled together based on results of various tests, observations and calculations. Comparison of partial results and their cross-checking also rises their reliability while considerable inaccuracies and flaws can be identified.



The idea about combining results of NDT tests together in order to rise their reliability is not new – over the years considerable effort has been dedicated to development of such approaches. Probably the most popular one is the *SonReb method* which allows to estimate the compressive strength of concrete based on both UPV and rebound hammer test results. The method was developed by RILEM and in [93] a conversion diagram is proposed, see Fig. 6-20. The diagram is meant to be the basic one derived for usual concrete strengths and mixtures while correction coefficients should be used for specific investigated concrete. Beside it the compressive strength can be also calculated. The most usual form of such equation can be seen in Eq. (6-10). Many authors propose the coefficients  $a$ ,  $b$  and  $c$  based on conducted regression analysis [78, 95, 96]. However, there is still no broad consensus among proposed relationships and with respect to natural variability of concrete properties it seems it cannot be achieved at all – the variability is even higher in case of thermally-damaged concrete. Therefore it seems that the best way is to conduct own regression analysis based on diagnosis results and obtain unique parameters  $a$ ,  $b$  and  $c$ . The main advantage of the SonReb method lies in enhancing the conversion accuracy only by combining results of both tests. The prediction accuracy can be expressed by coefficient of determination  $R^2$ , which should be higher than in case of correlation gained from one test method only (coming closer to  $R^2 = 1$ , which means 100% prediction agreement). Because the final prediction accuracy depends on accuracy of both single methods, their coefficients of determination should be reasonably close to each other (not 0,9 and 0,4) and according to author's opinion at least  $R_i^2 \geq 0,7$  in order to achieve satisfying accuracy.

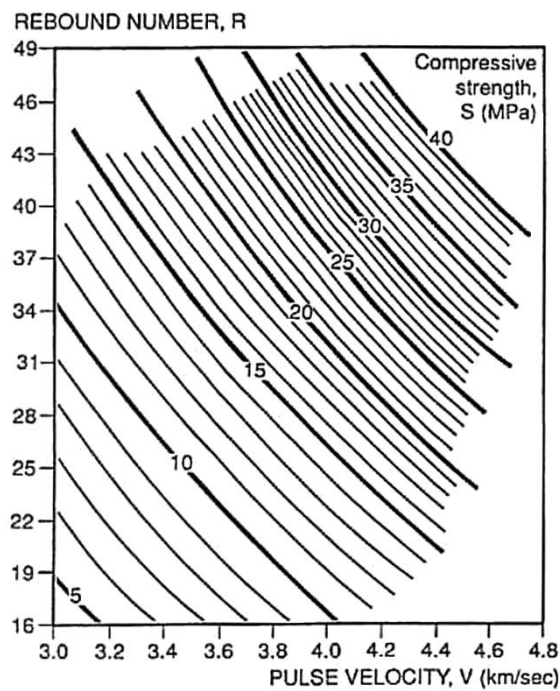


Fig. 6-20. Nomogram for estimating concrete compressive strength based on SonReb method [93].

$$f_c = a * UPV^b * RN^c \quad (6-10)$$

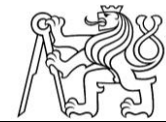
where  $f_c$  represents compressive strength of concrete in [MPa],

$UPV$  represents result of UPV test method in [m/s],

$RN$  represents result of rebound hammer test (the mean value of measurement set, either R- or Q-values) in [-],

$a, b, c$  represents correlation coefficients.





Example of the structural diagnosis output is elaborated in Fig. 6-21. It contains photo of the drilled core, information about probable temperature profile, positions of important isotherms, carbonation depth, colour profile, spots where NDT tests were conducted and finally the evolution of concrete compressive strength along the cross-section's depth estimated according to test results. This reduction diagram together with diagram of modulus of elasticity evolution (estimated by UPV tests) can be then used in calculations, see Chapter 8.

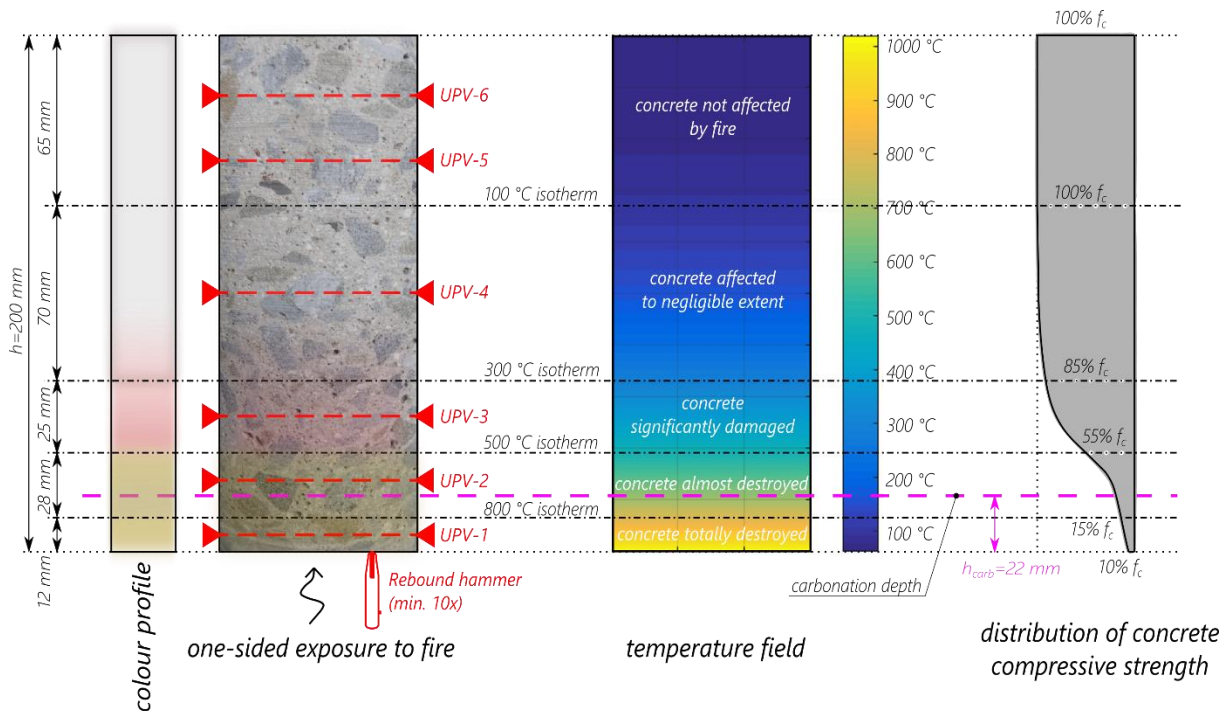


Fig. 6-21. Visual output of conducted structural diagnosis, temperature profile calculated in [53].

To end this chapter with, it is worth to remind the concrete mechanical properties of surface layers are usually very different when compared to the rest of the cross-section. This is due to several reasons: (i) surface layers are heated to the highest temperatures and for the longest time, (ii) surface layers suffer from spalling and sloughing off, (iii) surface layers are influenced by fire brigade intervention and possible quick cooling down the most. One should have these aspects on his mind when conducting the post-fire assessment in order to avoid misleading assumptions.



## 7 Global Structural Analysis

### 7.1 Importance of Conducting Global Analysis

In the field of structural engineering concerning on fire resistance of concrete structures and their performance during fire situations enormous effort has been dedicated to understanding of material behaviour and deterioration of mechanical properties caused by exposure to high temperatures. These efforts still continue as innovative and brand-new material composites are being developed and introduced into building industry. As it was already mentioned in [Chapter 2.6](#), nowadays there are several widely accepted methods how to assess fire resistance of certain structural RC element. Thanks to them the time during which RC structure shall withstand fire event (usually represented by ISO834 temperature-time curve) can be estimated. The calculation-based methods then focus on ways how to take into account the material deterioration and consequent decay of load-bearing capacity. At the end of the assessment the load-bearing capacity during fire event is obtained and can be compared with the effect of acting loads, as is defined by the basic inequation, see [Eq. \(7-1\)](#).

$$E < R \quad (7-1)$$

where  $E$  represents effect of loads acting on given element,

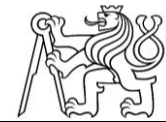
$R$  represents resistance of given element against acting loads.

It is worth to notice that most of the effort is related to the right side of the inequation given above. Traditionally much more attention has been dedicated to material behaviour and sectional analysis at high temperatures rather than global analysis, mainly because of its complexity and difficulty. For a long time, there were no adequate software capabilities that would enable solving such problems. However, if the assessment shall be meaningful and reliable, the effect of applied loads have to be estimated correctly, which might be unexpectedly tricky and misleading in some situations. Reason for this statement is the fact that the distribution of inner forces along given structural element might differ from the one related to ambient temperature prior to fire significantly and might vary over fire duration as some boundary conditions and element's structural characteristics are not constant, which is a consequence of transient nature of exposure to fire.

#### Thermal Loadings

When fire starts in certain fire compartment, air temperature inside the room increases and layer of hot smoke usually accumulates under the ceiling. With such boundary conditions the structural elements are gradually being heated. According to element's thermal analysis decay of mechanical properties is estimated. Beside the material deterioration the exposure to elevated temperature causes also volumetric expansion. Because the dominant dimension is typically element's length it is usually referred to as (thermal) elongation. Moreover, very often the cross-sections are not heated regularly and symmetrically from all sides (typically the floor slab is heated only from bottom, wall is heated only from one side, perimeter column and girder are heated from 3 sides). Due to it and relatively high thermal inertia of concrete thermal gradient creates in the direction of heat flux which tends to bend the cross section (more heated fibres tend to elongate more than the cooler ones). Existence of thermal gradient results in (thermal) bowing of elements, while the deflection propagates towards the source of heat.

So the structure or its part tends to deform. However, propagation of thermal deformation is strongly connected to the particular structural system. Generally, it can be stated that if the structure can be described as statically-determinate, thermal deformations are not restrained anyhow and thus can propagate. This results in the already mentioned elongation a bowing. At the same time, since the thermal deformations are not restrained, no additional mechanical stresses develop. Graphical interpretation of such example can be seen in [Fig. 7-1](#). Contrary, if the structure is described as statically-indeterminate, thermal deformations are restrained and cannot propagate. This results in creation of



additional inner stresses and forces, respectively. Restrained elongation causes creation of compressive axial force, restrained bowing causes creation of negative (hogging) bending moment. Graphical interpretation of such example can be seen in Fig. 7-2.

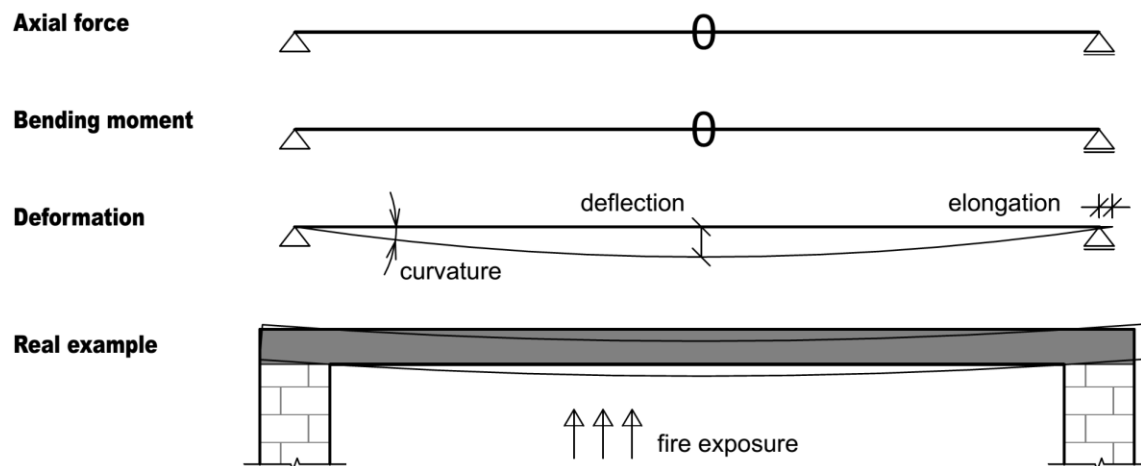


Fig. 7-1. Effect of thermal loading on statically-determinate structure.

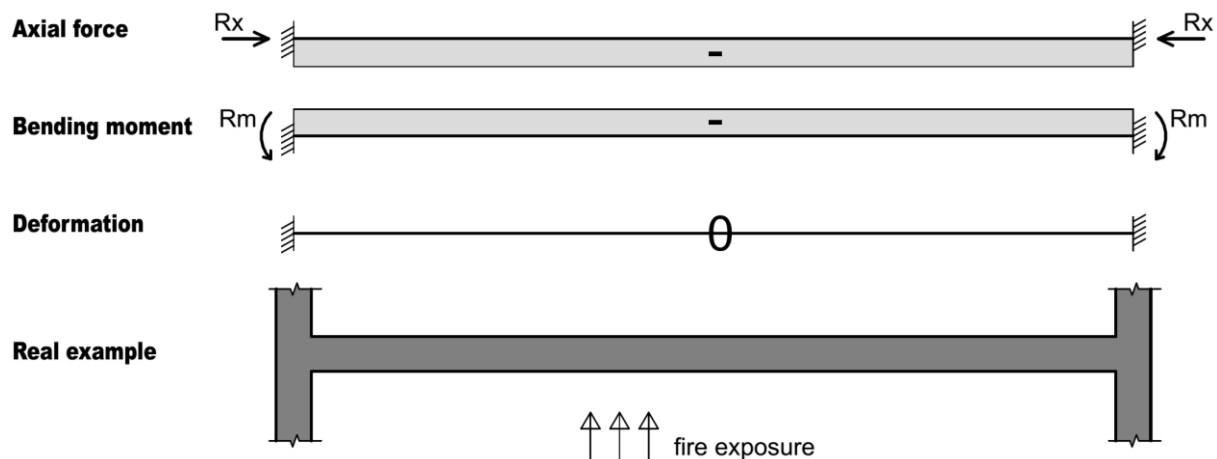
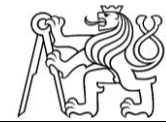


Fig. 7-2. Effect of thermal loading on statically-indeterminate structure.

Both limit situations when thermal deformation is completely free to propagate and completely restrained are rather theoretical. When speaking about real concrete structures, only minority of them can be described as purely statically-determinate. Structures casted on-site behave from their nature as statically-indeterminate since the elements are connected to each other by reinforcement and often also by concrete casted in one working step. Concrete floor slabs and beams supported by masonry walls and pillars are not perfectly free to move in longitudinal direction due to friction between materials, so some part of the deformation is restrained and reaction develops. Rotation at supports is not perfectly free due to loading from load-bearing wall of upper floors which partially restrains it and again, moment reaction develops. Floor slab composed of precast floor panels behaves as stiff diaphragm as single panels are connected to each other by reinforcement and joints are concreted afterwards. Probably a structure of (e.g. industrial) hall composed of single precast RC elements with hinge joints is closest to statically-determinate type of structure, however also in this case the hinges are not perfect due to the friction and limited width of spaces enabling horizontal movement. On the other hand, statically-indetermined structures can be usually characterized by allowing zero vertical and horizontal movement and zero rotation in stiff joints between elements, which is in calculation represented by appropriate zero members in the vector of movements. But in case of real structures the mentioned joint deformations are not equal to absolute zero, they are only limitedly approaching it – consequently the stiffness's are



not infinite. The value of stiffness can be then iteratively calculated<sup>7</sup>. This is very important if thermal loadings are about to be estimated.

Estimating thermal deformation and consequent additional inner forces on concrete element which is subjected to elevated temperatures is also complicated due to existence of LITS, which was discussed in detail in [Chapter 2.5.1](#). Thanks to it, not-negligible part of thermal strain is relaxed and do not contribute to thermal deformations or additional stresses. However, this strain component is not constant over fire duration as it depends on stiffness of subjected member and supports as well and also on the actual load level, which generally vary with time.

From the mentioned above it is clear the effect of thermal loadings must be solved on whole structure within global analysis (or at least on reasonably big part of it), due to the structural effects which cannot be described properly by sectional analysis. Certain simplification can be done by choosing one element to be inspected in detail separately. Supports of such element should be then generic in order to enable setting the actual stiffness of supports representing the adjacent structure. Example of such simplified calculation model can be seen in [Fig. 7-3](#).

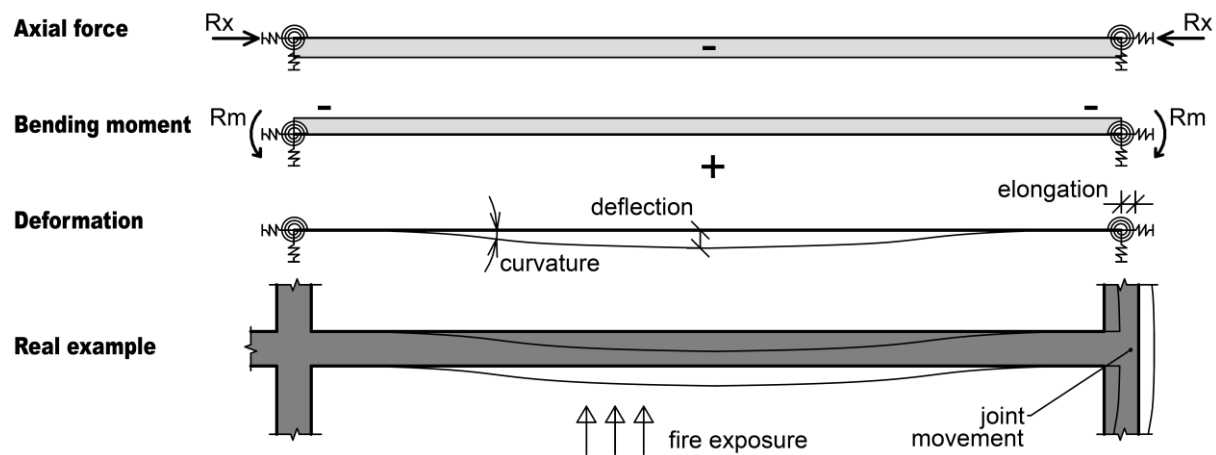


*Fig. 7-3. Effect of thermal loading on generic computational element.*

### Stiffness Evolution

Another aspect which makes global analysis necessary to be conducted is the fact that the elements stiffness (both axial and flexural) does not remain constant during fire. In case the structure is statically-determinate it does not represent problem since the distribution of internal forces (either from external or thermal loading) does not change due to it. However, in case of statically-indeterminate structure this stiffness evolution causes redistribution of internal forces.

Moreover, gradual decay of elements stiffness must be taken into account if simplified calculation model of global analysis is used, as is described above. If the global analysis was conducted on whole construction, stiffness decay would be properly attributed to all elements exposed to fire and thus the mutual stiffness ratios and consequently distribution of internal forces would be correct. However, if only one element is being inspected in the simplified model, it is necessary to set the stiffness's of spring supports as a function of fire duration in order to represent the stiffness decay of adjacent structure properly.

---

<sup>7</sup> The finite value of stiffness can approximately be found iteratively when force or moment reactions at spring supports differ from the ones gained from model with perfectly fixed supports by 5-10 %. Moreover, it does not make much sense to reach lower difference as the value of finite stiffness would rise steeply due to the singular nature of theoretical absolutely stiff supports.



As a result of the above described, list of implications is given below:

- Evolution of element's or spring supports stiffness's influence directly values of additional forces resulting from (partially) restrained thermal deformation. Because of that the analysis has to be coupled taking into account both evolution of additional forces and stiffness decay together according to chosen time of fire.
- Due to stiffness decay of the thermally damaged elements the internal forces move towards adjacent part of structure with higher stiffness and which is less damaged or even undamaged at all.
- Although damaged elements are unloaded by external loading a bit, their load-bearing capacity is reduced at the same time. To continue, distribution of internal forces is affected also by temperature-induced additional forces which vary over time. Thus, the load-bearing capacity of element exposed to fire cannot be assessed without detailed time-dependent analysis.
- As a consequence, adjacent not-damaged structural elements might exhibit increase of inner forces, especially in the spans closest to the damaged ones. These members would not usually be inspected and all attention would be dedicated to the members directly affected by fire, however due to such forces redistribution and change of structural system potentially dangerous situation might occur.
- One has to think about the structural system changes not only during fire, but during the forthcoming post-fire investigation as well. Big part of material deterioration and cross-sectional damage is irreversible and the process of cooling period might contribute to damage level as well. Then the structural system may be changed permanently which has to be reflected in the post-fire analysis.

Simplified idea about the reduction of flexural stiffness can be obtained assuming the principle of *isotherm 500 °C* method. For different standard fire durations distance of 500° C isotherm from the heated surface was estimated conducting thermal analysis. Then the layer of concrete heated to 500 °C or more was excluded from the cross-section while rest of the cross-section preserves initial strength and modulus of elasticity. For such dimensions the moment of inertia was calculated (rectangular cross-section heated only from bottom is assumed). Because height is cubed in the formula ( $I_y = 1/12 bh^3$ ), moment of inertia decreases quite progressively being approximately 75% at 60 min, 55% at 120 min and only 40% at 240 min duration of standard fire, see in [Fig. 7-04](#). The calculation is only illustrative assuming linear elastic behaviour of material without cross-section being weakened by cracks.



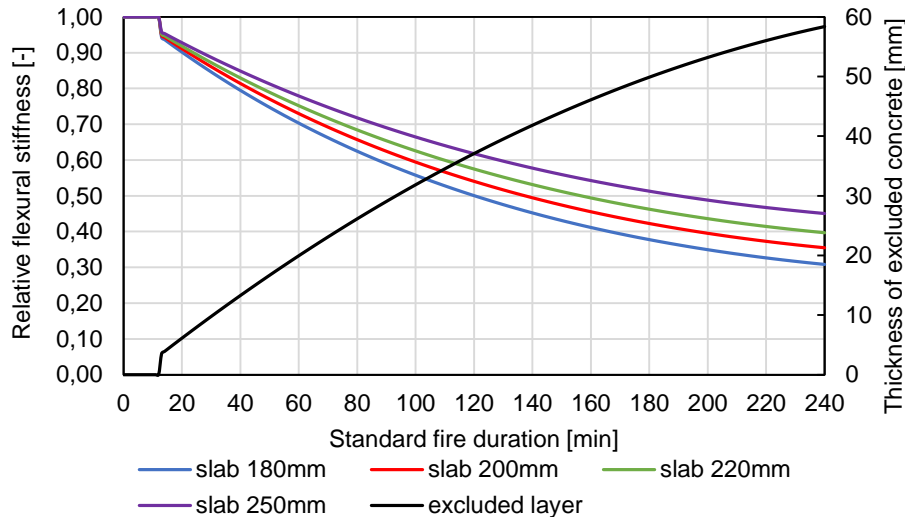


Fig. 7-4. Evolution of flexural stiffness decay and thickness reduction according to standard fire duration.

To illustrate the effect of element's stiffness decay an example was created, see Fig. 7-5. Let's have a continuous one-way RC slab 200 mm thick. Usual loading is assumed (dead load 2 kN/m<sup>2</sup> plus self-weight, live load 1,5 kN/m<sup>2</sup>). All spans are 5 m long. Inner 5 spans are inspected and the middle one is exposed to standard fire of various durations. Height of the cross-section is gradually reduced according to the diagram shown above in Fig. 7-4. Distribution of bending moment, calculated according to linear elastic theory, is then drawn for different durations of fire. Gradual movement of moment towards 2<sup>nd</sup> and 4<sup>th</sup> span can be seen which is a result of reduced stiffness of the middle element. Then one more situation is shown. It can happen that the cross-sections above supports of the fire-exposed element get overloaded during fire and that the linear behaviour is exceeded towards plastic region. Thus, these cross-sections do not preserve their flexural stiffness and (partial) plastic hinges create. This can happen when yield plateau of reinforcement is reached while ultimate strain of concrete is not – the structure still works but certain rotation at supports propagates and vertical deflection rises. And again, in case of statically-indeterminate structures redistribution of inner forces happens, which might significantly change their so far distribution. This possible change is then important mainly for post-fire assessments.

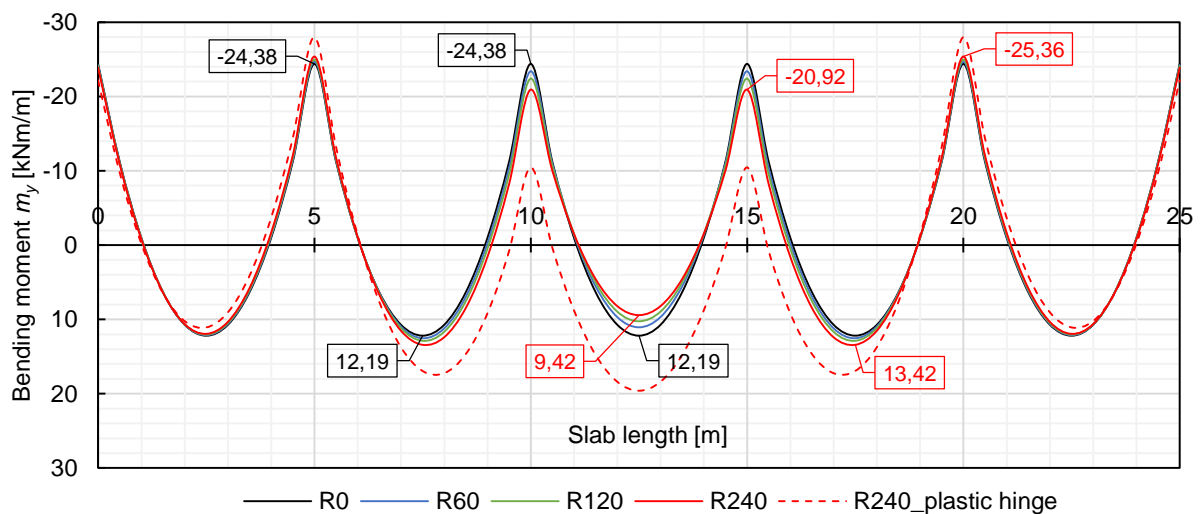


Fig. 7-5. Movement of bending moment line on continuous one-way RC slab th.200 mm, ISO834 fire assumed, middle span exposed.



## 7.2 Estimating Fire Resistance with Respect to Global Analysis

### Tabular Methods According to EC2

Available methods for assessing fire resistance of RC elements are briefly described in [Chapter 2.6](#). The popular tabular method is based on very many fire experiments and experience with real fires. It is said to be conservative in most cases, especially for longer fire durations. Because of the empirical nature of this method, effects of the mentioned transient processes are indirectly incorporated in the tables. Unfortunately, one does not have particular idea about reserves in the assessment and level of element exploitation. Therefore, one should be careful assessing unconventional and courageous structures or ordinary structures heavily or unconventionally loaded when using this method. In such cases performance-based methods seem to be more suitable.

There is also simplified calculation method for beams and slabs presented in Annex E, EC2-1-2 [16]. The method is created as an extension of tabular methods when minimal distance of reinforcement from heated surface is not respected. Using this method fire resistance with smaller distance of reinforcement can be proved. However, this calculation method cannot describe anything else and none of the actual structural behavior during fire.

### Simplified Calculation Methods According to EC2

Simplified calculation methods presented in Annex B, EC2-1-2 [16] are briefly described in [Chapter 2.6](#). Both of the methods take into account material deterioration due to exposure to high temperatures. Mechanical properties of both steel and concrete are lowered with respect to the temperature distribution along the cross-section and the element itself as well. In both methods also certain part of concrete cross-sectional area is excluded from calculations. Although the methods are based on simplified assumptions, according to many conducted reviews and studies [28] it is stated the accuracy of these methods is in most cases sufficient. Thanks to the simplifications the methods are relatively easy to use, fast and user-friendly. They are also implemented in commercial structural software (e.g. *FINE Beton požár* [97]) which can be used for such purposes.

On the contrary to the benefits mentioned above, although these methods are performance-based, their ability to describe the actual structural behaviour during fire is very limited. First of all, these methods allow conducting sectional analysis only, it means no global structural effects including temperature-induced loading are taken into account implicitly. If the assessment shall be conducted properly, these effects must be calculated by-hand or in another computational model and included in the assessment in the member of acting loads effect on the left side of the inequation, see [Eq. \(7-1\)](#).

### Advanced Calculation Methods According to EC2

Advanced calculation methods represent the most detailed approach how to assess fire resistance of concrete structural members. The assessment can be conducted either on cross-section, chosen part of structure or whole structure. Such assessment is then suitable for conducting global analysis since all structural effects connected to the structural system can be incorporated in the calculation. However, it is not easy to use such methods because EC2 [16] gives only very limited common guidelines.

Using advanced calculation methods leads to detailed FEM calculations either in commercial software or in in-house built applications. Beside some in-house built, not-generic applications developed at universities all over the world, there are two universal commercial computer programmes that can be used for such purposes. The first programme, SAFIR [48] has been developed at University of Liege, Belgium. The second one, VULCAN [98] has been developed by Sheffield Structural Fire Research Group, England. Both programmes are primarily aimed at calculating either steel or steel-concrete composite structures, but solving only concrete structure is possible as well. Both applications represent robust software which can be very useful when solving specific and challenging problems, however for regular use they are rather cumbersome and not user-friendly. They are also relatively



expensive and used by only small groups of engineers or scientists, respectively (for instance, in Czech Republic the programmes are not widely known and are used only by individuals, if ever).

Beside the two mentioned programmes which are aimed only at calculating structural fire resistance, there are also powerful generic software solutions, e.g. ANSYS or ABAQUS. In such software very broad field of problems can be simulated, among them also exposure to high temperature as a result of fire. It is possible to couple the thermal and mechanical analysis and to set the temperature-dependency of thermal and mechanical material properties. However, despite these promising assumptions it is very problematical to set the concrete stress-strain diagram correctly in order to respect LITS and relaxation of thermal loadings. Moreover, inserting reinforcement into the 3D model is enormously laborious. Idea of modelling more than one selected element from the structure, which should be one of the main goals of global analysis, is practically impossible. Thus, using such programmes can be possible for scientific purposes only and not engineering practise.

### Commentary to Eurocode 2 Guidelines

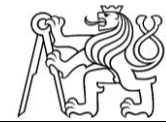
Since fire event is considered to be extraordinary design situation it is possible to reduce live loads to certain extent due to the limited probability of its occurrence in full extent during fire situation [49]. Beside the ordinary external loads, indirect thermal loads generally have to be incorporated in the calculation as well. On the other hand, structural elements are being damaged due to the exposure to high temperatures which results not only in decay of their load-bearing capacity, but reduction of their flexural and axial stiffness as well. Both mentioned phenomena are closely related to the particular structural system. It can be stated they both are relevant especially in case of statically-indeterminate structures. Additional inner forces caused by thermal loads are generally variable over fire duration as thermal gradient and reduction of stiffness's keep changing in nonlinear way. As a result, distribution of inner forces during fire is different to the state prior to it. Due to these reasons the approach allowed and suggested by EC1-1-2 [16] (par. 4.3.2) and EC2-1-2 [16] (par. 2.4.2), when the value of appropriate inner force can be taken and lowered by coefficient  $\eta_{fi}$  might not be accurate enough.

To continue, paragraph numbers relating to EC2 [16] with commentary are given in the list below:

- par. 2.4.2 (4): It is stated that *when conducting sectional analysis, the effects of thermal bowing must be taken into account, but thermal elongation can be neglected*. This assumption is not correct since additional inner forces are strongly dependant on particular structural system and cannot be separated; the assessment is then about to be done in N-M diagram where compressive force induced by restrained elongation might provide much-needed compressive reserve thanks to which the element's load-bearing capacity might be sufficient.
- par. 2.4.2 (5) and 2.4.3 (5): It is stated that *when conducting sectional analysis or solving chosen part of structure, the boundary and supports conditions at the ends of chosen element are constant over the fire time*. This assumption is not correct as the rotational stiffness at the supports is changing over the time of fire due to the material degradation, see Fig. 7-4 and Fig. 7-5 above.

## 7.3 Incorporation of Thermal Loading into the Assessment

As it was already mentioned, the best way how to investigate and estimate effects of thermal loadings of concrete structures subjected to fire, is conducting global analysis in the means of advanced calculating methods. It was also mentioned nowadays no easy way exists for this purposes. Therefore, it was decided that working group of Department of Concrete and Masonry Structures at Czech Technical University in Prague will develop its own computational application.



The idea about this application is following:

- It will work with one chosen structural element, see Fig. 7-6;
- Supports conditions at the ends will respect actual structural system using spring supports with finite stiffness's;
  - The value of stiffness's would be dependent on time of fire or temperature due to material deterioration (especially flexural stiffness, see Fig. 7-4);
- Concrete stress-strain diagram will be defined with respect to the actual behaviour of concrete structures under fire conditions including LITS and relaxation of thermal stresses;
  - It would be interesting to have an option to choose the stress-strain diagram according to the definition published by different authors (see Chapter 2.5.1)
- It will be possible to insert any temperature-time curve including cooling phase;
  - Alternatively, only ISO 834 temperature-time curve would be possible – other curves could be converted to ISO 834, see Fig. 5-13;
- Then coupled thermal and mechanical analysis will be conducted;
  - The cross-section will be divided into horizontal strips with its own mean temperature;
  - Decay of material strength and Young's modulus according to reached temperature will be implemented – either according to Eurocode or ACI assumptions or universally (results from material tests could be used)
  - Thermal strains will be included;
- Cooling regime will be taken into account (possible additional lowering mechanical properties);
- Slip of reinforcement as a result of different thermal strain will be taken into account.

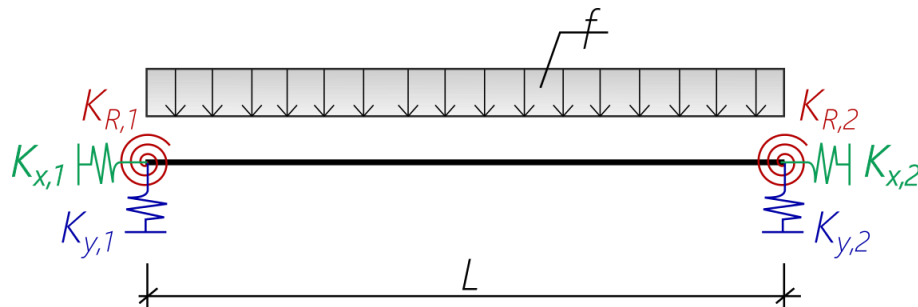


Fig. 7-6. Planned structural model of selected element analysed in the application.

As can be seen from the list above, the application must contain and properly describe many phenomena while most of them are nonlinear. Development of such software needs plenty of time and programming skills. Due to the total needed amount of labour and time it was decided the application will not be a part of this Ph.D. thesis. Instead of it, it will be developed and published separately after proper validation with other published research.

Until the application is finished and validated, an approximate approach how to take temperature-induced loading into account is given in forthcoming paragraphs. Graphical interpretation of the approach can be seen in the flowchart in Fig. 7-7 below. It is worth to notice that although the calculation approach is universal, it primarily deals with slabs and beams of rectangular cross-section in bending.

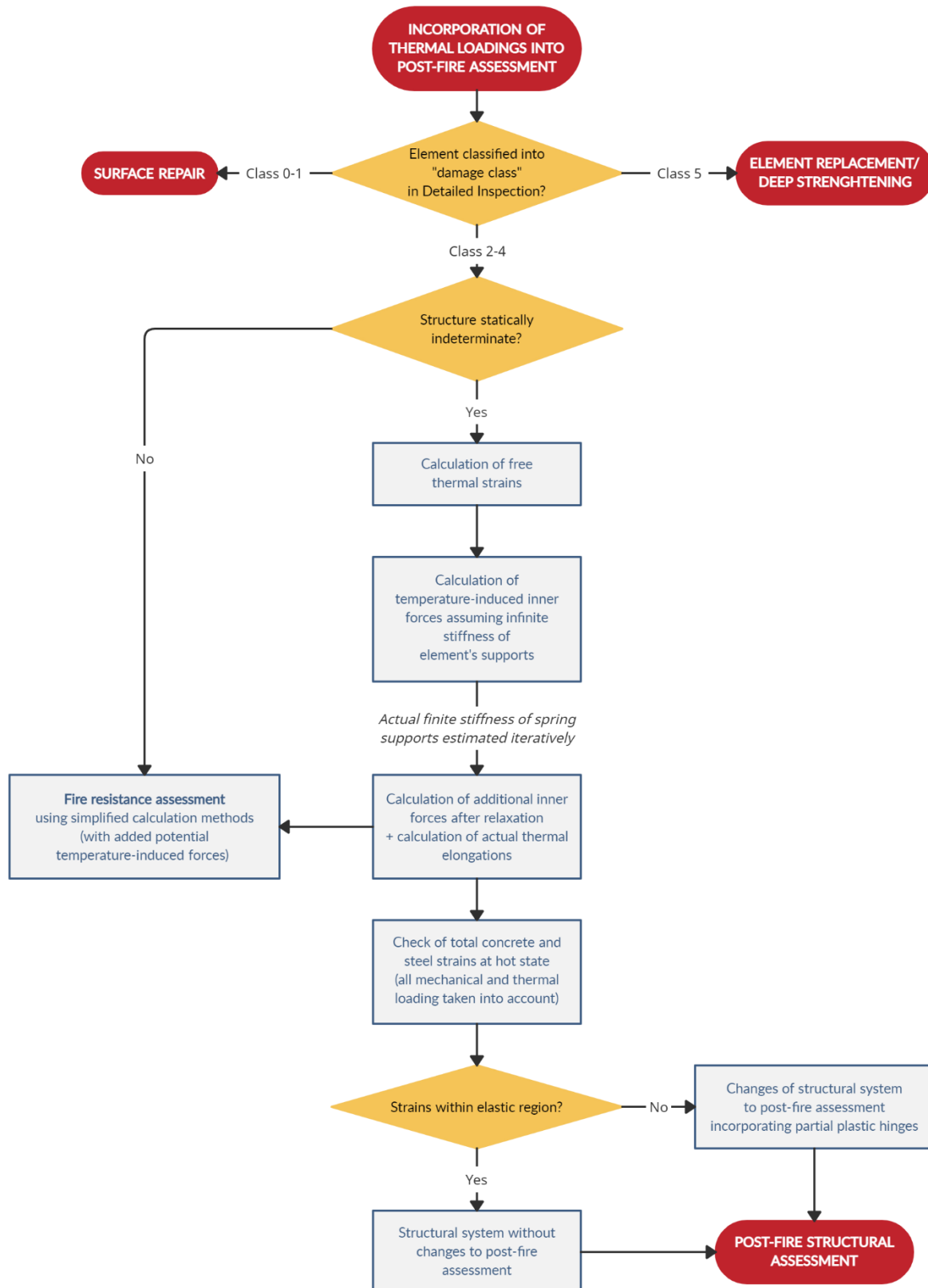
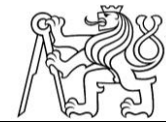


Fig. 7-7. Flowchart of taking thermal loading into account.





### Fundamentals of Thermal Strains Simplified Calculation

Calculation of temperature-induced additional inner forces proposed herein is based on the approach published in Annex D in the previous design code ENV 1992-1-2 [99]. According to it, the given cross-section is divided into horizontal strips. For each strip free thermal strain is calculated according to its temperature assuming the strips are able to deform axially freely without being restrained by the rest of the cross-section, see Fig. 7-8. Because of the strips nonlinear strains over the element height, which is a result of nonlinear temperature distribution, the cross-section would not stay plane, which is one of the basic assumptions of Bernoulli-Navier hypothesis. Therefore, a hypothetical compressive stress is applied to each strip in order to restrain the thermal strains and keep cross-section plane. To ensure force equilibrium, eccentric axial force is assumed to act on the cross-section with the very same but opposite overall effect to the hypothetical stresses, see Fig. 7-9. Such forces are then called self-equilibrating.

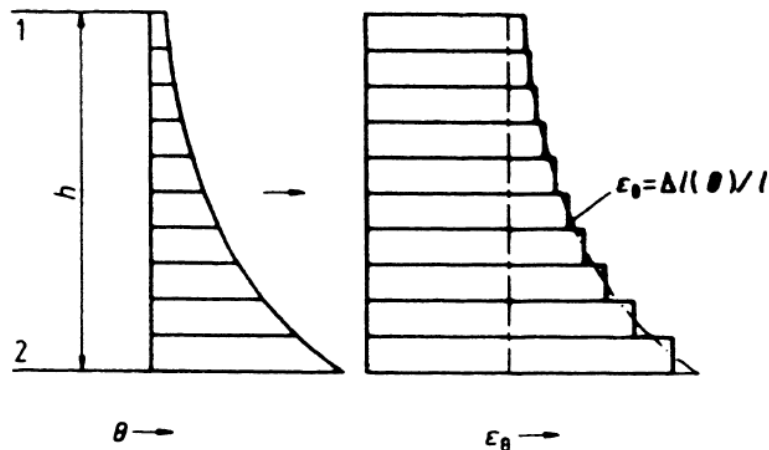


Fig. 7-8. Thermal strains of free strips, taken over [99].

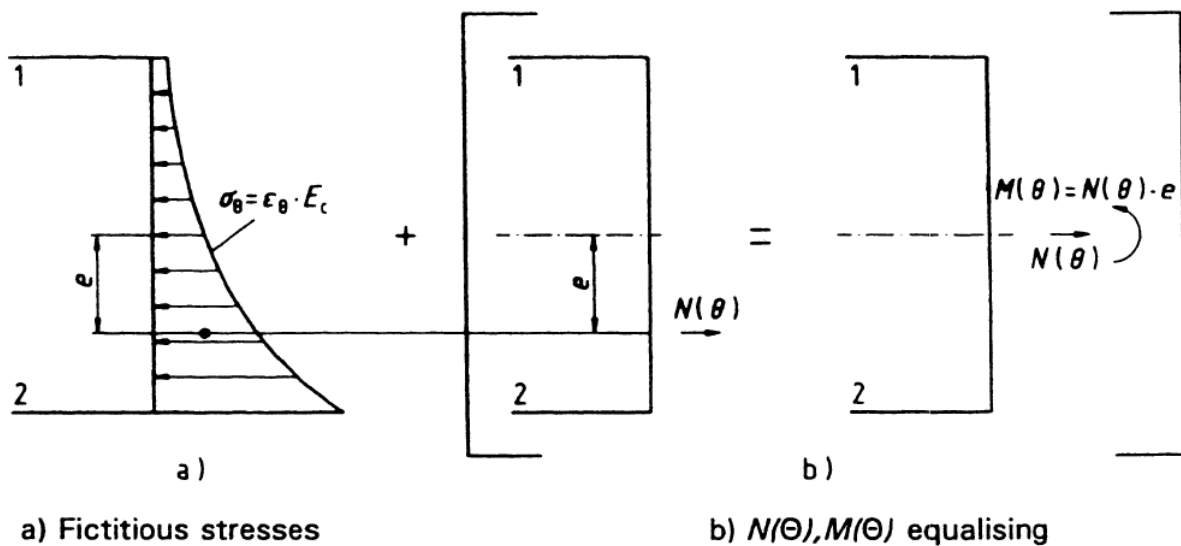


Fig. 7-9. Ensuring force-equilibrium over cross-section, taken over [99].

In case of rectangular cross-section of floor slab, it is presumed the element is heated only from the bottom side of cross-section. Then the thermal analysis can be done only in 1D direction along the element's height. In case of T-shaped or rectangular beams cross-sections, it is presumed it is heated from the bottom surfaces and from the web sides as well. The thermal field then has to be calculated in 2D. However, it is possible to make a simplification in the calculation of temperature-induced forces, as can be seen in Fig. 7-10. At given height mean temperature of the element over its thickness is calculated – then the cross-section is treated as rectangular.

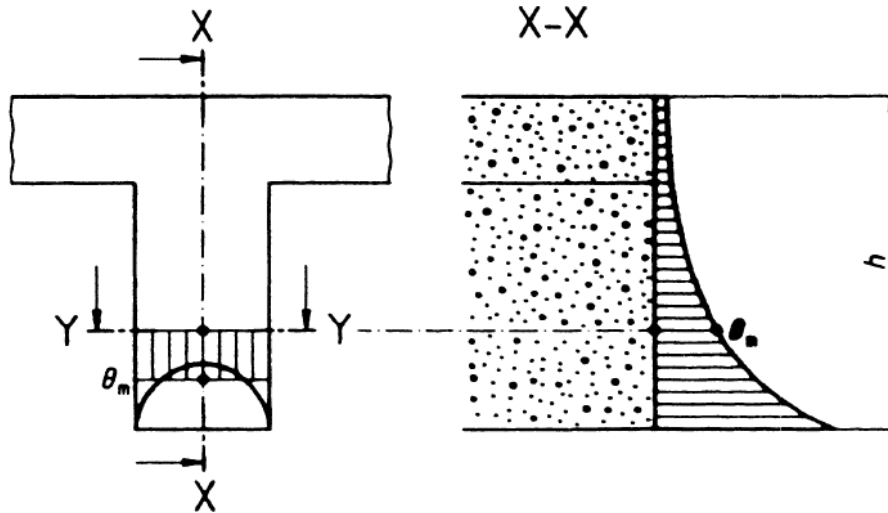


Fig. 7-10. Simplifying 2D thermal field into 1D, taken over [99].

To describe the calculation approach more in detail, the steps follow as it is given in the list below. For each strip these parameters are calculated:

- Distance of the strip axis to the heated surface  $x_{strip,i}$ ;
- Mean temperature of the strips  $\theta_{strip,i,mean}$  calculated as an average of temperatures on the strip edges (see Eq. (7-2));
- Temperature difference  $\Delta\theta_{strip,i}$  between mean strip temperature at hot state and the initial temperature prior to fire (see Eq. (7-3));
- Reduced Young's modulus of concrete  $E_{c,\theta}$  according to the concrete strength class and mean strip temperature at hot state (elasticity modulus decay e.g. [23], see Chapter 2.1.1);
- Free thermal strain of the strip  $\varepsilon_{free,strip,i}$  according to the temperature difference and EC2 [16];
- Stress in each strip  $\sigma_{strip,i}$  according to free thermal strain and reduced Young's modulus, thermal strain assumed to be absolutely restrained (see Eq. (7-4));
- Axial force  $N_{strip,i}$  as a result of the stress in the strip (see Eq. (7-5)).

After this procedure total sum of axial forces  $N_{\theta,total}$  can be calculated together with estimating the eccentricity  $e_{\theta}$  with respect to the centroid of the cross-section. After that axial force  $N_{\theta,total}$  and bending moment  $M_{\theta,total}$  can be expressed related to the centroid, see Eqs. (7-6) - (7-8).

$$\theta_{strip,i,mean} = 0,5 * (\theta_{strip,i,top} + \theta_{strip,i,bottom}) \quad (7-2)$$

$$\Delta\theta_{strip,i} = \theta_{strip,i,mean} - \theta_{strip,i,20} \quad (7-3)$$

$$\sigma_{strip,i} = \varepsilon_{free,strip,i} * E_{strip,i} \quad (7-4)$$

$$N_{strip,i} = A_{strip} * \sigma_{strip,i} \quad (7-5)$$

$$N_{\theta,total} = \sum_{i=1}^n N_{strip,i} \quad (7-6)$$

$$e_{\theta} = \frac{h}{2} - \frac{\sum N_{strip,i} * x_{strip,i}}{N_{\theta,total}} \quad (7-7)$$

$$M_{\theta,total} = N_{\theta,total} * e_{\theta} \quad (7-8)$$



### Calculation of Thermal Strains Assuming Zero Axial Support's Stiffness

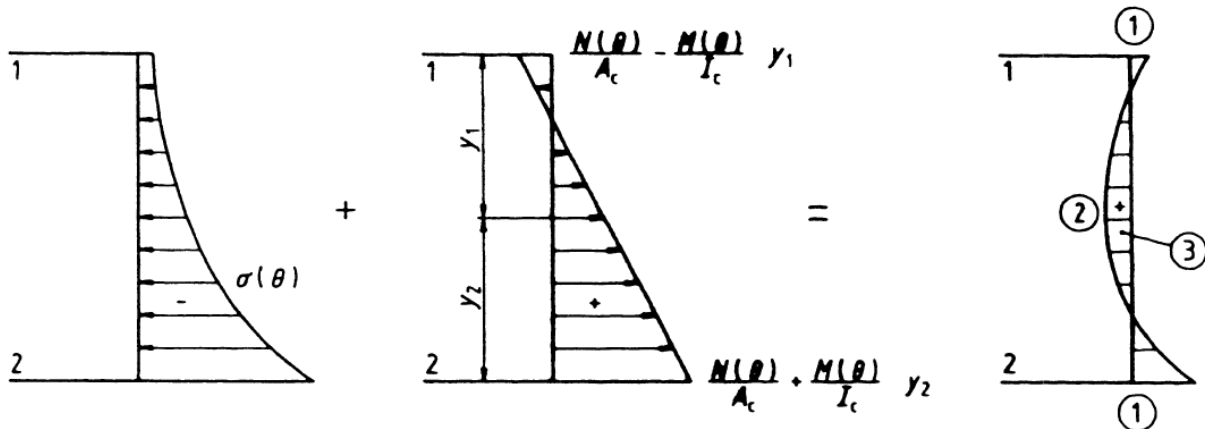
Calculation of free thermal strains continues in the approach given by ENV 1992-1-2 [99]. If the structural element is not restrained anyhow in horizontal direction, it will elongate according to the effective strain  $\varepsilon_{eff}$ , see Eq. (7-9). If the element is not restraint against bowing, it will rotate according to effective curvature  $(1/r)_{eff}$ , see Eq. (7-10). Final strains over the cross-section's height after imposing thermal and self-equilibrating stresses are displayed below in Fig. 7-11. The mean Young's modulus  $E_{c,\theta,1}$  refers to the weighted average of the part of cross-section, which is in compression by acting  $N_{\theta,total}$  and  $M_{\theta,total}$ .  $E_{c,\theta,2}$  represents weighted average of the value for the part of cross-section in tension by the same couple of internal forces.

$$\varepsilon_{eff} = \frac{\varepsilon_2 + \varepsilon_1}{2} \cong \frac{N_{\theta,total}}{2 * A_c} * \left( \frac{1}{E_{c,\theta,2}} + \frac{1}{E_{c,\theta,1}} \right) + \frac{M_{\theta,total}}{2 * I_y} * \left( \frac{y_2}{E_{c,\theta,2}} + \frac{y_1}{E_{c,\theta,1}} \right) \quad (7-9)$$

$$\left( \frac{1}{r} \right)_{eff} = \frac{\varepsilon_2 - \varepsilon_1}{h} \cong \frac{N_{\theta,total}}{2 * A_c * h} * \left( \frac{1}{E_{c,\theta,2}} - \frac{1}{E_{c,\theta,1}} \right) + \frac{M_{\theta,total}}{2 * I_y * h} * \left( \frac{y_2}{E_{c,\theta,2}} - \frac{y_1}{E_{c,\theta,1}} \right) \quad (7-10)$$

$$E_{c,\theta,1} = \frac{\sum E_{c,\theta,strip,i} * \varepsilon_{free,strip,i}}{\sum \varepsilon_{free,strip,i}} \quad (7-11)$$

$$E_{c,\theta,2} = \frac{\sum E_{c,\theta,strip,j} * \varepsilon_{free,strip,j}}{\sum \varepsilon_{free,strip,j}} \quad (7-12)$$



(1) compression, (2) tension, (3) possible internal micro-cracking

Fig. 7-11. Final strain over cross-section, taken over [99].



### Calculation of Temperature-Induced Forces Assuming Infinite Axial Support's Stiffness

In case the thermal strains are absolutely restrained they cannot even partially propagate and thus all energy that tend to deform the element results in additional internal stresses and internal forces, respectively. If the elongation is restrained, compressive stress develops along the element. If the stress is integrated over the cross-section negative axial force is obtained. If the rotation of element is restrained, the already mentioned negative axial force acts eccentrically with respect to the centroid of cross-section. If the temperature-induced axial force is expressed with respect to the centroid additional negative bending moment is obtained.

So the axial force and bending moment are the same values as already calculated  $N_{\theta, total}$  and  $M_{\theta, total}$ , but opposite signs since they are restraining the thermal strains to propagate. Theoretically these forces are directly the ones we can expect on the elements. However, due to the LITS and thermal stresses relaxation the actual forces which really develop on structural elements are much lower – which is very important and beneficial at the same time. The extent of relaxation according to the level of restraint in supports will be discussed in next paragraphs.

### Validation of Calculations

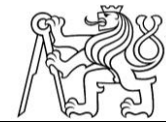
By using equations above it is possible to calculate actual free thermal strains of floor slabs and beams with respect to temperature distribution and also material “weakening” due to exposure to high temperatures. In order to validate gained results it is necessary to compare them with results of either experimental or numerical studies conducted on author’s own or by other researchers. Conducting full-scale experimental tests to analyse this phenomenon is extremely demanding (laboratory equipment, financial demands, etc.) and for the author of the Thesis unrealistic. On the other hand, conducting numerical study is closely connected to used software and its capabilities (see Chapter 7.2). Therefore, decision was made that for the comparative purposes validated numerical study published in the literature will be used – to be specific, parametric study published in Chapter 4.3.1 within *fib bulletin 46* [28].

In the study, among other analysed structures concrete precast floor panels and beams with variable supports conditions are chosen. The study is conducted in the ABAQUS software with specially implemented definition of concrete and reinforcement behaviour. Concrete stress-strain diagram should correspond with the implicit definition according to EC2 [16].

The first compared structural element is precast concrete floor panel. It is 6 m long, 250 mm thick and 1250 mm wide. Its bottom and top reinforcement is set to be 6 rods of diameter 12 mm. Ordinary loadings corresponding with use of such component in usual residential building is assumed. The panel is exposed to ISO834 fire heating bottom surface only. The structural behaviour is conducted up to 240 min of fire duration. In the study effect of changing axial stiffness of right support is analysed which influence the amount of LITS relaxing thermal stresses. At first (case A, see Fig. 7-12 below) zero axial stiffness is presumed while the rotation is restrained<sup>8</sup> (e.g. continuous floor slab supported by very rigid concrete wall on the left end and masonry wall on the right end). In cases B-D, the axial stiffness is being gradually increased up to the infinite stiffness, which tends to be rather theoretical case. Finite values of axial stiffness are expressed in the following form, see Eq. (7-13). This seems to be practical since the value of stiffness varies mainly with the length of adjacent structure (slab or beam continuing over next  $X$  spans). In some cases, the support’s stiffness is not based on the length of adjacent structure (e.g. outer span of slab or beam restrained by perimeter wall or column) – however in such cases the value can be also easily expressed in the form given below.

---

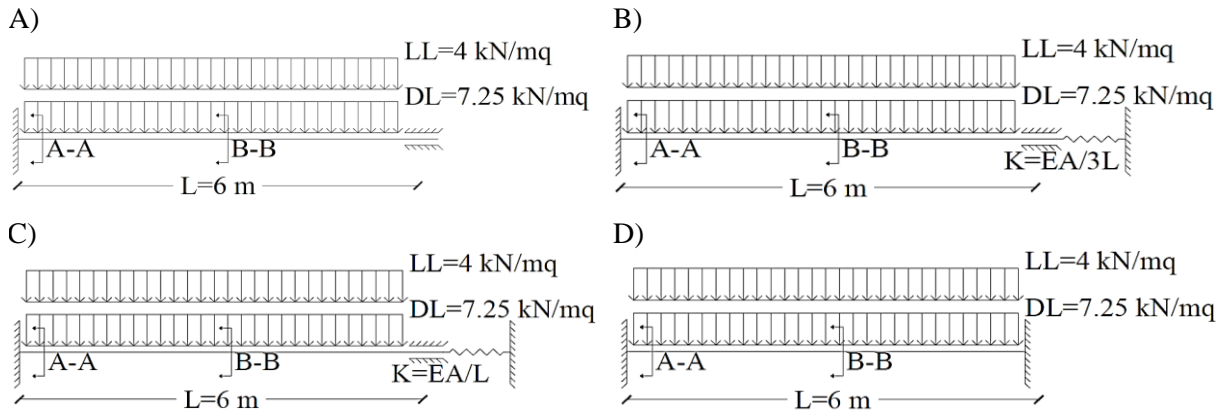
<sup>8</sup> This configuration seems to be unexpectedly dangerous as the negative bending moment develops due to rotation restraint, but no compressive reserve increasing flexural resistance is present due to free axial elongation.



$$K_i = \alpha_i * \left(\frac{EA}{L}\right) \quad (7-13)$$

where  $\alpha$  represents multiplier of the basic value of axial stiffness according to particular structural system,

$EA/L$  represents the basic value of axial stiffness.



Longitudinal reinforcement:

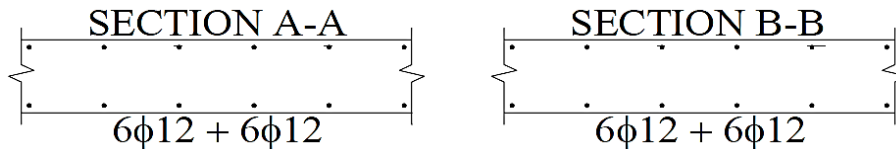


Fig. 7-12. Configuration of the parametric study, taken over [28].

The first value which is compared is the elongation of the panel at different times of fire. It is assumed the axial stiffness of the right supports is equal to zero, which corresponds with the case A. The calculated effective axial strain is multiplied by the length of the panel. The final values are displayed in the diagram below, see Fig. 7-13. In the same diagram also values resulting from the parametric study are drawn. It can be stated the panel elongates by approximately 14 mm at 60 minutes of standard fire and 24 mm at 240 minutes. From the comparison of the values it can be stated the values gained by simplified calculations fit to results of the parametric study very well.

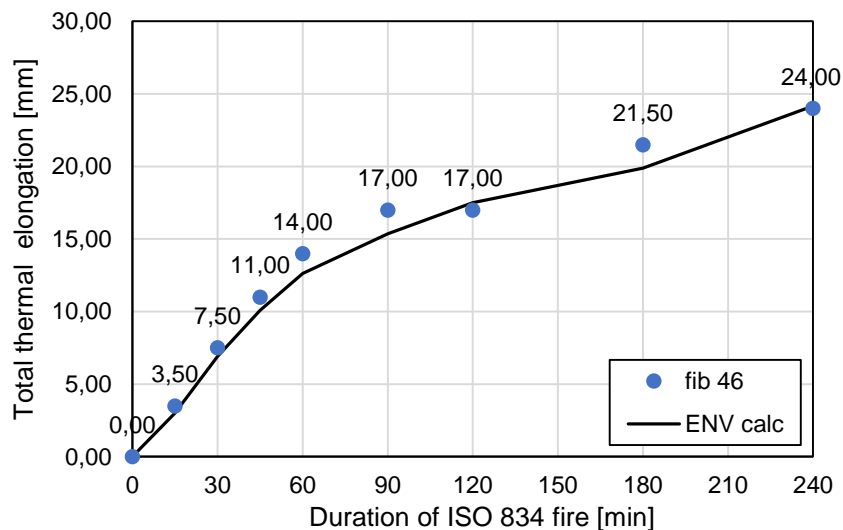


Fig. 7-13. Comparison of panel's elongation with zero axial restraint.





To continue, case D is compared – in this case the thermal strains are absolutely restrained. The theoretical evolution of temperature-induced axial force and bending moment without LITS is plotted in Fig. 7-14 according to the length of fire duration as well as values obtained in the parametric study. After the correlation it can be stated that the actual values of negative axial force after relaxation are only approximately 1/3 of the theoretical values – in other words 2/3 of the forces relax and disappear due to LITS. If the actual value of axial force is combined with the theoretically calculated eccentricity, the actual bending moments tend to be approximately 1/3 as well – at least up to 60 minutes. For longer fire durations, the bending moments are lower than the mentioned 1/3 of theoretical value (that is probably due to gradually decreasing flexural stiffness of the cross-sections which is incorporated in the advanced calculation model but not in the simplified one) – the simplified calculations are thus more conservative. The level of LITS relaxation in case of dominantly compressed elements (columns, walls and struts) reach up to 100 % [28] thanks to the prestress during heating, see Fig. 2.26. Thus, no additional compressive force develops; bending moment from restrained bowing still takes place.

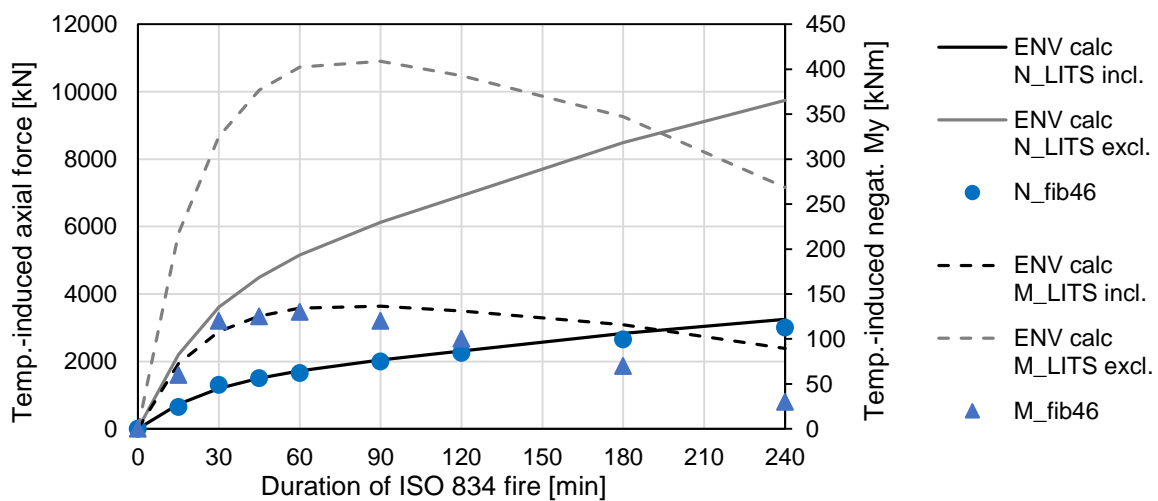


Fig. 7-14. Comparison of additional inner forces evolution with absolutely stiff axial restraint.

When speaking about the eccentricity of axial force generated by restrained thermal strain it is interesting to plot the evolution of the eccentricity which is a result of the thermal gradient. In Fig. 7-15 it can be seen that the eccentricity reaches its maximum at the very beginning of the fire as the thermal gradient is the highest as well due to very big difference between temperature of the already heated surface layers and still cool rest of the cross-section. With continuing fire duration, the thermal gradient gets gradually lower and so does the eccentricity.

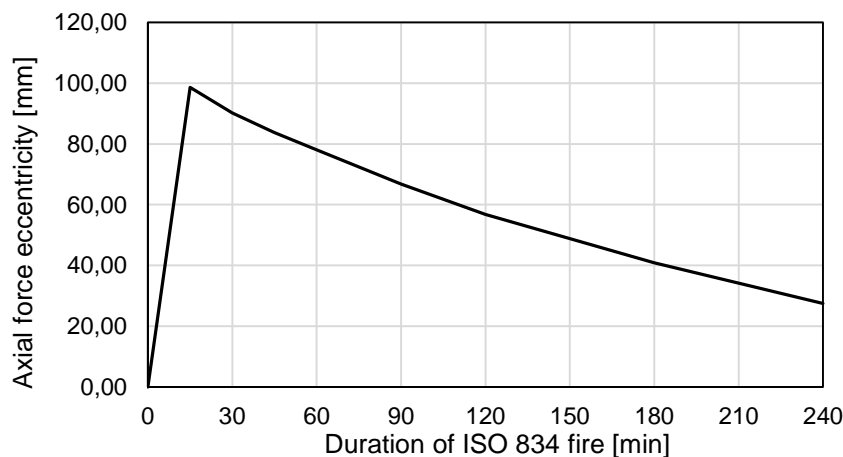


Fig. 7-15. Evolution of axial force eccentricity and thermal gradient.



Then it is interesting to think about the maximum of temperature-induced bending moment at 60 minutes, which is a combination of still increasing axial force and gradually decreasing thermal gradient. Nevertheless, the standard fire time 60 minutes seems to be critical as the temperature-induced bending moment reaches its maximum but the compressive axial force which helps to mitigate the tension in the cross-section does not.

### Calculation of Temperature-Induced Forces Assuming Actual Support's Stiffness

To begin this chapter, three diagrams based on the cited parametric study are given. In Figs. 7-16 to 7-18 evolution of temperature-induced axial forces, bending moments and axial elongation with fire duration and according to axial support stiffness can be seen. Based on the diagrams it can be stated that the value of stiffness influences the particular size of inner force and deformation, respectively, but the trend of evolution with fire duration keeps the same. Axial force together with elongation keep rising with lasting fire time and the bending moment reaches its maximum in 60<sup>th</sup> minute.

In the diagram of temperature-induced inner forces and elongation, respectively, there are also highlighted points of values obtained from simplified calculations according to the regression analysis dealing with changing stiffness – see equations Eq. (7-14) to (7-20) below. It can be stated the simplified calculation leads to slightly more conservative values than it is obtained from parametric study (colour of points respects colour of curves).

In case of temperature-induced bending moment the proportionality between axial force after relaxation (according to particular support stiffness) and bending moment does not work properly – the curves related to different stiffness's are practically identical up to 90 minutes of standard fire and after exceeding 90 minutes they are gradually decreasing in similar pace. Therefore, only values of additional bending moment gained by simplified calculations estimated assuming infinite stiffness's are showed in the diagram below. Then it can be stated that up to 60 minutes the curves representing parametric study and points representing simplified calculations correlate to each other very well. After exceeding 60 minutes of standard fire duration, the values from simplified calculations tend to be higher than curves of parametric study – it means the simplified calculations are more conservative. It is also worth to mention that in case the axial support stiffness is equal to zero and thus all axial elongation is not restrained (in other words the axial force is equal to zero), the bending moment develops as the thermal gradient still takes place. The theoretical axial force which induces the bending moment is approximately 22-25 % of the directly induced force  $N_{\theta, total}$  – thus it is conservative enough to assume 33 % as in case the axial force is not equal to zero.

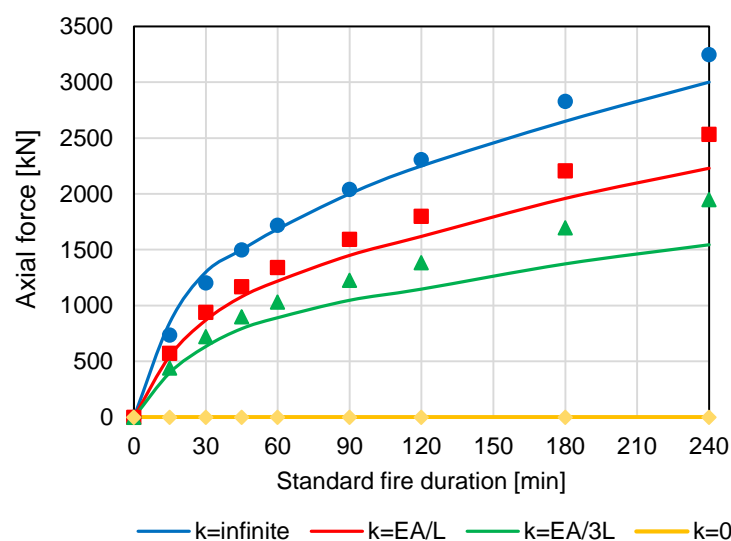


Fig. 7-16. Evolution of temperature-induced axial force according to support's axial stiffness [28].

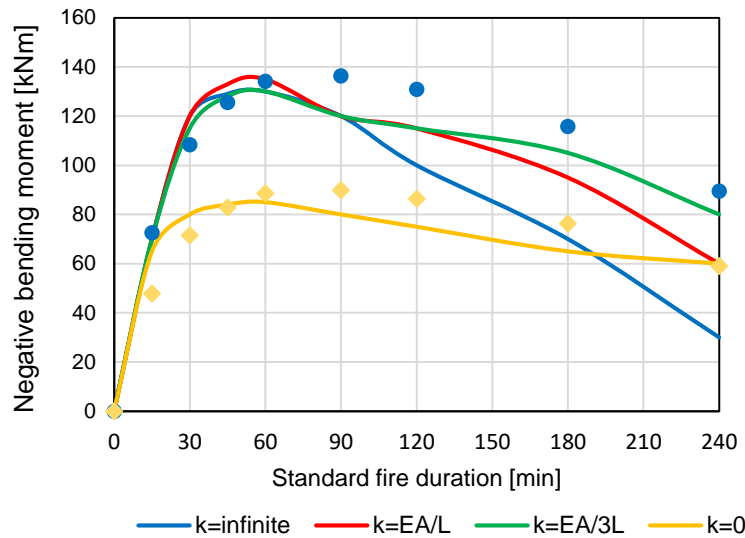


Fig. 7-17. Evolution of temperature-induced bending moment according to support's axial stiffness [28].

The same approach of simplified calculation can be applied in order to approximate the element's elongation if it is restrained to certain extent by supports – which is the situation that can be expected almost in every case. In the diagram given in Fig. 7-18 curves describing the elongation according to changing axial stiffness of supports from the parametric study are plotted. Based on their evolution it can be stated that the elongation decreases quite rapidly if some kind of axial restraint is present (e.g. nearly 25 mm in 240<sup>th</sup> minute of standard fire with no restraint versus 5 mm in the same fire time if restraint  $K = EA/3L$  can be taken into account). Since the elongation is very important for stress development in statically-indeterminate adjacent parts of structure (basically forced movements of joints), it is necessary to calculate also this kind of deformation to assess the fire resistance properly.

Beside the curves related to the parametric study also points of elongation obtained by simplified calculation can be found in the diagram. From comparison of these approximately estimated values and curves from parametric study it can be stated the simplified calculation provides satisfactory accuracy.

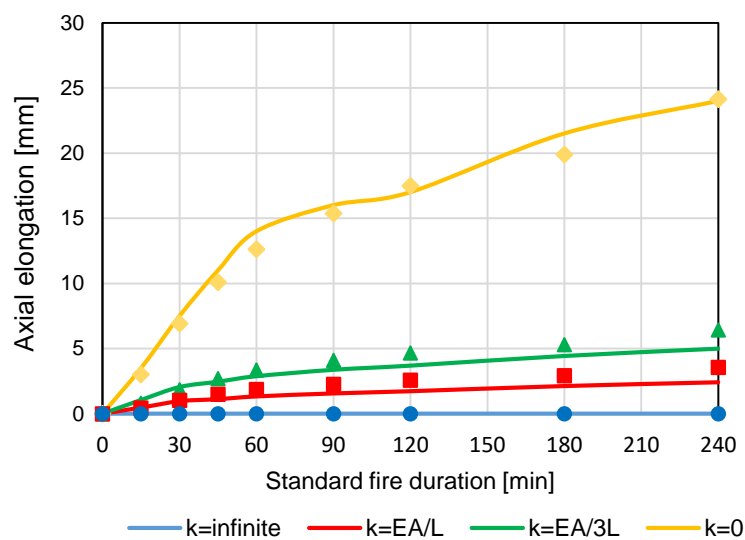
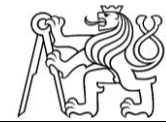


Fig. 7-18. Evolution of temperature-induced axial elongation according to support's axial stiffness [28].



$$N_{\theta,relax} = a_1 * a_2 * a_3 * N_{\theta,total} \quad (7-14)$$

$$\Delta L_{\theta,relax} = (1 - a_1) * (1 - a_2) * a_3 * \Delta L_{\theta,free} \quad (7-15)$$

$$M_{\theta,relax} = a_1 * N_{\theta,total} * e_{\theta} \quad (7-16)$$

$$\varepsilon_{eff,relax} = (1 - a_1) * (1 - a_2) * \varepsilon_{eff} \quad (7-17)$$

(according to correlation,  
see Figs. 7-16 to 7-18)

$$a_1 = 0,33 \quad (7-18)$$

or  $a_1 = 0,25$  if  $\alpha = 0$

$$a_2 = \max\left(0,87 - \frac{0,09}{\alpha}; 0,57 + 0,17 * \ln(\alpha)\right) \wedge a_2 \leq 1,0 \quad (7-19)$$

$$a_3 = 1 - \text{elements dominantly in bending (slabs, beams)} \quad (7-20)$$

$$a_3 = 0 - \text{elements dominantly in compression (columns, walls)}$$

where  $a_1$  represents the ratio of theoretically calculated temperature-induced forces which propagates on element after relaxation due to LITS if infinite axial supports stiffness is assumed,  
 $a_2$  represents the effect of supports with finite value of axial stiffness, see Fig. 7-19 below,  
 $a_3$  represents the difference between LITS relaxation level for elements in bending and compression,  
 $\alpha$  represents the multiplier of basic axial stiffness ( $EA/L$ ).

In order to take the changing value of axial support stiffness into account regression analysis is conducted where mutual mathematical relationship between stiffness and level of propagated inner forces is being searched. Two types of mathematical functions are used: (i) inverse function due to the rapid growth at low values of stiffness multiplier  $\alpha$ , (ii) logarithmic function for higher values of  $\alpha$  where only slow growth of variable  $a_2$  can be observed. Then, higher value from both equations is taken into account while  $a_2 \leq 1$  is assumed. If the support stiffness is very close to infinity  $\rightarrow a_2 = 1$  – which means all energy will result in the axial force and the elongation will be equal to zero, see Eq. (7-19). On the other hand, if the support stiffness is very low or equal to zero  $\rightarrow a_2 = 0$  – all energy will result in the elongation and the temperature-induced force will be equal to zero, see Eq. (7-19).

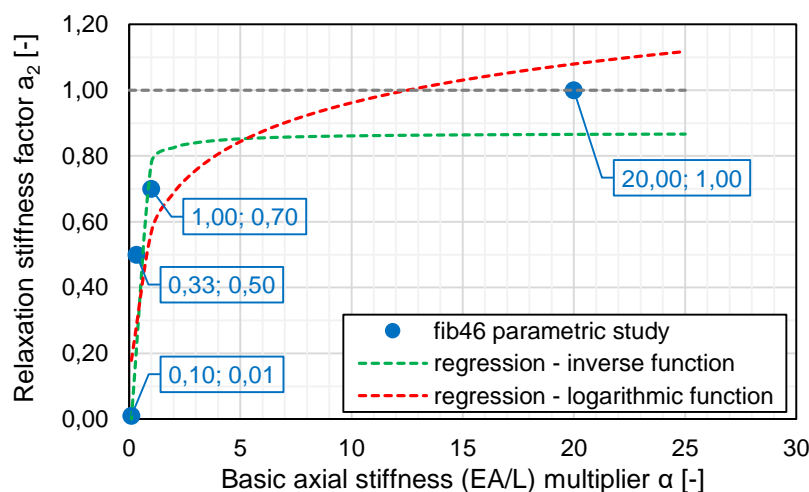


Fig. 7-19. Influence of support stiffness on relaxation level, expressed by factor  $a_2$ <sup>9</sup>.

<sup>9</sup> As it is stated in the flowchart in Fig. 7-07, the finite value of stiffness is estimated iteratively in order to achieve the result close to those obtained with infinitely stiff supports (results difference about 10 %).



If it is necessary to estimate both supports movement and thus direction of element's elongation on its both ends the value calculated according to the approach given above can be divided in the mutual ratio of supports stiffness's.

### Check of Cross-Section Elastic Behaviour During Fire

Check of total strains on cross-section whether they are within the elastic region is another step of global analysis which is about to be conducted. In this step the summed mechanical and thermal strains are analysed. Values of top and bottom reinforcement strains as well as strains of concrete in compression are studied and compared with the limit strain for both materials. In case of reinforcement the strain connected to reaching yield strength and the ultimate strain connected to bars rupture are taken into account. In case of concrete strain connected to reaching peak compressive strength and the ultimate strain connected to concrete crushing are taken into account. In the calculation it is also distinguished whether the concrete in compression and reinforcement in tension are heated by the fire – according to it the limit strain values are assumed as a function of temperature.

This assessment is advised to be done in order to have an idea about the stress state in the cross-section. If the calculated strains are still in the elastic region, it is good marker the cross-section is not overloaded and the ultimate load-bearing capacity is not close. It also means that after the end of fire event strains which can be attributed to unloading and cooling back to ambient temperature will disappear and no<sup>10</sup> plastic strains will remain. In case the strains are beyond the elastic limits it means that after the end of fire and unloading the relevant strains will disappear only partly – the other part of them will remain as residual due to reaching the plastic behaviour of materials. From the calculations below it seems the nearest elastic limit strain which is to be reached is the tensile reinforcement strain related to yield strength. After reaching this state following can be stated:

- The ultimate load-bearing capacity is getting close – one should be aware of it and careful;
- The statically indeterminate structure can still work and carry the loading until ultimate limit strains of concrete or reinforcement are reached;
  - This ability is attributed to the ductility of materials and is called *rotational capacity* of certain cross-section;
- Within this state the cross-section is rotating around its neutral axis more and more;
  - Plastic hinge starts to create at this cross-section and the structural scheme is irreversibly changing which is important mainly for post-fire assessments;
  - Practically it means the structure is not perfectly continuous which results in change of inner forces distribution (mainly hogging moments which generally decrease);
  - In the conventional computational models this can be implemented by inserting internal hinge with spring stiffness in rotation, the value of stiffness can be estimated iteratively by obtaining  $M_{Ed,plastic\ hinge}$  after calculation according to Eq. (7-20);
    - After lowering the hogging bending moment at the support cross-section the sagging bending moment in the mid-span cross-section rises<sup>11</sup>.

---

<sup>10</sup> When speaking about strains on concrete cross-section after exposure to fire, very probably some of the thermal strains will remain as residual due to the irreversible nature of thermal damage. It is connected mainly to the decay of Young's modulus of concrete and moment of inertia (both relating to the internal microcracking and loss of water), concrete spalling, etc. All of this results in residual deflections which are often reported.

<sup>11</sup> This aspect must be considered carefully in the post-fire assessment because even with the same loading and not reduced strength of bottom reinforcement the post-fire load-bearing capacity might not be sufficient.





$$M_{Ed,plastic\ hinge} = M_{Ed,full} * \frac{\min(\varepsilon_{su}^T; \varepsilon_{cu}^T) - \varepsilon_s^T}{\min(\varepsilon_{su}^T; \varepsilon_{cu}^T) - \varepsilon_{sy}^T} \quad (7-20)$$

where  $M_{Ed,plastic\ hinge}$  represents the reduced hogging bending moment due to partial plastification of the cross-section,  
 $M_{Ed,full}$  represents full hogging bending moment at the supports cross-section prior to fire,  
 $\varepsilon_{cu}^T$  represents the ultimate concrete strain in compression when concrete is being crushed with respect to reached temperature,  
 $\varepsilon_{su}^T$  represents the ultimate reinforcement strain when bars rupture with respect to reached temperature,  
 $\varepsilon_{sy}^T$  represents the reinforcement strain when yield strength is reached with respect to reached temperature,  
 $\varepsilon_s^T$  represents the actual reinforcement strain with respect to the reached temperature which is being studied.

Since the evolution of temperature-induced forces (axial force and its eccentricity, thus bending moment) keep changing with fire time and the limit elastic strains and both steel and concrete strength are changing with rising temperature as well, it is not clear at first sight which time is the critical from this point of view. Therefore, this check should be conducted for series of fire durations (the standard times 15, 30, 45, 60, 90, 120, 180 and 240 minutes). It seems this approach is the most correct one, but laborious at the same time. Thus a compromise can be made and only final time and 60 minutes (if the final time is longer than 60 minutes) can be checked. In the final time the highest temperatures, lowest strengths of concrete and steel and thus lowest limit elastic strains can be expected. On the other hand, in 60 minutes the highest temperature-induced bending moment mainly causing the tensile strain of reinforcement can be expected.

To illustrate the studied problem two examples are made. The first example deals with the already-known precast concrete floor panel 6 m long, 1,25 wide and 250 mm thick. It is made of concrete C30/37 with reinforcement class B500B (both top and bottom bars 6Ø12). It is assumed it is exposed to standard ISO 834 fire which heats the bottom side of panel only. In the 60<sup>th</sup> minute of fire the cross-section strains are checked. Mean temperature of concrete chords in compression is assumed to be 500 °C while the tensile reinforcement is not affected by temperature. At this time the summed internal forces induced by temperature and external loadings in the support cross-section are  $N_{Ed} = -1685\ kN$  and  $M_{Ed} = -170\ kNm$ . With such inputs the strains are calculated and can be seen in Fig. 7-20. Cross-section properties are calculated with excluded concrete in tension and limit strains for concrete and steel are assumed as temperature-dependent. Based on it following can be stated:

- The compressive axial force moves the neutral axis from the bottom surface inside the cross-section significantly which reduces the tensile strain of reinforcement;
- The ultimate strains for both concrete and reinforcement are very close to each other which determines the overall cross-sectional ductility;
- The actual strain of concrete in compression is way under the elastic limit, i.e. the possible changes would be governed by tensile reinforcement;
- The actual strain of tensile reinforcement lies under the limit elastic strain of steel which means no excessive elongation of tensile bars and thus rotation of cross-section together with creation of plastic hinge are expected; the structural scheme does not change.

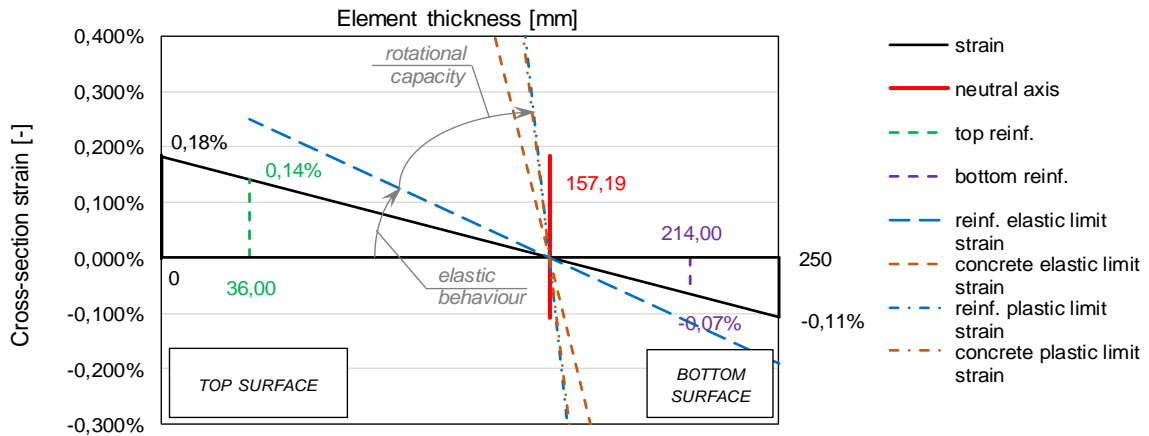


Fig. 7-20. Example 1: total cross-section linear strain with highlighted elastic and ultimate limit strains of both steel and concrete.

The second worked example deals with monolithic concrete floor slab 5m long, 200 mm thick and assumed width 1 m. It represents older structure made of concrete C20/25 and reinforcement with yield strength  $f_{yk,20} = 410 \text{ MPa}$  (corresponding with steel grade 10 425 (V) commonly used in Czech Republic in previous decades; top reinforcement 5Ø10, bottom reinforcement 5Ø8). The strains are checked in 180<sup>th</sup> minute of ISO 834 fire while only bottom surface is exposed. Mean temperature of concrete chords in compression is assumed to be 600 °C while the tensile reinforcement is not affected by temperature. At this time the summed internal forces induced by temperature and external loadings in the support cross-section are  $N_{Ed} = -1000 \text{ kN}$  and  $M_{Ed} = -100 \text{ kNm}$ . With such inputs the strains are calculated and can be seen in Fig. 7-21. Based on it following can be stated:

- The actual strain of tensile reinforcement exceeds the elastic limit strain of steel which means the plastic region of stress-strain diagram is reached; the internal plastic hinge starts to create according to the overload of the cross-section;
- The region of plastic deformations is highlighted in the diagram below, where can be seen the actual steel strain and its position within the rotational capacity which governs the subsequent hogging moment decrease;
- Assuming lower strength class of both concrete and steel results in higher cross-section strains and lower limit strains at the same time; This assessment seems to be important mainly in case of older concrete structures where materials of lower quality can be expected (e.g. concrete C16/20 and steel with yield strength equal to 200 MPa).

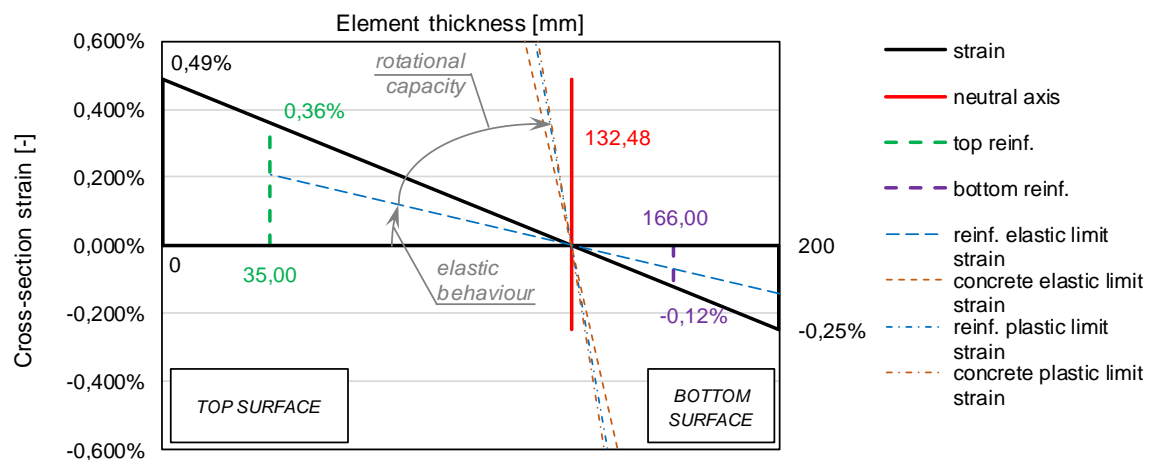


Fig. 7-21. Example 2: total cross-section linear strain with highlighted elastic and ultimate limit strains of both steel and concrete.



## 8 Estimation of Residual Load-Bearing Capacity

The previous [Chapters 2-7](#) are presented in the Thesis in order to help to understand the material and structural behaviour of RC structures during fire situations and after their end, as well as to collect as much information about the fire event as possible, make the investigation approach clear and conclusions understandable. The post-fire assessment and calculation of residual load-bearing capacity is the final and probably the most important step of the whole post-fire investigation.

### 8.1 Aspects to Be Taken into Account Prior to Post-Fire Assessment

With respect to the nature of fire events and conducting structural diagnosis as well as assessments of older structures a list of aspects that should be taken into account prior to calculation of residual load-bearing capacity is given below:

- If a structure previously subjected to fire is about to be used by public or some kind of industry and serve for certain purpose again, the state is considered to be usual design situation in terms of ULS and SLS. Therefore, appropriate loadings and material coefficients have to be incorporated in the calculations again;
  - Material coefficients might be lowered to certain level according to number of conducted material tests during structural diagnosis taking into account actual material properties.
- The load bearing capacity of structural elements during fire is generally going to be higher than the residual one, sometimes even at different durations of fire (e.g. fire performance at 90<sup>th</sup> minute might be higher than the residual one after 60-minutes fire). Since both calculations are done according to different design situation (extraordinary ULS versus ordinary ULS), different loadings and material coefficients are used – therefore both values are not comparable which may be misleading sometimes.
- According to the findings of global analysis (see [Chapter 7](#)), the structural model for forthcoming residual calculations might be updated in terms of stiffness reduction, inserting spring supports with finite values of stiffness's (especially rotational), incorporating residual deformations and joint movements, etc.;;
  - Due to the plastic deformations and joint movements it is suggested to always conduct calculations according to the *second-order theory*, which is important especially for vertical and mainly slender structures, where either local or global stability can become the critical aspect of the structural performance.
- If material deterioration according to carried out material tests is lower than one would expect according to design codes assumptions, one has to think twice if the experimental results are reliable enough. In case of any uncertainties lower and thus more conservative values should be used;
  - Moreover, if origin of concrete and reinforcement used in the assessed structure after fire are not known in detail (which basically are not) and design codes predictions of their deterioration due to high temperatures are used, concrete should be treated as with siliceous aggregate and reinforcement as cold-worked – which is conservative option in both cases.
- Although shear failure is not referred to be usual during fire [16], it should be included in the post-fire assessment of different types of structural members (slabs, beams, columns and walls). In case of slabs special attention should be attributed to punching as especially recent structures are often designed as locally supported without girders. The post-fire shear load-bearing capacity can be calculated analogically to the approach given in EC2-1-2 [16] with modifications of the simplified methods, see [Chapter 8.2](#).



- The post-fire assessment should also take into account the actual condition and load-bearing capacity of reference part of structure which was not subjected to fire. Especially in case of elderly buildings their load-bearing capacity might have decreased over the years due to progression of corrosion processes, design faults or unprofessional interventions. The final assessment should then be represented by both relative and absolute decrease of load-bearing capacity;
  - Theoretically a situation may occur when old RC structure was partially subjected to fire. Its damage is deep and strengthening would be necessary. However, it shows up that even the rest of the building which was not damaged by fire is in bad state and the strengthening would be necessary for whole building. This is very important in the decision process since a conclusion that the general strengthening is not worth may be made.
- The assumed fire scenario and derived temperature-time curve should include also the cooling phase with either gradual natural cooling after the end of fire or rapid cooling due to fire brigade intervention. The forthcoming thermal analysis should be then conducted with whole temperature-time curve including cooling phase as well. This is because of the thermal inertia of concrete when inner parts of cross-section might be heated to higher temperatures even after the moment when surface temperature reached its maximum and started to decrease;
  - If spalling of surface concrete layers occurs on structural elements after which some rebars (typically the corner ones) are directly exposed to fire, these should be treated as directly exposed to high temperatures for whole fire duration as the spalling usually occurs in the beginning part of fire due to vapour migration. For such bars the surface temperature can be assumed with the consequences to the post-fire assessment;
  - Another aspect connected to the risk of spalling is that due to it the cross-section becomes smaller and thus the inner parts close to the spalled areas (typically in corners again) reach higher temperatures.
- As a result of RC element's exposition to high temperatures, strength of concrete and reinforcement gradually decrease and its residual load-bearing capacity consequently decrease as well. Deterioration of these two materials affect the bond and cohesion between rebars and concrete. According to EC2-1-1 [25] the bond strength is directly dependent on tensile strength of concrete and also surface finish of rebars (smooth bars or ribbed bars), even though Eurocode does not assume any other type except ribbed bars.
  - Tensile strength of concrete drops quickly when exposed to high temperatures and its post-fire values do not get back to initial strength. As a result the residual bond strength decrease and the needed anchoring / overlapping length increase – which is impossible in case of existing building, therefore the maximal allowed stress in relevant rebars and whole bending resistance should be lowered by ratio  $f_{bd,residual}/f_{bd,initial}$ ;
  - Another phenomena affecting cohesion between rebars and concrete after fire is the differential thermal strains of rebars and concrete (see Fig. 2-20 in Chapter 2.2) which causes additional stress at the mutual interface. However, it seems [100] that similarly to free thermal elongation and LITS most of these differential interface stresses mitigate, especially in longer fire durations.
  - Problems with damaged bond strength is much more pronounced in case of smooth rebars used in past decades [100].



- In some situations, the structures might be damaged by fire to the extent that one would expect them to collapse since the basic presumptions of their behaviour are not fulfilled anymore. An example is given in Fig. 8-1. An RC slab after fire test in Cardington [101, 102, 103] lost majority of the cover layer at the bottom surface while most of bottom reinforcement became incoherent with the adjacent concrete. According to ordinary design approach the tensile forces at bottom face of the slab are carried by reinforcement which cannot fulfil this function in this situation. At this moment the slab is working thanks to the membrane action (see e.g. [104]) thanks to which its behaviour can be understood but not taken for granted. The membrane action is an example of alternative way of loads transfer which may occur with respect to the degree of structural indeterminacy, number of supports, material ductility etc. In such situations one has to be careful because even though the structures are still working, they cannot be assessed as reliable and safe.

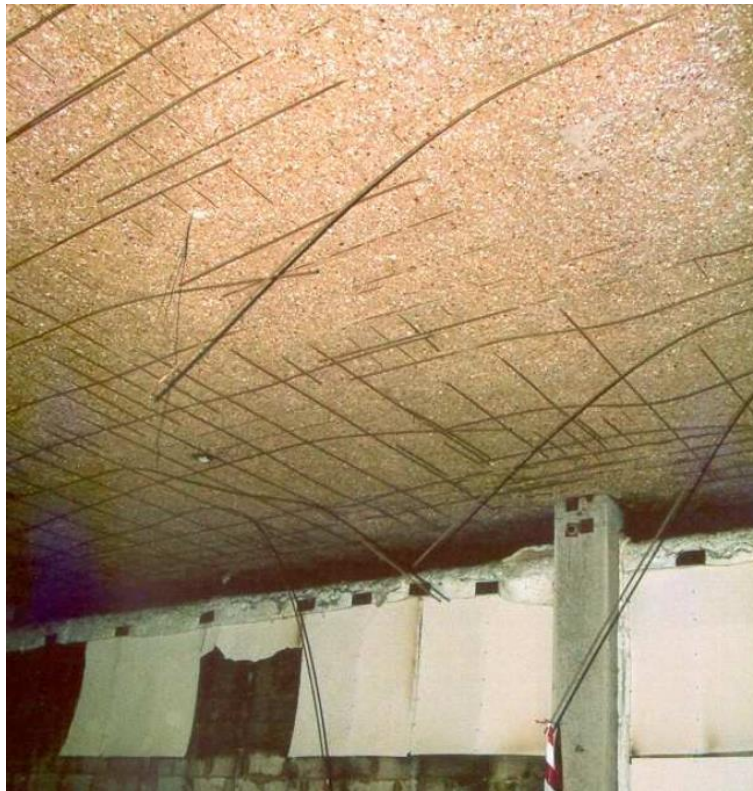


*Fig. 8-1. Cardington full-scale fire tests: concrete slab after fire with incoherent bottom reinforcement, taken over [105].*

- Generally, it is advised to pay attention to all structural aspects within the post-fire assessment, including:
  - Global analysis proving sufficient spatial stability and rigidity of whole structure or its parts;
  - Local analysis proving sufficient load-bearing capacity of all damaged elements ( $N$ - $M$  interaction, shear and punching capacity);
  - Local analysis proving adequate detailing, state of supports, locally-loaded spots, anchoring, etc.





## 8.2 Methods of Residual Load-Bearing Capacity Estimation

### Surface Deterioration Method

The first method of post-fire assessment proposed herein is called *Surface deterioration method* and is based on the assumption that the reduced concrete compressive strength of surface layers, which is obtained after conducting in-situ Schmidt rebound hammer test, is attributed to whole cross-section, while yield strength of reinforcement is not reduced.

This method is meant to be used as very simplified, quick and conservative assessment. In the list below general assumptions of the method are given:

- According to the building type (family house/residential or office building/industry hall) the nature of burning can be roughly assumed (cellulose, hydrocarbon or burning of specific petroleum products);
  - The method should be used **in case of fire scenario similar to ISO834 fire only** and not others due to their different pace of temperature evolution.
- Probable duration of fire is known; however maximal reached temperatures are not;
  - Theoretical ISO834 fire lasting 45 minutes would cause mean temperature of the surface concrete cover layers approximately 650 °C which is expected to correspond to 70% decay of compressive strength, see [Chapter 2.4.1](#). At this time maximal temperatures of rebars with typical thickness of concrete cover reach approximately 300 °C (see [Fig. 8-2](#)) which is below temperature when residual yield strength decrease (approximately 450 °C, see [Fig. 2-23 in Chapter 2.4.2](#)). **Therefore, residual yield strength can be assumed equal to the initial and duration 45 min is limiting for using this method;**
    - It is worth to note that one should be careful in case of spalled surfaces since the presumption of maximal rebar temperatures might not be true.
- Rebound hammer provides mean information about approximately 30 mm thick surface layer, it also means it provides information about mean maximal reached temperature in this layer.
  - With respect to conducting rebound hammer test it should not be used in case of old concrete buildings (more than 50 years) due to expected progressed carbonation and misleading obtained results, see [Chapter 6.2.1](#).
- In case the subjected element was exposed to fire from more than one side, the rebound hammer test has to be conducted from all heated sides, then the biggest strength decay is taken into account.
- Referential tests of the same but not fire-damaged structure should be done in order to compare results and obtain relative strength decays.
- **According to conducted parametric study (see [Fig. 8-8](#) and [Fig. 8-9](#)) it showed the method is always conservative in case of walls and columns dominantly loaded by centric compressive force, however non-conservative in case of elements subjected to bending.**
  - In case of assessing residual shear resistance the methods principals are still valid.





The assessment of residual load-bearing capacity of RC column loaded by centric axial force can be done as follows in Fig. 8-2. Duration 45 minutes of ISO834 fire is assumed. It can be seen the temperature of corner rebars is equal to 299 °C.

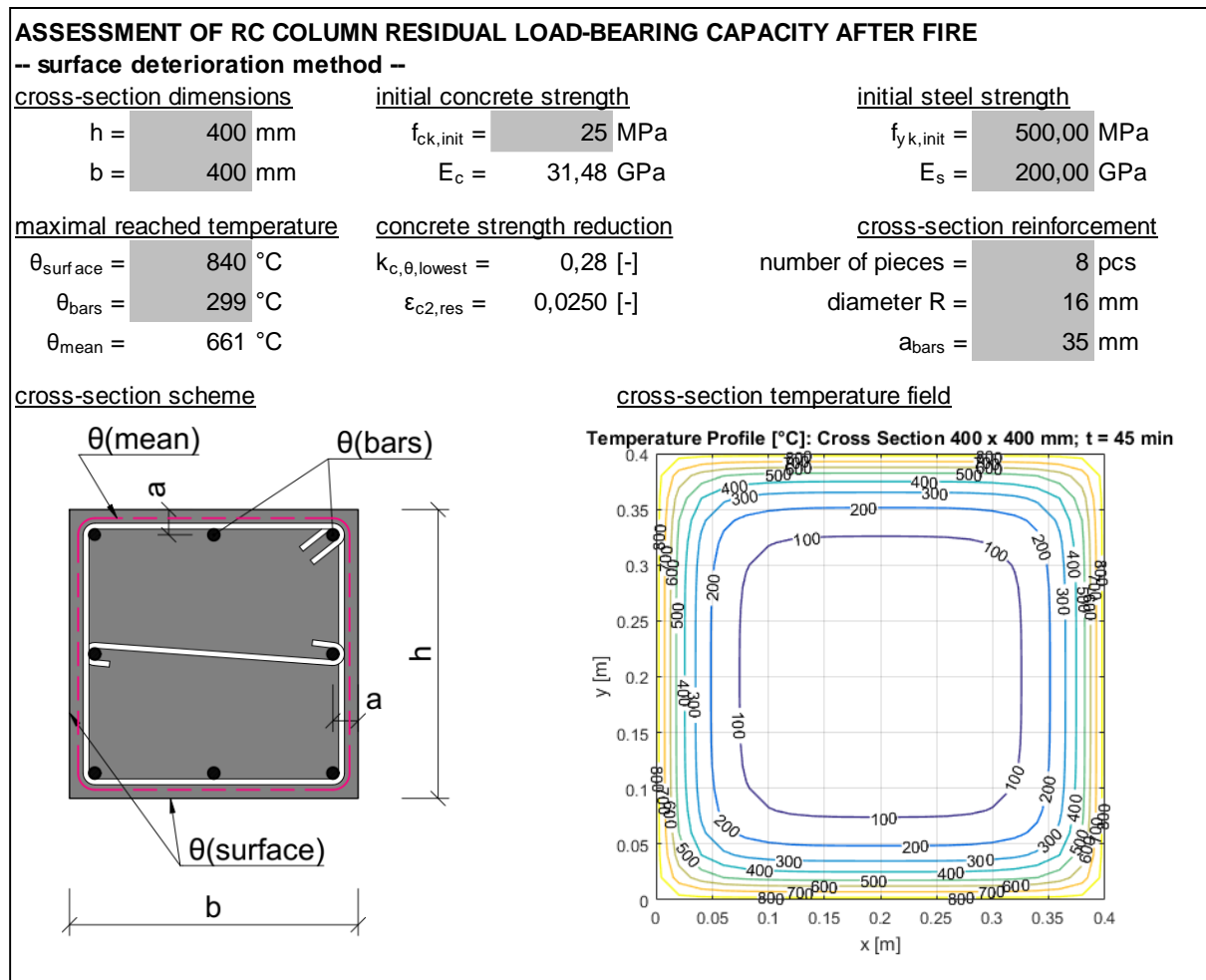


Fig. 8-2. Assessment of residual load-bearing capacity of RC column using Surface Deterioration method after ISO834 fire lasting 45 minutes.

$$\begin{aligned}
 N_{Rd,res} &= \alpha_{imperfect,ENV} * A_c * k_{c,\theta,lowest} * \frac{f_{ck}}{\gamma_c} + A_s * \min\left(\frac{f_{yk}}{\gamma_s}; \epsilon_{c2,res} * E_s\right) = \\
 &= 0,85 * 0,4 * 0,4 * 0,28 * \frac{25}{1,5} + 1608 * \min\left(\frac{500}{1,15}; 0,025 * 200\right) = \mathbf{1334 \text{ kN}}
 \end{aligned}$$

### Isotherm 300 °C Method

In case of the Isotherm 500 °C method its main principle is the assumption that concrete heated to temperatures above 500 °C is damaged to such extent it contributes to the cross-sectional load-bearing capacity either very limitedly or even not at all. On the other hand, concrete with maximal reached temperatures under 500 °C is said to preserve initial mechanical properties. Both of the assumptions are not precisely correct, they are meant as simplification and compromising average, however comparison with more precise methods and experiments as well proved satisfying accuracy. The yield strength of reinforcement is lowered directly according to the reached temperatures. At the same time, it is worth to note that EC2-1-2 [16] suggests lowering the compressive strength of concrete to 60 % of the initial values (valid for siliceous aggregates) at hot state during fire when 500 °C is reached.

In case of post-fire assessment similar approach can be applied since it is very convenient and user-friendly. However, it is important to note the residual compressive strength of concrete tend to be



lower than the strength right at hot state, see Chapter 2.4.1 – it also means the “critical” temperature important for the assessment method is going to be different to 500 °C. If it is possible, it is recommended to conduct material tests in order to assembly own curve of strength decrease according to reached temperatures. Based on this curve “critical” temperature can be found when strength is lowered to approximately 60 % of the initial one similarly to the approach of *Isotherm 500 °C method*. If conducting such tests is not possible, it can be assumed the residual compressive strength of concrete is lower by 15-20 % when compared to the strength at hot state [28]. The diagram of coefficient  $k_c(\theta)$  according to temperatures at hot and residual state can be seen in Fig. 8-3 (20% decay is presumed). Then it can be seen that for temperature 300 °C decay to approximately 65 % of initial strength is attributed. This “critical” temperature agrees well with the findings published in [38] – therefore the method is called *Isotherm 300 °C method*.

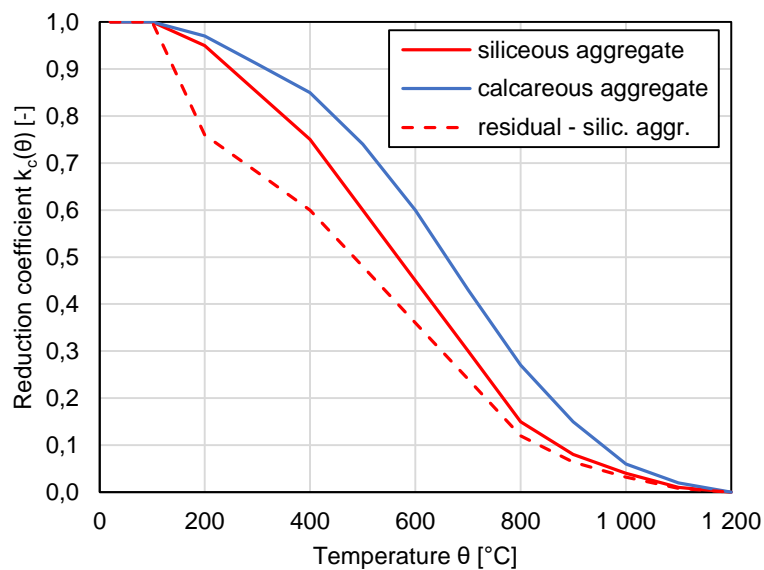


Fig. 8-3. Decay of concrete compressive strength at hot (EC2-1-2 [16]) and residual state [28].

Mechanical properties of reinforcement are taken into account according to Fig. 2-23 in Chapter 2.4.2 with respect to the highest reached temperature. It can be expected reached temperatures in single bars will differ, then weighted average or the most conservative value should be used.

According to the results of parametric study (see Fig. 8-8 and Fig. 8-9) using this method provides slightly more conservative values than more detailed methods, especially for longer fire durations where large cross-sectional areas are excluded. However, simplifications of the calculations are so beneficial it is worth to use this method. **The method can be used without deriving own curve of concrete strength decay when fire scenario with heating rate and dynamics similar to ISO834 fire is expected and the structures have not been cooled quickly with water streams by fire brigade at the same time. In the opposite case own curve has to be derived which specifies the “critical” temperature more in detail.**

Examples of post-fire assessment of RC column loaded by centric axial force and RC slab using *Isotherm 300 °C method* are shown in Fig. 8-4 and Fig. 8-5.

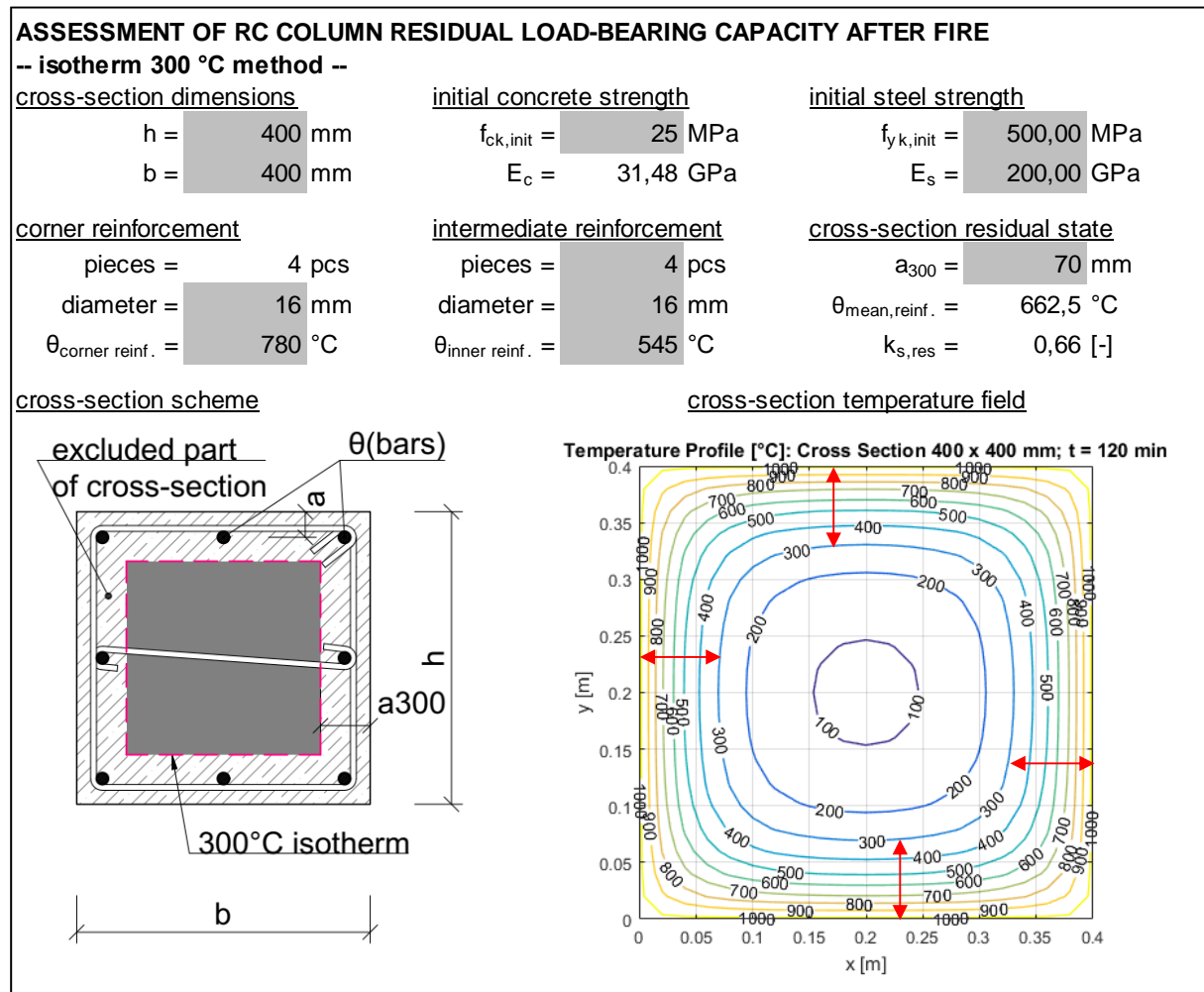
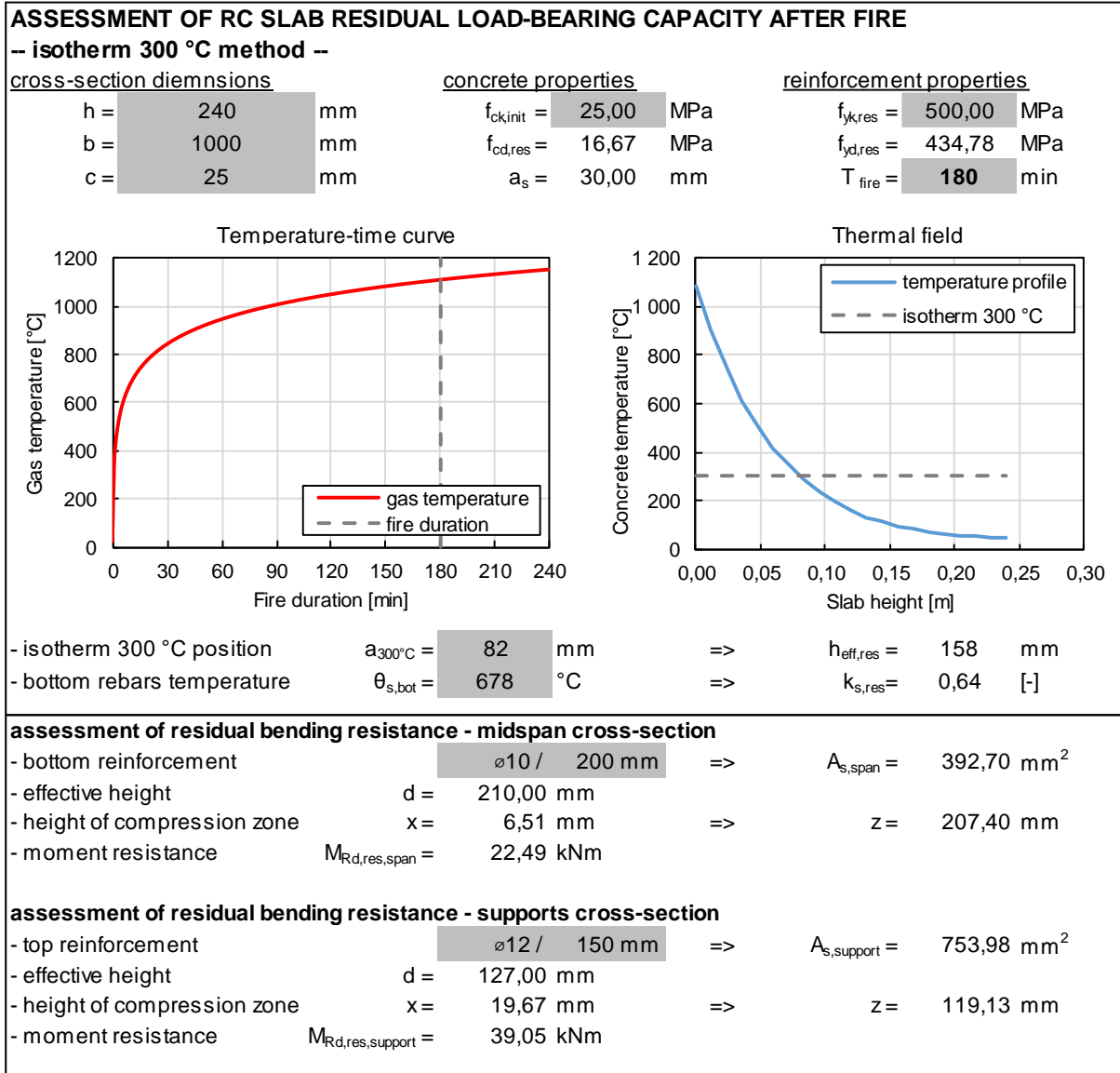


Fig. 8-4. Assessment of residual load-bearing capacity of RC column using Isotherm 300 °C method after ISO834 fire lasting 120 minutes.

$$\begin{aligned}
 N_{Rd,res} &= \alpha_{imperfect,ENV} * A_{c,residual} * \frac{f_{ck}}{\gamma_c} + A_s * \min \left( k_{s,res} * \frac{f_{yk}}{\gamma_s}; \varepsilon_{c2,res} * E_{s,res} \right) = \\
 &= 0,85 * (0,4 - 2 * 0,07) * (0,4 - 2 * 0,07) * \frac{25}{1,5} + 1608 \\
 &* \min \left( 0,66 * \frac{500}{1,15}; 0,025 * 200 * 0,66 \right) = \mathbf{1419\ kN}
 \end{aligned}$$



**Fig. 8-5.** Assessment of residual load-bearing capacity of RC slab using Isotherm 300 °C method after ISO834 fire lasting 180 minutes.



### Adjusted Zone Method

Probably the best ratio between accuracy and working demands together with usability in engineering practice can be provided by using the *Adjusted zone method*. As it is clear from its name the method is based on the well-known zone method proposed in EC2-1-2 [16]. It uses the same approach with dividing the cross-section into zones, however the coefficients  $k_c(\theta)$  and  $k_s(\theta)$  expressing deterioration of concrete and reinforcing steel are adjusted to the residual state.

If no information about actual decay of concrete compressive strength according to reached temperatures are available, the simplification according to [28] can be used and the strength assumed as by 15-20 % lower than the strength at certain temperature right at hot state as EC2-1-2 [16] proposes. However, deriving own curve of strength decay based on material test results is beneficial with respect to the calculation accuracy, especially together with smooth dividing the cross-section into zones. The reinforcement is treated in the same way as in case of *Isotherm 300 °C method* with adjusted values of coefficient  $k_s(\theta)$ .

Examples of post-fire assessment of RC column loaded by centric axial force and RC slab using *Adjusted zone method* are shown in Fig. 8-6 and Fig. 8-7.

**If the coefficients of concrete strength reduction are assumed simplified according to [28], the actual fire scenario had to be similar to ISO834 fire. In all other cases or when no information about the fire event is available, the reduction curve of concrete strength has to be derived according to experimental results. Then the method can be used universally with no limitations.**



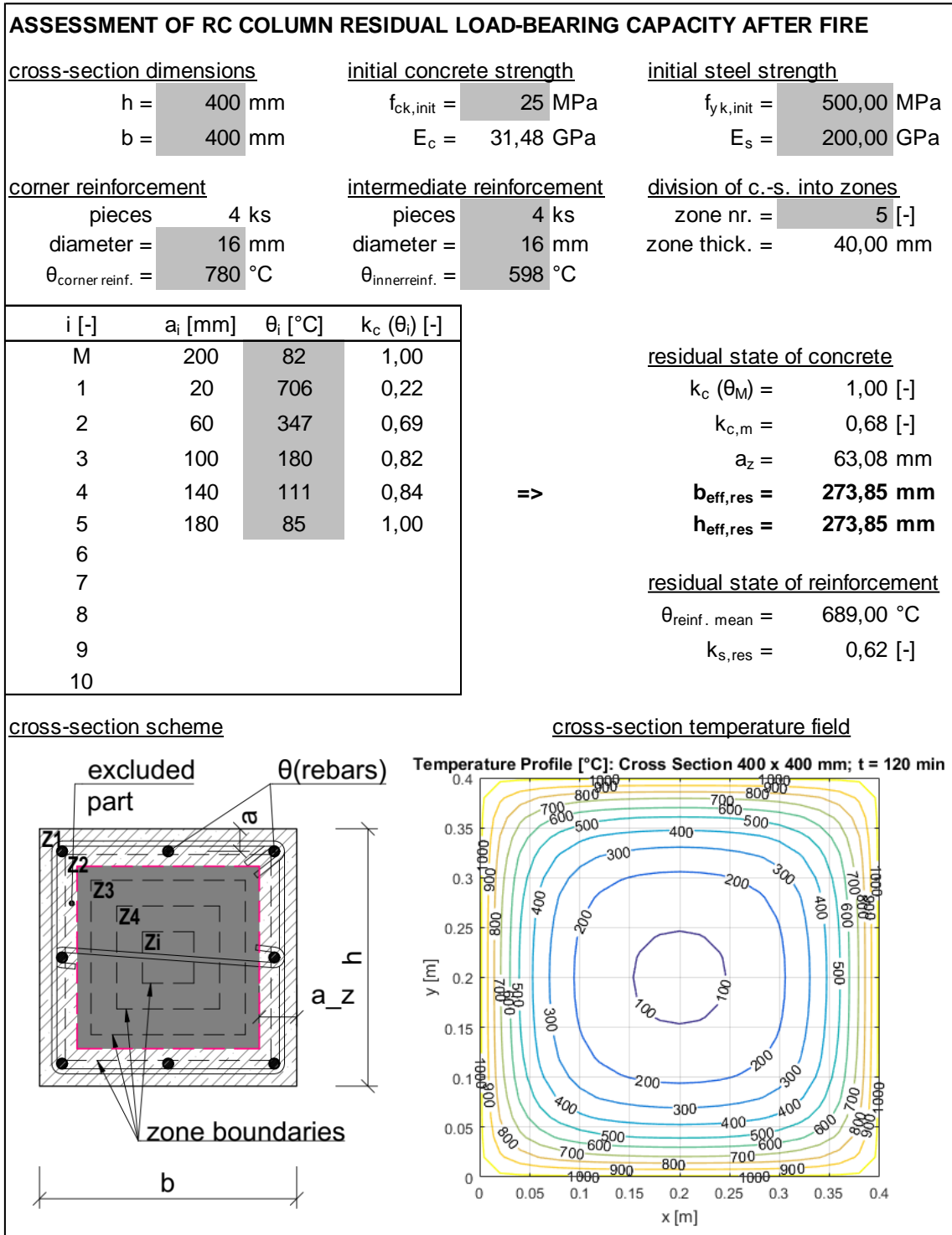


Fig. 8-6. Assessment of residual load-bearing capacity of RC column using Adjusted zone method after ISO834 fire lasting 120 minutes.

$$\begin{aligned}
 N_{Rd,res} &= \alpha_{imperfect,ENV} * A_{c,residual} * \frac{k_{c,\theta M} * f_{ck}}{\gamma_c} + A_s * \min \left( k_{s,res} * \frac{f_{yk}}{\gamma_s}; \varepsilon_{c2,res} * E_{s,res} \right) = \\
 &= 0,85 * 0,273^2 * \frac{1 * 25}{1,5} + 1608 * \min \left( 0,62 * \frac{500}{1,15}; 0,025 * 200 * 10^3 * 0,62 \right) = \\
 &= \mathbf{1495 \text{ kN}}
 \end{aligned}$$

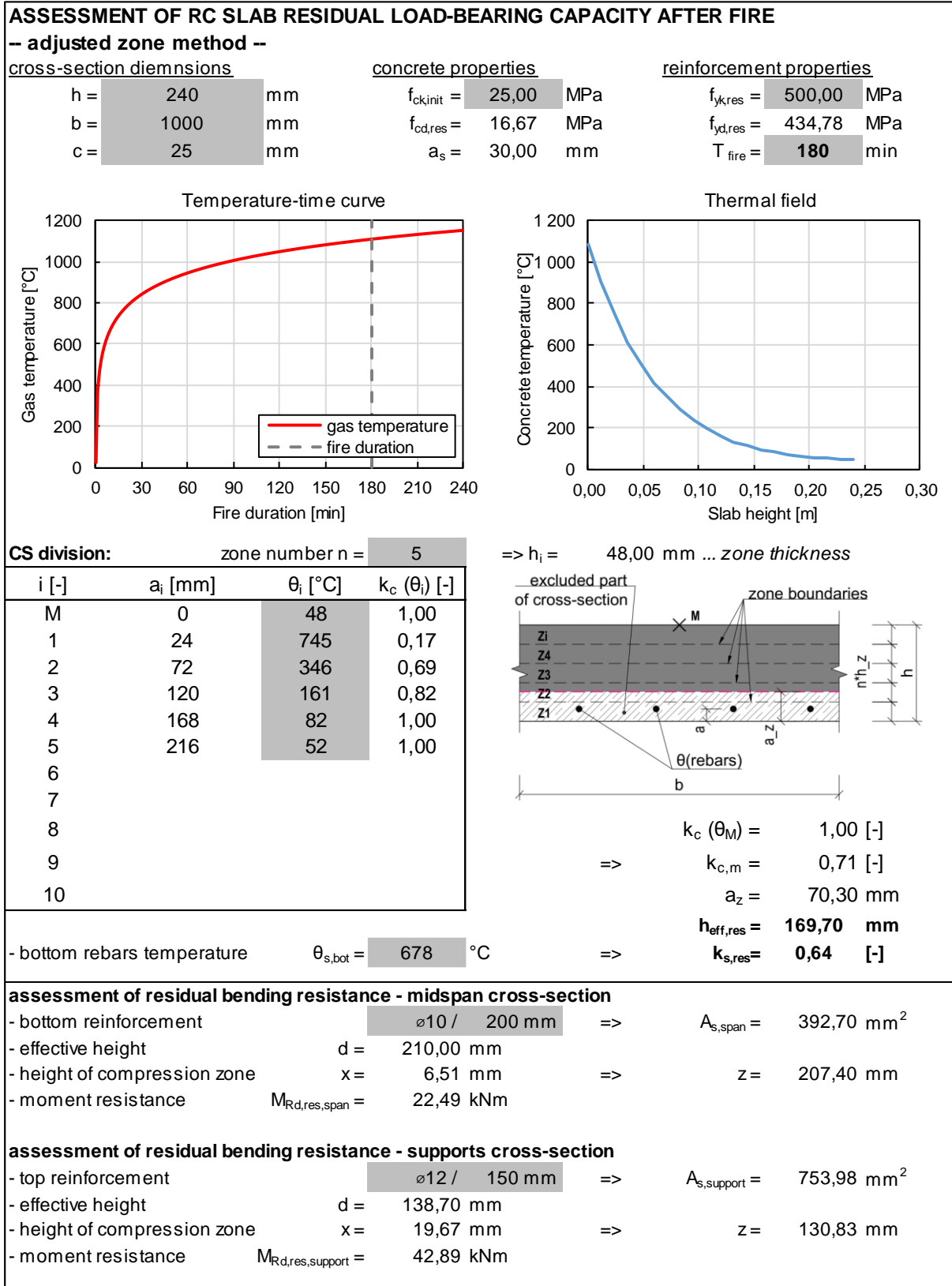


Fig. 8-7. Assessment of residual load-bearing capacity of RC slab using Adjusted zone method after ISO834 fire lasting 180 minutes.



### Detailed Strip Method

The last assessment method to be proposed is the *Detailed strip method*, which can be understood as advanced calculation method in terms of EC2-1-2 [16]. Using this method leads to creation of numerical calculation model where selected material model with stress-strain diagram, thermal properties and temperature boundary conditions can be implemented. Then the residual load-bearing capacity is estimated using sectional analysis and moment-curvature diagram. This method was for example used at ambient and high temperatures in order to calculate load-bearing capacity of slender columns, as can be seen in [106]. The same approach can be applied in the residual state with updating the stress-strain diagram of both concrete and steel.

Calculating the residual capacity using the *Detailed strip method* should provide the most accurate results, however there is no commercial software based on this method and in-house made applications are not universal. Using this method in engineering practise is rather cumbersome, not user-friendly and thus problematic.

### Parametric Study of Proposed Methods

In order to compare results of residual load-bearing capacity obtained by using different assessment methods parametric study was conducted while RC columns and slabs were analysed. Within the study *Surface deterioration method*, *Isotherm 300 °C method* and *Adjusted zone method* were used.

In case of columns, concrete grade C25/30 and cross-sectional dimensions 250x250 mm, 400x400 mm and 650x650 mm were assumed with uniform reinforcement of 8 rods 16 mm in diameter. The residual capacity was calculated only in means of no slenderness effect and only centric axial force with theoretical no bending moment (therefore no M-N diagram was created). Mutual comparison of calculated load-bearing capacities according to duration of ISO834 fire is shown in Fig. 8-8. Based on the results it can be stated, that results obtained by using *Surface deterioration method* are always conservative (the bigger cross-section the more conservative) up to 45 minutes. After exceeding this fire duration, the reinforcement is affected in residual state which is not incorporated in the method. In case of *Isotherm 300 °C method* the results are also always conservative, but they keep very close to those from *Adjusted zone method* which are understood as precise enough.

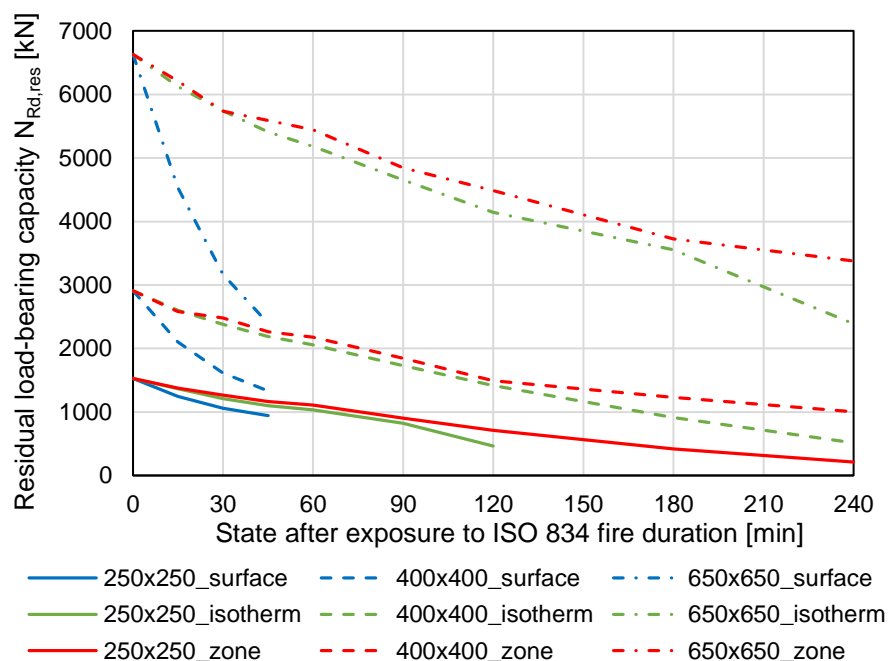
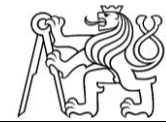


Fig. 8-8. Parametric study: residual load-bearing capacity of RC columns estimated with different assessment methods.



In case of slabs, thicknesses 180 mm, 240 mm and 300 mm were assumed. In all cases concrete grade C25/30, bottom reinforcement  $\varnothing 10/200$  mm and top reinforcement  $\varnothing 12/150$  mm were taken into account; in the mid-span and support cross-section assessment only tensile reinforcement is taken into account. Calculated load-bearing capacities at mid-span cross section according to ISO834 fire duration are show in Fig. 8-9. From the diagram below it is clear the curves attributed to different methods are hiding each other that it seems only curves of adjusted zone method are displayed. In fact, they all exhibit the same course (up to 45 minutes in case of surface deterioration method) since deterioration of tensile reinforcement is incorporated in the same way and different approach to damaged concrete do not take place in case of mid-span support as the compression zone at the top is not damaged.

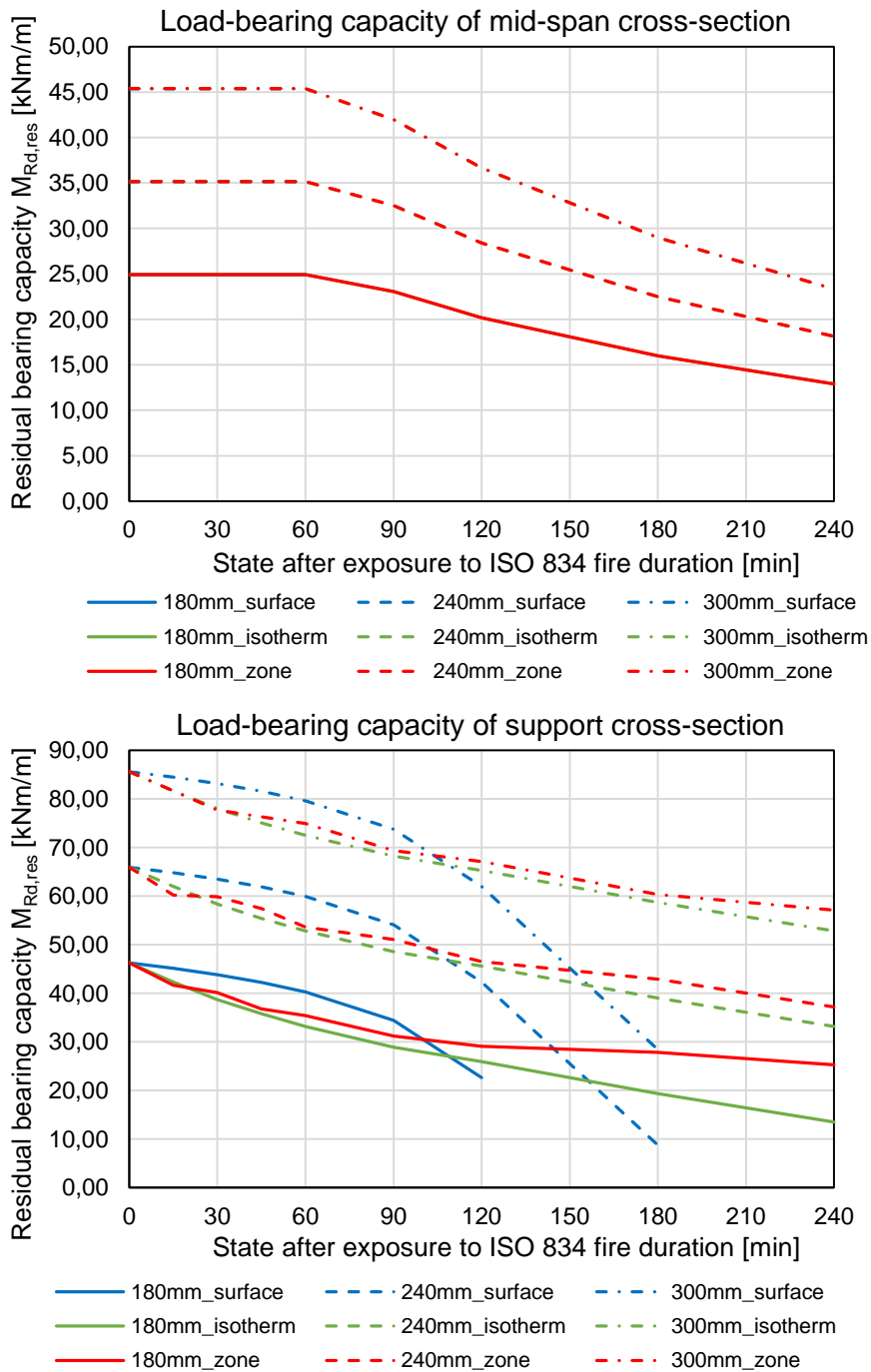


Fig. 8-9. Parametric study: residual load-bearing capacity of RC slabs estimated with different assessment methods.



In the second diagram of Fig. 8-9 showing residual capacities of slab's support cross-sections it can be seen the *Surface deterioration method* provides higher load-bearing capacities than the rest of methods which is not conservative. Probably the effect of taking into account whole cross-section thickness with lowered concrete strength provides higher values than reduced thickness with initial strength – therefore the *Surface deterioration method* is not advised to be used when assessing RC slabs after fire, which complies with the conclusions given above in the method description. To continue, results of *Isotherm 300 °C method* follows results of *Adjusted zone method* very well being on the conservative side at the same time, which is very similar to the findings of columns assessment. The *Isotherm 300 °C method* thus confirms its principle and usability for simplified post-fire assessment. Nevertheless, for most accurate results and option of experimental test results incorporation the *Adjusted zone method* is the most suitable one.

### 8.3 Quick Estimations of Load-Bearing Capacity Decay

During the post-fire investigation, it is usually necessary to approximately estimate the severity of structural damage caused by fire event and also to have an idea about probable residual capacity decay already at early stages of the investigation process, e.g. right after conducting the preliminary on-site inspection. It means at this stage the precise calculations are not needed while material test data are not available anyway, but decision about the forthcoming approach has to be made. Then the presumptions and findings of preliminary inspection together with rough estimation of structural capacity decay is fundamental.

The quick estimation of load-bearing capacity decay can be made according to different indications:

- According to classification to the damage classes – during the preliminary inspection the structural elements are classified into damage classes as it is described in Chapter 4.2;
  - Elements classified into classes 0-2 are expected to be damaged only minor or on the surface only with very limited or none effect on the structural capacity in terms of ULS or SLS;
  - Elements classified into class 3 are expected to be damaged to not-negligible extent with load-bearing capacity decay up to 25 % and visible residual deflection which might be a problem in case of SLS assessment;
  - Elements classified into class 4 are expected to be deeply damaged with load-bearing capacity decay 25-100 % and excessive residual deflection making SLS assessment very problematic.
- According to residual deflections – significant growth of deflections is usual accompanying phenomenon during structures exposition to fire while part of the deflections stays residual even after the end of fire and temperatures decrease to ambient values. They are caused mainly by decrease of concrete Young's modulus as well as propagating cracking of cross-sections.
  - Generally, if the comparison between measured residual deflection of damaged element and identical non-damaged element in other part of the subjected building  $\delta_{residual} / \delta_{initial} > 2$ , it can be expected the element is considerably damaged and if the ratio is higher than 5, the element is very probably deeply damaged with substantial loss of load-bearing capacity.
  - The deflections can be described in simplified way by using analytical equation, see e.g. Eq. (8-1) for uniformly distributed loading. The coefficients  $A$  and  $B$  can be estimated according to conducted global analysis and material tests. All together it can provide or confirm information about the deterioration.



$$\delta_{residual} = A * k_{\delta} * \frac{f * L^4}{B * (EI)} \quad (8-1)$$

where  $k_{\delta}$  represents characteristic number attributed to specific structural scheme, e.g.  $k_{\delta} = 5/384$  for simply supported beam;

$A \leq 1$  represents the coefficient of structural scheme change due to global fire action,

$B \leq 1$  represents the coefficient lowering flexural stiffness due to material deterioration.

- According to duration of fire exposition – the conducted parametric study provides valuable information about the rate of load-bearing capacity decay. If ISO834 fire scenario and usual concrete cover thicknesses are assumed, it can be expected, that:
  - Load-bearing capacity of mid-span cross-sections of slabs and beams in bending is fully preserved until temperature of rebars approximately 400 °C is reached which corresponds to 60 minutes ISO834 fire duration. After exceeding 400 °C of reinforcement temperature 20% decay of load-bearing capacity per 60 minutes of ISO834 fire can be expected.
    - Although bending moment resistance is not reduced until temperature in rebars reaches 400 °C, decay of bond strength between rebars and concrete should be expected, which is important mainly for extra reinforcement in the mid-span shorter than span length.
  - Load-bearing capacity of support cross-sections of slabs and beams in bending is expected to decrease by 15-25 % per 60 minutes of ISO834 fire according to the slab thickness.
  - In case of walls and columns decrease in compressive force resistance without eccentricity is expected to be by 15-25 % per 60 minutes of fire according to cross-section dimensions and reinforcement.

#### 8.4 Brief Commentary to Strengthening Design and Final Refurbishment

Phenomenon of structural strengthening and refurbishment is not in scope of this Thesis, however since it is connected to the post-fire assessment very closely, brief commentary is given below and the most important aspects are highlighted.

It was already discussed in [Chapter 3.2](#) and summed up in [Fig. 3.3](#): prior to designing and conducting refurbishment and strengthening it is essential to carry out the cost-effectiveness analysis in order to have an idea whether the option of damaged building renewal makes economic sense. Generally, the refurbishment works are expensive and cannot be made by anybody, both get even more pronounced in case of big areas to be repaired.

If the refurbishment is going to be conducted it is substantial to know at the design stage how many elements need to be repaired and if only surface or deep refurbishment together with structural strengthening is needed. The surface refurbishment is usually carried out due to durability, design and fire resistance reasons, whereas in case of deep refurbishment the repair works are beside the already mentioned reasons also connected to restoration of original cross-section dimensions, cracks injection, adding new reinforcement, shotcreting or installing steel or fibre-composite bandages. Another aspect which has to be clear at the design stage is knowing the full list of requirements (connected to the repaired structure and its re-use) which has to be fulfilled. These requirements contain the level of live loads which have to be carried by the structure, the needed fire resistance, durability with respect to the environment, or how to deal with the residual deflections.





For members requiring surface refurbishment the works usually consist of following steps:

- Cleaning surface using vacuum cleaner, water- or sand-jets;
- Treating uncovered reinforcement with anticorrosion coating;
- During the structural diagnosis concrete cores were taken from the structure and test of carbonation depth was conducted – if the depth is dangerously close to reinforcement and the risk of possible reinforcement corrosion together with possibly reduced durability is probable, penetrating subjected surfaces with anti-carbonation solution is advised;
- Local surface damages are patched with special filler and smooth finishing mortars.

On the other hand, if deep refurbishment and structural strengthening are required following works can be expected:

- Adding extra reinforcement bars or replacing damaged bars using ordinary ribbed bars, welded mesh, helical reinforcement, glass-fibre bars, fibre-reinforced polymer (FRP) strips, etc.
- Getting rid of any incoherent or delaminated parts of concrete;
- Restoration of original cross-sectional dimensions using mortars or shotcreting;
- Concreting (or shotcreting) extra layer around original cross-section;
- Installing steel or FRP bandages;
- Adding extra support;
- Post-tensioning the structure with external tendons.

In cases when dimensions of cross-section are being restored or enlarged the essential requirement is to ensure adequate bond and cohesion between the old and new part of cross-section in order to obtain element behaving as one together and to guarantee the transfer of forces on their interface. This can be achieved by roughing the surface concrete or installing transverse anchoring bars. Another universally valid note is that the structural element, which is going to be strengthened, should be unloaded as much as possible prior to strengthening, because the new part of cross-section is activated only after carrying some forces – it means the effect of strengthening is beneficial only for the part of loading applied after the refurbishment is done. In other words, the more unloaded the original damaged element is, the more effective the strengthening is.

To end with, when repairing RC structure after fire it is necessary to take into account the nature of damage caused by high temperatures and adequately design the strengthening.



## 9 Discussion

### 9.1 General Conclusions

In the submitted Thesis detailed approach to conducting analysis of concrete structures after fire is introduced. Within eight chapters, (i) fundamental material properties of concrete and reinforcing steel at high and back cooled down ambient temperatures are described, (ii) the preliminary and detailed inspections of burned out building with classification of damage level, on-site material tests and extraction of testing samples are discussed, (iii) structural diagnosis with special attention to damage caused by fire is described, (iv) global analysis taking into account temperature-induced forces using simplified calculation is given, and (v) methods for estimating the residual load-bearing capacity are presented. In the Thesis' annex several worked examples of complete post-fire assessment are given.

Main contribution of the Thesis lies according to author's opinion in following:

- Elaboration of detailed methodology to conduct post-fire investigation and assessment;
- Elaboration of graphical template to express the findings of preliminary and detailed inspection of damaged building;
- Selection of most suitable material test methods (and their combination), correct interpretation of test results with respect to damage nature caused by fire, elaboration of graphical template to visualise test results;
- Elaboration of simplified approach for estimation of temperature-induced additional inner forces and deformations, incorporation of such forces into the assessment;
- Adjustment of simplified calculation methods for estimating the residual load-bearing capacity;
- Elaboration of tool to quickly estimate the decay of load-bearing capacity according to fire duration.

### 9.2 Recommendation for Further Research

It is clear that such a vast topic as post-fire structural assessment is cannot be completely described within one thesis. Attention was dedicated primarily to the goals according to author's priorities, but also to those which were possible to be fulfilled (with respect to time, labour, theoretical and computational demands). Due to it, there are several topics left which need to be finished.

The future of post-fire assessments very probably lies in numerical modelling, since using this approach complicated processes (such as damage by fire) can be simulated. However, as it was already mentioned numerical modelling is enormously time- and labour-consuming and in engineering practise it is rather unrealistic. Simplified application based on FEM calculations working with chosen part of structure might be compromise – as it is described in [Chapter 7.3](#). Developing such application would be very useful. For this purposes, wide agreement on the most suitable stress-strain diagram of concrete during and after the fire incorporating LITS as well will be needed, since up to now several models providing more or less different results exist and different authors use different models.

Another phenomenon which is worth to study is the decay of bond-strength between concrete and rebars. As it is described in [Chapter 2](#), its irreversible deterioration due to high temperatures was experimentally proved on simple testing elements, however full-scale tests and conclusions about affecting the residual load-bearing capacity are missing so far. This would be beneficial to be scrutinised, because in some cases the post-fire performance will probably be lower after incorporating this.

To end with, it would be very useful to include all these findings into some kind of technical regulation on national or even European level in case of wide acceptance.



## Author's publications

MÜLLER, P., J. NOVÁK, and J. HOLAN. Destructive and non-destructive experimental investigation of polypropylene fibre reinforced concrete subjected to high temperature. *Journal of Building Engineering*. 2019, 26 ISSN 2352-7102. DOI 10.1016/j.job.2019.100906. (*contribution 65 %*)  
Available from: <https://www.sciencedirect.com/science/article/pii/S2352710219302360>

MÜLLER, P.; BENÝŠEK, M.; ŠTEFAN, R. Post-Fire Structural Assessment of a Firefighting Training Facility: A Case Study. In: *Journal of Fire Sciences*, 2021. Submitted (*contribution 40 %*)

MÜLLER, P. Zohlednění nepřímých teplotních zatížení při posuzování ŽB konstrukcí po požáru. In: HORÁKOVÁ, A. and M. PETŘÍK, eds. *Proceedings of PhD Workshop, Department of Concrete and Masonry Structures 2021*. 10th PhD Workshop of the Department of Concrete and Masonry Structures 2021, Praha, 2021-05-21. Praha: CTU FCE. Department of Concrete and Masonry Structures, 2021. ISBN 978-80-01-06842-7.

Available from: [https://concrete.fsv.cvut.cz/phdworkshop/proceedings/2021/pdf/Muller\\_Petr.pdf](https://concrete.fsv.cvut.cz/phdworkshop/proceedings/2021/pdf/Muller_Petr.pdf)

MÜLLER, P. Statická analýza konstrukce po požáru. In: HORÁKOVÁ, A. and M. PETŘÍK, eds. *Proceedings of PhD Workshop, Department of Concrete and Masonry Structures 2020*. 9th PhD Workshop of the Department of Concrete and Masonry Structures 2020, Praha, 2020-11-13. Praha: CTU FCE. Department of Concrete and Masonry Structures, 2020. ISBN 978-80-01-06774-1.

Available from: <https://concrete.fsv.cvut.cz/phdworkshop/proceedings/2020/>

MÜLLER, P. Vyšetřování materiálových parametrů betonových konstrukcí po požáru. In: PETŘÍK, M. and A. HORÁKOVÁ, eds. *Proceedings of the 8th PhD Workshop of the Department of Concrete and Masonry Structures*. 8th PhD Workshop of the Department of Concrete and Masonry Structures 2019, Praha, 2019-05-31. Praha: CTU FCE. Department of Concrete and Masonry Structures, 2019. ISBN 978-80-01-06574-7.

Available from: [https://concrete.fsv.cvut.cz/phdworkshop/proceedings/2019/pdf/Muller\\_Petr.pdf](https://concrete.fsv.cvut.cz/phdworkshop/proceedings/2019/pdf/Muller_Petr.pdf)

MÜLLER, P. Analýza železobetonových konstrukcí po požáru. In: DVORSKÝ, T. and M. PETŘÍK, eds. *PhD Workshop 2018 - CD*. PhD Workshop 2018, Praha, 2018-05-25. Praha: CTU FCE. Department of Concrete and Masonry Structures, 2018. ISBN 978-80-01-06417-7.

MÜLLER, P. Analýza stěnového nosníku objektu školy. In: DVORSKÝ, T. and M. PETŘÍK, eds. *PhD Workshop - Full Texts*. PhD Workshop 2017, Praha, 2017-05-26. Praha: CTU FCE. Department of Concrete and Masonry Structures, 2017. ISBN 978-80-01-06132-9.

MÜLLER, P. Analýza vybraných nosných prvků objektu školy. Praha 2017. Master Thesis. CTU FCE. Department of Concrete and Masonry Structures.



## References

- [1] Andraus Building. *Wikipedia: the free encyclopedia* [online]. San Francisco (CA): Wikimedia Foundation [cit. 2022-01-30]. Dostupné z: [https://en.wikipedia.org/wiki/Andraus\\_Building](https://en.wikipedia.org/wiki/Andraus_Building)
- [2] Joelma Building. *Wikipedia: the free encyclopedia* [online]. San Francisco (CA): Wikimedia Foundation [cit. 2022-01-30]. Dostupné z: [https://en.wikipedia.org/wiki/Joelma\\_Building](https://en.wikipedia.org/wiki/Joelma_Building)
- [3] Grenfell Tower fire. *Wikipedia: the free encyclopedia* [online]. San Francisco (CA): Wikimedia Foundation [cit. 2022-01-30]. Dostupné z: [https://en.wikipedia.org/wiki/Grenfell\\_Tower\\_fire](https://en.wikipedia.org/wiki/Grenfell_Tower_fire)
- [4] Lakanal House fire. *Wikipedia: the free encyclopedia* [online]. San Francisco (CA): Wikimedia Foundation [cit. 2022-01-30]. Dostupné z: [https://en.wikipedia.org/wiki/Lakanal\\_House\\_fire](https://en.wikipedia.org/wiki/Lakanal_House_fire)
- [5] *Fire Safety Statistics* [online]. Modern Building Alliance [cit. 2022-01-30]. Dostupné z: <https://www.modernbuildingalliance.eu/fire-safety-statistics/>
- [6] *Statistiky* [online]. Hasičský záchranný sbor České republiky [cit. 2022-01-30]. Dostupné z: <https://www.hzscr.cz/info-servis-statistiky.aspx>
- [7] Great Fire of London. *Wikipedia: the free encyclopedia* [online]. San Francisco (CA): Wikimedia Foundation [cit. 2022-01-30]. Dostupné z: [https://en.wikipedia.org/wiki/Great\\_Fire\\_of\\_London](https://en.wikipedia.org/wiki/Great_Fire_of_London)
- [8] *ČSN 73 0802: Požární bezpečnost staveb - Nevýrobní objekty*. Praha: Úřad pro technickou normalizaci, metrologii a státní zkušebnictví.
- [9] List of building or structure fires. *Wikipedia: the free encyclopedia* [online]. San Francisco (CA): Wikimedia Foundation [cit. 2022-01-30]. Dostupné z: [https://en.wikipedia.org/wiki/List\\_of\\_building\\_or\\_structure\\_fires](https://en.wikipedia.org/wiki/List_of_building_or_structure_fires)
- [10] CALAVERA, JOSÉ et al.: Fire in the Windsor building, Madrid: Survey of the fire resistance and residual bearing capacity of the structure after fire. Madrid: INTEMAC, 2005. ISSN 1885-4575
- [11] LI, YI & LU, XINZHENG & GUAN, HONG & YING, MINGJIAN & YAN, WEIMIN. (2015). A Case Study on a Fire-Induced Collapse Accident of a Reinforced Concrete Frame-Supported Masonry Structure. *Fire Technology*. 52. 10.1007/s10694-015-0491-0.
- [12] Plasco Building. *Wikipedia: the free encyclopedia* [online]. San Francisco (CA): Wikimedia Foundation [cit. 2022-01-30]. Dostupné z: [https://en.wikipedia.org/wiki/Plasco\\_Building](https://en.wikipedia.org/wiki/Plasco_Building)
- [13] LI, Y., LU, X., GUAN, H. *et al.* A Case Study on a Fire-Induced Collapse Accident of a Reinforced Concrete Frame-Supported Masonry Structure. *Fire Technol* **52**, 707–729 (2016). <https://doi.org/10.1007/s10694-015-0491-0>
- [14] *Ausgebrannt: Feuer frisst sich durch Riesen-Hochhaus in Dubai - Bilder & Fotos* [online]. Welt [cit. 2022-01-30]. Dostupné z: <https://www.welt.de/vermishtes/weltgeschehen/gallery111251709/Feuer-frisst-sich-durch-Riesen-Hochhaus-in-Dubai.html>
- [15] *Fire design of concrete structures: materials, structures and modelling : state-of-art report*. Lausanne: International Federation for Structural Concrete. Bulletin. ISBN 978-2-88394-078-9.
- [16] *ČSN EN 1992-1-2: Eurokód 2: Navrhování betonových konstrukcí – Část 1-2: Obecná pravidla – Navrhování konstrukcí na účinky požáru*. Praha: Český normalizační institut.
- [17] *ACI 216.1: Code Requirements for Determining Fire Resistance of Concrete and Masonry Construction Assemblies*. Michigan: American Concrete Institute.
- [18] *Model Code 2010: bulletin 65*. Lausanne: International Federation for Structural Concrete. ISBN 978-2-88394-105-2.
- [19] AKANSHU SHARMA, JOSIPA BOŠNJAK, SASKIA BESSERT. *Experimental investigations on residual bond performance in concrete subjected to elevated temperature*, Engineering Structures, Volume 187, 2019, Pages 384-395, ISSN 0141-0296, <https://doi.org/10.1016/j.engstruct.2019.02.061>.



- [20] NESMA GHAZALY, AHMED RASHAD, MOHAMED KOHAIL, OMAR NAWAWY, Evaluation of bond strength between steel rebars and concrete for heat-damaged and repaired beam-end specimens, *Engineering Structures*, Volume 175, 2018, Pages 661-668, ISSN 0141-0296, <https://doi.org/10.1016/j.engstruct.2018.08.056>.
- [21] O. BAHR, P. SCHAUMANN, B. BOLLEN, J. BRACKE. *Young's modulus and Poisson's ratio of concrete at high temperatures: Experimental investigations*, *Materials & Design*, Volume 45, 2013, Pages 421-429, ISSN 0261-3069, <https://doi.org/10.1016/j.matdes.2012.07.070>
- [22] ALBREKTSSON, Joakim, Mathias FLANSBJER, Jan Erik LINDQVIST a Robert JANSSON. *Assessment of concrete structures after fire: SP Report 2011:19*. Borås: SP Technical Research Institute of Sweden. ISBN 978-91-86622-50-3. ISSN 0284-5172.
- [23] BASTAMI, MORTEZA & ASLANI, F. & OMRAN, M.. (2010). *High-Temperature Mechanical Properties of Concrete*. *International Journal of Civil Engineering*. 8. 337-351.
- [24] CHUDZIK, PAWEŁ & KOWALSKI, ROBERT & ABRAMOWICZ, MARIAN. (2017). *Strains of Concrete in RC Structures Subjected to Fire*. *Procedia Engineering*. 193. 377-384. 10.1016/j.proeng.2017.06.227.
- [25] ČSN EN 1992-1-1: Eurokód 2: Navrhování betonových konstrukcí – Část 1-1: Obecná pravidla a pravidla pro pozemní stavby. Ed. 2. Praha: Úřad pro technickou normalizaci, metrologii a státní zkušebnictví.
- [26] PETR MÜLLER, JOSEF NOVÁK, JAKUB HOLAN. *Destructive and non-destructive experimental investigation of polypropylene fibre reinforced concrete subjected to high temperature*, *Journal of Building Engineering*, Volume 26, 2019, 100906, ISSN 2352-7102, <https://doi.org/10.1016/j.jobe.2019.100906>.
- [27] LUIGI BIOLZI, SARA CATTANEO, GIANPAOLO ROSATI. *Evaluating residual properties of thermally damaged concrete*, *Cement and Concrete Composites*, Volume 30, Issue 10, 2008, Pages 907-916, ISSN 0958-9465, <https://doi.org/10.1016/j.cemconcomp.2008.09.005>.
- [28] *Fire design of concrete structures: structural behaviour and assessment : state-of-the-art report*. Lausanne: International Federation for Structural Concrete. Bulletin. ISBN 978-2-88394-086-4.
- [29] QIANMIN MA, RONGXIN GUO, ZHIMAN ZHAO, ZHIWEI LIN, KECHENG HE. *Mechanical properties of concrete at high temperature – A review*, *Construction and Building Materials*, Volume 93, 2015, Pages 371-383, ISSN 0950-0618, <https://doi.org/10.1016/j.conbuildmat.2015.05.131>.
- [30] HAGER, IZABELA. *Behaviour of cement concrete at high temperature*. *Bulletin of the Polish Academy of Sciences. Technical Sciences*, 2013, 61.1: 145-154.
- [31] ULRICH SCHNEIDER. *Concrete at high temperatures — A general review*, *Fire Safety Journal*, Volume 13, 1988, Pages 55-68, ISSN 0379-7112, [https://doi.org/10.1016/0379-7112\(88\)90033-1](https://doi.org/10.1016/0379-7112(88)90033-1).
- [32] ŠTEFAN, RADEK. *Transport Processes in Concrete at High Temperatures: Mathematical Modelling and Engineering Applications with Focus on Concrete Spalling*. Praha, 2015. Disertační práce. ČVUT.
- [33] D.V. BOMPA, A.Y. ELGHAZOULI. *Elevated temperature characteristics of steel reinforcement incorporating threaded mechanical couplers*, *Fire Safety Journal*, Volume 104, 2019, Pages 8-21, ISSN 0379-7112, <https://doi.org/10.1016/j.firesaf.2018.12.006>.
- [34] BAŽANT, ZDENĚK A MAURICE F. KAPLAN. *Concrete at high temperatures: material properties and mathematical models*. Harlow: Longman. Concrete design and series construction. ISBN 0-582-08626-4.
- [35] FELICETTI, ROBERTO & GAMBAROVA, PIETRO. (1998). *Effects of High Temperature on the Residual Compressive Strength of High-Strength Siliceous Concretes*. *ACI Materials Journal*. 95. 395-405.
- [36] ČSN EN 1994-1-2: Eurokód 4: Navrhování sprážených ocelobetonových konstrukcí – Část 1-2: Obecná pravidla – Navrhování konstrukcí na účinky požáru. Praha: Český normalizační institut.





- [37] MACIEL, PRISCILA & FRANSOZO, HELDER & M CLARET, ANTONIO & CARVALHO, ESPEDITO & NETO, JOÃO & SOARES JUNIOR, PAULO ROBERTO & BEZERRA, AUGUSTO. (2019). *Influence of Cooling Methods on the Residual Mechanical Behavior of Fire-Exposed Concrete: An Experimental Study*. Materials. 12. 3512. 10.3390/ma12213512.
- [38] *TR 68 Assessment, design and repair of fire-damaged concrete structures*. Camberley: The Concrete Society. ISBN 978-1904482512.
- [39] NESMA GHAZALY, AHMED RASHAD, MOHAMED KOHAIL, OMAR NAWAWY. *Evaluation of bond strength between steel rebars and concrete for heat-damaged and repaired beam-end specimens*, Engineering Structures, Volume 175, 2018, Pages 661-668, ISSN 0141-0296, <https://doi.org/10.1016/j.engstruct.2018.08.056>.
- [40] JAMAL KHALAF, ZHAOHUI HUANG. *The bond behaviour of reinforced concrete members at elevated temperatures*, Fire Safety Journal, Volume 103, 2019, Pages 19-33, ISSN 0379-7112, <https://doi.org/10.1016/j.firesaf.2018.12.002>.
- [41] ROBERTO FELICETTI, PIETRO G. GAMBAROVA, ALBERTO MEDA. *Residual behavior of steel rebars and R/C sections after a fire*, Construction and Building Materials, Volume 23, Issue 12, 2009, Pages 3546-3555, ISSN 0950-0618, <https://doi.org/10.1016/j.conbuildmat.2009.06.050>.
- [42] VAŠEK, Milan. *Havárie, poruchy a rekonstrukce: dřevěné a ocelové konstrukce*. Praha: Grada. Stavitel. ISBN 978-80-247-3526-9.
- [43] T. GERNAY, J.-M. FRANSSSEN. *A formulation of the Eurocode 2 concrete model at elevated temperature that includes an explicit term for transient creep*, Fire Safety Journal, Volume 51, 2012, Pages 1-9, ISSN 0379-7112, <https://doi.org/10.1016/j.firesaf.2012.02.001>.
- [44] GIACOMO TORELLI, PARTHASARATHI MANDAL, MARTIN GILLIE, VAN-XUAN TRAN, *Concrete strains under transient thermal conditions: A state-of-the-art review*, Engineering Structures, Volume 127, 2016, Pages 172-188, ISSN 0141-0296, <https://doi.org/10.1016/j.engstruct.2016.08.021>.
- [45] ANDERBERG Y, THELANDERSSON S. *Stress and deformation characteristics of concrete at high temperature: 2. Experimental investigation and material behaviour model*. Bull. No. 46, Lund; 1976, p. 86
- [46] NIELSEN CV, PEARCE CJ, BICANIC N. *Theoretical model of high temperature effects on uniaxial concrete member under elastic restraint*. Mag Concr Res 2002; 54:239–49. <http://dx.doi.org/10.1680/macr.54.4.239.38809>
- [47] DIEDERICHS U. Modelle zur Beschreibung der Betonverformung bei instantion {ä}ren Temperaturen. Abschluss{kolloquium–Bauwerke Unter. Brand 1987:25–34
- [48] SAFIR [online]. Liege: University of Liege [cit. 2022-01-30]. Dostupné z: [https://www.uee.uliege.be/cms/c\\_6331644/en/safir](https://www.uee.uliege.be/cms/c_6331644/en/safir)
- [49] ČSN EN 1990: Eurokód: Zásady navrhování konstrukcí. Ed. 2. Praha: Úřad pro technickou normalizaci, metrologii a státní zkušebnictví.
- [50] ČSN EN 1995-1-2: Eurokód 5: Navrhování dřevěných konstrukcí – Část 1-2: Obecná pravidla – Navrhování konstrukcí na účinky požáru. Praha: Český normalizační institut.
- [51] OLIVEIRA, JAQUELINE & RIBEIRO, JOSÉ & PEDROTI, LEONARDO & FARIA, CAMILA & NALON, GUSTAVO & OLIVEIRA, ANDRÉ. (2019). *Durability of Concrete After Fire Through Accelerated Carbonation Tests*. Materials Research. 22. 10.1590/1980-5373-mr-2019-0049.
- [52] *Central Group nabídne designové byty na pražské Harfě* [online]. Praha [cit. 2022-01-30]. Dostupné z: <https://www.central-group.cz/page.aspx?page=tz-03052018&jv=1>
- [53] *TempAnalysis: Výpočetní program pro teplotní analýzu průřezů vystavených účinkům požáru* [online]. [cit. 2022-01-30]. Dostupné z: <http://people.fsv.cvut.cz/www/stefarad/software/ta/ta.cz.html>
- [54] ČSN EN 1991-1-2: Eurokód 1: Zatížení konstrukcí – Část 1-2: Obecná zatížení – Zatížení konstrukcí vystavených účinkům požáru. Praha: Český normalizační institut.





- [55] *OZone: The Design Fire Tool OZone V2.0 - Theoretical Description and Validation On Experimental Fire Tests* [online]. Liege: University of Liege [cit. 2022-01-30]. Dostupné z: [https://dan.ct.upt.ro/fire/files/OZone\\_V2.pdf](https://dan.ct.upt.ro/fire/files/OZone_V2.pdf)
- [56] *FIN EC: Dimenzační a posudkové programy*. FINE spol. s r.o. Dostupné z: <https://www.fine.cz/vypocty-statiky/>
- [57] CFAST, Fire Growth and Smoke Transport Modeling [online]. NIST [cit. 2022-01-30]. Dostupné z: <https://www.nist.gov/el/fire-research-division-73300/product-services/consolidated-fire-and-smoke-transport-model-cfast>
- [58] BENÝŠEK, MARTIN. *Analysis of Fire Resistance of Concrete Structures Based on Different Fire Models*. Praha. Disertační práce. ČVUT.
- [59] MÜLLER, P.; BENÝŠEK, M.; ŠTEFAN, R. Post-Fire Structural Assessment of a Firefighting Training Facility: A Case Study. In: *Journal of Fire Sciences*, 2021. Submitted (contribution 40 %)
- [60] *ČSN ISO 13822: Zásady navrhování konstrukcí - Hodnocení existujících konstrukcí*. Ed. 2. Praha: Úřad pro technickou normalizaci, metrologii a státní zkušebnictví.
- [61] *ČSN EN 13791: Posuzování pevnosti betonu v tlaku v konstrukcích a v prefabrikovaných betonových dílcích*. Praha: Evropský výbor pro normalizaci.
- [62] *ČSN EN 12504: Zkoušení betonu v konstrukcích*. Praha: Evropský výbor pro normalizaci.
- [63] *ČSN EN 12390: Zkoušení ztvrdlého betonu*. Praha: Evropský výbor pro normalizaci.
- [64] *ČSN EN 206+A2: Beton - Specifikace, vlastnosti, výroba a shoda*. Praha: Evropský výbor pro normalizaci.
- [65] PATTAMAD PANEDPOJAMAN, DANUPON TONNAYOPAS. *Rebound hammer test to estimate compressive strength of heat exposed concrete*, *Construction and Building Materials*, Volume 172, 2018, Pages 387-395, ISSN 0950-0618, <https://doi.org/10.1016/j.conbuildmat.2018.03.179>.
- [66] *Rebound Hammer Test on Concrete: Principle, Procedure, Advantages & Disadvantages* [online]. The Constructor [cit. 2022-01-30]. Dostupné z: <https://theconstructor.org/concrete/rebound-hammer-test-concrete-ndt/2837/>
- [67] *Silver Schmidt: Operating Instructions* [online]. proceq [cit. 2022-01-30]. Dostupné z: [https://www.screeningeagle.com/Downloads/SilverSchmidt\\_Operating%20Instructions\\_English\\_high.pdf](https://www.screeningeagle.com/Downloads/SilverSchmidt_Operating%20Instructions_English_high.pdf)
- [68] *ČSN 73 1373: Nedestruktivní zkoušení betonu - Tvrdoměrné metody zkoušení betonu*. Praha: Evropský výbor pro normalizaci.
- [69] LESLIE J. R., CHEESEMAN W. J.: An ultrasonic method for studying deterioration and cracking in concrete structures. *Amer. Concrete Inst., Proceedings*. Vol. 46. Sept. 1949. p. 17–36
- [70] *Guidebook on non-destructive testing of concrete structures*. Vienna: International Atomic Energy Agency. ISSN 1018–5518.
- [71] CIKRLE, Petr, Dalibor KOCÁB a Ondřej POSPÍCHAL. *Zkoušení betonu ultrazvukovou impulsovou metodou*. *BETON TKS* [online]. 2013(3), 74-79 [cit. 2022-01-30]. Dostupné z: <https://www.ebeton.cz/clanky/2013-3-74-zkouseni-betonu-ultrazvukovou-impulsovou-metodou/>
- [72] LESLIE J. R., CHEESEMAN W. J.: An ultrasonic method for studying deterioration and cracking in concrete structures. *Amer. Concrete Inst., Proceedings*. Vol. 46. Sept. 1949. p. 17–36
- [73] *ČSN 73 2011: Nedestruktivní zkoušení betonových konstrukcí*. Praha: Úřad pro technickou normalizaci, metrologii a státní zkušebnictví.
- [74] *ČSN 73 1371: Nedestruktivní zkoušení betonu - Ultrazvuková impulzová metoda zkoušení betonu*. Praha: Úřad pro technickou normalizaci, metrologii a státní zkušebnictví.
- [75] ANTON, Ondřej. *Zkušebnictví a technologie: Laboratorní cvičení* [online]. 1. Brno: VUT Brno -FAST [cit. 2017-10-26]. Dostupné z: <http://lences.cz/domains/lences.cz/skola/subory/Skripta/BI02->



- [Zkusenictvi%20a%20technologie/Zkusebnictvi%20a%20technologie%20M04-Laboratorni%20cviceni.pdf](#)
- [76] DENYS, BREYSSE. (2012). *Nondestructive evaluation of concrete strength: An historical review and a new perspective by combining NDT methods*. Construction and Building Materials. 33. 139–163. 10.1016/j.conbuildmat.2011.12.103.
- [77] PANZERA, T. & CHRISTOFORO, ANDRÉ & COTA, FABIO & RIBEIRO BORGES, PAULO & BOWEN, CHRIS. (2011). *Ultrasonic Pulse Velocity Evaluation of Cementitious Materials*. 10.5772/17167.
- [78] MAITHAM FADHIL ABBAS ALWASH. *Assessment of concrete strength in existing structures using nondestructive tests and cores : analysis of current methodology and recommendations for more reliable assessment*. Mechanics [physics]. Université de Bordeaux, 2017. English. ffNNT : 2017BORD0587ff. fftel-01531241
- [79] Gregor Trtnik, Franci Kavčič, Goran Turk, Prediction of concrete strength using ultrasonic pulse velocity and artificial neural networks, Ultrasonics, Volume 49, Issue 1, 2009, Pages 53-60, ISSN 0041-624X, <https://doi.org/10.1016/j.ultras.2008.05.001>
- [80] *ACI 228.1R: Report on Methods for Estimating In-Place Concrete Strength*. Michigan: American Concrete Institute.
- [81] *ASTM Test Designation C 597-02, Standard Test Method for Pulse Velocity through Concrete*, Annual Book of ASTM Standards, Vol. 04.02, West Conshohocken, PA, 2003
- [82] FELICETTI, ROBERTO. (2004). *Digital Camera Colorimetry for the Assessment of Fire Damaged Concrete*.
- [83] HAGER, I. *Colour Change in Heated Concrete*. Fire Technology, Vol. 50, 2014, pp. 945–958
- [84] KONG, WEIKANG & WAN, CHENG & WANG, YA-QIONG. (2019). *The Colorimetry Method in Assessing Fire-Damaged Concrete*. Journal of Advanced Concrete Technology. 17. 282-294. 10.3151/jact.17.282.
- [85] Short - Assessment of fire damaged concrete using colour image analysis (2000)
- [86] CHROMÁ, MARKÉTA. *Studium a modelování karbonatace betonu*. Brno. Disertační práce. VYSOKÉ UČENÍ TECHNICKÉ V BRNĚ. Dostupné online: [https://www.vutbr.cz/www\\_base/zav\\_prace\\_soubor\\_verejne.php?file\\_id=47248](https://www.vutbr.cz/www_base/zav_prace_soubor_verejne.php?file_id=47248), výpočetní program dostupný online: <http://freet.cz/rc-lifetime/index.php>
- [87] VÁVRA, ZDENĚK. *Koroze konstrukcí*. Betosan: seminář [online]. Dostupné z: <https://docplayer.cz/108543749-Koroze-konstrukci-ing-zdenek-vavra.html>
- [88] *ASTM C39 / C39M-18, Standard Test Method for Compressive Strength of Cylindrical Concrete Specimens*, ASTM International, West Conshohocken, PA, 2018
- [89] *ČSN 73 1317: Stanovení pevnosti betonu v tlaku*. Praha: Úřad pro normalizaci a měření.
- [90] KOLÍSKO, JIŘÍ. *Posuzování pevnosti betonu v tlaku v konstrukcích: seminář*. In: BETON UNIVERSITY [online]. Dostupné z: <https://www.betonuniversity.cz/stahnout-soubor?id=1525>
- [91] ROBERTO FELICETTI, *The drilling resistance test for the assessment of fire damaged concrete*, Cement and Concrete Composites, Volume 28, Issue 4, 2006, Pages 321-329, ISSN 0958-9465, <https://doi.org/10.1016/j.cemconcomp.2006.02.009>.
- [92] FELICETTI, ROBERTO. (2014). *Assessment of fire damage in concrete structures: new inspection tools and combined interpretation of results*.
- [93] TC 177-MDT. Rilem Recommendation MDT.D.1 – Indirect determination of the surface strength of unweathered hydraulic cement mortar by the drill energy method. Mater Struct 2004;37:485–7.



- [94] ČSN EN ISO 6892-1: *Kovové materiály - Zkoušení tahem - Část 1: Zkušební metoda za pokojové teploty*. Praha: Evropský výbor pro normalizaci.
- [95] CHINGĂLATĂ, COSTEL, MIHAI BUDESCU a RADU LUPĂȘTEANU. Accuracy in Predicting the Compressive Strength of Concrete using Sonreb Method. In: *BULETINUL INSTITUTULUI POLITEHNIC DIN IAȘI* [online]. 63. Universitatea Tehnică „Gheorghe Asachi” din Iași, 2017.
- [96] M.T. CRISTOFARO, S. VITI, M. TANGANELLI. *New predictive models to evaluate concrete compressive strength using the SonReb method*, Journal of Building Engineering, Volume 27, 2020, 100962, ISSN 2352-7102, <https://doi.org/10.1016/j.jobbe.2019.100962>.
- [97] *FIN EC: Beton požár*. FINE spol. s r.o. <https://www.fine.cz/vypocty-statiky/beton-pozar/>
- [98] HUANG Z, BURGESS IW, PLANK RJ. *Nonlinear analysis of reinforced concrete slabs subjected to fire*. ACI Structural Journal 1999;96:127–35.
- [99] *ENV 1992-1-2: Eurocode 2: Design of concrete structures — Part 1.2 General rules — Structural fire design*. Brussels: European Committee for Standardization.
- [100] V.K.R. KODUR, ANKIT AGRAWAL. *Effect of temperature induced bond degradation on fire response of reinforced concrete beams*, Engineering Structures, Volume 142, 2017, Pages 98-109, ISSN 0141-0296, <https://doi.org/10.1016/j.engstruct.2017.03.022>.
- [101] M. GILLIE, A.S. USMANI, J.M. ROTTER. *A structural analysis of the Cardington British Steel Corner Test*, Journal of Constructional Steel Research, Volume 58, Issue 4, 2002, Pages 427-442, ISSN 0143-974X, [https://doi.org/10.1016/S0143-974X\(01\)00066-9](https://doi.org/10.1016/S0143-974X(01)00066-9).
- [102] M GILLIE, A.S USMANI, J.M ROTTER. *A structural analysis of the first Cardington test*, Journal of Constructional Steel Research, Volume 57, Issue 6, 2001, Pages 581-601, ISSN 0143-974X, [https://doi.org/10.1016/S0143-974X\(01\)00004-9](https://doi.org/10.1016/S0143-974X(01)00004-9).
- [103] S LAMONT, A.S USMANI, D.D DRYSDALE. *Heat transfer analysis of the composite slab in the Cardington frame fire tests*, Fire Safety Journal, Volume 36, Issue 8, 2001, Pages 815-839, ISSN 0379-7112, [https://doi.org/10.1016/S0379-7112\(01\)00041-8](https://doi.org/10.1016/S0379-7112(01)00041-8).
- [104] JIAN JIANG, HONGHUI QI, YAOLIANG LU, GUO-QIANG LI, WEI CHEN, JIHONG YE. *State-of-the-art review on tensile membrane action in reinforced concrete floors exposed to fire*, Journal of Building Engineering, Volume 45, 2022, 103502, ISSN 2352-7102, <https://doi.org/10.1016/j.jobbe.2021.103502>.
- [105] RADEK ŠTEFAN, JAROSLAV PROCHÁZKA. *Students lecture nr. 2, voluntary course Fire Design of Concrete And Masonry Structures*, 2013, available online: [http://people.fsv.cvut.cz/www/stefarad/vyuka/133YPNB/133YPNB\\_Prednaska\\_2.pdf](http://people.fsv.cvut.cz/www/stefarad/vyuka/133YPNB/133YPNB_Prednaska_2.pdf)
- [106] ŠTEFAN, R., SURA, J., PROCHÁZKA, J., KOHOUTKOVÁ, A., WALD, F. *Numerical investigation of slender reinforced concrete and steel-concrete composite columns at normal and high temperatures using sectional analysis and moment-curvature approach*. Engineering Structures, 190, 285-305, (2019)
- [107] Scia Engineer: *Structural Analysis & Design Software*. Nemetschek Group. <https://www.scia.net/cs/software/scia-engineer>



## List of Figures

<b>Nr.</b>	<b>Figure name</b>	<b>Page</b>
1-1	Evolution of human life losses caused by fire, taken over [5].	11
1-2	Official Czech fire brigade statistics per one month (average) over last 4 years [6].	11
1-3	Official Czech fire brigade statistics during year 2019 [6].	12
1-4	Windsor Tower fire, Madrid 2005 [10].	14
1-5	Grenfell Tower fire, London 2017 [3].	15
1-6	Partial fire-induced collapse of Hengzhou building, China 2003 [13].	15
1-7	Fire-induced collapse of Plasco building, Tehran 2017 [12].	16
1-8	Fire of Torch skyscraper, Dubai 2015 [14].	16
1-9	Flowchart of typical fire event.	17
2-1	Overview of changes in concrete exposed to fire.	20
2-2	Reduction coefficient of compressive strength according to EC2 [16].	21
2-3	Reduction coefficient of tensile strength according to EC2 [16].	22
2-4	Diagrams of compressive strength reduction according to ACI 216.1 (left: siliceous aggregate concrete, right: calcareous aggregate concrete) [17].	22
2-5	Diagram of bond strength reduction according to experimental results [19].	23
2-6	Scatter of Young's modulus decay based on test results according to [22].	24
2-7	Experimental results of Young's modulus decay at high temperatures [23].	24
2-8	Specific heat capacity of concrete according to EC2 [16].	26
2-9	Bulk density of concrete according to EC2 [16].	26
2-10	Thermal conductivity of concrete according to EC2 [16].	27
2-11	Free thermal strain of concrete according to EC2 [16].	27
2-12	Derived coefficient of thermal expansion of concrete.	28
2-13	Microscopic images of concrete matrix at ambient temperature (left) and 750 °C (right) - taken over [27].	29
2-14	Thermal strain of different types of aggregate - taken over [31].	30
2-15	Overview of aggregate types used in concrete production and their thermal stability, taken over [15].	30
2-16	Reduction coefficient of yield strength according to EC2 [16].	32
2-17	Reduction diagram of tensile strength according to ACI 216.1, taken over [17].	33
2-18	Reduction diagram of Young's modulus of reinforcing steel according to EC2 [16].	34
2-19	Free thermal strain of steel according to EC2 [16].	34
2-20	Temperature induced bond stress between reinforcement and concrete.	35
2-21	Comparison of relative compressive strength of concrete with calcareous aggregate according to test arrangement, taken over [28].	36
2-22	Time-dependent residual compressive strength of concrete specimen after exposure to 250 °C, taken over [35].	38
2-23	Reduction coefficient of residual yield strength according to [38].	40
2-24	Visual interpretation of LITS, taken over [44].	42
2-25	Total strain decomposition and constituents interpretation, taken over [44].	42
2-26	Total thermal strain of concrete at high temperatures with different applied load levels, taken over [44].	43
2-27	Stress-strain diagram with unloading branch, taken over [43].	44
2-28	Stress-strain diagram of siliceous aggregate concrete at high temperatures with linear descending branch, according to EC2 [16].	45
2-29	Thermal deformation of concrete column axially compressed and subjected to Japanese standard fire according to different numerical models and test results, taken over [43].	46
2-30	Stress-strain diagram of cold-worked reinforcing steel in tension at high temperatures, according to EC2 [16].	48



2-31	Stress-strain diagram of reinforcing steel in compression at high temperatures, according to EC2 [16].	48
3-1	Content of firefighting report related to post-fire structural assessment.	52
3-2	Flowchart of the structural assessment after fire.	56
3-3	Simplified interpretation of possible ways of fire damaged building treatment related to CEA.	60
4-1	Visual aspects of possible serious damage of concrete structure caused by fire event.	61
4-2	Example of graphical output based on preliminary post-fire inspection.	65
5-1	Example of amended graphical output based on detailed post-fire inspection.	67
5-2	Temperature profiles of 250 mm thick concrete slab, subjected to one-sided standard fire exposure for various durations; thermal analysis conducted in TempAnalysis software [53].	69
5-3	Temperature-time curves according to different fire scenarios and compartment parameters.	70
5-4	Temperature profiles of 250 mm thick concrete slab, subjected to one-sided fire exposure according to different fire scenarios and durations; thermal analysis conducted in TempAnalysis [53].	70
5-5	Temperature profiles of 400x400 mm concrete cross-section, subjected to four-sided fire exposure for different fire scenarios and durations (one quarter of cross-section displayed); thermal analysis conducted in TempAnalysis software [53].	72
5-6	Simulation of temperature evolution in T=5 min displayed on the transverse plane section, CFAST fire software [57].	73
5-7	Simulation of temperature evolution in T=42 min displayed on the longitudinal plane section, CFAST fire software [57].	73
5-8	Simulation of smoke production in T=8 min, CFAST fire software [57].	73
5-9	CFD simulation; left: overall 3D model, right: surface temperatures at time T=3 min [59].	74
5-10	CFD simulation; left: surface temperatures at time T=3 min with obstacle above flames source, right: smoke visualisation with vectors of convection [59].	74
5-11	Temperature evolution of gas and concrete (depth 30 mm from heated surface) according to various fire scenarios; thermal analysis conducted in TempAnalysis software [53].	75
5-12	Temperature-time curves according to different fire scenarios.	76
5-13	Temperature profiles of 250 mm thick concrete slab according to zone method temperature-time curves and their equivalent standard fire curves; thermal analysis conducted in TempAnalysis software [53].	77
5-14	Possible effect of internal forces redistribution on element not directly affected by fire.	78
6-1	Visual overview of post-fire diagnosis methods.	81
6-2	Evolution of deflections due to fire exposure.	84
6-3	Classic Schmidt rebound hammer, Proceq model N.	85
6-4	Conversion diagram of classic rebound number to compressive strength according to [67].	86
6-5	Diagram of average concrete cover temperature (30 mm thick) and corresponding decay of compressive strength and related measured rebound index.	88
6-6	Options of UPV test arrangement.	89
6-7	Aspects inside concrete element affecting pulse travel time, taken over [75].	91
6-8	Calibration diagrams of concrete compressive strength based on UPV tests according to various standards and experimental results.	92
6-9	Varying colour profile of concrete according to exposure temperatures, taken over [83].	93
6-10	Different colour systems – left: HSI [85], right: XYZ after RGB transformation [84].	94





6-11	Left: Whole chromaticity diagram in XY plane [82], right: concrete colour alteration caused by exposure to high temperatures put down into XY chromaticity diagram [84].	95
6-12	Expected velocity of concrete carbonation, based on [86].	96
6-13	Visual result of concrete carbonation test, taken over [87].	96
6-14	Effect of slenderness ratio on compressive strength, based on [90].	97
6-15	Strut & tie model in concrete specimen during destructive compressive strength test.	99
6-16	Left: electric drilling-machine equipped with measuring gadget; right: measured a calculated parameters needed for test evaluation, taken over [91].	100
6-17	Visual evaluation of drilling resistance test, taken over [91].	100
6-18	Histogram of data set A.	104
6-19	Standard probability distribution of two data sets.	104
6-20	Nomogram for estimating concrete compressive strength based on SonReb method [93].	106
6-21	Visual output of conducted structural diagnosis, temperature profile calculated in [53].	107
7-1	Effect of thermal loading on statically-determinate structure.	109
7-2	Effect of thermal loading on statically-indeterminate structure.	109
7-3	Effect of thermal loading on generic computational element.	110
7-4	Evolution of flexural stiffness decay and thickness reduction according to standard fire duration.	112
7-5	Movement of bending moment line on continuous one-way RC slab th.200 mm, ISO834 fire assumed, middle span exposed.	112
7-6	Planned structural model of selected element analysed in the application.	115
7-7	Flowchart of taking thermal loading into account.	116
7-8	Thermal strains of free strips, taken over [99].	117
7-9	Ensuring force-equilibrium over cross-section, taken over [99].	117
7-10	Simplifying 2D thermal field into 1D, taken over [99].	118
7-11	Final strain over cross-section, taken over [99].	119
7-12	Configuration of the parametric study, taken over [28].	121
7-13	Comparison of panel's elongation with zero axial restraint.	121
7-14	Comparison of additional inner forces evolution with absolutely stiff axial restraint.	122
7-15	Evolution of axial force eccentricity and thermal gradient.	122
7-16	Evolution of temperature-induced axial force according to support's axial stiffness [28].	123
7-17	Evolution of temperature-induced bending moment according to support's axial stiffness [28].	124
7-18	Evolution of temperature-induced axial elongation according to support's axial stiffness [28].	124
7-19	Influence of support stiffness on relaxation level, expressed by factor $a_2$ .	125
7-20	Example 1: total cross-section linear strain with highlighted elastic and ultimate limit strains of both steel and concrete.	128
7-21	Example 2: total cross-section linear strain with highlighted elastic and ultimate limit strains of both steel and concrete.	128
8-1	Cardington full-scale fire tests: concrete slab after fire with incoherent bottom reinforcement, taken over [105].	131
8-2	Assessment of residual load-bearing capacity of RC column using surface Deterioration method after ISO834 fire lasting 45 minutes.	133
8-3	Decay of concrete compressive strength at hot (EC2-1-2 [16]) and residual state [28].	134
8-4	Assessment of residual load-bearing capacity of RC column using Isotherm 300 °C method after ISO834 fire lasting 120 minutes.	135
8-5	Assessment of residual load-bearing capacity of RC slab using Isotherm 300 °C method after ISO834 fire lasting 180 minutes.	136
8-6	Assessment of residual load-bearing capacity of RC column using Adjusted zone method after ISO834 fire lasting 120 minutes.	138





8-7	Assessment of residual load-bearing capacity of RC slab using Adjusted zone method after ISO834 fire lasting 180 minutes.	139
8-8	Parametric study: residual load-bearing capacity of RC columns estimated with different assessment methods.	140
8-9	Parametric study: residual load-bearing capacity of RC slabs estimated with different assessment methods.	141
A-1	Graphical results of preliminary and detailed object inspection.	159
A-2	Temperature-time curve of assumed fire scenario [53].	160
A-3	Temperature field of column's cross-section at $t = 93$ min [53].	161
A-4	Temperature field of lintel's cross-section at $t = 93$ min [53].	161
A-5	Temperature profile of slab with soffit at $t = 93$ min (plasterboard layer neglected) [53].	161
A-6	Relative strength decay of concrete based on UPV tests.	163
A-7	Equation of actual concrete strength decay according to reached maximal temperature obtained by regression analysis.	163
A-8	2D structural model with highlighted part affected by fire.	168
A-9	Other dead load incorporated in the calculations in $[\text{kN}/\text{m}^2]$ .	169
A-10	Live load incorporated in the calculations, categories B and H in $[\text{kN}/\text{m}^2]$ .	169
A-11	Linear elastic deflections at SLS in $[\text{mm}]$ .	170
A-12	Axial forces at ULS in $[\text{kN}]$ .	170
A-13	Bending moments at ULS in $[\text{kNm}]$ .	171
A-14	Shear forces at ULS in $[\text{kN}]$ .	171
A-15	Linear elastic deflections at extraordinary ULS in $[\text{mm}]$ .	173
A-16	Axial forces at extraordinary ULS in $[\text{kN}]$ .	173
A-17	Bending moments at extraordinary ULS in $[\text{kNm}]$ .	174
A-18	Shear forces at extraordinary ULS in $[\text{kN}]$ .	174
A-19	Estimation of stiffness coefficients based on deflections from unit forces – left span.	175
A-20	Estimation of stiffness coefficients based on deflections from unit forces – right span.	175
A-21	Incorporation of thermal strains into structural model as external loading.	178
A-22	Linear elastic deflections at extraordinary ULS in 60 <sup>th</sup> minute of fire in $[\text{mm}]$ .	178
A-23	Axial forces at extraordinary ULS in 60 <sup>th</sup> minute of fire in $[\text{kN}]$ .	179
A-24	Bending moments at extraordinary ULS in 60 <sup>th</sup> minute of fire in $[\text{kNm}]$ .	179
A-25	Shear forces at extraordinary ULS in 60 <sup>th</sup> minute of fire in $[\text{kN}]$ .	180
A-26	Linear elastic deflections at extraordinary ULS in 120 <sup>th</sup> minute of fire in $[\text{mm}]$ .	183
A-27	Axial forces at extraordinary ULS in 120 <sup>th</sup> minute of fire in $[\text{kN}]$ .	183
A-28	Bending moments at extraordinary ULS in 120 <sup>th</sup> minute of fire in $[\text{kNm}]$ .	184
A-29	Shear forces at extraordinary ULS in 120 <sup>th</sup> minute of fire in $[\text{kN}]$ .	184
A-30	Strains in maximally loaded slab cross-section referring to 60 <sup>th</sup> minute of fire.	187
A-31	Strains in maximally loaded wall cross-section referring to 120 <sup>th</sup> minute of fire.	188
A-32	Changes in structural model respecting overloading of critical cross-sections.	189
A-33	Maximal linear elastic deflections of adjusted model at extraordinary ULS in $[\text{mm}]$ .	189
A-34	Maximal axial forces in adjusted model at extraordinary ULS in $[\text{kN}]$ .	190
A-35	Maximal bending moments in adjusted model at extraordinary ULS in $[\text{kNm}]$ .	190
A-36	Maximal shear forces in adjusted model at extraordinary ULS in $[\text{kN}]$ .	191
A-37	Linear elastic deflections of adjusted model at SLS after fire in $[\text{mm}]$ .	191
A-38	Axial forces at ULS after fire in $[\text{kN}]$ .	192
A-39	Bending moments at ULS after fire in $[\text{kNm}]$ .	192
A-40	Shear forces at ULS after fire in $[\text{kN}]$ .	193
A-41	Bending moments at ULS after fire in $[\text{kNm}]$ with highlighted cross-sections according to assessment results.	194



## List of Tables

<b>Nr.</b>	<b>Table name</b>	<b>Page</b>
2-1	Overview of physical and chemical changes in concrete at increasing temperatures [15].	20
2-2	Overview of thermal properties of building materials at 20 °C.	28
3-1	Overview of common household material's reactions on increasing temperatures [28, 38].	53
4-1	Classification of structural damage caused by fire according to [38].	63
6-1	Overview of structural aspects investigated during diagnosis of concrete structures.	79
6-2	Overview of non-destructive diagnosis methods usable for investigation of concrete structures damaged by fire, according to [28].	82
6-3	Advantages and disadvantages of on-site NDT techniques, according to [22].	82
6-4	Expected concrete quality according to rebound hammer test [66].	86
6-5	Expected concrete quality according to UPV test, based on [71,72].	90
6-6	Conversion coefficient to static modulus of elasticity according to ČSN 73 2011 [73].	90
6-7	Assignment of temperature ranges to colouring and structural damage, based on [38].	94
6-8	Values of $k_n$ for 5% characteristic value, based on [49].	102
6-9	Example of data set gained experimentally and its evaluation according to EN 1990 [49].	103



## Annex – Worked Examples of Complete Fire and Post-Fire Resistance Assessment

### Case no. 1 – Assessment of RC Column and Lintels after Fire

Imaginary four-storey residential building was subjected to fire situation when fire spread in one fire compartment in first floor. Structural drawing of the 1<sup>st</sup> floor is given in Fig. A-1 below. It can be seen that the subjected structure was made of masonry walls (sand-lime bricks), one RC columns as the inner local support and RC floor slab. Structural system in all floors is identical making the static action predictable.

#### Information about Fire Event

From the firefighting report elaborated and provided by fire brigade it is known the fire was reported to fire brigade late making extinguishing rather impossible as the moment of flashover had already happened. Therefore, the fire brigade ensured the fire would not spread to other compartments and floors, and the fire in epicentre was extinguished after reaching peak temperature. Whole fire lasted for nearly three hours with peak temperatures taking place in between 80-100<sup>th</sup> minute, and which were estimated to reach approximately 900 °C. Within the fire brigade intervention inhabitants of the building were evacuated with no human life losses or harms.

#### Information from Preliminary and Detailed Object Inspection

After the end of fire brigade intervention police closed the subjected building with adjacent area for public. Few days after the end of fire preliminary inspection of the burned-out house was done by firefighters, police, representative of public administration and foremost structural engineer-specialist. Based on the preliminary inspection following statements were made:

- Only the compartment with fire epicentre was visibly affected by fire while rest of the 1<sup>st</sup> floor together with other floors appeared not-affected with maximally localised spots of blacked surface by soot;
- Probable ignition spot of fire was estimated according to the burned rests of items very firmly connected to floor tiles;
- Reaching at least 800 °C was confirmed as the glass pieces from windows were melted in case of two windows closer to the ignition spot;
- From the structural point of view masonry walls together with lintels and RC inner column were directly exposed to fire with no protective layers.
- 2<sup>nd</sup> floor RC slab was protected by plasterboard soffit with acoustic insulation made of mineral wool.

Beside the aforementioned statements also visual assessment of structural elements was made. Subsequently, these elements were classified into *damage classes* according to Tab. 4-1. The masonry walls exhibited only surface crazing and blackened plastering, which fell down from the bricks on several spots. The walls exhibited no residual deformation, no cracks, no local nor global collapses. Compressive strength of bricks was tested on several spots using rebound hammer, at the same time it was tested in the other compartment as referential. According to the results the compressive strength of sand-lime bricks subjected to fire exhibit 5-10% decay with respect to the referential ones. Therefore, the masonry walls were classified into damage class 1 expecting them to be damaged only minimally. Almost all plastering of the RC column fell off, moreover the column exhibited moderate surface spalling, especially in the corner zones making four corner rebars and stirrups directly exposed to fire; on contrary, the middle bars on every side were covered with the concrete cover of full thickness. No rebars were buckled or ruptured. Beside spalling there were particles in the concrete matrix without cover of sooth clearly coloured to red/orange. Results of the rebound hammer test showed 50-65% decay of surface compressive strength when compared to the referential measurement in the second



compartment. Therefore, the column was classified into damage class 3 expecting it to be significantly damaged. Moreover, extraction of drilled core from the column was requested for laboratory tests. RC lintels in outer walls overheads were significantly affected by fire when flames were flickering out of the windows making lintels cross-sections exposed to fire from 3 sides. Surface crazing together with cracks of width up to 0,6 mm at the bottom face of lintels in the mid-span and colour change to whitish grey/buff were visible. Also residual deflection up to 18-20 mm was present in case of 3 m long lintel. Only limited damage signs were present in case of lintel in the doorhead, which was exposed to high temperatures from 2 sides only. Rebound hammer test conducted from the bottom side showed 30-70% strength decay. The lintels were thus classified into damage class 2 (lintel in the doorhead) and 3-4 (lintels in the outer walls), expecting them to be considerably damaged. RC floor slab was protected by soffit consisting of 12,5 mm plasterboard together with 100 mm mineral wool, therefore it was not directly exposed to high temperatures. Due to the fire extinguishing the soffit was destroyed and pulled down in whole area. The bottom face of the slab looked nearly unaffected without spalled spots, cracks or residual deflections. The rebound hammer test of surface strength was conducted on two spots. As a referential measurement the test was conducted also in the other compartment through a service opening in the soffit. After results comparison mutual difference up to  $\pm 5\%$  was observed. The slab is not expected to be affected by fire in the residual state and thus it was classified into damage class 0. One drilled core is requested to be extracted from the slab in order to have referential specimen. All holes after extracted cores were immediately afterwards concrete back.

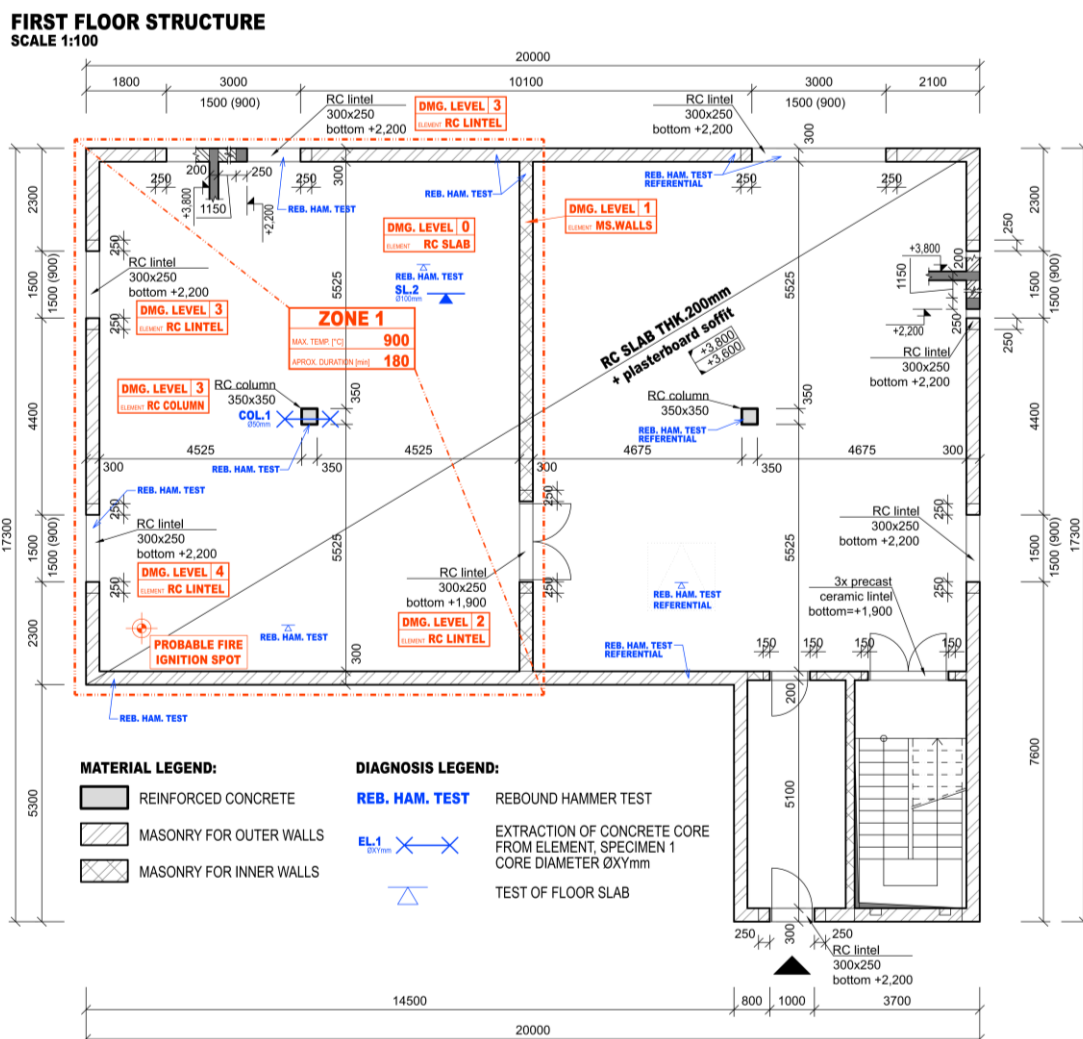


Fig. A-1. Graphical results of preliminary and detailed object inspection.



### Approximation of Fire Scenario, Thermal Analysis

In order to have an idea about probable fire scenario parametric temperature-time curve according to Annex A, EN 1991-1-2 [16] was constructed. Actual geometry of compartment, thermal properties of enclosures, fire loads according to dwelling nature of the building with fire safety measures were taken into account resulting into parameters given below:

- opening factor  $O = 0,039 m^{0,5}$
- thermal inertia  $b = 1184,327 J/m^2 s^{0,5} K$
- fire load density  $q_{t,d} = 301,9 MJ/m^2$
- medium fire growth rate

The curve can be seen in Fig. A-2. It can be stated the peak temperature  $\theta_{max} = 997 \text{ }^\circ\text{C}$  was reached in  $t_{max} = 93 \text{ min}$  after which the cooling phase had started. The peak temperature together with corresponding time agrees well with the information from fire brigade and the evidence of melted glass. The temperature-time curve assumed natural cooling after reaching the peak temperature which lasted for almost 160 min. The actual fire scenario was shorter as firefighters extinguished the fire within 90 minutes after reaching peak temperature; the cooling branch was then steeper. It means the structures were exposed to high temperatures for shorter duration and the critical time causing highest temperature distribution is assumed to be the already mentioned 93 minutes.

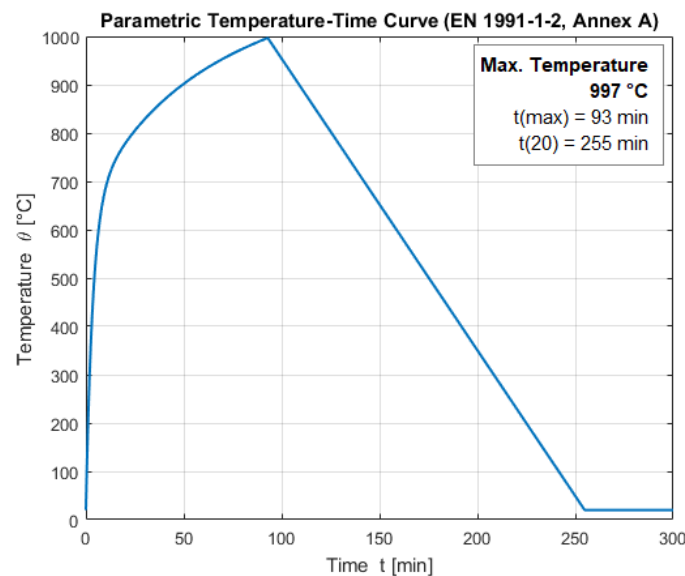


Fig. A-2. Temperature-time curve of assumed fire scenario [53].

According to the estimated duration of elements' exposure to high temperatures (see Chapter 8.3), it is expected the column would probably suffer 25-35% decay of load-bearing capacity, while decay up to 15-25 % is expected in case of lintels.



With such inputs thermal analysis of column, lintel and RC slab together with soffit are conducted, see Figs. A-3 to A-5.

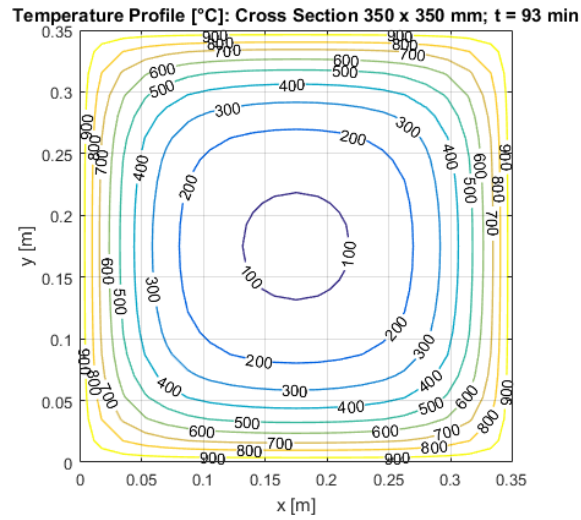


Fig. A-3. Temperature field of column's cross-section at  $t = 93$  min [53].

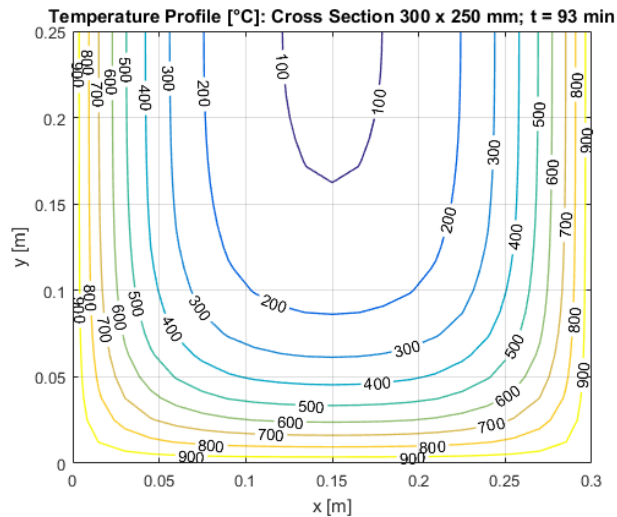


Fig. A-4. Temperature field of lintel's cross-section at  $t = 93$  min [53].

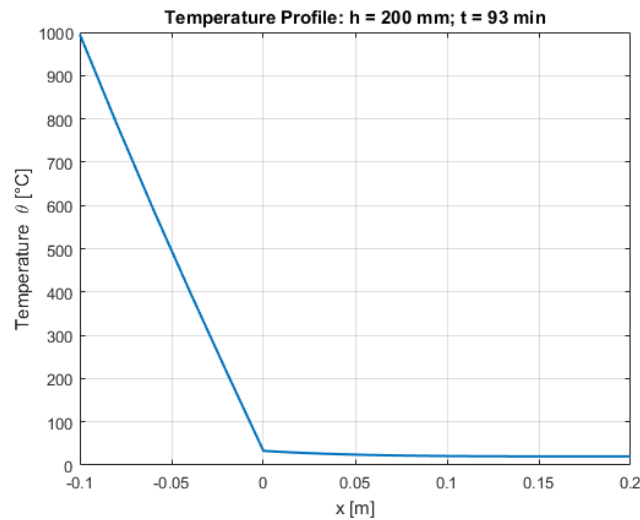


Fig. A-5. Temperature profile of slab with soffit at  $t = 93$  min (plasterboard layer neglected) [53].





## Structural Diagnosis

In order to estimate the decay of mechanical properties after exposition to fire, the inspected elements were subjected to on-site and laboratory material tests including rebound hammer test, destructive and UPV tests on cut-out concrete cores. In all cases beside tests on damaged elements also referential tests of undamaged elements were carried out, so the relative comparison can be made. Type of conducted material test with its position is evident in Fig. A-1 above.

Rebound hammer tests were conducted as first already during the preliminary inspection of the building in order to have an idea about damage severity and extent. All rebounds were conducted directly on concrete surface and not plastering, which required to remove the plaster at some spots. In all cases 10 rebounds were made which the rebound hammer automatically processed and provided the mean value and standard deviation. These two values were then used to calculate the characteristic value of rebound number according to EN 1990, Annex D [49]. Characteristic rebound number was afterwards converted to concrete compressive strength. For the conversion the basic formula given by hammer producer was used with correlation according to comparison of referential specimen strength obtained from rebound hammer test and destructive test. Within the results evaluation also thickness of carbonated layer was taken into account, which was measured on extracted concrete cores. As it was already mentioned, the strength decays were obtained as follows:

- masonry – relative decay up to 5-10 %
- column – relative decay in range 50-65 %
- lintels – relative decay in range 30-70 %
- slab – negligible decay or even slightly higher values in relative range  $\pm 5$  %

Destructive test of concrete compressive strength was performed on two specimens in accredited laboratory. Referential specimens taken out of the not-damaged column and slab were tested. The drilled core from column was shortened to length 100 mm in order to achieve optimal slenderness ratio. Prior to destructive test all cores were analysed in the means of carbonation depth, which was then used when evaluating rebound hammer tests. Results of both tests were close to each other and showed cylinder compressive strength  $f_{c,cyl,ls} = 24 \text{ MPa}$  (mean value) which corresponds well with information from original project documentation specifying the strength class C20/25 for concrete structures in this building. The core from damaged column was not tested destructively due to problematic evaluation of obtained test result with respect to different damage level depending on maximal reached temperatures at different depths.

The ultrasonic pulse velocity tests were conducted on all concrete cores doing 10 measurements in different depth in transverse direction through the core. According to the mutual comparison of obtained pulse velocities and concrete strength obtained from destructive test correlation equation was found by regression analysis. Therefore, all obtained pulse velocities could be transformed to the concrete compressive strength. This was important foremost in case of damaged core when strength decay could be investigated according to depth and expected highest reached temperature (see Fig. A-6). Mutual dependency of reached temperatures and strength decay was then expressed by linear function (see Fig. A-7).

The residual yield strength of reinforcement was not scrutinised experimentally due to problematic specimen extraction out of column and lintels. However, the theoretical idea about reached temperatures in cross-section based on thermal analysis and evidence based on material tests inspecting concrete are relatively consistent, therefore it was assumed the theoretical information of maximal reached temperatures and decay of residual strength are sufficient in this case.

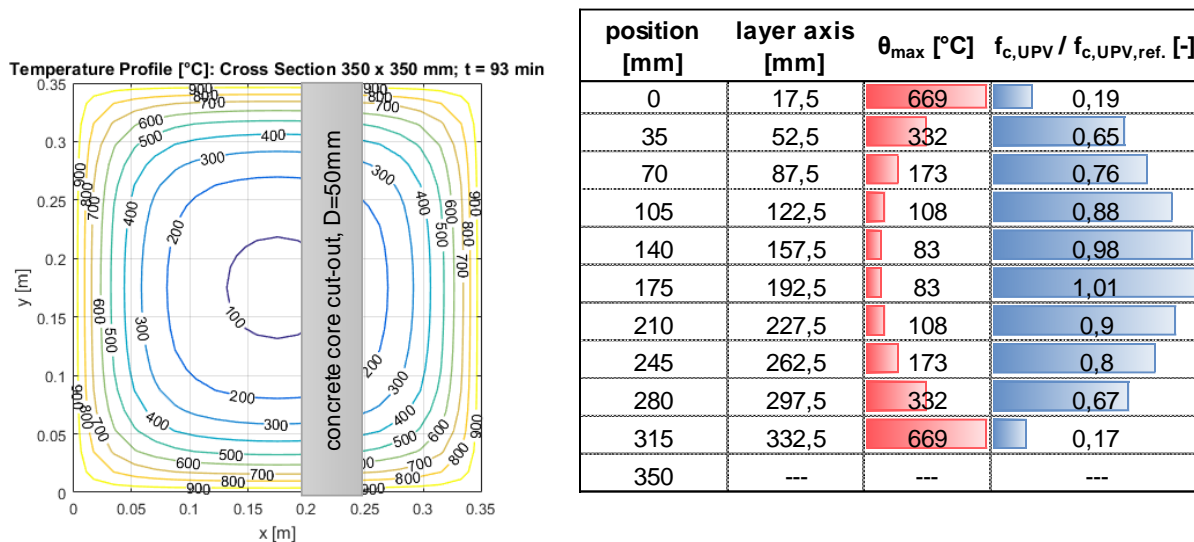


Fig. A-6. Relative strength decay of concrete based on UPV tests.

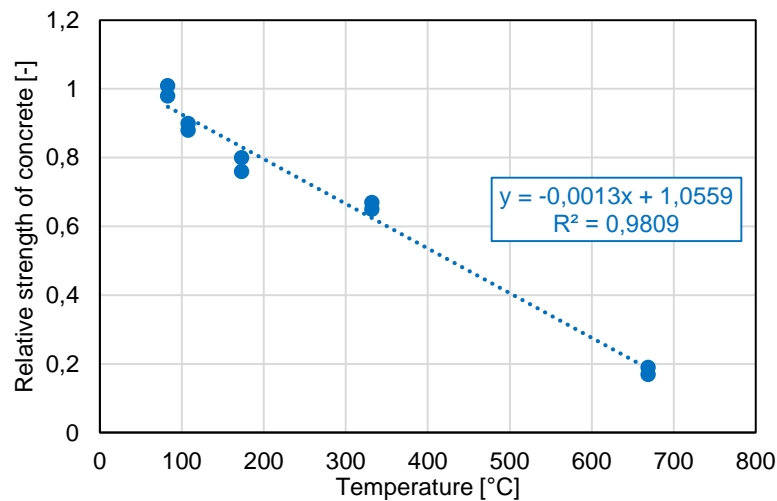


Fig. A-7. Equation of actual concrete strength decay according to reached maximal temperature obtained by regression analysis.

### Global Analysis

The effect of fire and high temperatures on global static action is assessed in this section. The RC column was assumed to be heated uniformly from all faces, thus no bowing (and potential bending moment) was expected. Thermal elongation was not expected thanks to LITS effect and complete relaxation of thermal strains (effect of compressive stress applied prior to and during heating).

RC lintels were assumed to act as simply supported beams. Potential thermal deformation would be probably enabled by local crushing of bricks, but with respect to the lintels dimensions and length these deformations were expected to be minimal. Lintels are not connected to other structures in the means of static indeterminacy.

RC floor slab was protected by the soffit which ensured the highest temperature of bottom face of the slab did not reach even 50 °C, see Fig. A-5 above. Hence, the slab is assumed not to be affected by the fire event anyhow.

Therefore, assessment of the column's and lintels' residual load-bearing capacity can be conducted with incorporated material degradation only. No change of static scheme is expected.



### Assessment of Residual Load-Bearing Capacity

Based on gained information and obtained evidence from the object inspection and structural diagnosis it was possible to assess the residual load-bearing capacity of damaged elements: (i) RC column, (ii) RC lintel 1 in outer wall – damage level 4 and (iii) RC lintel 2 in outer wall – damage level 3.

Following loadings are assumed:

- dead loads
  - self-weight of the slab  $g_{0,k} = \gamma_{conc} * h = 25 * 0,2 = 5 \text{ kN/m}^2$
  - weight of floor layers  $(g - g_0)_k = 1,5 \text{ kN/m}^2$
- variable loads
  - live load – category A  $q_k = 1,5 \text{ kN/m}^2$
- loading areas carried by elements
  - RC column  $A_{loads,column} = 29 \text{ m}^2$
  - RC lintel 1,5 m long  $A_{loads,lintel 1} = 1,7 \text{ m}^2$
  - RC lintel 3 m long  $A_{loads,lintel 2} = 4,5 \text{ m}^2$
- column carries 4 identical storeys

$$\begin{aligned} N_{Ed,column} &= n_{storeys} * A_{loads,column} * (\gamma_G * g_k + \gamma_Q * q_k) \\ &= 4 * 29 * (1,35 * (5 + 1,5) + 1,5 * 1,5) = 1279 \text{ kN} \end{aligned}$$

$$M_{Ed,lin 1} = \frac{1}{8} * f_{d,lin 1} * l_{lin 1} = \frac{1}{8} * 13,5 * 1,5^2 = 3,8 \text{ kNm}$$

$$V_{Ed,lin 1} = \frac{1}{2} * f_{d,lin 1} * l_{lin 1} = \frac{1}{2} * 13,5 * 1,5 = 10,1 \text{ kN}$$

$$M_{Ed,lin 2} = \frac{1}{8} * f_{d,lin 2} * l_{lin 2} = \frac{1}{8} * 20 * 3^2 = 17,5 \text{ kNm}$$

$$V_{Ed,lin 2} = \frac{1}{2} * f_{d,lin 2} * l_{lin 2} = \frac{1}{2} * 20 * 3 = 30 \text{ kN}$$



Assessment of RC column using *adjusted zone method*:

### ASSESSMENT OF RC COLUMN RESIDUAL LOAD-BEARING CAPACITY AFTER FIRE

<u>cross-section dimensions</u>	<u>initial concrete strength</u>	<u>initial steel strength</u>
h = 350 mm	$f_{ck,init} = 24$ MPa	$f_{yk,init} = 500,00$ MPa
b = 350 mm	$E_c = 31,19$ GPa	$E_s = 200,00$ GPa
<u>corner reinforcement</u>	<u>intermediate reinforcement</u>	<u>division of c.-s. into zones</u>
pieces = 4 pcs	pieces = 4 pcs	zone nr. = 10 [-]
diameter = 14 mm	diameter = 14 mm	zone thick. = 17,50 mm
$\theta_{corner\ reinf.} = 850$ °C	$\theta_{inner\ reinf.} = 429$ °C	

i [-]	a <sub>i</sub> [mm]	θ <sub>i</sub> [°C]	k <sub>c</sub> (θ <sub>i</sub> ) [-]
M	175	286	0,68
1	9	812	0,00
2	26	571	0,31
3	44	398	0,54
4	61	286	0,68
5	79	205	0,79
6	96	154	0,86
7	114	120	0,90
8	131	101	0,92
9	149	88	0,94
10	166	82	0,95

residual state of concrete

$k_c(\theta_M) = 0,68$  [-]

$k_{c,m} = 0,68$  [-]

$a_z = 2,10$  mm

**=>  $b_{eff,res} = 345,80$  mm**

**$h_{eff,res} = 345,80$  mm**

residual state of reinforcement

$\theta_{reinf.\ mean} = 639,50$  °C

$k_{s,res} = 0,70$  [-]

cross-section scheme

cross-section temperature field

**RESIDUAL LOAD-BEARING CAPACITY IN PLAIN COMPRESSION**

$$N_{Rd,res} = 0,85 * A_{c,res} * (k_{cM} f_{ck} / \gamma_c) + A_s * \min(k_{s,res} * f_{yk} / \gamma_s; \epsilon_{c2} * E_s) = 1485,63 \text{ kN}$$

$$N_{Rd,res} = 1485 \text{ kN} > N_{Ed} = 1279 \text{ kN}$$

**SATISFY**

165



Assessment of RC lintel 1 using *isotherm 300 °C method*:

### ASSESSMENT OF RC BEAM RESIDUAL LOAD-BEARING CAPACITY AFTER FIRE

<b>cross-section dimensions</b>	<b>concrete properties</b>	<b>reinforcement properties</b>
h = 250 mm	$f_{ck,init} = 24,00$ MPa	$f_{yk} = 500,00$ MPa
b = 300 mm	$f_{cd,res} = 16,00$ MPa	$f_{yd} = 434,78$ MPa
c = 25 mm		

**Parametric Temperature-Time Curve (EN 1991-1-2, Annex A)**

Max. Temperature  
997 °C  
t(max) = 93 min  
t(20) = 255 min

**Temperature Profile [°C]: Cross Section 300 x 250 mm; t = 93 min**

- 300°C isotherm position	$a_{300°C} = 60$ mm	=>	$h_{res,300} = 190$ mm
- bottom corner bars temp.	$\theta_{s,bot,corner} = 638$ °C	=>	$k_{s,res,bot} = 0,70$ [-]
- bottom inner bars temp.	$\theta_{s,bot,inner} = 441$ °C	=>	$k_{s,res,bot} = 1,00$ [-]
- stirrups temp.	$\theta_{s,stir.} = 641$ °C	=>	$k_{s,res,stir.} = 0,69$ [-]
- refer. height for stir. temp.	$x_{stir. temp.} = 60$ mm		

	pcs	∅	spacing	$A_s$ [mm <sup>2</sup> ]
- bottom rebars	2x	8 mm		100,53
- top rebars	2x	8 mm		100,53
- stirrups		6 mm	/ 300 mm	56,55

**assessment of residual bending resistance - midspan cross-section**

- effective height	d = 215,00 mm		
- height of compression zone	x = 10,61 mm	=>	z = 210,76 mm
- moment resistance	$M_{Rd,res,span} = 6,44$ kNm	>	$M_{Ed,span} = 3,80$ kNm

**SATISFY**

**assessment of residual bending resistance - supports cross-section**

- effective height	d = 155,00 mm		
- height of compression zone	x = 15,18 mm	=>	z = 148,93 mm
- moment resistance	$M_{Rd,res,support} = 6,51$ kNm	>	$M_{Ed,support} =$ kNm

**assessment of residual shear resistance**

- shear crack angle	cotg θ = 1,5 [-]		
- compressed strut resistance	$V_{Rd,max,res} = 151,95$ kN	>	$V_{Ed} = 10,10$ kN
- shear reinf. resistance	$V_{Rd,s,res} = 17,99$ kN	>	

**SATISFY**



Assessment of RC lintel 2 using *isotherm 300 °C method*:

### ASSESSMENT OF RC BEAM RESIDUAL LOAD-BEARING CAPACITY AFTER FIRE

<b>cross-section dimensions</b>	<b>concrete properties</b>	<b>reinforcement properties</b>
h = 250 mm	$f_{ck,init} = 24,00$ MPa	$f_{yk} = 500,00$ MPa
b = 300 mm	$f_{cd,res} = 16,00$ MPa	$f_{yd} = 434,78$ MPa
c = 25 mm		

Parametric Temperature-Time Curve (EN 1991-1-2, Annex A)  
Max. Temperature 997 °C  
t(max) = 93 min  
t(20) = 255 min

Temperature Profile [°C]: Cross Section 300 x 250 mm; t = 93 min

- 300°C isotherm position	$a_{300°C} = 60$ mm	=>		$h_{res,300} = 190$ mm	
- bottom corner bars temp.	$\theta_{s,bot,corner} = 638$ °C	=>		$k_{s,res,bot} = 0,70$ [-]	
- bottom inner bars temp.	$\theta_{s,bot,inner} = 441$ °C	=>		$k_{s,res,bot} = 1,00$ [-]	
- stirrups temp.	$\theta_{s,stir.} = 641$ °C	=>		$k_{s,res,stir.} = 0,69$ [-]	
- refer. height for stir. temp.	$x_{stir. temp.} = 54$ mm				

	pcs	Ø	spacing	A <sub>s</sub> [mm <sup>2</sup> ]
- bottom rebars	3x	10 mm		235,62
- top rebars	2x	10 mm		157,08
- stirrups		8 mm	/ 250 mm	100,53

**assessment of residual bending resistance - midspan cross-section**

- effective height	d = 212,00 mm				
- height of compression zone	x = 28,44 mm	=>		z = 200,63 mm	
- moment resistance	$M_{Rd,res,span} = 16,43$ kNm	<		$M_{Ed,span} = 17,50$ kNm	<b>DO NOT SATISFY</b>

**assessment of residual bending resistance - supports cross-section**

- effective height	d = 152,00 mm				
- height of compression zone	x = 23,71 mm	=>		z = 142,51 mm	
- moment resistance	$M_{Rd,res,support} = 9,73$ kNm	>		$M_{Ed,support} = 5,00$ kNm	<b>SATISFY</b>

**assessment of residual shear resistance**

- shear crack angle	cotg θ = 1,5 [-]				
- compressed strut resistance	$V_{Rd,max,res} = 144,65$ kN	>		$V_{Ed} = 30,00$ kN	
- shear reinf. resistance	$V_{Rd,s,res} = 36,54$ kN	>			<b>SATISFY</b>

## Discussion

Thanks to conducted post-fire assessment, it was proved the damaged RC column as well as shorter RC lintels in outer walls provide sufficient load-bearing capacity, however the longer RC lintel in outer wall do not satisfy the ULS (mid-span in bending). Due to it strengthening of this element would be necessary. If the lintels' residual deflections do not satisfy the requirements of SLS, the curved shape can be hidden e.g. by plasterboard cladding.





## Case no. 2 – Assessment of RC Floor Slabs and Walls in Global Fire Action

Second worked example of post-fire structural assessment deals with imaginary three-storey office building made of RC floor slabs and walls. The assessment is aimed at global analysis with incorporation of temperature-induced deformations and forces, respectively, loadings history and consequences to the residual state. The initial phases of assessment including gathering information about fire event, object inspections, fire scenario approximation together with elements thermal analysis and structural diagnosis would be carried out analogically to Case 1 described above and therefore they are not described herein in full length.

It is assumed part of the structure was subjected to fire which could be described with ISO834 temperature-time curve. The fire situation lasted for 120 minutes after which it was extinguished by fire brigade while no structural elements suffered thermal shock. As a simplification the material deterioration at hot and residual state is incorporated according to EC2 [16] and fib 46 [28] recommendations.

### Structural Model and Inserted Loadings

The structural system consists of regular one-way RC floor slabs 250 mm thick and RC walls 250 mm thick as well. The span length is equal to 6 m while storey height is equal to 3,5 m. The structure is identical in all storeys but in 2<sup>nd</sup> and 3<sup>rd</sup> storey only two spans continue instead of four. During fire situation two spans of floor slab, one outer wall and two inner walls were directly exposed to high temperatures with no protection. Characteristic transverse section through the building in structural model made in commercial software Scia Engineer 20 [107] can be seen in Fig. A-8 below. Load cases for other dead loads and live loads were created, while self-weight was incorporated automatically by the software.

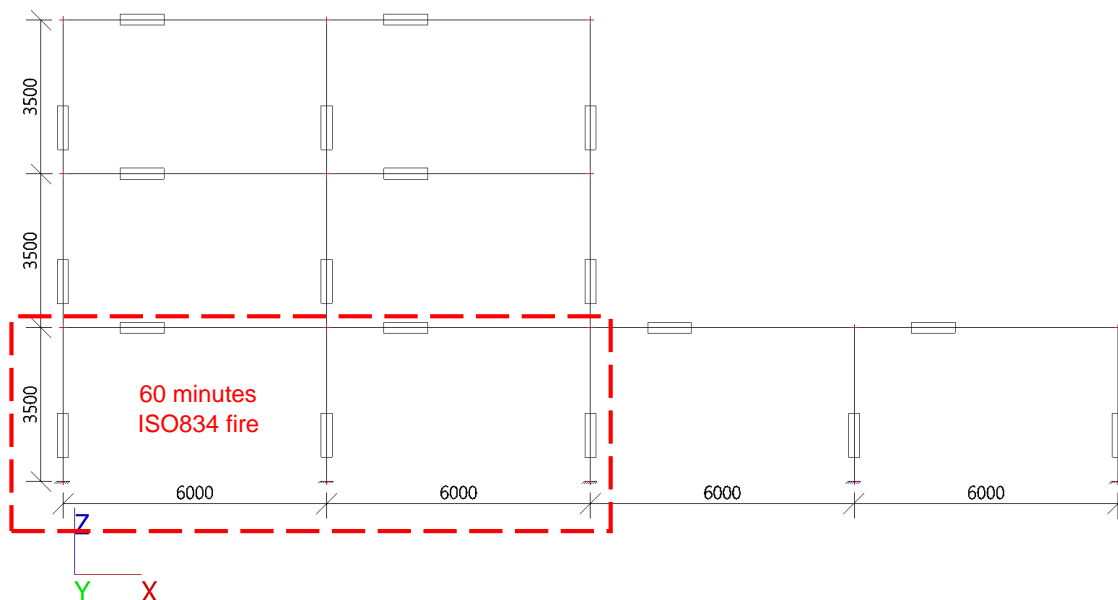


Fig. A-8. 2D structural model with highlighted part affected by fire.

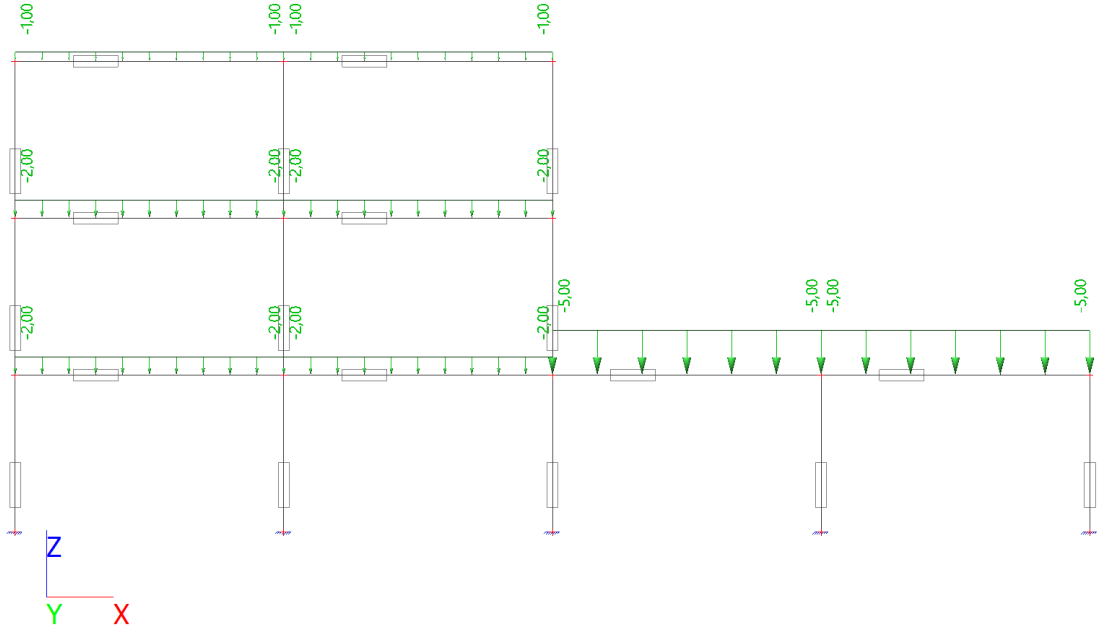


Fig. A-9. Other dead load incorporated in the calculations in [kN/m<sup>2</sup>].

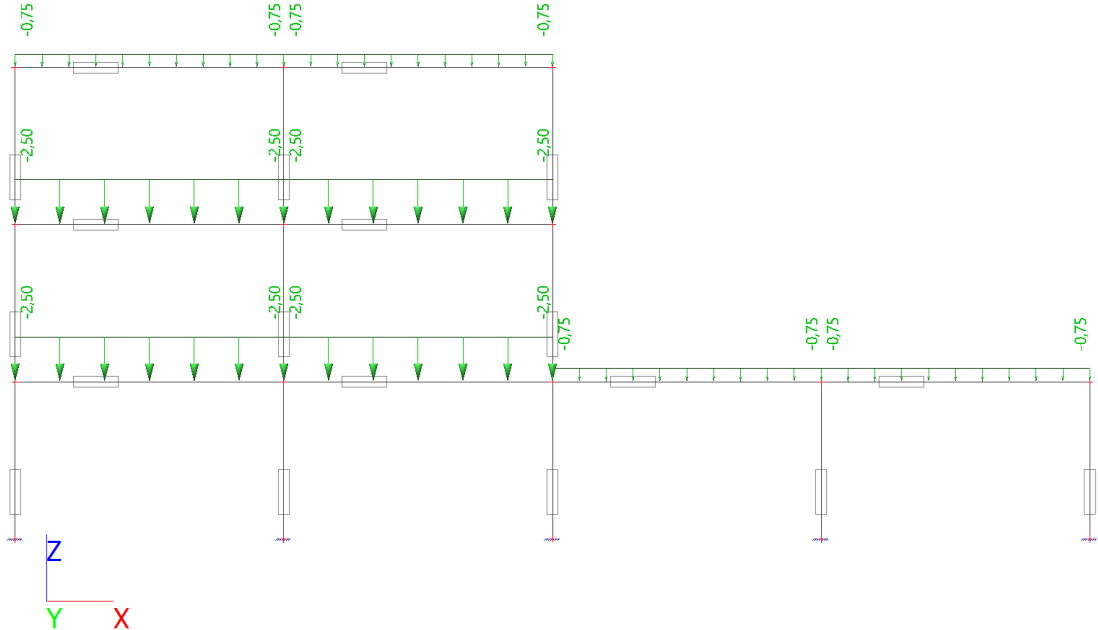


Fig. A-10. Live load incorporated in the calculations, categories B and H in [kN/m<sup>2</sup>].



### Calculation Results at Normal Temperatures

At first results of FEM calculations in the means of deflections and inner forces are given and then the assessments are carried out in commercial software FINE EC [56].

Hodnoty:  $U_{total}$

Lineární výpočet

Kombinace: MSP-Char (auto)

Výběr: Vše

Poloha: V uzlech s průměrováním.

System: Globální

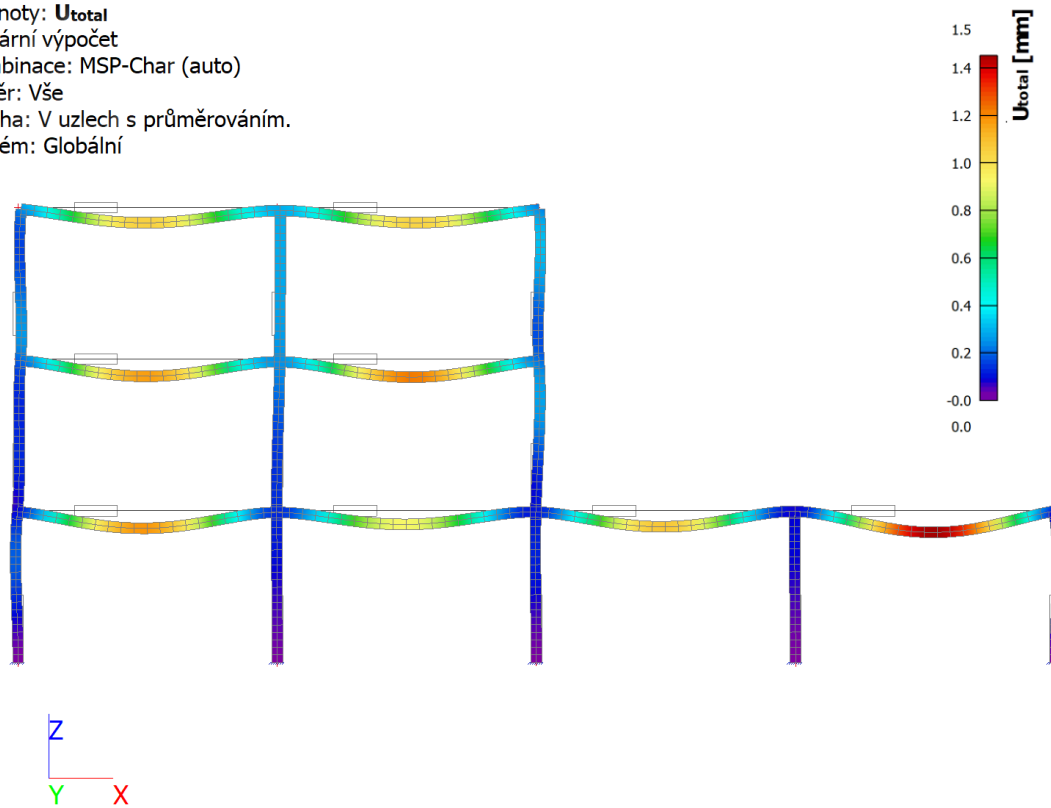


Fig. A-11. Linear elastic deflections at SLS in [mm].

Hodnoty:  $N$

Lineární výpočet

Kombinace: MSÚ-Sada B (auto)

Souřadný systém: Dílec

Extrém 1D: Lokální

Výběr: Vše

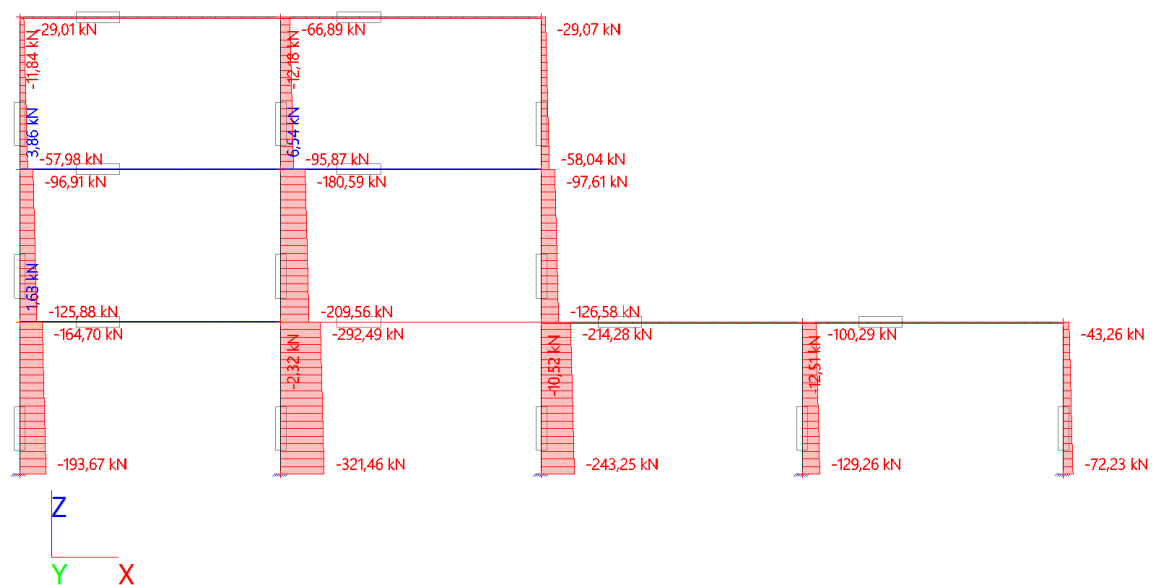


Fig. A-12. Axial forces at ULS in [kN].



Hodnoty:  $M_y$   
Lineární výpočet  
Kombinace: MSÚ-Sada B (auto)  
Souřadný systém: Dílec  
Extrém 1D: Lokální  
Výběr: Vše

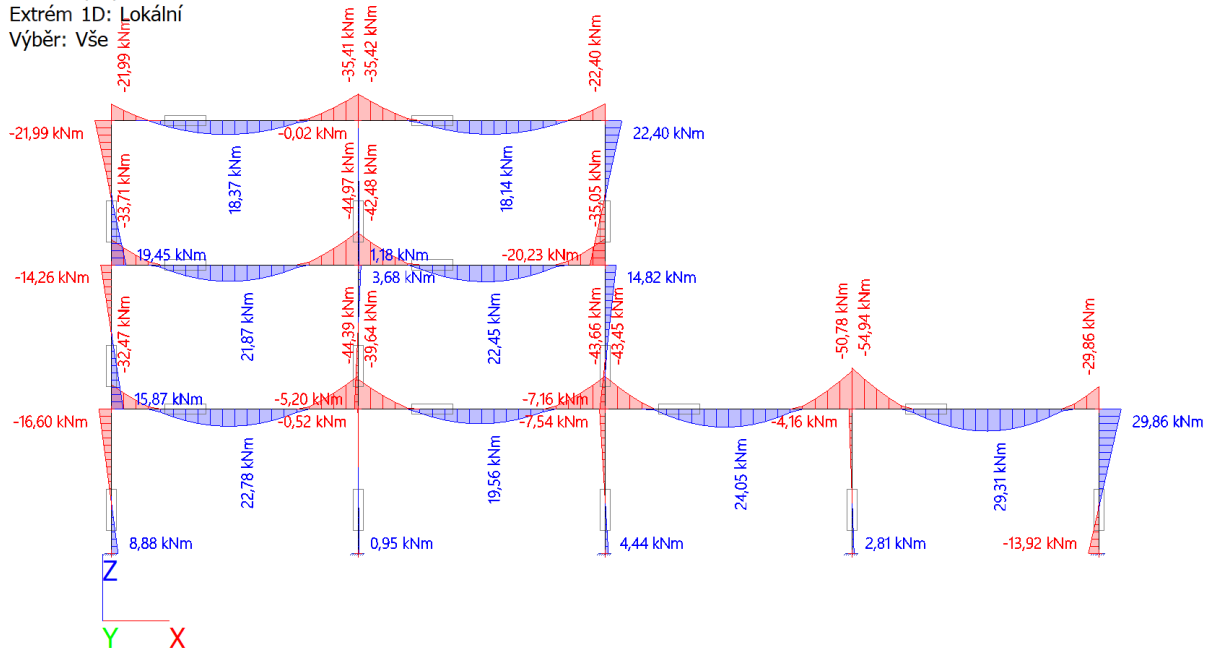


Fig. A-13. Bending moments at ULS in [kNm].

Hodnoty:  $V_z$   
Lineární výpočet  
Kombinace: MSÚ-Sada B (auto)  
Souřadný systém: Dílec  
Extrém 1D: Lokální  
Výběr: Vše

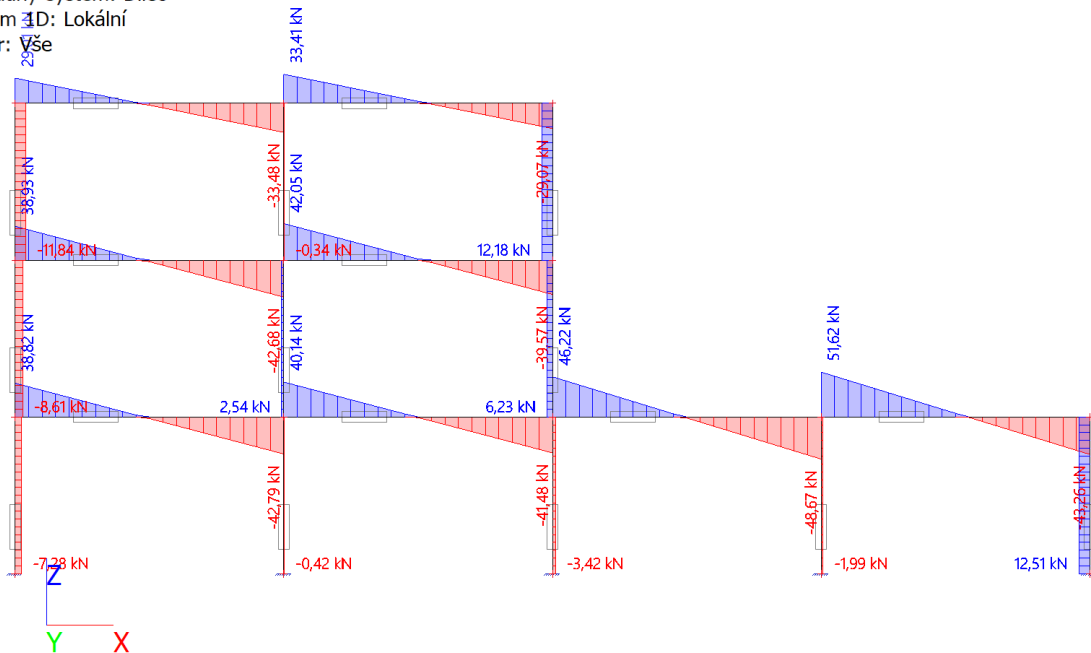


Fig. A-14. Shear forces at ULS in [kN].

Based on the linear elastic calculations of inner forces longitudinal reinforcement  $\varnothing 10/200\text{ mm}$  were designed as bottom reinforcement in all span length and  $\varnothing 12/150\text{ mm}$  were designed as top reinforcement in support cross-sections. The middle third of span length on top surface was reinforced with supplementary reinforcement  $\varnothing 8/150\text{ mm}$ . No shear reinforcement was designed. The walls were reinforced with vertical bars  $\varnothing 10/200\text{ mm}$  on both faces.



## Reinforcement Designs and Assessments at Normal Temperatures

**floor slab**

Typ prvku: deska  
Prostředí: XC1  
**Beton: C 25/30**  
 $f_{ck} = 25,0 \text{ MPa}$ ;  $f_{ctm} = 2,6 \text{ MPa}$ ;  $E_{cm} = 31000 \text{ MPa}$   
**Ocel podélná: B500B** ( $f_{yk} = 500,0 \text{ MPa}$ ;  $E_s = 200000 \text{ MPa}$ )  
**Ocel příčná: B500** ( $f_{yk} = 500,0 \text{ MPa}$ ;  $E_s = 200000 \text{ MPa}$ )  
**Vzpěr**  
Vzpěr není uvažován  
S tlačnou výztuží není počítáno.  
Průřez bez smykové výztuže.

**Posouzení mezního stavu únosnosti**

č.	Název	$N_{Ed}$ [kN]	$N_{Rd}$ [kN]	$M_{Edy}$ [kNm]	$M_{Rdy}$ [kNm]	$V_{Edz}$ [kN]	$V_{Rdz}$ [kN]	Využití [%]	Posouzení
1	Zat. případ 1	-0,68	-4166,67	-35,00	-72,24	35,26	106,02	48,4	Vyhovuje
2	Zat. případ 2	-1,60	-4166,67	-39,64	-72,33	40,14	106,15	54,8	Vyhovuje
3	Zat. případ 3	-1,60	-4166,67	19,56	40,72	-0,67	-106,24	48,0	Vyhovuje
4	Zat. případ 4	-1,60	-4166,67	-43,66	-72,33	-41,48	-106,15	60,4	Vyhovuje
5	Zat. případ 5	1,33	534,27	22,78	40,44	-1,99	-105,85	56,4	Vyhovuje
6	Zat. případ 6	1,33	534,27	-44,39	-72,05	-42,79	-105,76	61,6	Vyhovuje

**61,6 % VYHOVUJE**

**walls**

Typ prvku: stěna  
Prostředí: XC1  
**Beton: C 25/30**  
 $f_{ck} = 25,0 \text{ MPa}$ ;  $f_{ctm} = 2,6 \text{ MPa}$ ;  $E_{cm} = 31000 \text{ MPa}$   
**Ocel podélná: B500B** ( $f_{yk} = 500,0 \text{ MPa}$ ;  $E_s = 200000 \text{ MPa}$ )  
**Ocel příčná: B500B** ( $f_{yk} = 500,0 \text{ MPa}$ ;  $E_s = 200000 \text{ MPa}$ )  
**Vzpěr**  
Vzpěrná délka:  $l_{ef} = 3,50 \times 0,71 = 2,48 \text{ m}$   
S tlačnou výztuží je počítáno.  
Průřez bez smykové výztuže.

**Posouzení mezního stavu únosnosti**

č.	Název	$N_{Ed}$ [kN]	$N_{Rd}$ [kN]	$M_{Edy}$ [kNm]	$M_{Rdy}$ [kNm]	$V_{Edz}$ [kN]	$V_{Rdz}$ [kN]	Využití [%]	Posouzení
1	Zat. případ 1	-193,67	-4480,83	8,88 → 10,57	59,83	-7,28	-132,77	17,7	Vyhovuje
2	Zat. případ 2	-130,66	-4480,83	5,60 → 6,74	53,62	-4,54	-124,27	12,6	Vyhovuje
3	Zat. případ 3	-164,70	-4480,83	-16,60 → -18,04	-56,98	-7,28	-128,86	31,7	Vyhovuje
4	Zat. případ 4	-109,20	-4480,83	-10,28 → -11,24	-51,48	-4,54	-121,37	21,8	Vyhovuje
5	Zat. případ 5	-223,23	-4480,83	4,44 → 6,39	62,75	-3,42	-136,76	10,2	Vyhovuje
6	Zat. případ 6	-214,28	-4480,83	-6,22 → -8,09	-61,86	-2,85	-135,55	13,1	Vyhovuje
7	Zat. případ 7	-143,89	-4480,83	-5,59 → -6,85	-54,93	-2,54	-126,05	12,5	Vyhovuje
8	Zat. případ 8	-194,26	-4480,83	-7,54 → -9,24	-59,89	-3,42	-132,85	15,4	Vyhovuje

**31,7 % VYHOVUJE**

As can be seen the assessments at ordinary ULS are satisfactory in all cases.



### Calculation Results at Fire Design Situation

At first deflections and results of inner forces are showed in case of extraordinary design situation without incorporation of temperature-induced strains.

Hodnoty:  $U_{total}$   
Lineární výpočet  
Kombinace: MSÚ požár1  
Výběr: Vše  
Poloha: V uzlech s průměrováním.  
Systém: Globální

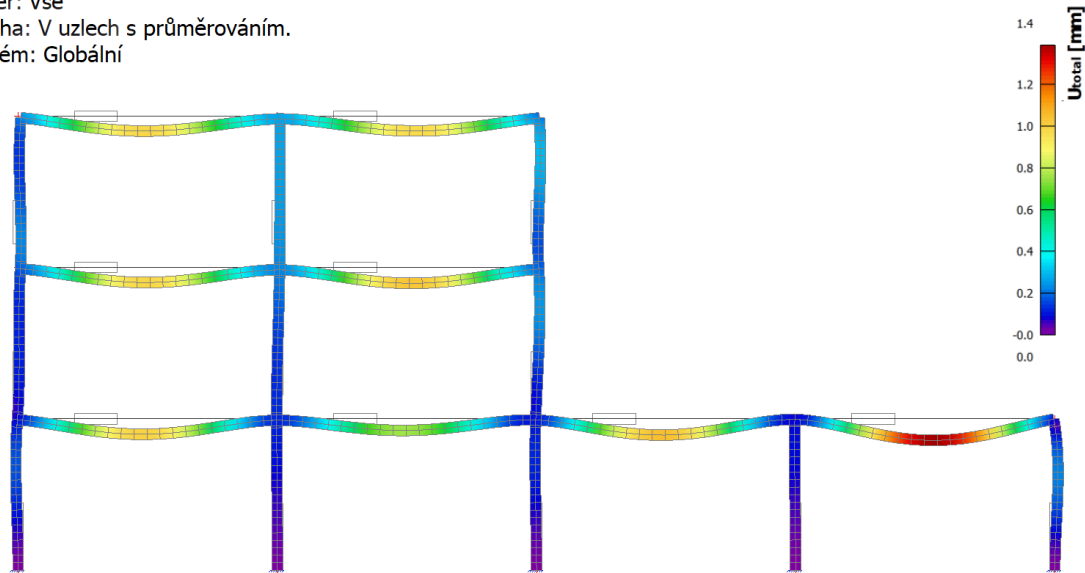


Fig. A-15. Linear elastic deflections at extraordinary ULS in [mm].

Hodnoty:  $N$   
Lineární výpočet  
Kombinace: MSÚ požár1  
Souřadný systém: Dílec  
Extrém 1D: Dílec  
Výběr: Vše

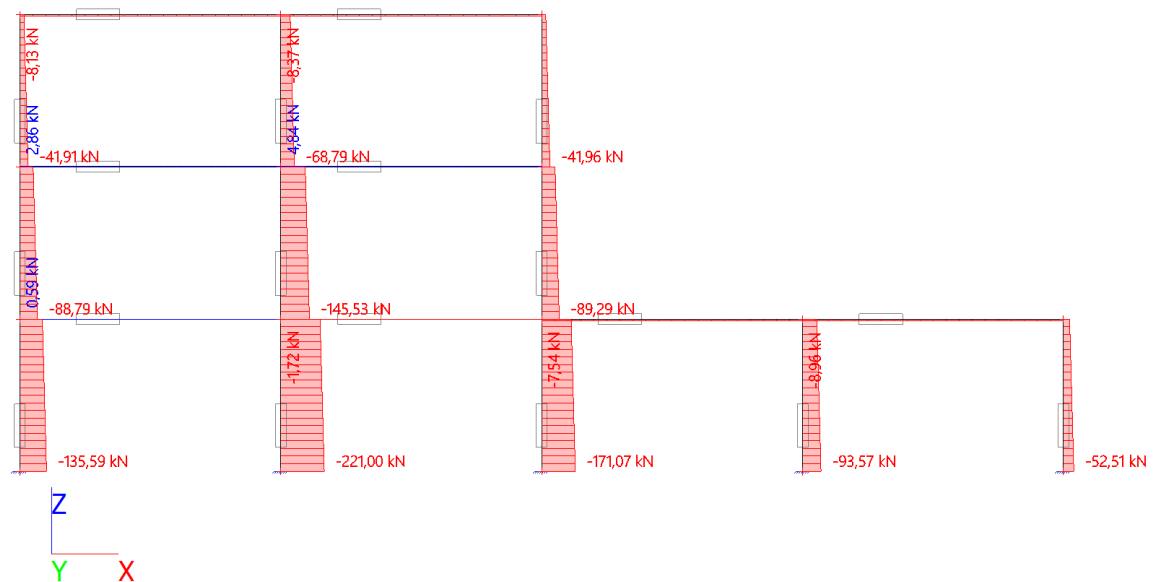


Fig. A-16. Axial forces at extraordinary ULS in [kN].





Hodnoty:  $M_y$   
Lineární výpočet  
Kombinace: MSÚ požár1  
Souřadný systém: Dílec  
Extrém 1D: Dílec  
Výběr: Vše

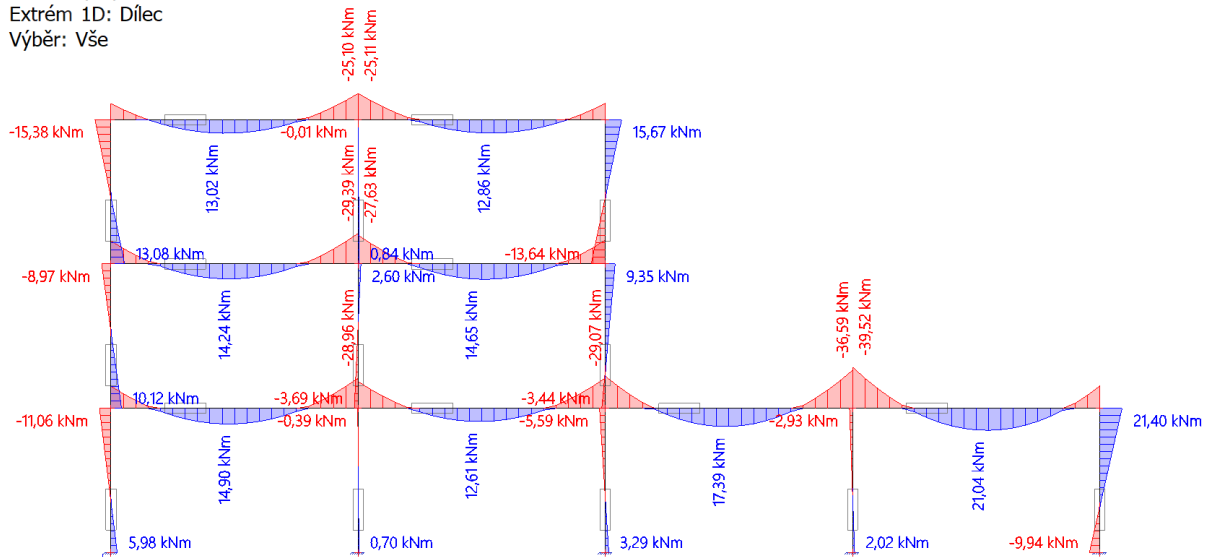


Fig. A-17. Bending moments at extraordinary ULS in [kNm].

Hodnoty:  $V_z$   
Lineární výpočet  
Kombinace: MSÚ požár1  
Souřadný systém: Dílec  
Extrém 1D: Dílec  
Výběr: Vše

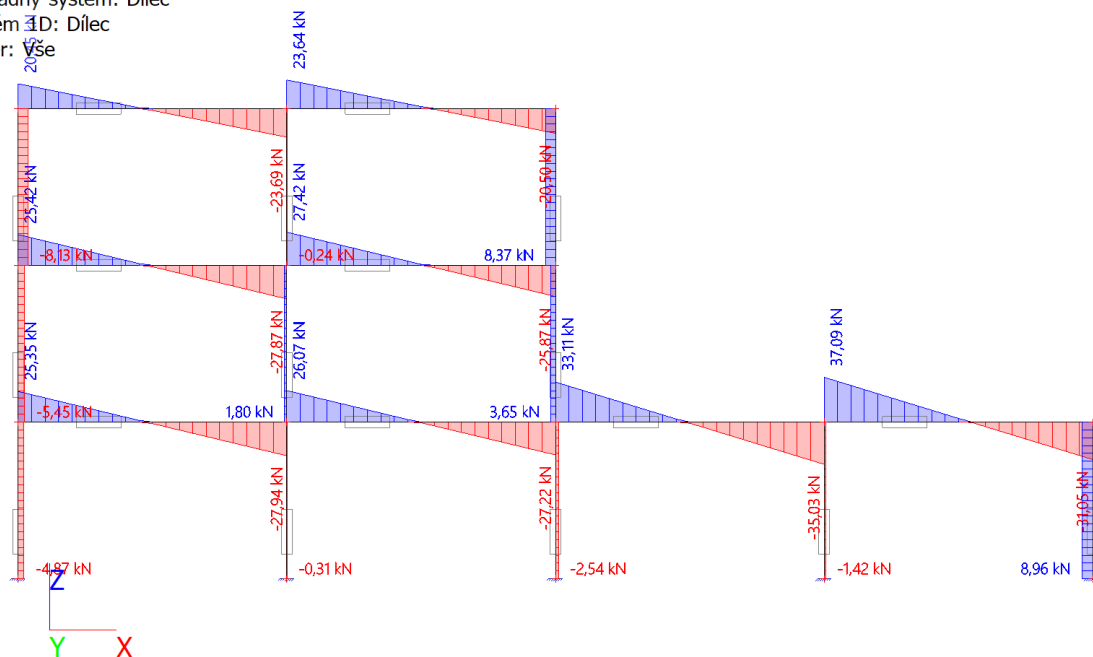


Fig. A-18. Shear forces at extraordinary ULS in [kN].

In order to incorporate thermal deformations, theoretical elongation and curvature have to be calculated in case of exposed elements. At the same time, level of their relaxation based on stiffness of the rest of the structure are estimated using *unit force and deflection method*, as can be seen below. The unit force is incorporated in horizontal direction at the ends of the scrutinised floor slab span, which is missing in the model (to exclude its axial stiffness). In case of walls it is assumed the level of longitudinal elongation relaxation is equal to 100 %, thus these elements do not elongate at all thanks to applied compressive stress prior to heating, see Chapter 2.5; thermal bowing caused by one-side heating is still valid in case of subjected walls.



Hodnoty:  $u_x$   
Lineární výpočet  
Zatěžovací stav: ZS2  
Souřadný systém: Globální  
Extrém 1D: Dílec  
Výběr: Vše

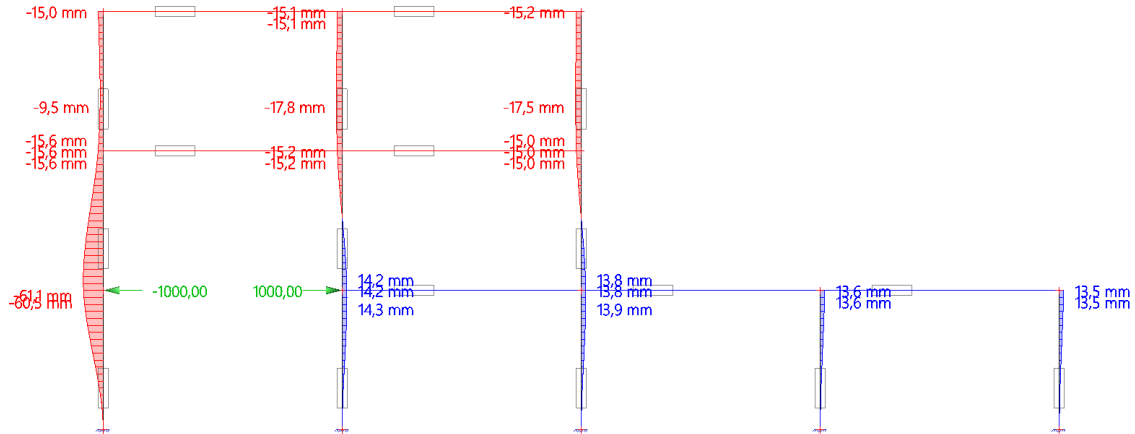


Fig. A-19. Estimation of stiffness coefficients based on deflections from unit forces – left span.

**Axial stiffness calculation if left floor slab elongates:**

$$K_{x,1} = \frac{F}{u_1} = \frac{1000 * 10^3}{61,1 * 10^{-3}} = 16,4 \text{ MN/m} \quad K_{x,2} = \frac{F}{u_2} = \frac{1000 * 10^3}{14,3 * 10^{-3}} = 71,4 \text{ MN/m}$$

Hodnoty:  $u_x$   
Lineární výpočet  
Zatěžovací stav: ZS2  
Souřadný systém: Globální  
Extrém 1D: Dílec  
Výběr: Vše

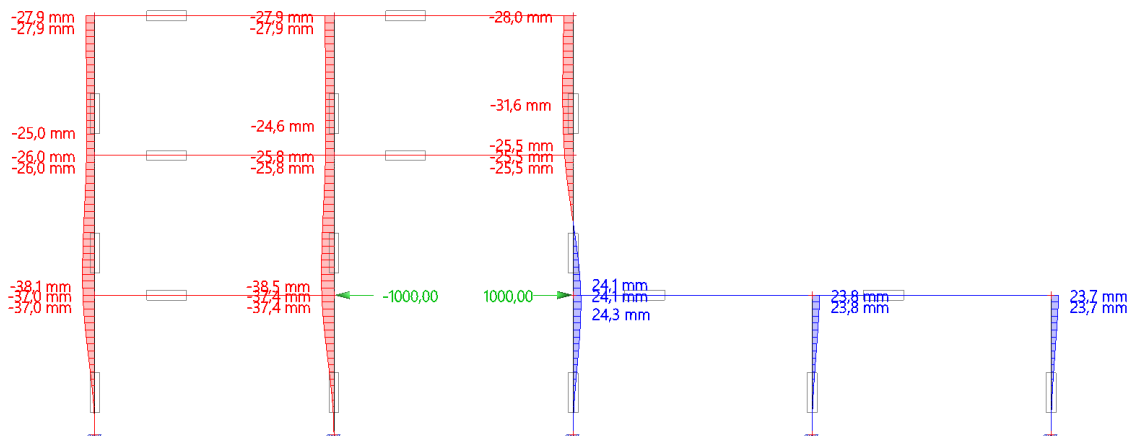


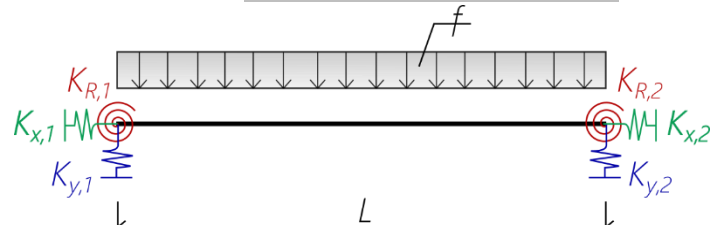
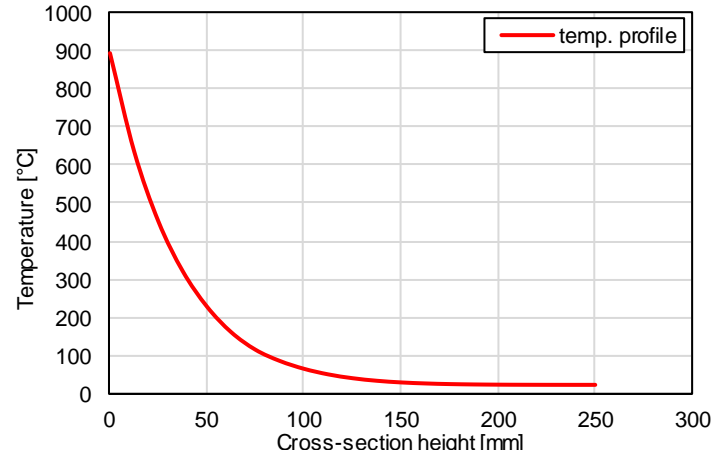
Fig. A-20. Estimation of stiffness coefficients based on deflections from unit forces – right span.

**Axial stiffness calculation if right floor slab elongates:**

$$K_{x,1} = \frac{F}{u_1} = \frac{1000 * 10^3}{38,5 * 10^{-3}} = 25,9 \text{ MN/m} \quad K_{x,2} = \frac{F}{u_2} = \frac{1000 * 10^3}{24,3 * 10^{-3}} = 41,2 \text{ MN/m}$$



Based on the calculation below effective mean change of temperature  $\Delta\theta_{eff}$  and longitudinal curvature  $(1/r)_{\theta}$  are estimated and inserted in the FEM software as additional loading in fire conditions. The calculation is always related to certain fire time. The thermal strains are checked in 60<sup>th</sup> minute of fire (when maximal thermal gradient can be expected) and then in 120<sup>th</sup> minute (when maximal elongation can be expected) representing the finish time of fire.

Thermal loadings calculation of RC element:	RC floor slab in fire conditions
<b>- cross-section dimensions</b>	
height $h =$ 250 mm	concrete strength $f_{ck} =$ 25,00 MPa
width $b =$ 1000 mm	concrete Young's modulus $E_{cm} =$ 31,48 GPa
length $L =$ 6,00 m	thermal elongation coeff. $\alpha_T =$ 1,00E-05 [-]
$I_y =$ 1,30E+09 mm <sup>4</sup>	initial temperature $t_0 =$ 20 °C
$a_{500} =$ 20 mm	fire duration $T =$ 60 min
<b>- static scheme</b>	
element in: in bending	axial stiffnesses
static scheme: edge span of continuous beam	$K_{x,1} =$ 16,4 MN/m
	$K_{x,2} =$ 71,4 MN/m
	resulting axial stiffness $K_x =$ 13,34 MN/m
	basic stiffness $EA/L =$ 1311,49 MN/m
	multiplier of basic stiffness $\alpha =$ 0,01 [-]
	stiffness coefficients $a_1 =$ 0,25 [-]
	$a_2 =$ 0,00 [-]
	$a_3 =$ 1,00 [-]
	relative decay of bending stiff. $EI_{red}/EI =$ 0,78 [-]
	ratio of additional $M^-$ $a_M =$ 1,00 [-]
	
<b>- deformations and inner forces</b>	
$\Delta L_{\theta, free} =$ 12,63 mm	...free elongation assuming $EA=0$
$N_{\theta, total} =$ -3953,96 kN	...theoretical axial force assuming $EA=infinity$
$M_{\theta, total} =$ -308,73 kNm	...theoretical bending moment assuming $EI=infinity$
$e_{\theta} =$ 78,08 mm	...resulting axial force eccentricity causing $M_{\theta, total}$
$\Delta L_{\theta, relax} =$ 9,46 mm	...total thermal elongation assuming LITS relax. and actual EA
$\Delta\theta_{eff} =$ 157,72 °C	...effective temperature change corresponding to $\Delta L_{\theta, relax}$
$M_{\theta, relax} =$ -60,16 kNm	...bending moment after LITS relax. and assuming actual EI
$(1/r)_{\theta} =$ 1,47 mrad/m	...effective curvature corresponding to $M_{\theta, relax}$



Thermal loadings calculation of RC element:		RC floor slab in fire conditions	
<b>- cross-section dimensions</b>			
height h =	250 mm	concrete strength	$f_{ck} = 25,00$ MPa
width b =	1000 mm	concrete Young's modulus	$E_{cm} = 31,48$ GPa
length L =	6,00 m	thermal elongation coeff.	$\alpha_T = 1,00E-05$ [-]
$I_y =$	$1,30E+09$ mm <sup>4</sup>	initial temperature	$t_0 = 20$ °C
$a_{500} =$	20 mm	fire duration	$T = 60$ min
<b>- static scheme</b>			
element in:	in bending	axial stiffnesses	
static scheme:	edge span of continuous beam	$K_{x,1} = 16,4$ MN/m	
		$K_{x,2} = 71,4$ MN/m	
		resulting axial stiffness	$K_x = 13,34$ MN/m
		basic stiffness	$EA/L = 1311,49$ MN/m
		multiplier of basic stiffness	$\alpha = 0,01$ [-]
		stiffness coefficients	
		$a_1 = 0,25$ [-]	
		$a_2 = 0,00$ [-]	
		$a_3 = 1,00$ [-]	
		relative decay of bending stiff.	$EI_{red}/EI = 0,78$ [-]
		ratio of additional M <sup>-</sup>	
		$a_M = 1,00$ [-]	
<b>- deformations and inner forces</b>			
$\Delta L_{\theta, free} =$	17,49 mm	...free elongation assuming $EA=0$	
$N_{\theta, total} =$	-5306,04 kN	...theoretical axial force assuming $EA=infinity$	
$M_{\theta, total} =$	-301,33 kNm	...theoretical bending moment assuming $EI=infinity$	
$e_{\theta} =$	56,79 mm	...resulting axial force eccentricity causing $M_{\theta, total}$	
$\Delta L_{\theta, relax} =$	13,11 mm	...total thermal elongation assuming LITS relax. and actual EA	
$\Delta \theta_{eff} =$	218,42 °C	...effective temperature change corresponding to $\Delta L_{\theta, relax}$	
$M_{\theta, relax} =$	-58,72 kNm	...bending moment after LITS relax. and assuming actual EI	
$(1/r)_{\theta} =$	1,43 mrad/m	...effective curvature corresponding to $M_{\theta, relax}$	

Only calculation of thermal strains attributed to floor slabs are shown. In case of walls heated from one side only, the bowing effect remains the same as the cross-section thicknesses are equal while the elongation effect is considered to be relaxed from 100 %. In case of wall heated from both sides the thermal bowing does not take place thanks to symmetry and the elongation is considered to be mitigated as well.

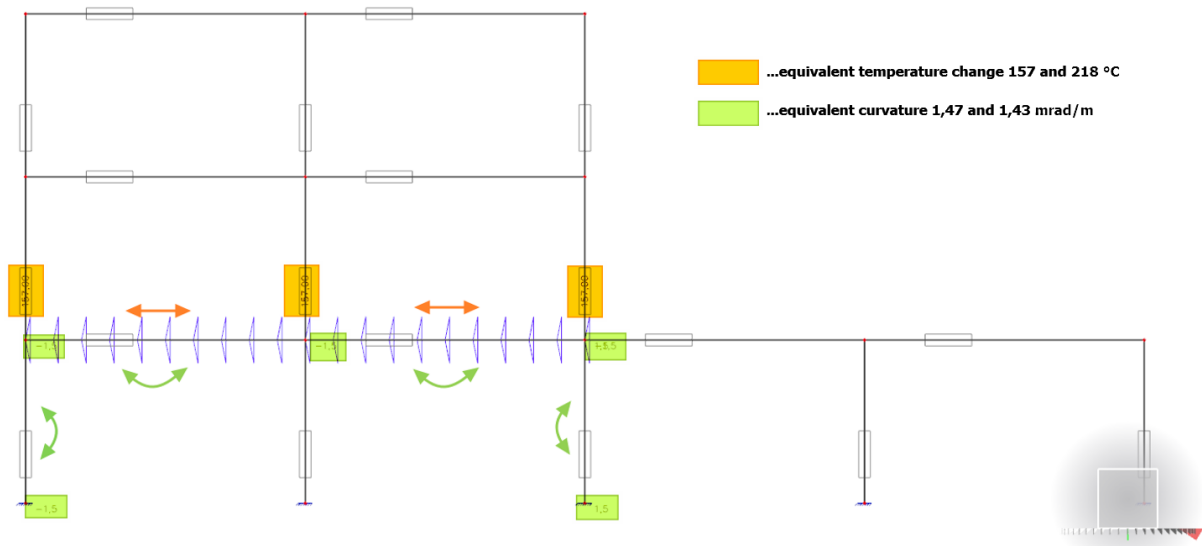


Fig. A-21. Incorporation of thermal strains into structural model as external loading.

Now deformations and inner forces with accounted thermal strains in 60<sup>th</sup> minute of fire are given. Afterwards assessment of load-bearing capacity in the same time are conducted using isotherm 500 °C method.

Hodnoty:  $U_{total}$   
Lineární výpočet  
Kombinace: MSÚ požár2  
Výběr: Vše  
Poloha: V uzlech s průměrováním.  
Systém: Globální

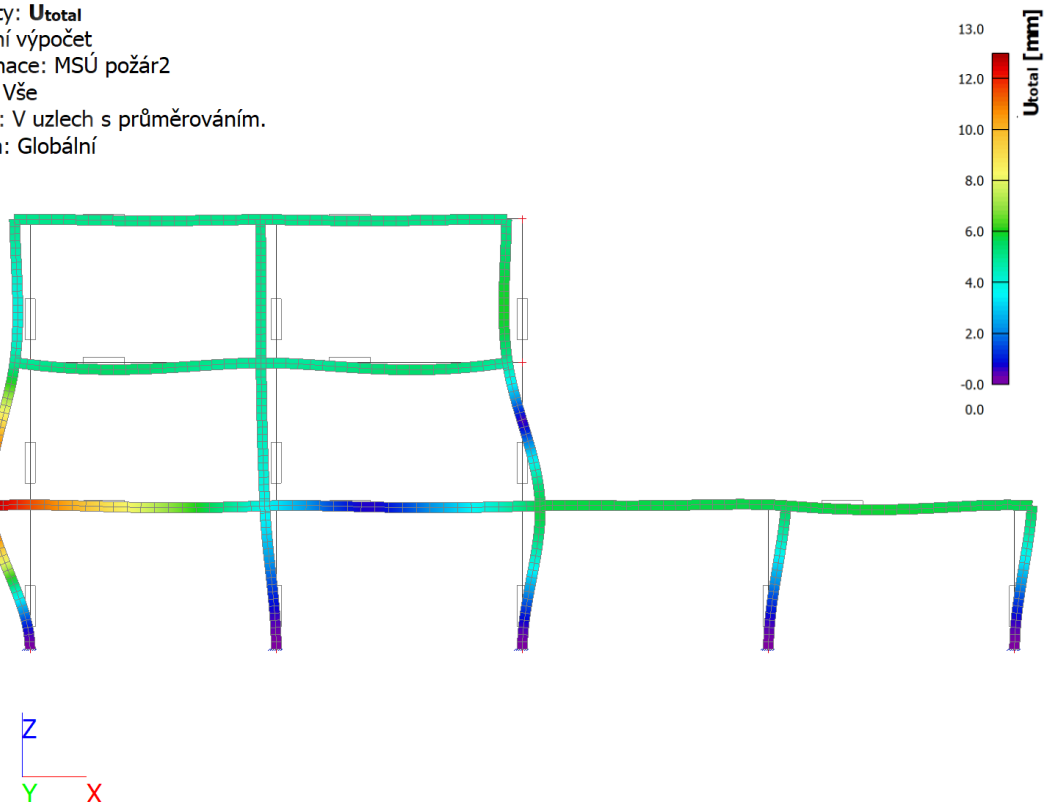


Fig. A-22. Linear elastic deflections at extraordinary ULS in 60<sup>th</sup> minute of fire in [mm].



Hodnoty: **N**  
Lineární výpočet  
Kombinace: MSÚ požár2  
Souřadný systém: Dílec  
Extrém 1D: Dílec  
Výběr: Vše

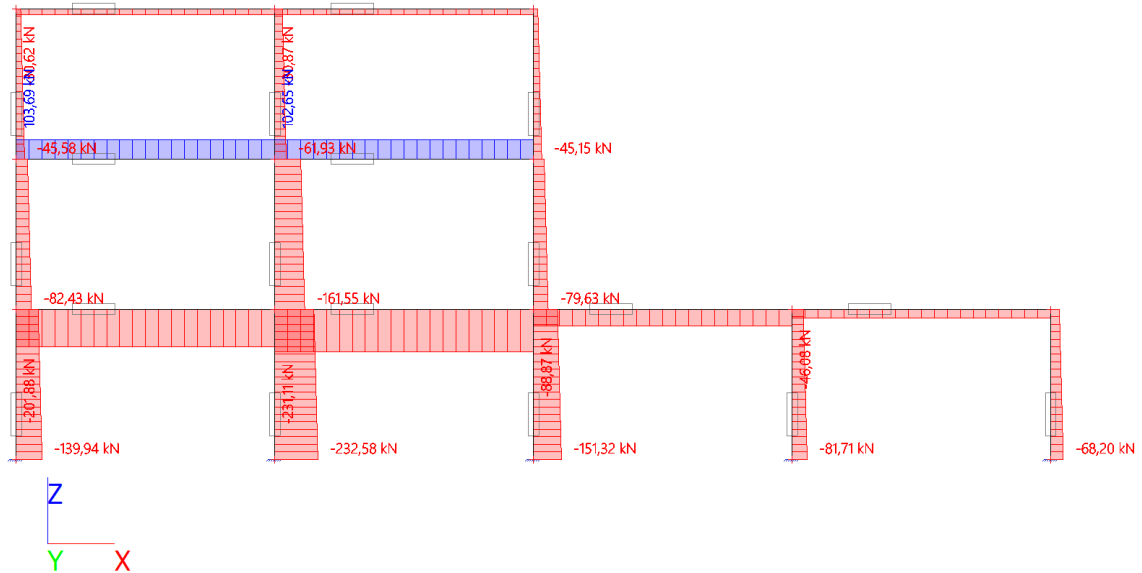


Fig. A-23. Axial forces at extraordinary ULS in 60<sup>th</sup> minute of fire in [kN].

Hodnoty: **M<sub>y</sub>**  
Lineární výpočet  
Kombinace: MSÚ požár2  
Souřadný systém: Dílec  
Extrém 1D: Lokální  
Výběr: Vše

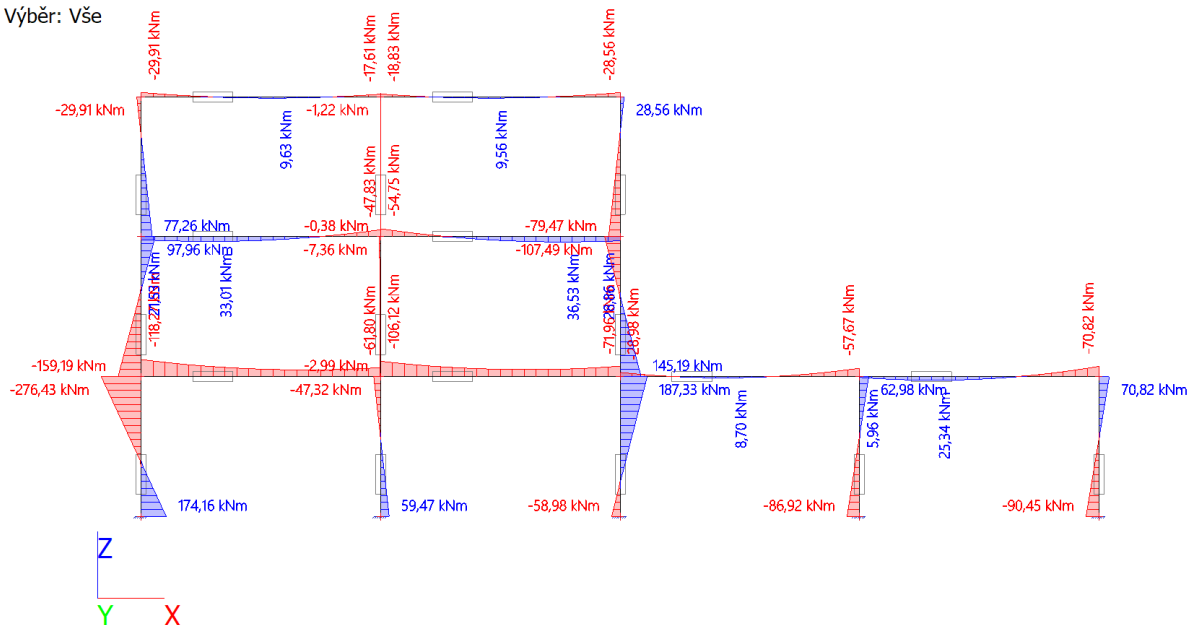


Fig. A-24. Bending moments at extraordinary ULS in 60<sup>th</sup> minute of fire in [kNm].





Hodnoty:  $V_z$   
Lineární výpočet  
Kombinace: MSÚ požár2  
Souřadný systém: Dílec  
Extrém 1D: Lokální  
Výběr: Vše

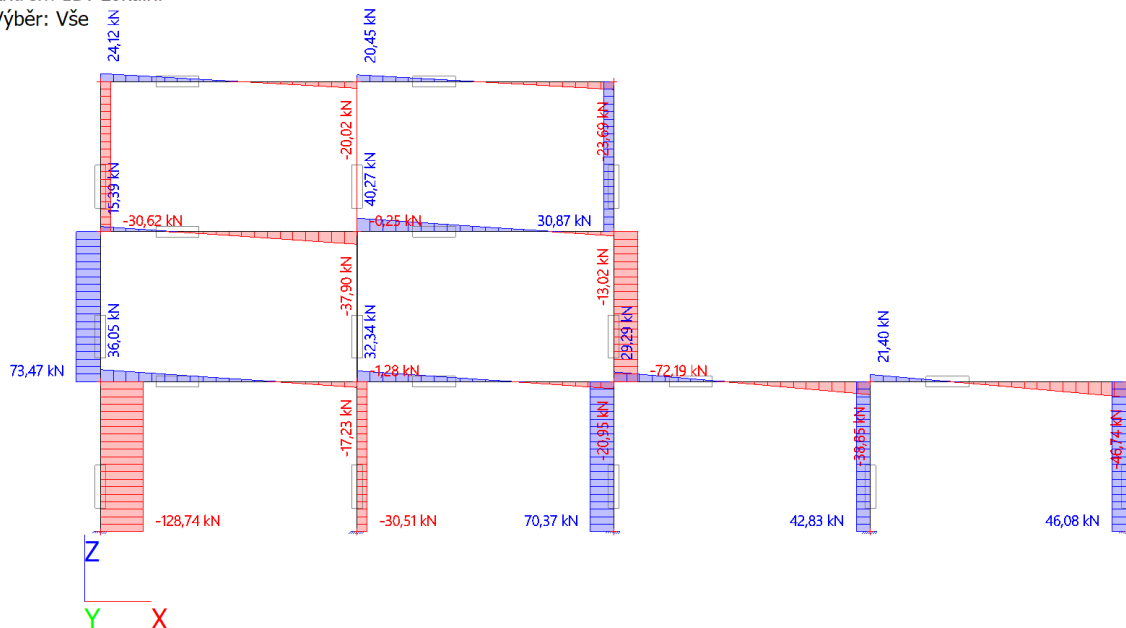


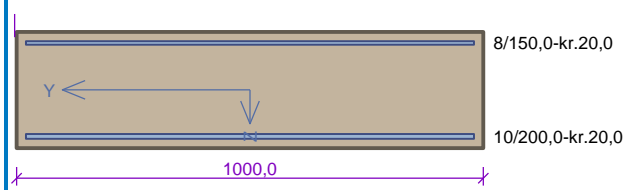
Fig. A-25. Shear forces at extraordinary ULS in 60<sup>th</sup> minute of fire in [kN].

Assessment of load-bearing capacity in 60<sup>th</sup> minute of fire duration with incorporated thermal strains:

floor slab-support CS_R60								
				Typ prvku: deska Prostedí: XC1 <b>Beton: C 25/30</b> $f_{ck} = 25,0$ MPa; $f_{ctm} = 2,6$ MPa; $E_{cm} = 31000$ MPa <b>Ocel podélná: B500B</b> ( $f_{yk} = 500,0$ MPa; $E_s = 200000$ MPa) <b>Ocel příčná: B500</b> ( $f_{yk} = 500,0$ MPa; $E_s = 200000$ MPa) <b>Vzpěr</b> Vzpěr není uvažován				
Posouzení v čase požadované požární odolnosti $t = 60,0$ min Metoda izotermu 500 °C								
Posouzení mezního stavu únosnosti								
č.	Název	$N_{Ed}$ $N_{Rd}$ [kN]	$M_{Edy}$ $M_{Rdy}$ [kNm]	$M_{Edz}$ $M_{Rdz}$ [kNm]	$V_{Edz}$ $V_{Rdz}$ [kN]	$V_{Edy}$ $V_{Rdy}$ [kN]	Využití [%]	Posouzení
1	Zat. případ 1	-231,11	-103,78 → -107,25	0,00	30,04	0,00	108,2	Nevyhovuje
		-6114,32	-99,05	0,00	182,61	0,00		
2	Zat. případ 2	-230,90	-106,12 → -109,58	0,00	32,34	0,00	110,6	Nevyhovuje
		-6114,32	-99,03	0,00	182,59	0,00		
3	Zat. případ 3	-201,88	-116,46 → -119,49	0,00	33,91	0,00	123,7	Nevyhovuje
		-6114,32	-96,47	0,00	178,77	0,00		
4	Zat. případ 4	-201,63	-118,27 → -121,29	0,00	36,05	0,00	125,6	Nevyhovuje
		-6114,32	-96,45	0,00	178,73	0,00		
<b>125,6 % NEVYHOVUJE</b>								



### floor slab-span CS\_R60



Typ prvku: deska  
Prostředí: XC1

**Beton: C 25/30**

$f_{ck} = 25,0$  MPa;  $f_{ctm} = 2,6$  MPa;  $E_{cm} = 31000$  MPa

**Ocel podélná: B500B** ( $f_{yk} = 500,0$  MPa;  $E_s = 200000$  MPa)

**Ocel příčná: B500** ( $f_{yk} = 500,0$  MPa;  $E_s = 200000$  MPa)

**Vzpěr**

Vzpěr není uvažován

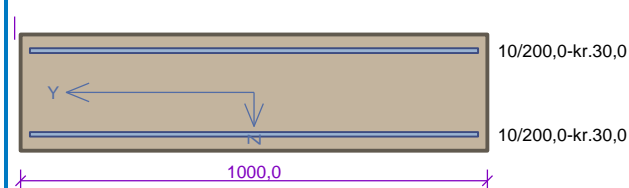
Posouzení v čase požadované požární odolnosti  $t = 60,0$  min  
Metoda izotermie  $500$  °C

#### Posouzení mezního stavu únosnosti

č.	Název	$N_{Ed}$ $N_{Rd}$ [kN]	$M_{Edy}$ $M_{Rdy}$ [kNm]	$M_{Edz}$ $M_{Rdz}$ [kNm]	$V_{Edz}$ $V_{Rdz}$ [kN]	$V_{Edy}$ $V_{Rdy}$ [kN]	Využití [%]	Posouzení
1	Zat. případ 1	-202,00	-54,00 → -57,03	0,00	0,00	0,00	98,6	Vyhovuje
		-5942,51	-57,85	0,00	0,00	0,00		
2	Zat. případ 2	-231,00	-52,00 → -55,46	0,00	0,00	0,00	91,1	Vyhovuje
		-5942,51	-60,92	0,00	0,00	0,00		

**98,6 % VYHOVUJE**

### outer wall\_R60



Typ prvku: stěna  
Prostředí: XC1

**Beton: C 25/30**

$f_{ck} = 25,0$  MPa;  $f_{ctm} = 2,6$  MPa;  $E_{cm} = 31000$  MPa

**Ocel podélná: B500B** ( $f_{yk} = 500,0$  MPa;  $E_s = 200000$  MPa)

**Ocel příčná: B500** ( $f_{yk} = 500,0$  MPa;  $E_s = 200000$  MPa)

**Vzpěr**

Vzpěrná délka:  $l_{ef,y} = 3,50 \times 0,50 = 1,75$  m

Posouzení v čase požadované požární odolnosti  $t = 60,0$  min  
Metoda izotermie  $500$  °C

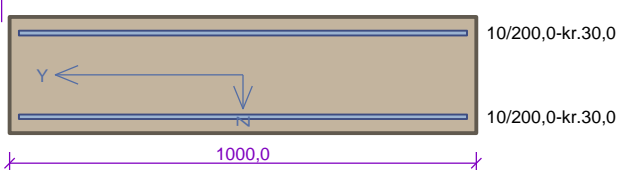
#### Posouzení mezního stavu únosnosti

č.	Název	$N_{Ed}$ $N_{Rd}$ [kN]	$M_{Edy}$ $M_{Rdy}$ [kNm]	$M_{Edz}$ $M_{Rdz}$ [kNm]	$V_{Edz}$ $V_{Rdz}$ [kN]	$V_{Edy}$ $V_{Rdy}$ [kN]	Využití [%]	Posouzení
1	Zat. případ 1	<b>-139,94</b>	<b>174,16 → 175,38</b>	<b>0,00</b>	-128,74	0,00	297,0	Nevyhovuje
		-5984,30	59,06	0,00	-145,89	0,00		
2	Zat. případ 2	<b>-135,00</b>	<b>173,78 → 174,96</b>	<b>0,00</b>	-128,41	0,00	297,9	Nevyhovuje
		-5984,30	58,73	0,00	-145,19	0,00		
3	Zat. případ 3	<b>-118,48</b>	<b>-276,43 → -277,47</b>	<b>0,00</b>	-128,74	0,00	> 300	Nevyhovuje
		-5984,30	-51,75	0,00	-134,69	0,00		
4	Zat. případ 4	<b>-113,54</b>	<b>-275,65 → -276,64</b>	<b>0,00</b>	-128,41	0,00	> 300	Nevyhovuje
		-5984,30	-51,26	0,00	-134,06	0,00		

**300,0 % NEVYHOVUJE**



**inner wall-two sides\_R60**



Typ prvku: stěna  
Prostředí: XC1  
**Beton: C 25/30**  
 $f_{ck} = 25,0 \text{ MPa}$ ;  $f_{ctm} = 2,6 \text{ MPa}$ ;  $E_{cm} = 31000 \text{ MPa}$   
**Ocel podélná: B500B** ( $f_{yk} = 500,0 \text{ MPa}$ ;  $E_s = 200000 \text{ MPa}$ )  
**Ocel příčná: B500** ( $f_{yk} = 500,0 \text{ MPa}$ ;  $E_s = 200000 \text{ MPa}$ )  
**Vzpěr**  
Vzpěrná délka:  $l_{ef,y} = 3,50 \times 0,50 = 1,75 \text{ m}$

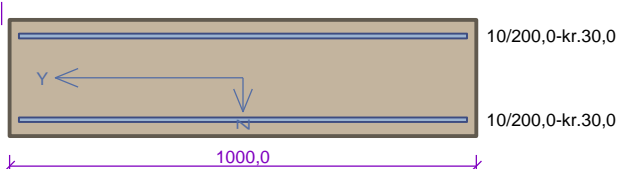
**Posouzení v čase požadované požární odolnosti  $t = 60,0 \text{ min}$**   
Metoda izotermie  $500 \text{ °C}$

**Posouzení mezního stavu únosnosti**

č.	Název	$N_{Ed}$ $N_{Rd}$ [kN]	$M_{Edy}$ $M_{Rdy}$ [kNm]	$M_{Edz}$ $M_{Rdz}$ [kNm]	$V_{Edz}$ $V_{Rdz}$ [kN]	$V_{Edy}$ $V_{Rdy}$ [kN]	Využití [%]	Posouzení
1	Zat. případ 1	<b>-232,58</b>	<b>59,45 → 61,49</b>	<b>0,00</b>	-30,50	0,00	106,7	Nevyhovuje
		-5403,97	57,61	0,00	-152,27	0,00		
2	Zat. případ 2	<b>-221,83</b>	<b>59,47 → 61,41</b>	<b>0,00</b>	-30,51	0,00	108,0	Nevyhovuje
		-5403,97	56,88	0,00	-150,76	0,00		
3	Zat. případ 3	-211,12	-47,31 → -49,16	0,00	-30,50	0,00	87,5	Vyhovuje
		-5403,97	-56,15	0,00	-149,26	0,00		

**108,0 % NEVYHOVUJE**

**inner wall-one side\_R60**



Typ prvku: stěna  
Prostředí: XC1  
**Beton: C 25/30**  
 $f_{ck} = 25,0 \text{ MPa}$ ;  $f_{ctm} = 2,6 \text{ MPa}$ ;  $E_{cm} = 31000 \text{ MPa}$   
**Ocel podélná: B500B** ( $f_{yk} = 500,0 \text{ MPa}$ ;  $E_s = 200000 \text{ MPa}$ )  
**Ocel příčná: B500** ( $f_{yk} = 500,0 \text{ MPa}$ ;  $E_s = 200000 \text{ MPa}$ )  
**Vzpěr**  
Vzpěrná délka:  $l_{ef,y} = 3,50 \times 0,50 = 1,75 \text{ m}$

**Posouzení v čase požadované požární odolnosti  $t = 60,0 \text{ min}$**   
Metoda izotermie  $500 \text{ °C}$

**Posouzení mezního stavu únosnosti**

č.	Název	$N_{Ed}$ $N_{Rd}$ [kN]	$M_{Edy}$ $M_{Rdy}$ [kNm]	$M_{Edz}$ $M_{Rdz}$ [kNm]	$V_{Edz}$ $V_{Rdz}$ [kN]	$V_{Edy}$ $V_{Rdy}$ [kN]	Využití [%]	Posouzení
1	Zat. případ 1	<b>-151,32</b>	<b>-58,98 → -60,30</b>	<b>0,00</b>	70,37	0,00	109,9	Nevyhovuje
		-5984,30	-54,89	0,00	138,86	0,00		
2	Zat. případ 2	<b>-145,60</b>	<b>-58,79 → -60,06</b>	<b>0,00</b>	70,21	0,00	110,5	Nevyhovuje
		-5984,30	-54,35	0,00	138,13	0,00		
3	Zat. případ 3	<b>-129,87</b>	<b>187,33 → 188,47</b>	<b>0,00</b>	70,37	0,00	> 300	Nevyhovuje
		-5984,30	58,40	0,00	144,47	0,00		

**300,0 % NEVYHOVUJE**



Deformations and inner forces with accounted thermal strains in 120<sup>th</sup> minute of fire are given as well. Afterwards assessment of load-bearing capacity in the same time are conducted using isotherm 500 °C method.

Hodnoty: **U<sub>total</sub>**  
Lineární výpočet  
Kombinace: MSÚ požár3  
Výběr: Vše  
Poloha: V uzlech s průměrováním.  
Systém: Globální

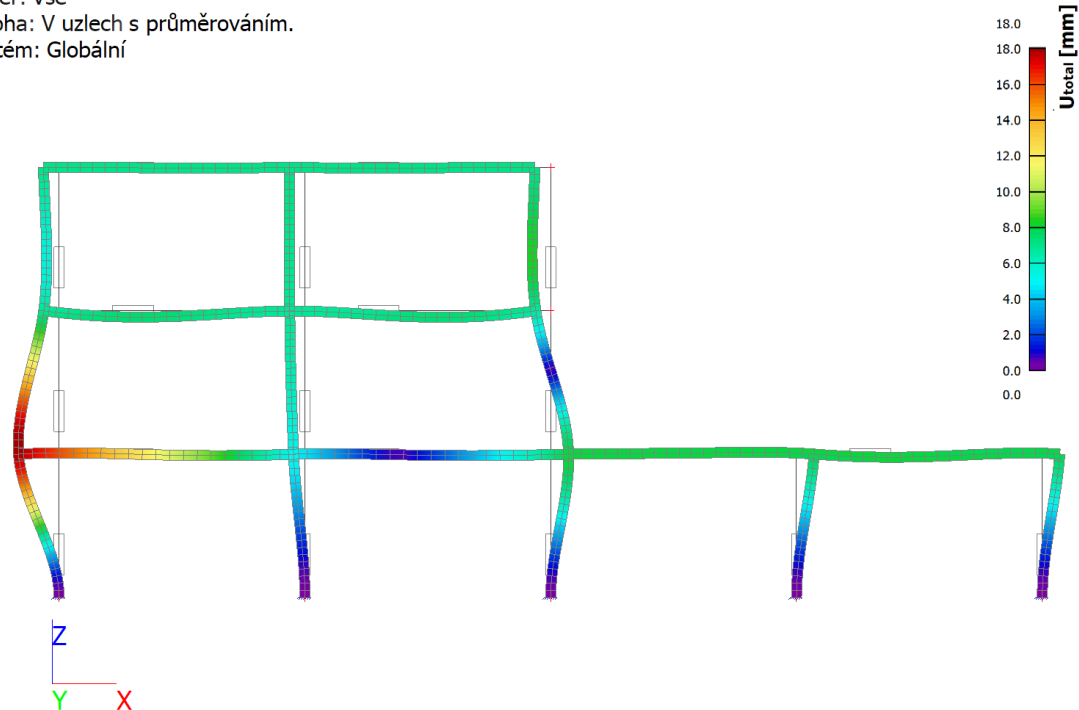


Fig. A-26. Linear elastic deflections at extraordinary ULS in 120<sup>th</sup> minute of fire in [mm].

Hodnoty: **N**  
Lineární výpočet  
Kombinace: MSÚ požár3  
Souřadný systém: Dílec  
Extrém 1D: Lokální  
Výběr: Vše

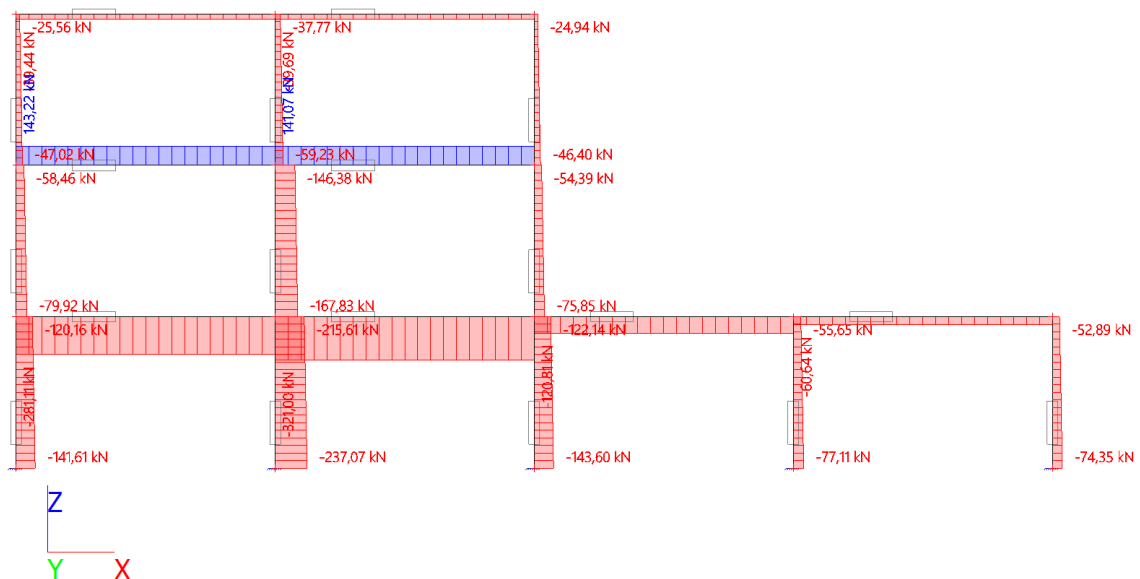


Fig. A-27. Axial forces at extraordinary ULS in 120<sup>th</sup> minute of fire in [kN].



Hodnoty:  $M_y$   
 Lineární výpočet  
 Kombinace: MSÚ požár3  
 Souřadný systém: Dílec  
 Extrém 1D: Lokální  
 Výběr: Vše

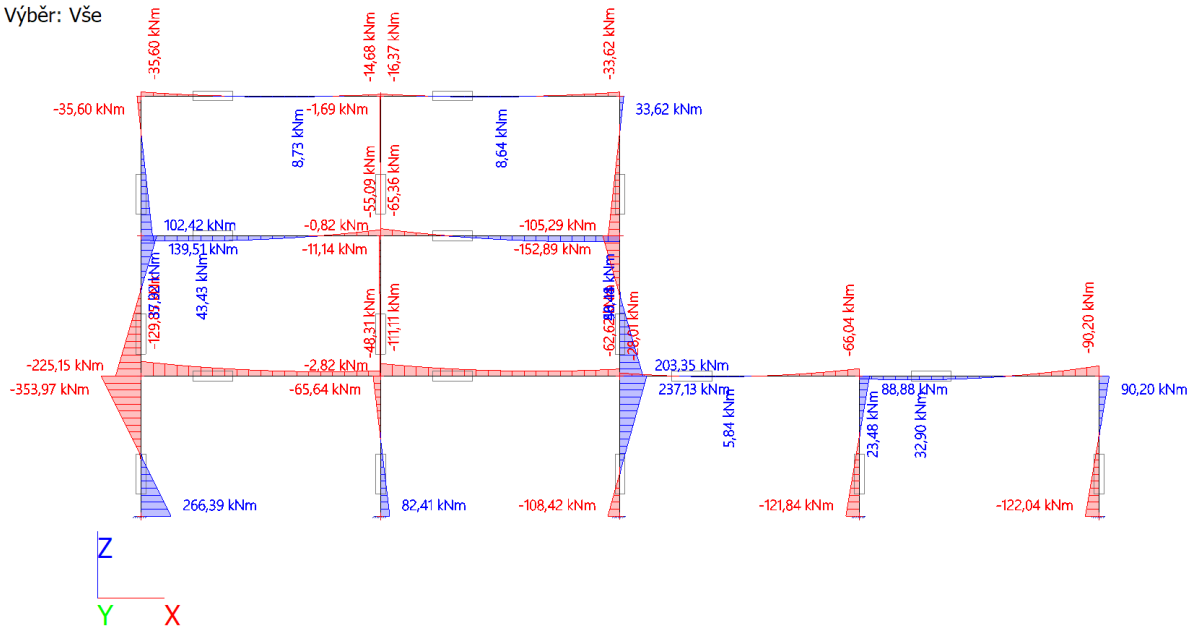


Fig. A-28. Bending moments at extraordinary ULS in 120<sup>th</sup> minute of fire in [kNm].

Hodnoty:  $V_z$   
 Lineární výpočet  
 Kombinace: MSÚ požár3  
 Souřadný systém: Dílec  
 Extrém 1D: Lokální  
 Výběr: Vše

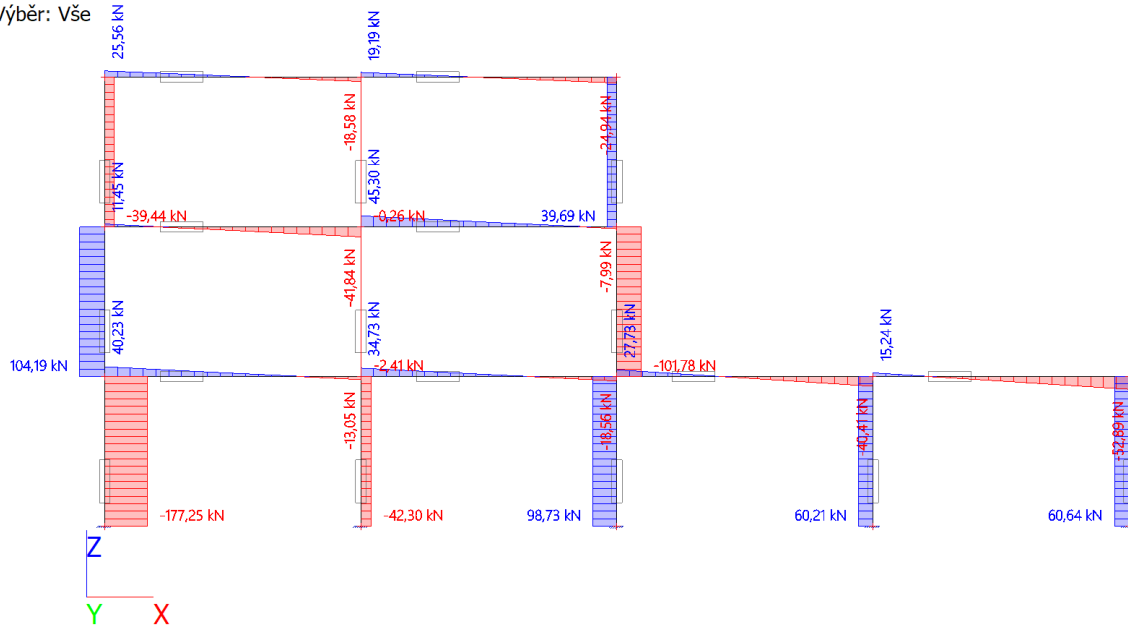
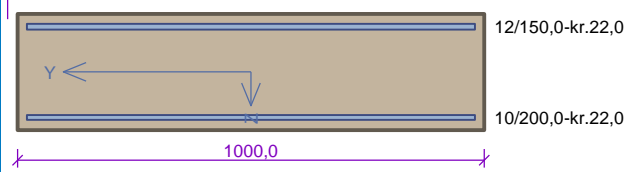


Fig. A-29. Shear forces at extraordinary ULS in 120<sup>th</sup> minute of fire in [kN].



### floor slab-support CS\_R120



Typ prvku: deska  
Prostředí: XC1

**Beton: C 25/30**

$f_{ck} = 25,0$  MPa;  $f_{ctm} = 2,6$  MPa;  $E_{cm} = 31000$  MPa

**Ocel podélná: B500B** ( $f_{yk} = 500,0$  MPa;  $E_s = 200000$  MPa)

**Ocel příčná: B500** ( $f_{yk} = 500,0$  MPa;  $E_s = 200000$  MPa)

**Vzpěr**

Vzpěr není uvažován

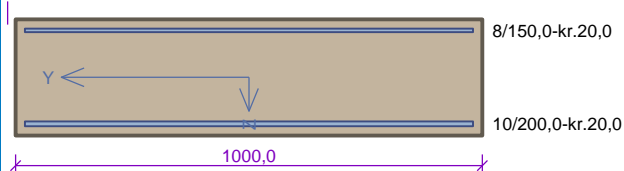
Posouzení v čase požadované požární odolnosti  $t = 120,0$  min  
Metoda izotermie  $500$  °C

#### Posouzení mezního stavu únosnosti

č.	Název	$N_{Ed}$	$M_{Edy}$	$M_{Edz}$	$V_{Edz}$	$V_{Edy}$	Využití [%]	Posouzení
		$N_{Rd}$ [kN]	$M_{Rdy}$ [kNm]	$M_{Rdz}$ [kNm]	$V_{Rdz}$ [kN]	$V_{Rdy}$ [kN]		
1	Zat. případ 1	<b>-320,79</b>	<b>-111,11 → -115,92</b>	<b>0,00</b>	34,73	0,00	118,5	Nevyhovuje
		-5684,25	-97,69	0,00	-186,36	0,00		
2	Zat. případ 2	<b>-281,11</b>	<b>-128,04 → -132,26</b>	<b>0,00</b>	38,09	0,00	139,5	Nevyhovuje
		-5684,25	-94,58	0,00	181,16	0,00		
3	Zat. případ 3	<b>-280,86</b>	<b>-129,85 → -134,06</b>	<b>0,00</b>	40,23	0,00	141,4	Nevyhovuje
		-5684,25	-94,57	0,00	181,13	0,00		

**141,4 % NEVYHOVUJE**

### floor slab-span CS\_R120



Typ prvku: deska  
Prostředí: XC1

**Beton: C 25/30**

$f_{ck} = 25,0$  MPa;  $f_{ctm} = 2,6$  MPa;  $E_{cm} = 31000$  MPa

**Ocel podélná: B500B** ( $f_{yk} = 500,0$  MPa;  $E_s = 200000$  MPa)

**Ocel příčná: B500** ( $f_{yk} = 500,0$  MPa;  $E_s = 200000$  MPa)

**Vzpěr**

Vzpěr není uvažován

Posouzení v čase požadované požární odolnosti  $t = 120,0$  min  
Metoda izotermie  $500$  °C

#### Posouzení mezního stavu únosnosti

č.	Název	$N_{Ed}$	$M_{Edy}$	$M_{Edz}$	$V_{Edz}$	$V_{Edy}$	Využití [%]	Posouzení
		$N_{Rd}$ [kN]	$M_{Rdy}$ [kNm]	$M_{Rdz}$ [kNm]	$V_{Rdz}$ [kN]	$V_{Rdy}$ [kN]		
1	Zat. případ 1	-281,00	-50,00 → -54,22	0,00	0,00	0,00	90,0	Vyhovuje
		-5508,70	-60,31	0,00	0,00	0,00		
2	Zat. případ 2	-321,00	-50,00 → -54,82	0,00	0,00	0,00	86,1	Vyhovuje
		-5508,70	-63,74	0,00	0,00	0,00		

**90,0 % VYHOVUJE**





**outer wall\_R120**

Typ prvku: stěna  
Prostředí: XC1  
**Beton: C 25/30**  
 $f_{ck} = 25,0 \text{ MPa}$ ;  $f_{ctm} = 2,6 \text{ MPa}$ ;  $E_{cm} = 31000 \text{ MPa}$   
**Ocel podélná: B500B** ( $f_{yk} = 500,0 \text{ MPa}$ ;  $E_s = 200000 \text{ MPa}$ )  
**Ocel příčná: B500** ( $f_{yk} = 500,0 \text{ MPa}$ ;  $E_s = 200000 \text{ MPa}$ )  
**Vzpěr**  
Vzpěrná délka:  $l_{ef,y} = 3,50 \times 0,50 = 1,75 \text{ m}$

**Posouzení v čase požadované požární odolnosti  $t = 120,0 \text{ min}$**   
Metoda izotermie  $500 \text{ °C}$

**Posouzení mezního stavu únosnosti**

č.	Název	$N_{Ed}$ $N_{Rd}$ [kN]	$M_{Edy}$ $M_{Rdy}$ [kNm]	$M_{Edz}$ $M_{Rdz}$ [kNm]	$V_{Edz}$ $V_{Rdz}$ [kN]	$V_{Edy}$ $V_{Rdy}$ [kN]	Využití [%]	Posouzení
1	Zat. případ 1	<b>-141,61</b>	<b>266,39 → 267,63</b>	<b>0,00</b>	<b>-177,25</b>	<b>0,00</b>	> 300	Nevyhovuje
		-5571,77	48,24	0,00	-147,54	0,00		
2	Zat. případ 2	<b>-136,68</b>	<b>266,01 → 267,21</b>	<b>0,00</b>	<b>-176,92</b>	<b>0,00</b>	> 300	Nevyhovuje
		-5571,77	47,88	0,00	-146,80	0,00		
3	Zat. případ 3	<b>-120,16</b>	<b>-353,97 → -355,02</b>	<b>0,00</b>	<b>-177,25</b>	<b>0,00</b>	> 300	Nevyhovuje
		-5571,77	-49,37	0,00	-128,40	0,00		

**300,0 % NEVYHOVUJE**

**inner wall-two sides\_R120**

Typ prvku: stěna  
Prostředí: XC1  
**Beton: C 25/30**  
 $f_{ck} = 25,0 \text{ MPa}$ ;  $f_{ctm} = 2,6 \text{ MPa}$ ;  $E_{cm} = 31000 \text{ MPa}$   
**Ocel podélná: B500B** ( $f_{yk} = 500,0 \text{ MPa}$ ;  $E_s = 200000 \text{ MPa}$ )  
**Ocel příčná: B500** ( $f_{yk} = 500,0 \text{ MPa}$ ;  $E_s = 200000 \text{ MPa}$ )  
**Vzpěr**  
Vzpěrná délka:  $l_{ef,y} = 3,50 \times 0,50 = 1,75 \text{ m}$

**Posouzení v čase požadované požární odolnosti  $t = 120,0 \text{ min}$**   
Metoda izotermie  $500 \text{ °C}$

**Posouzení mezního stavu únosnosti**

č.	Název	$N_{Ed}$ $N_{Rd}$ [kN]	$M_{Edy}$ $M_{Rdy}$ [kNm]	$M_{Edz}$ $M_{Rdz}$ [kNm]	$V_{Edz}$ $V_{Rdz}$ [kN]	$V_{Edy}$ $V_{Rdy}$ [kN]	Využití [%]	Posouzení
1	Zat. případ 1	<b>-237,07</b>	<b>82,39 → 84,46</b>	<b>0,00</b>	-42,29	0,00	187,1	Nevyhovuje
		-4548,10	45,15	0,00	-149,13	0,00		
2	Zat. případ 2	<b>-226,32</b>	<b>82,41 → 84,39</b>	<b>0,00</b>	-42,30	0,00	189,4	Nevyhovuje
		-4548,10	44,56	0,00	-147,49	0,00		
3	Zat. případ 3	<b>-215,61</b>	<b>-65,62 → -67,51</b>	<b>0,00</b>	-42,29	0,00	154,2	Nevyhovuje
		-4548,10	-43,78	0,00	-145,87	0,00		

**189,4 % NEVYHOVUJE**



**inner wall-one side\_R120**

Typ prvku: stěna  
Prostředí: XC1

**Beton: C 25/30**  
 $f_{ck} = 25,0 \text{ MPa}$ ;  $f_{ctm} = 2,6 \text{ MPa}$ ;  $E_{cm} = 31000 \text{ MPa}$

**Ocel podélná: B500B** ( $f_{yk} = 500,0 \text{ MPa}$ ;  $E_s = 200000 \text{ MPa}$ )

**Ocel příčná: B500** ( $f_{yk} = 500,0 \text{ MPa}$ ;  $E_s = 200000 \text{ MPa}$ )

**Vzpěr**  
Vzpěrná délka  $l_{ef,y} = 3,50 \times 0,50 = 1,75 \text{ m}$

**Posouzení v čase požadované požární odolnosti  $t = 120,0 \text{ min}$**   
Metoda izotermie  $500 \text{ °C}$

**Posouzení mezního stavu únosnosti**

č.	Název	$N_{Ed}$ $N_{Rd}$ [kN]	$M_{Edy}$ $M_{Rdy}$ [kNm]	$M_{Edz}$ $M_{Rdz}$ [kNm]	$V_{Edz}$ $V_{Rdz}$ [kN]	$V_{Edy}$ $V_{Rdy}$ [kN]	Využití [%]	Posouzení
1	Zat. případ 1	-143,60	-108,42 → -109,68	0,00	98,73	0,00	212,4	Nevyhovuje
		-5571,77	-51,60	0,00	131,34	0,00		
2	Zat. případ 2	-137,88	-108,23 → -109,44	0,00	98,57	0,00	214,2	Nevyhovuje
		-5571,77	-51,05	0,00	130,63	0,00		
3	Zat. případ 3	-122,14	237,13 → 238,20	0,00	98,73	0,00	> 300	Nevyhovuje
		-5571,77	46,79	0,00	144,60	0,00		
4	Zat. případ 4	-116,42	236,75 → 237,77	0,00	98,57	0,00	> 300	Nevyhovuje
		-5571,77	46,37	0,00	143,73	0,00		

**300,0 % NEVYHOVUJE**

Based on the calculated inner forces and conducted assessments it can be stated the elements were significantly overloaded in critical cross-sections in means of flexural resistance and also shear resistance in case of outer wall during fire situation. When speaking about flexural resistance, it means the elasticity limits were exceeded and materials started to work in plastic region. At the same time, flexural stiffness of overloaded cross-sections started to decrease which lead to redistribution of inner forces to those part of structure with lower damage level. Whether the redistribution can propagate in full extent it directly depends on the rotational capacity of subjected cross-sections. Maximal strains reached in reinforcement and concrete together with limit elastic and ultimate strains were checked in maximally loaded cross-sections of floor slabs and walls, see Fig. A-30 and A-31.

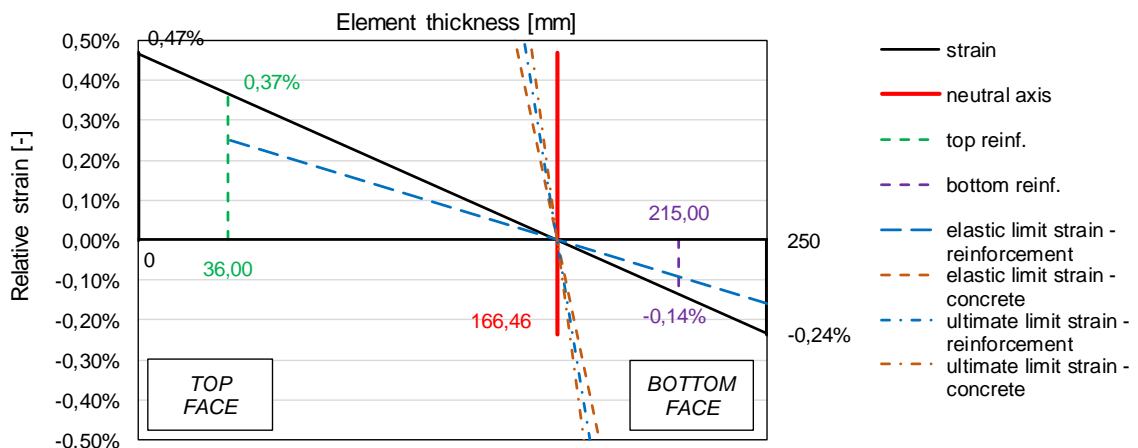


Fig. A-30. Strains in maximally loaded slab cross-section referring to 60<sup>th</sup> minute of fire.

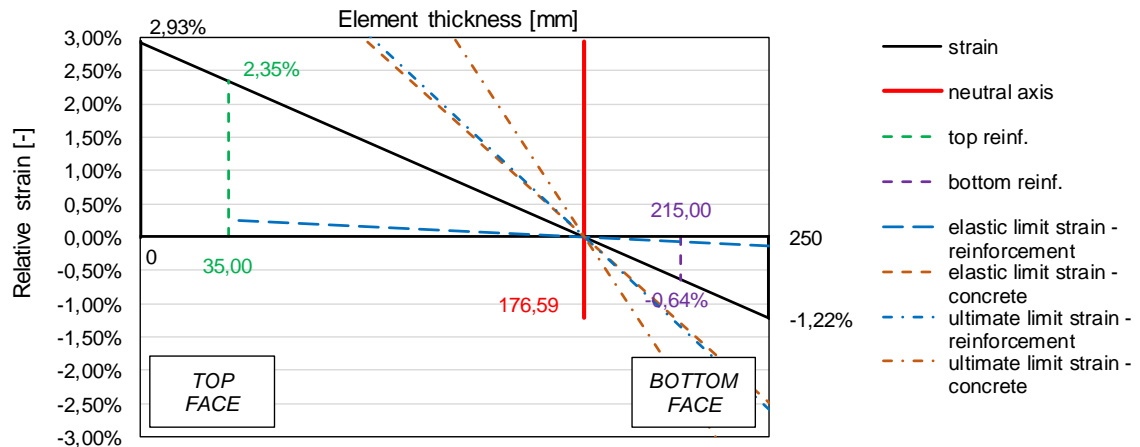


Fig. A-31. Strains in maximally loaded wall cross-section referring to 120<sup>th</sup> minute of fire.

In both cases it is evident the tensile reinforcement far exceeded the yield strain which triggers rotation of cross-section, decrease of flexural stiffness and thus forces redistribution. At the same time the ultimate strain of reinforcement referring to bars rupture nor elastic or ultimate limit strain of concrete referring to concrete crushing were not reached. It means the cross-sections exhibit sufficient rotational capacity and the redistribution is possible. It is worth to mention the bottom concrete chords exhibit high strain values which is due to higher ductility at high temperatures.

Beside the fact critical cross-sections were overloaded by bending moment the top cross-sections of outer RC wall were also overloaded by excessive shear forces that developed due to thermal elongation of floor slab. In case of flexural overloading it can be proved the structure can help itself with the redistribution, however in case of shear overloading the situation would very probably end with shear failure and possibly local collapse. This type of failure is often reported from real fire cases.



### Incorporation of Changes in Structural System

Based on the findings described above the structural model was adjusted in following way in order to take into account the structural damage and internal forces redistribution:

- Rotational stiffness of supports in the bottom walls cross-sections was set to finite value found iteratively;
- Internal plastic hinges were placed in cross-sections that were overloaded while their rotational stiffness was set to finite value found iteratively;
- To incorporate the shear failure of outer wall horizontal free movement was set to the already inserted internal hinge.

The changes made in structural model are indicated in Fig. A-32 below.

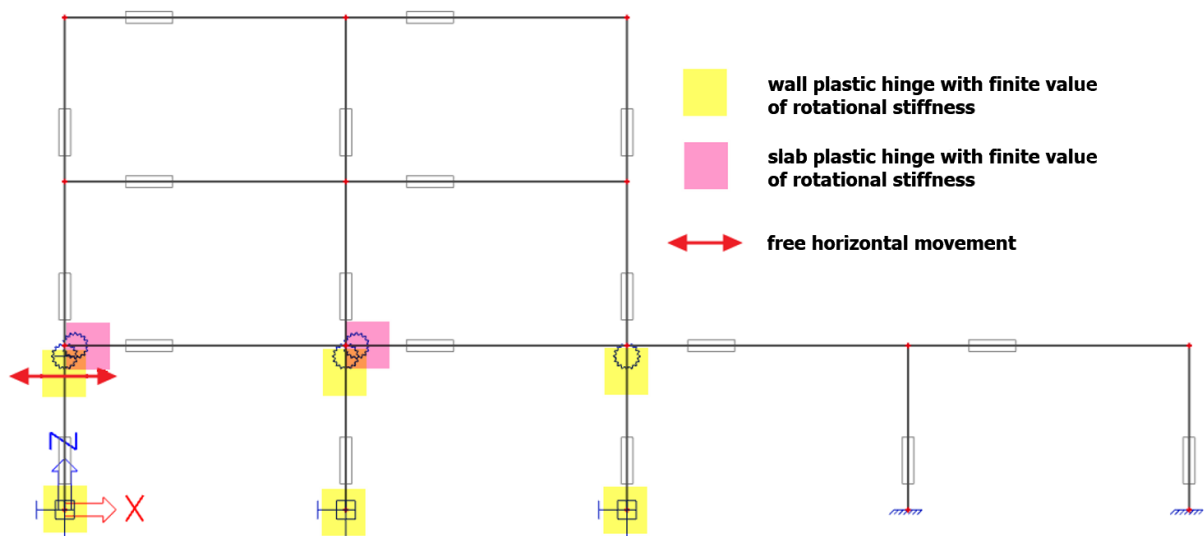


Fig. A-32. Changes in structural model respecting overloading of critical cross-sections.

Another set of calculation results with adjusted structural model is given below.

Hodnoty:  $U_{total}$   
Lineární výpočet  
Třída: MSÚ\_požár  
Výběr: Vše  
Poloha: V uzlech s průměrováním.  
Systém: Globální



Fig. A-33. Maximal linear elastic deflections of adjusted model at extraordinary ULS in [mm].



Hodnoty: **N**  
Lineární výpočet  
Třída: MSU\_požár  
Souřadný systém: Dílec  
Extrém 1D: Lokální  
Výběr: Vše

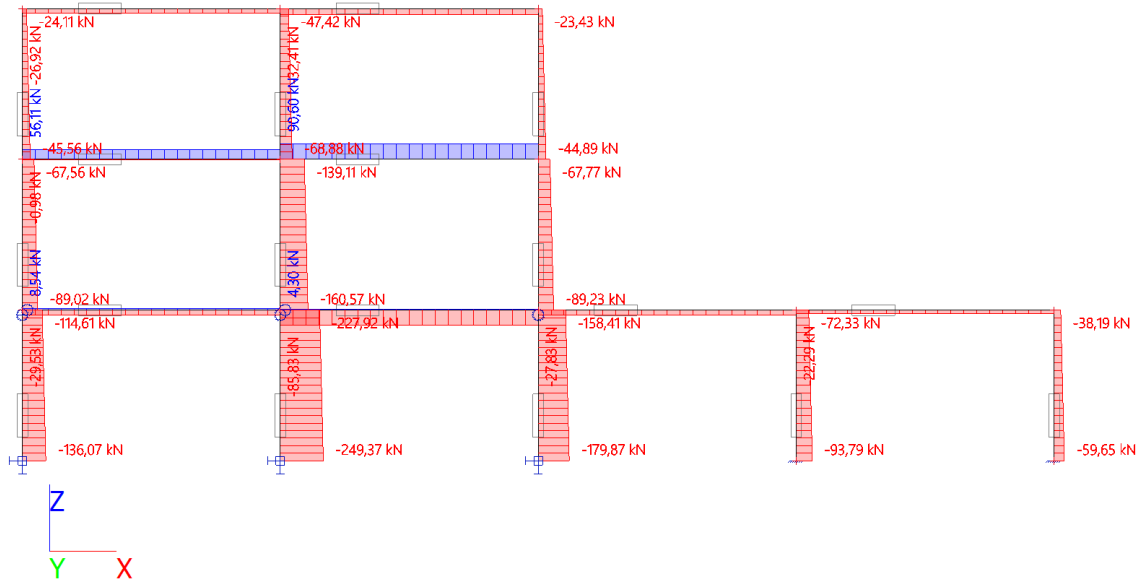


Fig. A-34. Maximal axial forces in adjusted model at extraordinary ULS in [kN].

Hodnoty: **M<sub>y</sub>**  
Lineární výpočet  
Třída: MSU\_požár  
Souřadný systém: Dílec  
Extrém 1D: Lokální  
Výběr: Vše

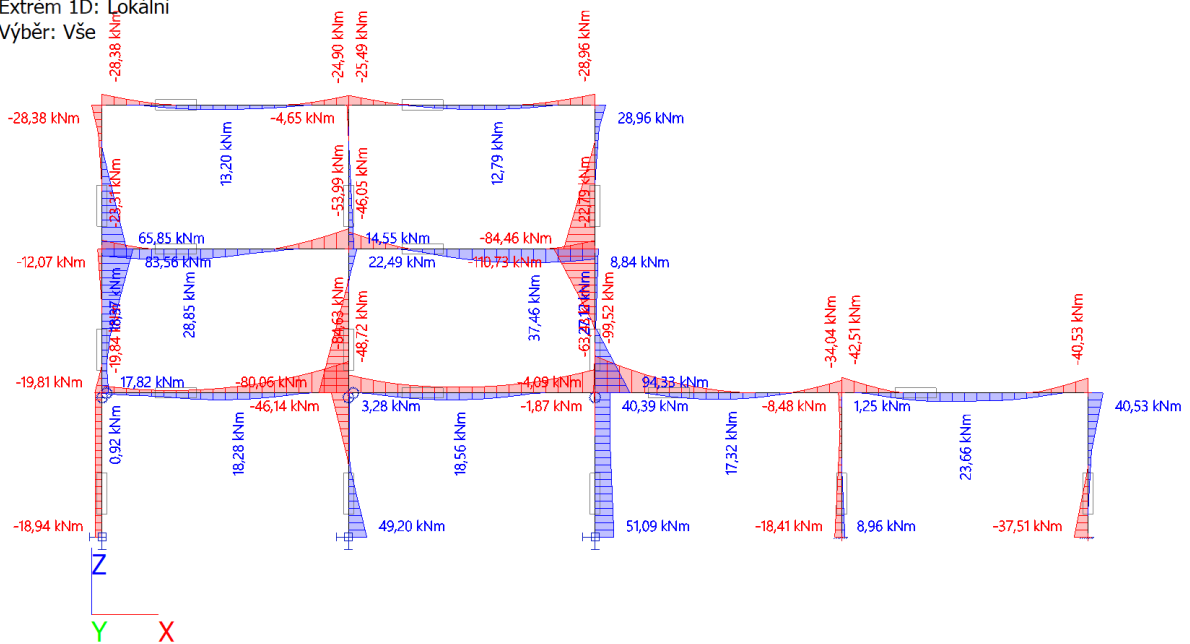


Fig. A-35. Maximal bending moments in adjusted model at extraordinary ULS in [kNm].



Hodnoty:  $V_z$   
Lineární výpočet  
Třída: MSÚ\_požár  
Souřadný systém: Dílec  
Extrém 1D: Lokální  
Výběr: Vše

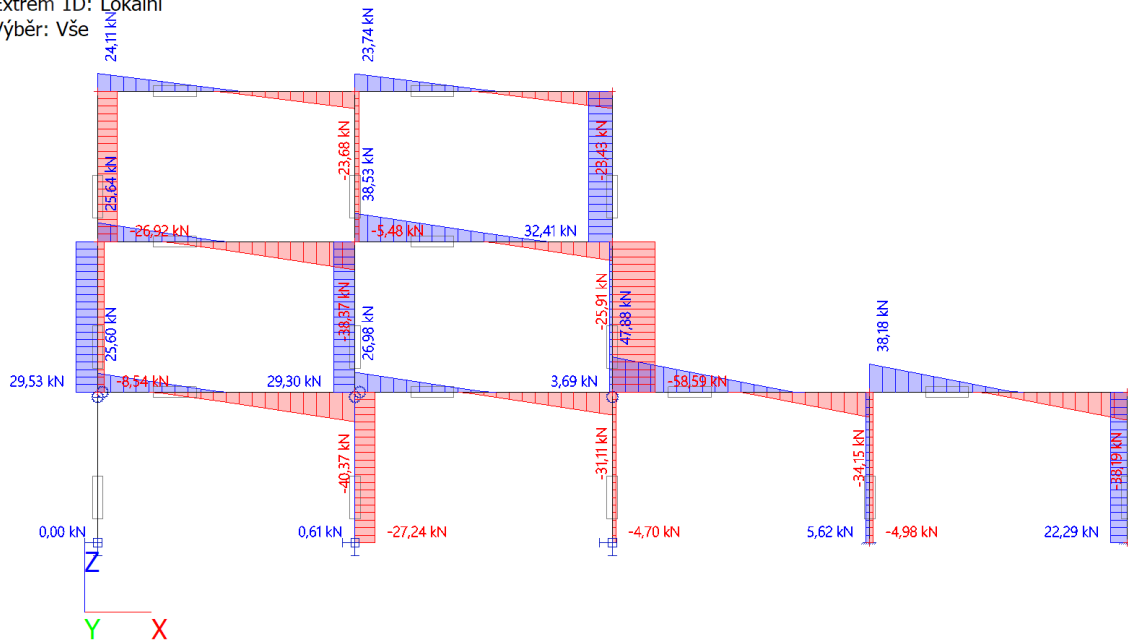


Fig. A-36. Maximal shear forces in adjusted model at extraordinary ULS in [kN].

### Assessment of Residual Load-bearing Capacity

Now results of internal forces and deflection calculation in residual state are given. It is assumed the level of dead and live loads stays the same in the residual state.

Hodnoty:  $U_{total}$   
Lineární výpočet  
Kombinace: MSP-Char (auto)  
Výběr: Vše  
Poloha: V uzlech s průměrováním.  
Systém: Globální

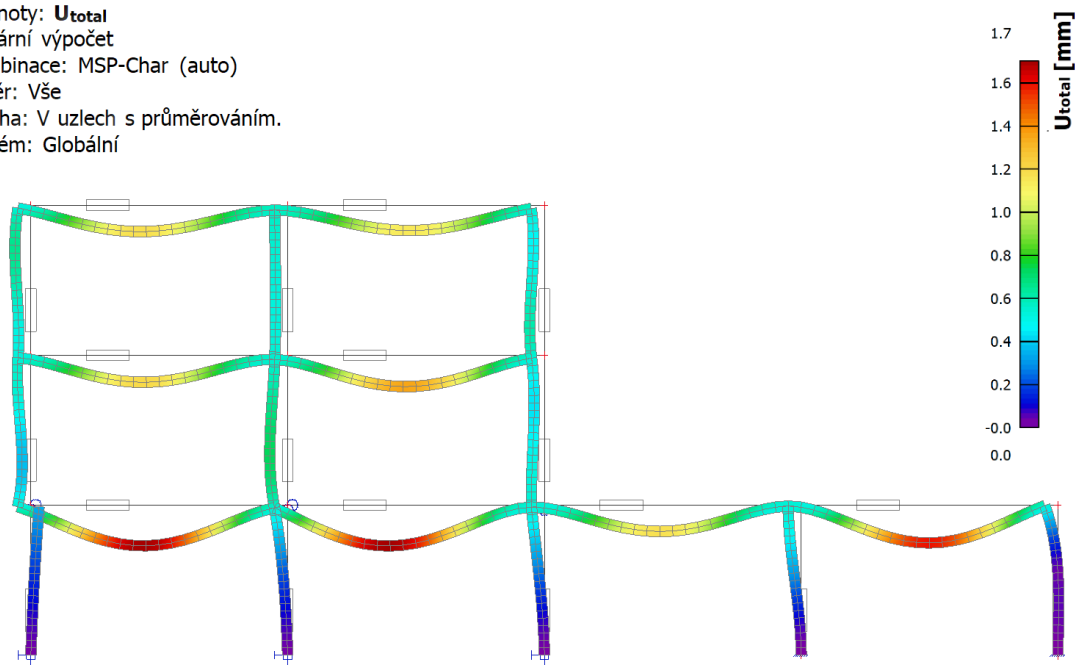


Fig. A-37. Linear elastic deflections of adjusted model at SLS after fire in [mm].





Hodnoty: **N**  
Lineární výpočet  
Kombinace: MSÚ-Sada B (auto)  
Souřadný systém: Dílec  
Extrém 1D: Lokální  
Výběr: Vše

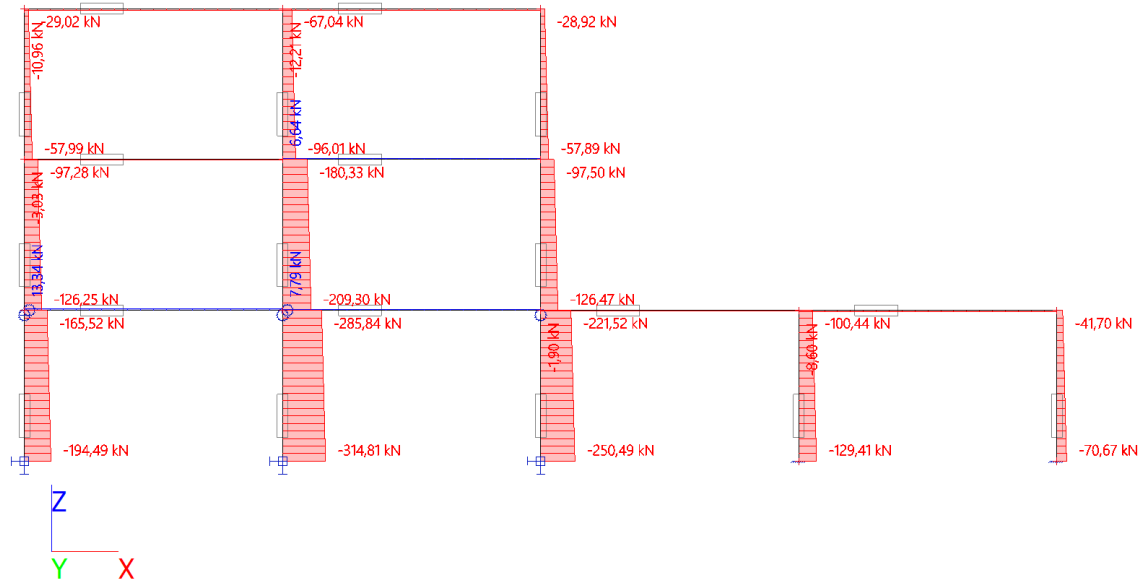


Fig. A-38. Axial forces at ULS after fire in [kN].

Hodnoty: **M<sub>y</sub>**  
Lineární výpočet  
Kombinace: MSÚ-Sada B (auto)  
Souřadný systém: Dílec  
Extrém 1D: Lokální  
Výběr: Vše

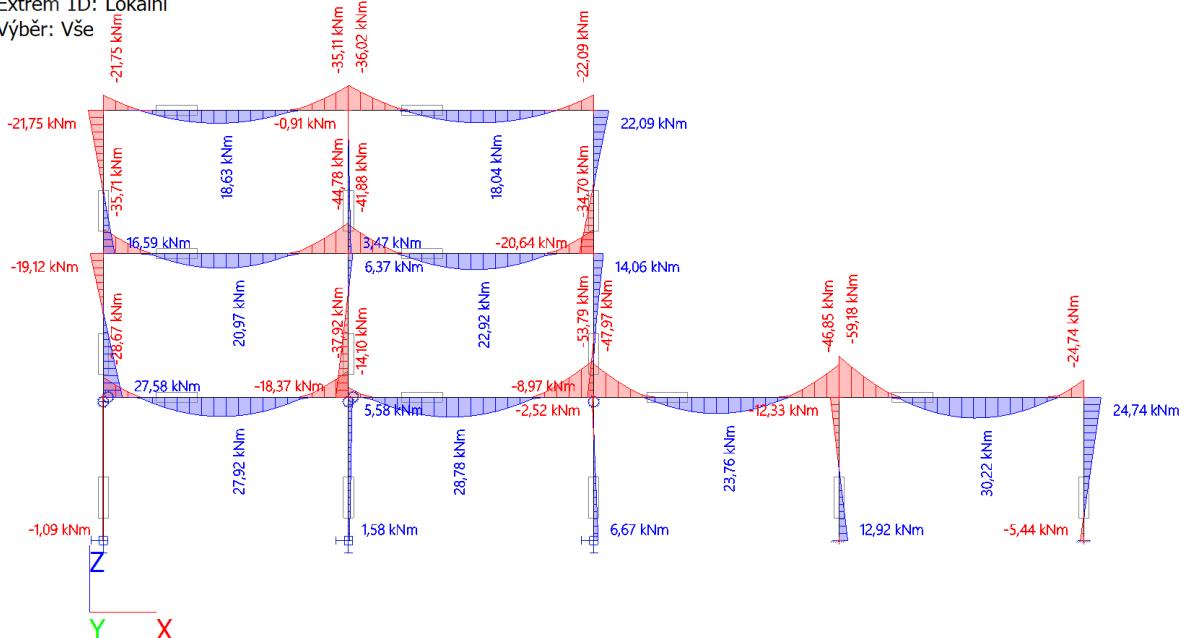


Fig. A-39. Bending moments at ULS after fire in [kNm].



Hodnoty:  $V_z$   
Lineární výpočet  
Kombinace: MSÚ-Sada B (auto)  
Souřadný systém: Dilec  
Extrém 1D: Lokální  
Výběr: Vše

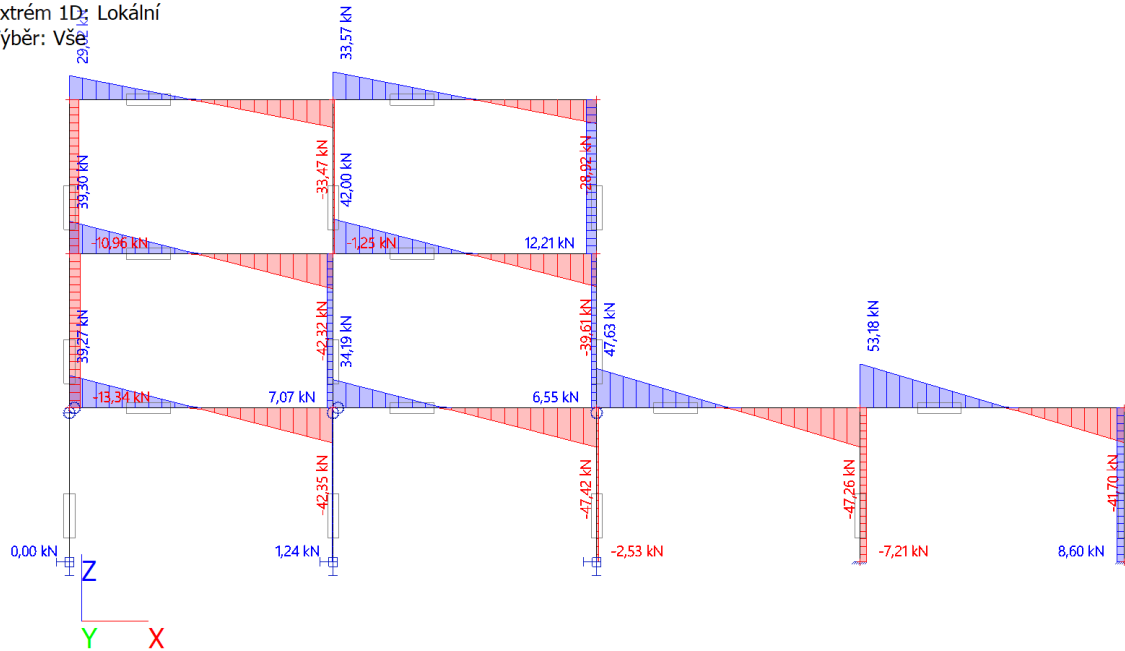


Fig. A-40. Shear forces at ULS after fire in [kN].

At this moment assessment of residual load-bearing capacity of floor slabs and walls can be done. Within the assessment following aspects are taken into account: (i) loading history during fire situation influencing structural system in residual state; (ii) acting internal forces on changed structural system; (iii) material deterioration of both concrete and reinforcing steel taking residual properties into account.

ASSESSMENT OF RC FLOOR SLAB RESIDUAL LOAD-BEARING CAPACITY AFTER FIRE		
cross-section dimensions	concrete properties	reinforcement properties
h = 250 mm	$f_{ck,init} = 25,00$ MPa	$f_{yk} = 500,00$ MPa
b = 1000 mm	$f_{cd,res} = 16,67$ MPa	$f_{yd} = 434,78$ MPa
c = 20 mm		
<p>Standard Temperature-Time Curve (ISO 834)</p>	<p>Temperature Profile: h = 250 mm; t = 120 min</p>	
- 300°C isotherm position	$a_{300°C} = 62$ mm	=> $h_{res,300} = 188$ mm
- bottom bars temperature	$\theta_{s,bot} = 628$ °C	=> $k_{s,res,bot} = 0,72$ [-]
<b>rebars specification</b>	$\varnothing$ spacing $A_s$ [mm <sup>2</sup> ]	
- bottom rebars	10 mm 200 mm	392,70
- top rebars	12 mm 150 mm	753,98



<b>assessment of residual bending resistance - midspan cross-section</b>			
- effective height	d =	225,00 mm	
- height of compression zone	x =	9,16 mm	=> z = 221,34 mm
- moment resistance	$M_{Rd, res, span}$ =	27,03 kNm	< $M_{Ed, span}$ = 28,70 kNm
<b>DO NOT SATISFY</b>			
<b>assessment of residual bending resistance - supports cross-section</b>			
- effective height	d =	162,00 mm	
- height of compression zone	x =	24,59 mm	=> z = 152,17 mm
- moment resistance	$M_{Rd, res, support}$ =	49,88 kNm	< $M_{Ed, support}$ = 53,80 kNm
<b>DO NOT SATISFY</b>			

Based on the assessment of residual load-bearing capacity cross-sections with sufficient load-bearing capacity were determined (in Fig. A-41 highlighted with green colour) as well as cross-sections without sufficient load-bearing capacity (highlighted with purple colour).

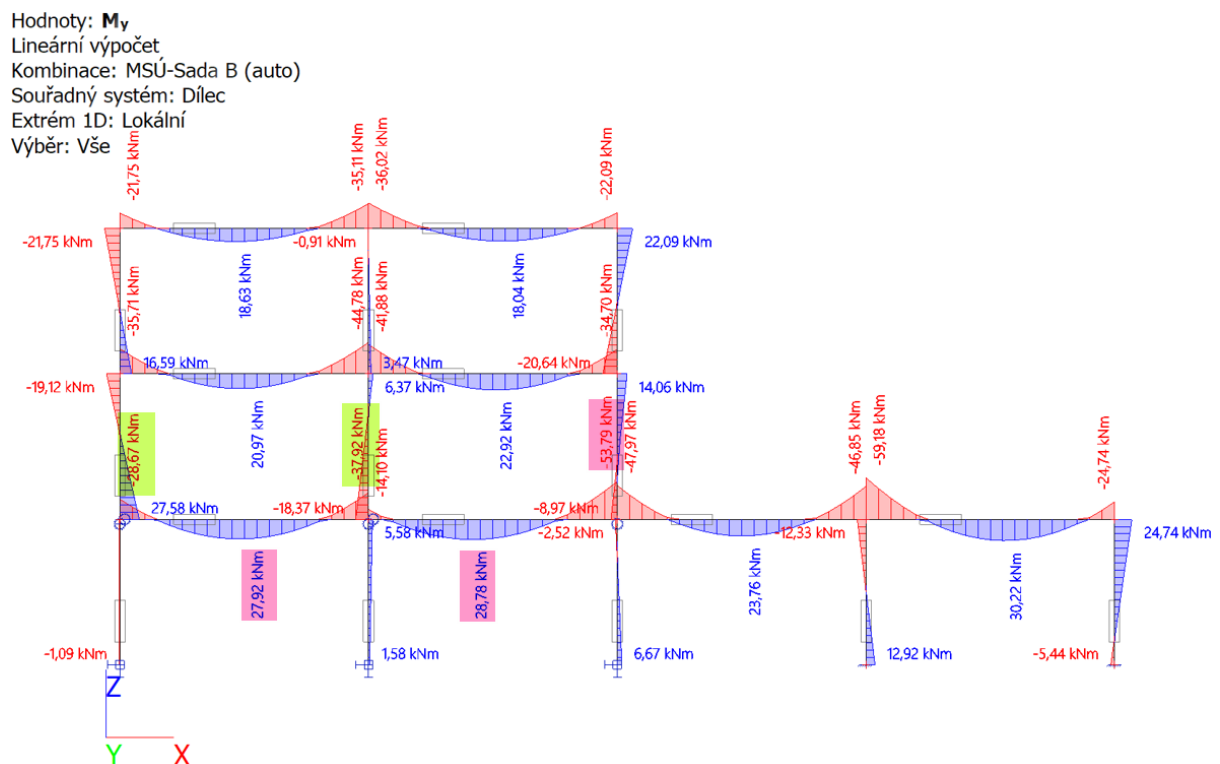


Fig. A-41. Bending moments at ULS after fire in [kNm] with highlighted cross-sections according to assessment results.



**ASSESSMENT OF RC WALL RESIDUAL LOAD-BEARING CAPACITY AFTER FIRE**  
-- wall subjected to fire from one side --

cross-section dimensions		initial concrete strength	initial steel strength		
h =	250 mm	$f_{ck,init} =$	25 MPa	$f_{yk,init} =$	500,00 MPa
b =	1000 mm	$E_c =$	31,48 GPa	$E_s =$	200,00 GPa
reinforcement (heated side)		reinforcement (opposite side)	division of c.-s. into zones		
pieces =	5 pcs	pieces =	5 pcs	zone nr. =	10 [-]
diameter =	10 mm	diameter =	10 mm	zone thick. =	25,00 mm
$\theta_{corner\ reinf.} =$	519 °C	$\theta_{inner\ reinf.} =$	20 °C		

i [-]	$a_i$ [mm]	$\theta_i$ [°C]	$k_c(\theta_i)$ [-]
M	250	20	1,00
1	13	796	0,10
2	38	488	0,52
3	63	301	0,74
4	88	184	0,81
5	113	113	0,84
6	138	74	1,00
7	163	50	1,00
8	188	36	1,00
9	213	39	1,00
10	238	26	1,00

**residual state of concrete**

$k_c(\theta_M) =$  1,00 [-]  
 $k_{c,m} =$  0,79 [-]  
 $a_z =$  67,45 mm  
 **$h_{eff,res} =$  182,55 mm**

**residual state of reinforcement**

$\theta_{reinf.\ mean} =$  269,50 °C  
 $k_{s,res} =$  1,00 [-]

**cross-section scheme**

**cross-section temperature field**

**RESIDUAL LOAD-BEARING CAPACITY IN PLAIN COMPRESSION**

$$N_{Rd,res} = 0,85 * A_{c,res} * (k_{cM} f_{ck} / \gamma_c) + A_s * \min(k_{s,res} * f_{yk} / \gamma_s; \epsilon_{c2} * E_s) = \mathbf{2900,34\ kN}$$

$$N_{Rd,res} = 2900\ kN > N_{Ed} = 251\ kN$$

**SATISFY**

The walls subjected to fire from one side only are loaded dominantly by axial force, therefore the assessment is done in the means of calculation of load-bearing capacity in plain compression.



Beside this assessment the outer wall is still presumed to be damaged with shear failure in its head making the wall rather unstable – **this would definitely be the place where the structure should be temporarily propped already during the investigation.**

### ASSESSMENT OF RC WALL RESIDUAL LOAD-BEARING CAPACITY AFTER FIRE

-- wall subjected to fire from two sides --

<u>cross-section dimensions</u>	<u>initial concrete strength</u>	<u>initial steel strength</u>
h = 250 mm	$f_{ck,init} = 25$ MPa	$f_{yk,init} = 500,00$ MPa
b = 1000 mm	$E_c = 31,48$ GPa	$E_s = 200,00$ GPa
<u>reinforcement (heated side)</u>	<u>reinforcement (opposite side)</u>	<u>division of c.-s. into zones</u>
pieces = 5 pcs	pieces = 5 pcs	zone nr. = 10 [-]
diameter = 10 mm	diameter = 10 mm	zone thick. = 12,50 mm
$\theta_{corner\ reinf.} = 519$ °C	$\theta_{inner\ reinf.} = 519$ °C	

i [-]	a <sub>i</sub> [mm]	θ <sub>i</sub> [°C]	k <sub>c</sub> (θ <sub>i</sub> ) [-]
M	125	151	0,83
1	6	917	0,03
2	19	715	0,21
3	31	568	0,41
4	44	444	0,58
5	56	357	0,68
6	69	284	0,75
7	81	233	0,79
8	94	193	0,81
9	106	168	0,82
10	119	154	0,83

residual state of concrete

$k_c(\theta_M) = 0,83$  [-]

$k_{c,m} = 0,58$  [-]

$a_z = 46,36$  mm

**=>  $h_{eff,res} = 157,28$  mm**

residual state of reinforcement

$\theta_{reinf.\ mean} = 519,00$  °C

$k_{s,res} = 0,89$  [-]

cross-section scheme

cross-section temperature field

Temperature Profile: h = 250 mm; t = 120 min

**RESIDUAL LOAD-BEARING CAPACITY IN PLAIN COMPRESSION**

$$N_{Rd,res} = 0,85 * A_{c,res} * (k_{cM} f_{ck} / \gamma_c) + A_s * \min(k_{s,res} * f_{yk} / \gamma_s; \epsilon_{c2} * E_s) = \mathbf{2147,46\ kN}$$

$$N_{Rd,res} = 2147\ kN > N_{Ed} = 315\ kN$$

**SATISFY**

196



## Discussion

Within previous chapters, fire resistance of chosen structural elements was scrutinised together with the loadings history. Temperature-induced forces and deformations were established for critical durations of fire and were consequently incorporated in the calculation. It showed that during fire certain cross-sections of walls and slabs (typically their mutual joints) were significantly overloaded which have essential impact not only to the behaviour during fire but also to the residual state as well.

Based on the complete post-fire structural assessment following statements can be made:

- The inspected structure withstood the fire of approximate duration 120 minutes with no global collapse.
- Local shear failure of outer RC wall was expected according to the calculations;
  - The shear failure was triggered by thermal elongation of floor slab in final time of fire duration.
- Permanent changes in structural system are expected based on the calculations regarding decrease of flexural stiffness's and partial plastic hinges formation;
  - The changes in structural system enabled the structure to withstand the extraordinary situation;
  - Redistribution of internal forces was enabled thanks to sufficient rotational capacity of cross-sections and materials ductility (enlarged in hot state);
  - The biggest overloading of slab's cross-sections was achieved around 60<sup>th</sup> minute of fire duration (biggest thermal gradient took place) while damage of wall's cross-sections was achieved at the very end of fire duration, in 120<sup>th</sup> minute (biggest thermal elongation of slab)
- Residual bending resistance of floor slabs is not sufficient in case of bottom reinforcement and right end of right span in case of top reinforcement. Structural strengthening or loadings reduction will be necessary to use the structure again in future.
- Residual compressive force resistance of all walls is sufficient.
- **Shear failure of cross-section in head of outer wall is understood as very severe since it could lead to global collapse and even if it did not happen, the structure has to be treated as potentially unstable and unsafe. This detail has to be inevitably and properly repaired!**
- Due to the structural system changes and creation of partial plastic hinges the spatial stability, rigidity and resistance to horizontal forces suffered and therefore shall be checked in residual state.
- Within this post-fire assessment only elements directly exposed to fire were assessed. However, due to the elements continuity and statically-indeterminate nature the temperature-induced forces influence also the adjacent parts of structure which might get overloaded as well, see bending moments in [Figs. A-24, 28, 35](#). These members have to be assessed as well a potential plastic hinges incorporated into the structural model.